Groundwater recharge and movement through mountain-basin systems of the Southwest: a case study in the Chiricahua Mountains-San Bernardino Valley system, Arizona and Sonora

by

Samuel Earman

Submitted in Partial Fulfillment
of the Requirements for the

Doctorate of Philosophy in Earth and Environmental Science
with Dissertation in Hydrology

Socorro, New Mexico

December, 2004

ABSTRACT

This dissertation discusses several aspects of the hydrogeology of a mountain-basin system (the Chiricahua Mountains, Arizona, USA, and the San Bernardino Valley, Arizona, USA, and Sonora, Mexico) . Detailed studies focused on four major phenomena: the hydrogeologic impacts of magmatically-active accommodation zones, the conditions necessary for the formation of the evaporite mineral trona ($Na_3CO_3HCO_3 \cdot 2H_2O$) groundwater recharge and movement in a high-elevation mountain range, and the proportion of snowmelt in groundwater recharge in the Southwest.

Although the San Bernardino Valley and its neighboring basins are bounded by highlands with of similar lithology, are of the same age, and share a common mode of formation, the San Bernardino Valley has distinct hydrogeologic properties, including groundwater anion evolution dominated by HCO_3^- (as opposed to SO_4^{2-} and Cl^-), high total dissolved solids content, low groundwater ages, and low storativity. The hydrogeologic differences are all related to the presence of the magmatically-active accommodation zone. The differences in hydrogeology between the San Bernardino Valley and its neighbors can be used as a basis for interpreting hydrogeological differences between other accommodation-zone basins and their neighbors.

The differences in water chemistry described above include a high ratio of $[HCO_3^-]$ to $[Ca^{2+}]$ in the San Bernardino aquifer due to injection of CO_2 related to the accommodation zone, which means that groundwaters from San Bernardino would form significant quantities of the mineral trona upon evaporation, but waters from its neighboring basins would not. Observation of this difference in mineral assemblages that would result from CO_2 injection led to an examination of other trona deposits

and trona-forming waters around the world, suggesting that CO_2 injection appears to be a necessary factor for trona formation. This refinement of the generally-accepted theory for trona formation helps to explain the limited distribution of trona deposits in the geologic record, and can aid future trona prospecting.

Among other findings, an examination of groundwater recharge and movement in the Chiricahuas shows that high-elevation mountain springs are not necessarily hydraulically isolated from lower systems; that the development of snowpack appears to be one of the factors that drives groundwater recharge; and that high-elevation zones of the range are the most important contributors of water to the mountain system and the adjacent San Bernardino aquifer.

Stable isotopes in snow are subject to post-fall alteration, which can have significant impacts on mass-balance calculations. Paired precipitation collectors of different designs can be used to determine the magnitude of alteration that occurs at a site. Because the collectors allow different amounts of alteration to take place, comparison of data gathered by different styles of collectors may yield misleading results if snow makes up a significant part of the sample collected. The alteration of snow by precipitation collectors may not be evident, as even samples that have undergone significant alteration can plot on or above the global meteoric water line. Many processes contribute to the alteration of snow, including isotope exchange with atmospheric water vapor. The effects of this process were observed in the field and the laboratory. The isotope signature of fresh snow is typically not representative of the bulk meltwater derived from the snow; because isotope evolution appears to increase with exposure time, samples of snow or melt collected on a given day are also unlikely to be representative of the bulk melt. As a result, isotope mixing models using fresh snow signatures as an end member contributing to groundwater recharge appear to underestimate the contribution of snowmelt. Mixing models using

snowmelt isotope composition from a precipitation collector designed to provide an improved value for meltwater input (compared to fresh precipitation or a sample of snow or melt from a given day) show that snowmelt accounts for a significant proportion of groundwater recharge (typically 40-60%) at four sites in New Mexico and Arizona. The proportion of snowmelt in groundwater at these sites is typically higher than the proportion of snow in average annual precipitation, showing that snow has a greater recharge efficiency than rain. Future climate change could significantly affect groundwater recharge in the western USA, because it could result in lower proportions of snow.

ACKNOWLEDGEMENTS

Many parts of the work described in this dissertation would not have been possible (or would have been of poorer quality) without the assistance of a number of individuals and organizations.

Funding for this work was provided by the New Mexico Water Resources Research Institute, the SAHRA Science and Technology Center of the National Science Foundation, and the U.S. Fish and Wildlife Service.

My committee members were all of great assistance during my time at New Mexico Institute of Mining and Technology. I am grateful to Andy Campbell for many thoughtful discussions of isotopic and chemical issues that greatly improved the quality of research; suggestions that improved the clarity of the analysis and presentation of data in this dissertation and abstracts submitted for various meetings along the way and will help me do so in the future; his great teaching style; his patient help with all manner of mass-spectrometry issues; and for keeping the mass spectrometer laboratory stocked with Atomic Fireballs. Brian J. O. L. McPherson got me started on the project that led to all the research described here, and provided a great deal of encouragement and support along the way in addition to very helpful reviews of draft versions of this manuscript. Brent Newman helped with the establishment of one of the field sites used in this study and with obtaining access to the site; he provided important suggestions for improving some experimental work, and suggested revisions that greatly improved the end product. Fred Phillips' attention to detail and desire for true scientific advancement can sometimes be a thorn in one's side—I know of several students who have deliberately avoided adding Fred to their committees because of the amount of work they fear would be entailed. However (at the risk of degenerating into kitsch), some thorns come attached to roses. As one example, were it not for his ideas and suggestions, the investigation of the

conditions necessary to form trona (described in Chapter 2) would never have reached fruition. Although countless hours of modeling, incredibly broad literature research and many other forms of hair pulling were involved, I feel the trona work is my best scientific accomplishment to date, and I hope to follow this example in the future. John Wilson helped to provide some of the funding that made the work in Chapters 3, 4 (and a small but highly significant part of the work in Chapter 2) possible. In addition, his ideas and input helped improve the quality of the research a good deal, and his reviews greatly improved the clarity of the reporting found in the text.

Chris Caldwell was of major assistance in helping me convert mental images of field equipment into working designs, often on short notice. Louie Pope and Ed du Bray both generously took the time to share their knowledge of the Chiricahua Mountains with me. Tom Biggs, Steve Skotnicki and Phil Pearthree were similarly generous in sharing their knowledge of the San Bernardino Valley. Chris Eastoe (whose hospitality is also appreciated), John Hawley, Randy Keller, Rong Kuo, Doug Towne, L. G. Wilson, and Jim Witcher provided otherwise-unobtainable data from previous studies.

Assistance with field work, technical, and logistical issues was provided by John Ayarbe, Dave Boutt, James Broska, Kevin Cobble, Barret Cole, Steve Cullinan, Dale Fox, Andrew Hautzinger, Nina King, Dan Klinglesmith, Kate Jones, B. J. Lechler, Matt Magoffin, Gerald Mitchell, Tony Lupo, Bill Radke, Gary Shellhorn, Paul Tashjian, Tony Velasco, and Tristan Wellman.

Access to many of the water samples discussed in this report due to the assistance of the U. S. Forest Service (especially Duane Bennet, Dave Heft, and Rick Robinson), Cynthia Stefanovic, and numerous private landowners and public land leaseholders. Thanks to Scotty Anderson, Ed Ashurst, Joe and Valer Austin, Roger Barnett, Drum Hadley, Don Kimble, Rob Krentz, Matt Magoffin, Tom Peterson and

Fred Eddington, Ben Snure, and Rick Snure for their assistance. The coöperation of the Southwestern Research Station of the American Museum of Natural History (and the assistance of Wade and Emily Sherbrooke, Diane Smith and Mike Stoehner), the Langmuir Laboratory for Atmospheric Research and the Steward Observatory was essential to establishing long-term sites for precipitation collection.

Finally, the support and friendship of a number of people, including Dave Boutt, Tim Callahan, Bayani Cardenas, "Ike" Chapin, Kate Jones, Garret Kramer, Ryan Jakubowski, Ellie Kurth, BJ Lechler, Alyssa Olson Callahan, Mike Rank, Dina Varano, Michelle Walvoord, and Rob Wykoff is appreciated.

TABLE OF CONTENTS

LIST OF FIGURES

LIST OF TABLES

This dissertation is accepted on behalf of the
Faculty of the Institute by the following committee:

Fred M Phillips

Advisor

John L Wilson

Brian McPherson

Andrew Campbell

10 September 2004

Date

I release this document to the New Mexico Institute of Mining and Technology.

10 September, 2004

Student's Signature Date

INTRODUCTION

This dissertation describes investigations of recharge, movement, and chemical characteristics of groundwater in a mountain-basin system in Arizona, New Mexico, and Sonora (Mexico). It includes investigations of groundwater flow in an accommodation-zone basin, the conditions necessary for the formation of the evaporite mineral trona, groundwater recharge and transfer from a mountain range to an adjacent alluvial aquifer, determination of the proportion of groundwater recharge composed of snowmelt at four sites in Arizona and New Mexico, and a study to determine if exchange with atmospheric water vapor can affect the stable isotope signature of snow. Although these subjects might seem disparate, they all relate to a common ancestor.

The work originated as a hydrogeologic reconnaissance study of the San Bernardino Valley in Arizona, USA and Sonora, Mexico. The hydrogeology of the basin had not been widely studied, so goals included identifying recharge areas and determining the hydraulic and hydrogeologic properties of the basin-fill aquifer. Analysis of the basin's geology indicated that it contains an accommodation zone that was magmatically active, and that the presence of the accommodation zone causes the water chemistry of the San Bernardino Valley to be unique compared to that of its neighboring basins. This investigation is described in Chapter 1.

Closer examination of the water chemistry of the San Bernardino Valley and its neighboring basins showed that the main mineral that would be produced by evaporating San Bernardino groundwater is trona (which is relatively rare in the geologic record), but evaporation of waters from the neighboring basins would yield more traditional evaporite mineral assemblages (*exempli gratia* calcite, halite, and gypsum). Chapter 2 investigates why this is the case for the San Bernardino Valley,

and applies the results to other major deposits of trona around the world, showing that injection of "excess" CO_2 plays a vital, role in driving the deposition of trona.

Research into the sources of recharge for the San Bernardino aquifer showed that the Chiricahua Mountains provided the majority of the basin's groundwater. Because of the range's importance to the water supply of the San Bernardino Valley, the means of recharge and avenues of transfer from the range to the basin aquifer were of interest; the investigation of these issues is described in Chapter 3.

Stable isotope data collected for the sourcing of recharge to the San Bernardino Valley clearly showed that the Chiricahuas were the major source, but the data seemed to show that low-elevation precipitation and summer precipitation were the major sources of recharge, but the physiographic characteristics of the range suggested that high-elevation precipitation, especially snow, should be the major source. Chapter 4 describes an investigation of the stable isotope evolution of snow and how this evolution affects the apparent proportion of snowmelt in recharge. Investigations were conducted in the Chiricahuas and three other sites in Arizona and New Mexico, showing that the proportion of snow in groundwater recharge can be underestimated if stable isotope metamorphism is not taken into account. During research on the stable isotope evolution of snow, it became apparent that there were disputing viewpoints on whether or not stable isotope exchange between snow and atmospheric water vapor could have a significant impact on the isotope composition of snow. While several sources state that this type of exchange is possible, they all appear to rely on anecdotal evidence. An experiment was designed to test this concept. Chapter 4 describes the experiment, and shows that isotope exchange can impact the isotope composition of snowpack, even at temperatures held below 0 °C.

In sum, these investigations track water from its fall as mountain precipitation through its travel to the center of an adjacent basin, examining some of the physical, chemical and isotopic processes that act on it along the way.

CHAPTER 1: Hydrogeology of an accommodation zone basin: The San Bernardino Valley, Arizona, USA and Sonora, Mexico

INTRODUCTION

The San Bernardino Valley, southeastern Arizona, USA and northern Sonora, Mexico (Figure 1-1), is located in the Basin and Range physiographic province. Groundwater in the basin is the only source for domestic supply, and is critical to cattle ranching (the main revenue source for valley residents). The groundwater is also used to maintain artificial streams and ponds in the San Bernardino National Wildlife Refuge that provide habitat for several species of endangered and threatened fish. The rapid population growth in the southwestern USA for the past several decades has increased the importance of understanding groundwater occurrence, movement, and chemical properties in the region as a whole.

In the San Bernardino Valley, average daily temperature ranges from about 14 to 16.5 °C, depending on altitude (Biggs *et alii*, 1999; Hawley *et alii*, 2000). According to the Western Regional Climate Center (URL <http://wrcc.dri.edu>), average annual precipitation varies from 200 to 410 mm, depending on location. In the mountain ranges bounding the valley, precipitation can be as low as that observed in the basin (Perilla Mountains) to "above" 910 mm/yr in the Chiricahua mountains.

As with most basins in the southwestern USA, groundwater in the San Bernardino Valley is obtained almost exclusively from the alluvial basin fill; only two wells used for water production are known to penetrate the consolidated rock beneath the alluvium. The San Bernardino Valley's basin fill differs from that found in typical basins in the region—it is relatively thin, and contains a significant proportion of interbedded basalt. The geological uniqueness of the San Bernardino Valley (compared to its neighboring basins) is the result of a structural high interpreted as a magmatically-

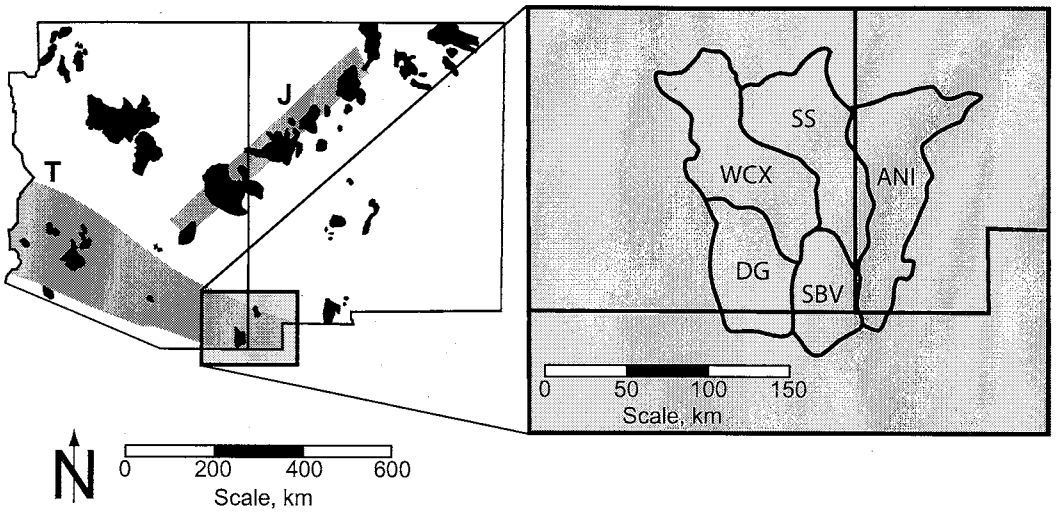

Figure 1-1A. Location of the San Bernardino Valley (SBV) and its neighboring basins (DG = Douglas Basin, WCX = Willcox Basin, SS = San Simon sub-basin of the Gila Basin, ANI = Animas Basin). Black outlines on index map indicate areas where volcanism was active during the Cenozoic; grey bands represent regional structural lineaments (J = Jemez lineament, T = Texas Lineament Belt). Areas of Cenozoic volcanism after from Aldrich, Jr. and Laughlin (1984); lineament locations after Aldrich, Jr. and Laughlin (1984) and Wertz (1970).

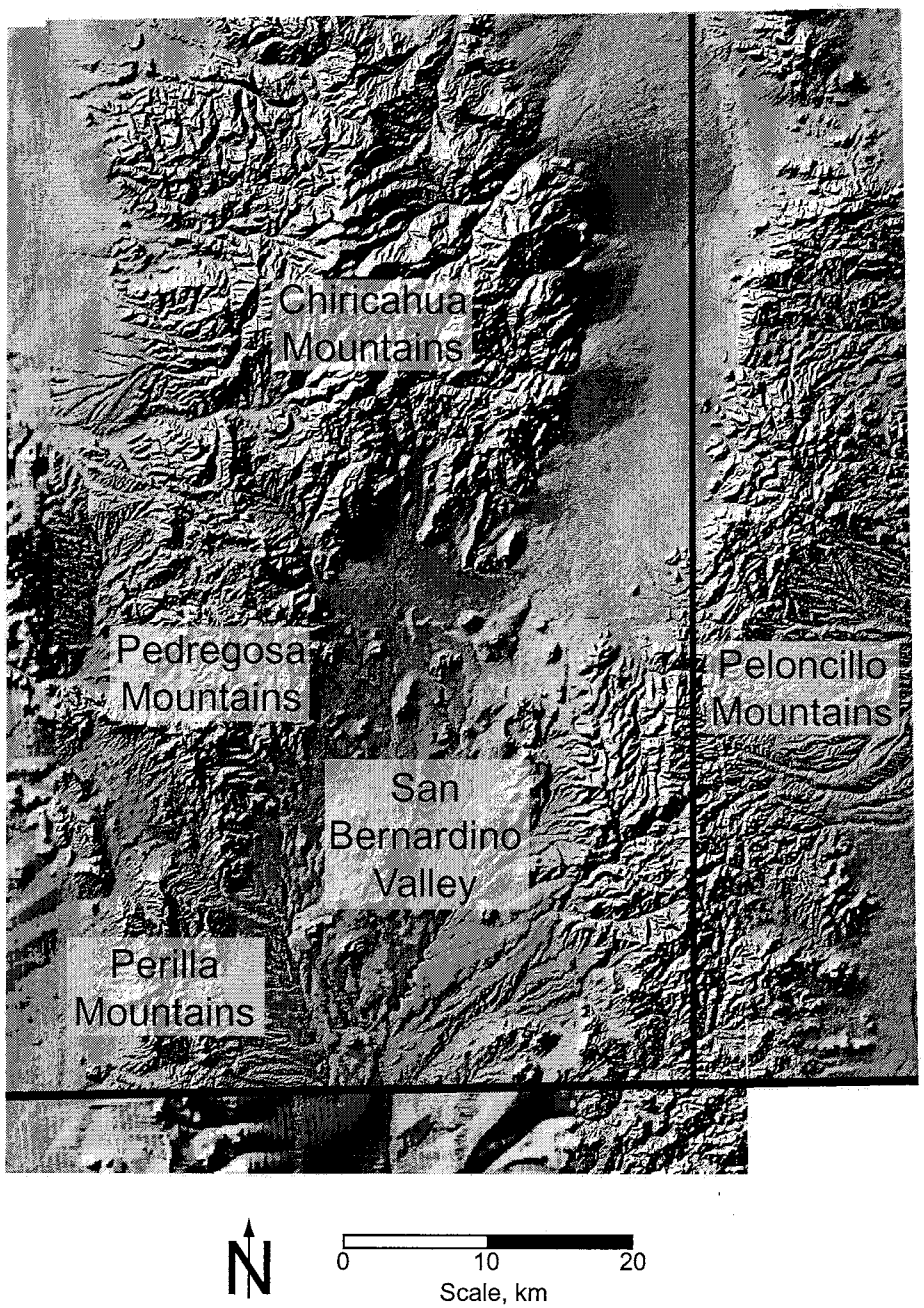

Figure 1-1B. Digital elevation model hillshade of the northern portion of San Bernardino Valley and its bounding mountain ranges. Vertical line represents the Arizona-New Mexico border, horizontal line represents the international border.

active accommodation zone; this uniqueness causes the chemical evolution of groundwater in the basin to differ from that observed in nearby basins.

GEOLOGY

Surrounding mountain ranges

The highlands surrounding the San Bernardino Valley are the primary source of material for the basin fill making up the San Bernardino aquifer. The ranges bounding the San Bernardino Valley are predominantly rhyolitic in composition; rhyolitic tuff and rhyolite are the most common units found in these ranges. In addition to the igneous rocks, there are a number of sedimentary units present; these rocks are primarily carbonates, predominantly limestone (Drewes, 1980).

San Bernardino Valley

The San Bernardino Valley's formation is the result of Basin-and-Range tectonic activity. The Basin and Range disturbance began locally in the early Oligocene (Drewes, 1981), and has continued through the present (Lynch, 1972). The structure of the basin was analyzed by examining the surficial geology, subsurface lithology, gravity, and hillshades of digital elevation models (DEMs). The northern portion of the basin is a half-graben dipping to the west, while the southern portion is a half graben dipping to the east (Figure 1-2). Our analysis shows the San Bernardino basin is offset from the San Simon Basin to the north by a transfer fault (a strike-slip fault that facilitates the transfer of strain between two extended domains that share a common strike but are offset), and the west-dipping half graben in the northern portion of San Bernardino Valley is split into 'mini-half grabens' by four other transfer faults. All five transfer faults strike NW-SE, aligned with the regional structural lineament intersecting the basin (Figure 1-1A). The area separating the northern and southern portions of the basin is a boundary in three senses: it separates two bedrock dip domains, it separates an area that experienced significant basaltic volcanism in the Cenozoic from

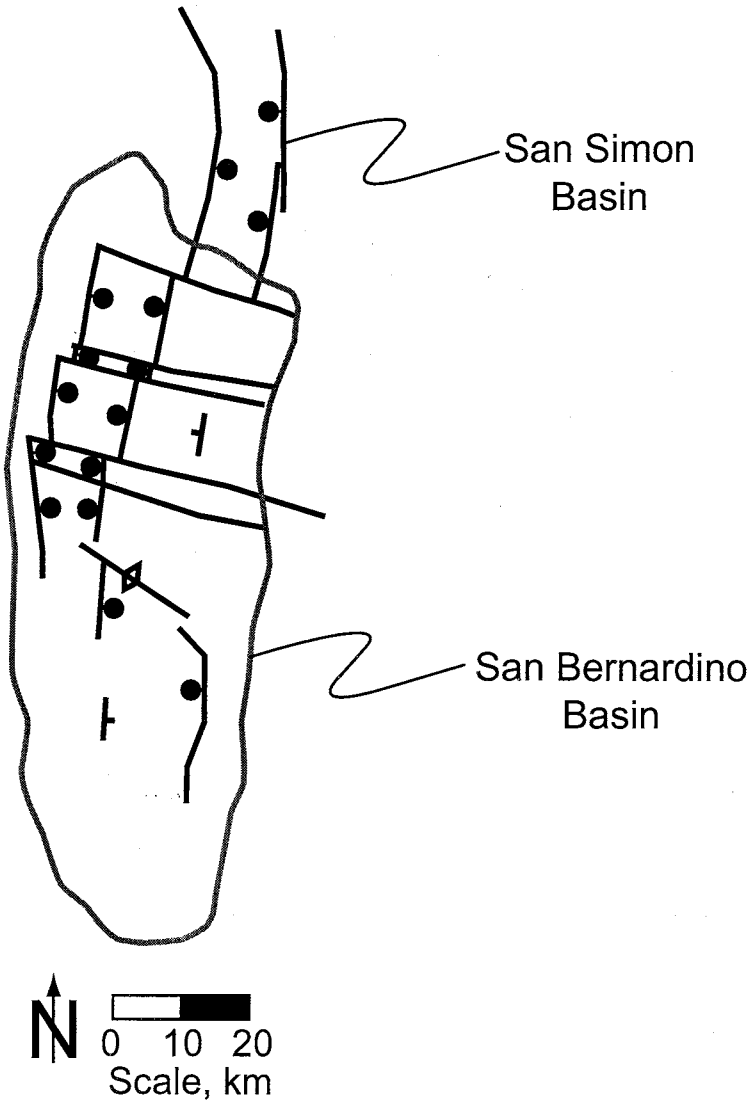

Figure 1-2. Major structural features of the San Bernardino Basin and southern San Simon Basin. Outline in grey represents the San Bernardino hydrologic basin boundary, which extends beyond range-front faults. Normal faults are shown with bar and ball on downthrown side; transfer faults are represented by plain lines; the anticline is indicated via a line with arrowheads. Note the NW-SE orientation of the transfer faults parallel to that of the Texas Lineament Belt (Figure 1-1A).

an area that has experienced minimal basaltic volcanism, and it separates an area with distinct NW-SE transfer faults from an area lacking such features.

This boundary is an accommodation zone, defined by Faulds and Varga (1998) as a belt "of overlapping fault terminations [that] can separate either systems of uniformly dipping normal faults or adjacent domains of oppositely dipping normal faults." Based on the geometry of the San Bernardino accommodation zone, it is classified as an oblique antithetic anticlinal accommodation zone using Faulds and Varga's (1998) terminology. Accommodation zones are often associated with major volcanic fields—over two-thirds of the accommodation zones identified in the Basin and Range Province are associated with major volcanic fields (Faulds and Varga, 1998). The fact that the San Bernardino accommodation zone marks the southern boundary of widespread basaltic volcanism suggests that the basalts are related to the accommodation zone. Because of the association between the basalts and the accommodation zone, the accommodation zone will be described as 'magmatically active.'

The basalts that make up a significant portion of the basin fill were originally called the 'Bernardino volcanic field' by Lynch (1972), but have since been renamed the 'Geronimo volcanic field' (Arculus *et alii*, 1977). They can be split into two groups based on age and chemical characteristics: flank lavas are present in the flanks of the ranges bounding the valley, are predominantly alkali-olivine basalts with ages from 3.5 to 4.7 Myr (and possibly as old as 9.2 Myr), and have relatively low ratios of magnesium to iron; valley lavas are found in the valley proper, are predominantly basinites with ages from 0.26 to 3.2 Myr, and have relatively high magnesium to iron ratios (Kempton, 1984; Kempton and Dungan, 1989).

According to Lynch (1972), the basalts cover an area of approximately 850 km^2 at the surface, but most individual flows cover less than 5 km^2. The younger basalt flows are typically less than 3 m thick, but the older basalts tend to be present in thick-

er deposits (Lynch, 1972). Well logs show that basalts are common as interbeds in the basin fill in much of the northern portion of the basin.

The majority of the alluvial material in the basin fill is derived from the mountains bounding the basin; reflecting the composition of these ranges, it is predominantly rhyolitic, but some zones have received high proportions of sediment derived from montane sedimentary units and contain significant proportions of carbonate minerals. Although most clays in the basin appear to be derived from weathering of the basaltic or rhyolitic sediments, in the center of the basin there is a lacustrine clay unit in the subsurface.

HYDROGEOLOGY

In the majority of the San Bernardino Valley, there is a single, unconfined basin-fill aquifer (the main aquifer of the basin). The lacustrine clay near the basin center serves as a confining unit for a small portion of the main aquifer (a number of flowing artesian wells are present in the area near the international border), and also forms the base of a second, shallower unconfined aquifer. This local unconfined aquifer is supplied mainly by upward leakage through the main aquifer's confining unit; mixing model analysis of stable isotope data show valley-floor precipitation contributes between 0 and 40 % of the water in local aquifer. In the remainder of this manuscript, unless specific mention to the contrary is made, all mentions of groundwater or an aquifer will be referring to the main aquifer and/or the water it contains.

Water samples were collected from a number of wells and springs in the basin, and from springs and streams in the surrounding highlands. Samples were analyzed for one or more of the following: $\delta\ ^{18}O$ and δ D, major-ion chemistry, dissolved gas content, ^{14}C activity, $\delta\ ^{13}C$, and ^{3}H activity. In addition, parameters such as pH, electrical conductivity (EC), and temperature were measured in the field at the time of sampling. Selected data are provided in Table 1-1; a complete compilation of water chem-

istry data is provided in the Appendices. All samples for $\delta\ ^{18}O$ and δ D analysis were either preserved in the field by means of mineral oil in specially-designed reservoir until collection in a glass bottle with Poly-Seal lid (in the case of samples of precipitation and snowmelt), or collected directly into a glass bottle with Poly-Seal lid (in the case of groundwater samples). Samples collected under mineral oil were separated in the laboratory, then stored in a glass bottle with Poly-Seal lid until analysis. $\delta\ ^{18}O$ and δ D (relative to Vienna Standard Mean Ocean Water) were determined via gas-source mass spectrometry. All $\delta\ ^{18}O$ results were obtained via analysis of CO_2 gas that had been equilibrated with a sample aliquot (similar to the methodology outlined by Clark and Fritz, 1997 and discussed in greater detail by Socki *et alii*, 1992). δ D values were obtained by analyzing hydrogen gas formed during an oxidation reaction (Clark and Fritz, 1997). During the initial portion of the study, a sample aliquot was reacted with zinc shavings at 450 °C for 30 min (Coleman *et alii*, 1982); later sample aliquots were reacted with powdered chromium at 750 °C for 60 s (Nelson and Dettman, 2001). The change in methodology coïncided with the transition to a new mass spectrometer. Multiple samples run using the old instrument and methodology were rerun (for both $\delta\ ^{18}O$ and δ D) on the new instrument to insure that values measured with the new instrument and methodology were identical (within analytical error).

Major-ion chemistry samples were collected in clean, field-rinsed containers; one sample was collected in a 1-L container and left unpreserved, second sample (for metals analysis) of 250 mL was preserved in the field by addition of trace-metal grade nitric acid such that the pH was less than two. Samples were submitted to the Chemistry Laboratory of the New Mexico Bureau of Mines and Mineral Resources (now known as the New Mexico Bureau of Geology and Mineral Resources) for analysis. Most radiocarbon samples were collected via field precipitation, similar to the method described by Clark and Fritz (1997), with approximately 75 L of water

collected at each site. Immediately upon collection, the pH of each sample was raised above 10 by addition of NaOH, carbon was precipitated by addition of $BaCO_3$, and flocculation of the precipitate was enhanced by addition of Percol 156. After being allowed to settle for at least 24 hr, the precipitate was collected and submitted to the Isotope Geochemistry Laboratory of the University of Arizona for determination of ^{14}C activity by scintillation counting (Clark and Fritz, 1997; Polach *et alii*, 1988) and $\delta\ ^{13}C$ by mass spectrometry (Clark and Fritz, 1997). A limited group of samples was collected in 1-L glass containers, then submitted to the Environmental Isotope Laboratory at University of Waterloo or Beta Analytic for extraction of C and analysis via accelerator mass spectrometry (Clark and Fritz, 1997; Jull *et alii*, 2004). ^{3}H samples were collected in 1-L glass containers and submitted to the Rare Gas Laboratory of the University of Rochester or the Isotope Geochemistry Laboratory of the University of Arizona for electrolytic enrichment and determination of ^{3}H activity by scintillation counting (Clark and Fritz, 1997; Hulston *et alii*, 1981). The collection and analysis of dissolved-gas samples is discussed in the "Dissolved-gas methods and results" section of Chapter 3.

Groundwater source areas

Stable isotope data from the mountain ranges surrounding the San Bernardino Valley, valley-floor precipitation, and wells and springs discharging water from the main aquifer are shown in Figure 1-3 (values shown in the plot are provided in Appendix 1). Waters from the Chiricahua Mountains are the most isotopically depleted, as would be expected based on their high elevation (maximum elevation of 2975 m above sea level) compared to the other ranges (maximum elevations above sea level of 1966, 1993, and 1947 m for the Peloncillo, Pedregosa, and Perilla ranges, respectively).

Some Peloncillo waters have undergone significant evaporation (for the sake of clarity, some highly-evaporated Peloncillo waters are not shown in Fig. 1-3), likely

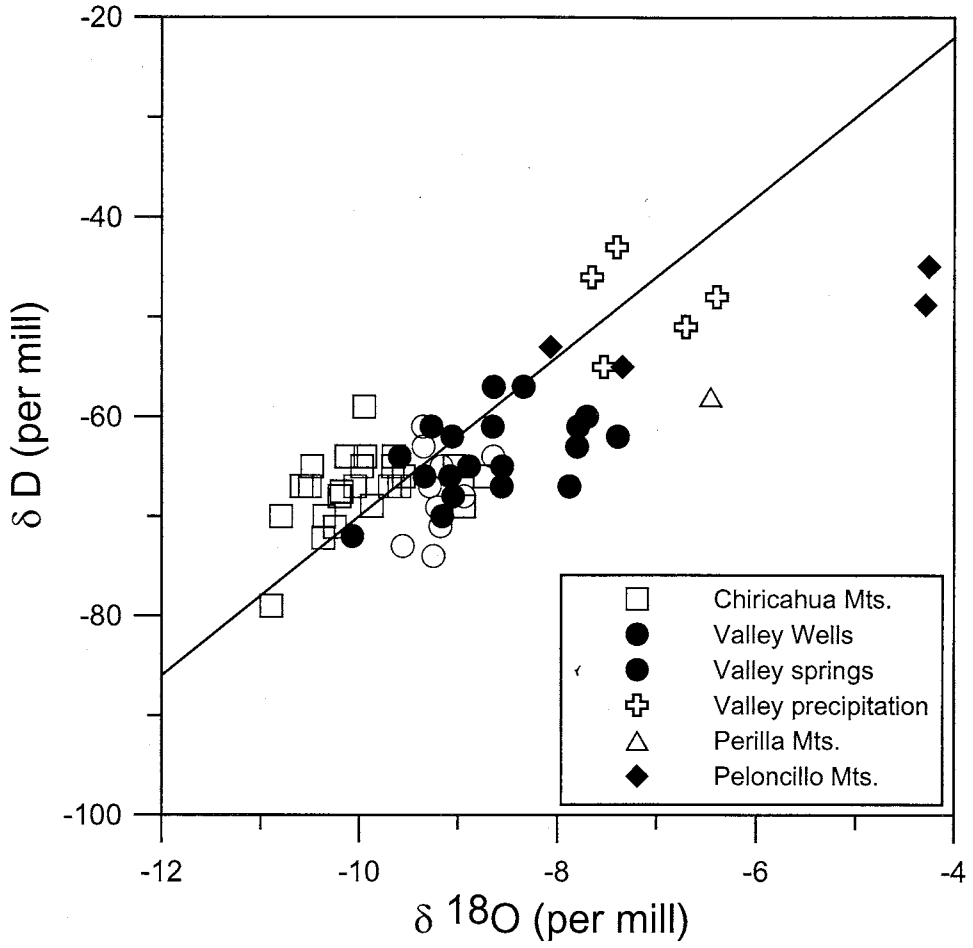

Figure 1-3. Stable isotope content for waters from the San Bernardino Valley and bounding ranges shown with the global meteoric water line. Well waters from the San Bernardino Valley are most closely related to groundwater from the Chiricahua Mountains.

due to the fact that some of the samples were collected during a drought, and, as a result, only stagnant pools were available for sampling rather than flowing spring water. The less-evaporated samples and the intercept of the global meteoric water line and the local evaporation line (the best-fit line for the samples that have undergone evaporation, slope = 3.8) show that Peloncillo waters are slightly lighter than valley-floor precipitation. Only one mapped spring in the Perilla Mountains had water present during sampling, and this water appears to have been affected by evaporation. The assumed signature of the Perilla water prior to evaporation (using the Peloncillo evaporation line slope) is slightly lighter than the Peloncillo waters, overlapping with the most enriched valley spring waters.

Well waters from the main aquifer overlap with the heaviest samples from the Chiricahua Mountains, suggesting that the Chiricahuas are the main recharge area for the aquifer. Two of the main aquifer wells are anomalously enriched; both are located near major ephemeral stream channels that could provide focused recharge of isotopically-heavier valley-floor precipitation that could mix with high-elevation recharge water in the aquifer, thus enriching the isotope signature. With one exception, spring waters from the valley tend to be more enriched than well waters. These springs all emerge in the area where the main aquifer is confined. All the enriched springs appear to have undergone one of two processes to yield the enriched signature: either water has undergone evaporation prior to sampling, or the discharge is a mix between high-elevation recharge that has leaked upward through the confining unit and valley-floor precipitation. Using the mean value of the $\delta\ ^{18}O$ of main aquifer water from wells in the area where the springs are located (near the basin center) of -9.19 ‰, a mean valley-floor precipitation $\delta\ ^{18}O$ of -7.24 ‰, and non-evaporated spring $\delta\ ^{18}O$ values ranging from -9.23 ‰ (given the analytical error for $\delta\ ^{18}O$, a value indistinguishable for the main aquifer water from the area) to -8.37 ‰, mixing calculations show that springs

discharging mixed waters contain a minimum of 60 % main aquifer water, and in some cases, are composed entirely of main aquifer water. No correlation was found between the two enrichment mechanisms and local geology.

Groundwater ages

A set of wells in the basin was selected to approximate a flowpath from the Chiricahua Mountains to the basin center (Figure 1-4). Due to the limitations of available well locations and depths, the approximated flowpath differs from a true flowpath in the x, y, and z directions. The ^{3}H activities (Table 1-1) of all waters on the flowpath approximation suggest that the waters are "submodern" (recharged prior to 1952) using the characterization system described by Clark and Fritz (1997). Because the waters were too old to be dated with tritium, ^{14}C dating appeared to be the most appropriate method for determining groundwater ages. Because reactions such as carbonate dissolution and isotope exchange with the aquifer matrix can affect the ^{14}C activity of water, the computer code NETPATH (Plummer *et alii*, 1991) was used to estimate groundwater ages while taking into account non-decay geochemical processes that have the potential to influence the radiocarbon activity. NETPATH interprets the geochemical reactions that occurred as water moves along a flowpath, based on the changes in molality of the chemical constituents and a set of plausible minerals and gases that could have participated in chemical reactions. For ^{14}C dating, NETPATH uses the mass transfer reactions to calculate a 'corrected' ^{14}C activity, factoring out changes to ^{14}C activity resulting from chemical reactions, and indicating what the ^{14}C activity would be at a given well if radioactive decay were the only process that had affected it. A description of the models used and the calculated mass transfers is provided in Appendix 2).

The NETPATH-calculated ages are shown in Table 1-1. In general, the ages show a logical progression from younger to older as distance along the flowpath

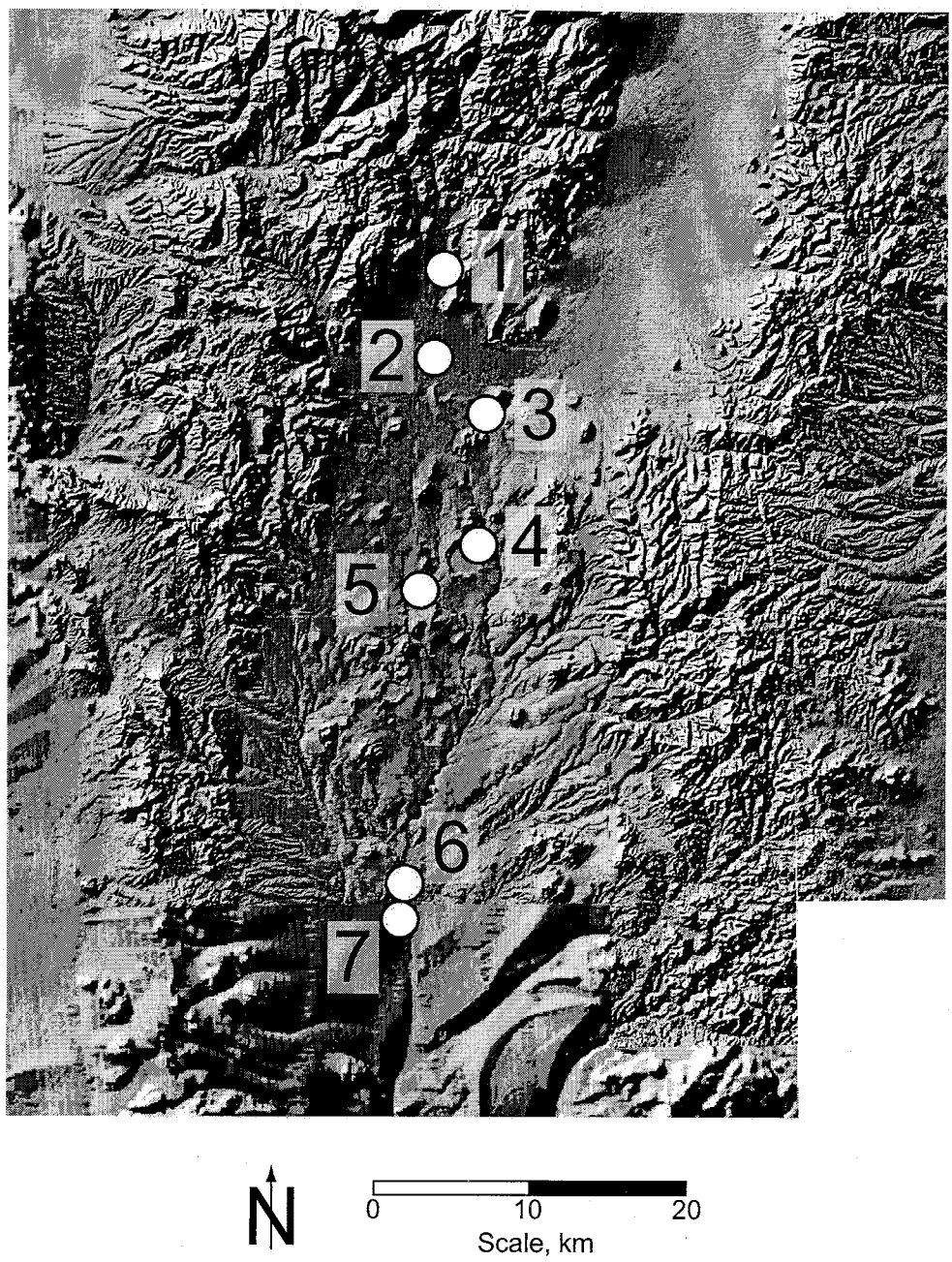

Figure 1-4. Locations of wells used to approximate a flowpath through the basin. Numerals correspond to a given "Flowpath Well" in Table 1-1; low well identification numbers refer to nearest the main recharge area, higher numbers represent increased distance south.

approximation increases, but the age of water in the Gibbons Well (900 yr) is less than the Anderson Well upgradient (1470 yr). This is an artifact of the imperfect nature of the flowpath approximation. The total depth of the Anderson Well is 190 m greater than that of Gibbons Well, and the difference in elevation above sea level for the maximum depth of the two wells is 90 m. The deeper Anderson Well is sampling water from a deeper flowpath than that being sampled by the Gibbons Well; water on the shallower flowpath was recharged more recently than that on the deeper flowpath, causing the apparently anomalous age of the Gibbons Well.

Chemical evolution of groundwater

The chemical signatures of waters from the San Bernardino aquifer are shown in Figure 1-5 (values represented in the plot are provided in Appendix 3). Waters near the main recharge area have chemical signatures similar to those of low-elevation springs in the Chiricahuas that appear to be the main conduits for groundwater recharge to the San Bernardino Aquifer (Earman and Phillips, 2003). As water moves downgradient, the anion signature remains unchanged (HCO_3^--dominated), but the cation signature shifts from Ca^{2+}-dominated to a mixed-ion water, with greatly-increased proportions of Na^+ and Mg^{2+}. Spring waters are similar in chemical composition to well waters, but contain higher proportions of Mg^{2+}.

Processes contributing to the chemical evolution of San Bernardino groundwater are discussed in detail in Chapter 2. The chemical evolution follows two distinct patterns, as shown in Figure 1-6. On the initial portion of the flowpath (wells one through three), there is a linear relationship between HCO_3^- and Ca^{2+}, with increases in HCO_3^- concentration accompanied by increases in Ca^{2+} concentration; on the latter portion of the flowpath, the concentration of HCO_3^- increases without any concomitant increase in Ca^{2+} concentration. On the initial segment of the flowpath, basalts are not present in the basin fill; on the latter portion of the flowpath, basalts

Water Source	pH (field)	Temp (° C)	DO (mg/L)	EC(µS/cm) (field)	Field Alkalinity (mg/L as $CaCO_3$)	pH (laboratory)	EC (µS/cm) (laboratory)	Hardness (CaCO3)	CO_3^{2-} (mg/L)
SBNWR Precip	-	-	-	-	-	-	-	-	-
SBNWR Precip	-	-	-	-	-	-	-	-	-
SBNWR Precip	-	-	-	-	-	-	-	15	0
SBNWR Precip	-	-	-	-	-	-	-	-	-
Flowpath Well 1	7.55	27.4	1.98	250	77	7.40	272	76	0
Flowpath Well 2	7.75	31.8	5.12	395	160	7.70	422	164	0
Flowpath Well 3	7.82	25.2	5.89	310	145	7.80	331	124	0
Flowpath Well 4	8.31	28.6	2.60	336	165	8.30	361	83	0
Flowpath Well 5	8.13	25.0	4.87	341	115	8.20	351	96	0
Flowpath Well 6	7.94	25.8	3.98	429	244	7.60	395	96	0
Flowpath Well 7	7.86	28.8	4.51	544	-	7.50	560	103	0
Astin Spring	8.20	11.5	6.92	440	214	7.80	410	139	0
Goat Tank Spring	-	-	-	-	-	7.30	650	212	0
Headquarters Spring	-	-	-	-	-	7.10	700	242	0
House Spring	8.11	14.7	7.15	465	221	7.70	440	148	0

Table 1-1. Selected water chemistry data from the study and calculated ^{14}C ages for well waters on the flowpath approximation.

Water Source	HCO_3^- (mg/L)	Cl^- (mg/L)	SO_4^{2-} (mg/L)	NO_3^- (mg/L)	F^- (mg/L)	Na^+ (mg/L)	K^+ (mg/L)	Mg^{2+} (mg/L)	Ca^{2+} (mg/L)
SBNWR Precip	-	-	-	-	-	-	-	-	-
SBNWR Precip	-	-	-	-	-	-	-	-	-
SBNWR Precip	0	1.7	1.5	0.55	0.79	2.8	3.2	0.91	4.4
SBNWR Precip	-	-	-	-	-	-	-	-	-
Flowpath Well 1	131	4.4	9.1	1.40	3.10	21.0	2.8	2.00	27.0
Flowpath Well 2	218	5.9	8.0	2.10	2.10	14.0	3.8	6.40	55.0
Flowpath Well 3	170	5.8	5.8	4.60	0.96	12.0	5.7	5.80	40.0
Flowpath Well 4	197	5.0	4.6	5.70	0.62	37.0	7.1	11.00	15.0
Flowpath Well 5	186	6.1	4.8	7.30	0.39	29.0	7.6	13.00	17.0
Flowpath Well 6	255	6.0	10.0	5.50	0.29	58.0	2.6	12.50	18.0
Flowpath Well 7	312	6.2	11.0	4.70	0.44	71.0	6.2	14.00	18.0
Astin Spring	265	7.0	9.0	4.70	0.32	40.0	8.5	21.00	21.0
Goat Tank Spring	345	18.0	30.0	20.00	ND	56.0	12.6	35.00	27.0
Headquarters Spring	375	22.0	38.0	26.00	ND	60.0	14.0	40.00	31.0
House Spring	270	10.0	13.0	4.80	0.27	40.0	11.0	25.00	18.0

Table 1-1 (continued). Selected water chemistry data from the study and calculated ^{14}C ages for well waters on the flowpath approximation.

Water Source	SiO_2 (mg/L)	Calc. TDS (mg/L)	δ D (per mill)	$\delta^{18}O$ (per mill)	^{14}C (pmc)	$\delta^{13}C$ (per mill)	^{3}H (TU)	Calculated age (yr)
SBNWR Precip	-	-	-55	-7.5	-	-	-	-
SBNWR Precip	-	-	-51	-6.7	-	-	-	-
SBNWR Precip	0	16	-43	-7.4	-	-	-	-
SBNWR Precip	-	-	-46	-7.7	-	-	-	-
Flowpath Well 1	112	314	-66	-9.3	35.6	-10.7	<1.1	1470
Flowpath Well 2	94	409	-62	-9.1	43.2	-9.6	<0.8	900
Flowpath Well 3	95	346	-65	-8.9	31.7	-8.6	<0.9	2100
Flowpath Well 4	55	338	-61	-9.3	8.6	-8.3	<1.2	3400
Flowpath Well 5	65	336	-70	-9.2	21.5	-7.6	<1.8	4200
Flowpath Well 6	32	400	-64	-8.6	13.7	-8.3	0.7	5700
Flowpath Well 7	64	508	-67	-9.1	21.4	-7.4	0.5	6400
Astin Spring	28	405	-67	-7.9	-	-	1.16 ± 1.03	-
Goat Tank Spring	32	576	-57	-8.6	-	-	-	-
Headquarters Spring	32	638	-65	-8.6	-	-	-	-
House Spring	21	413	-62	-7.4	-	-	1.83 ± 1.02	-

Table 1-1 (continued). Selected water chemistry data from the study and calculated ^{14}C ages for well waters on the flowpath approximation.

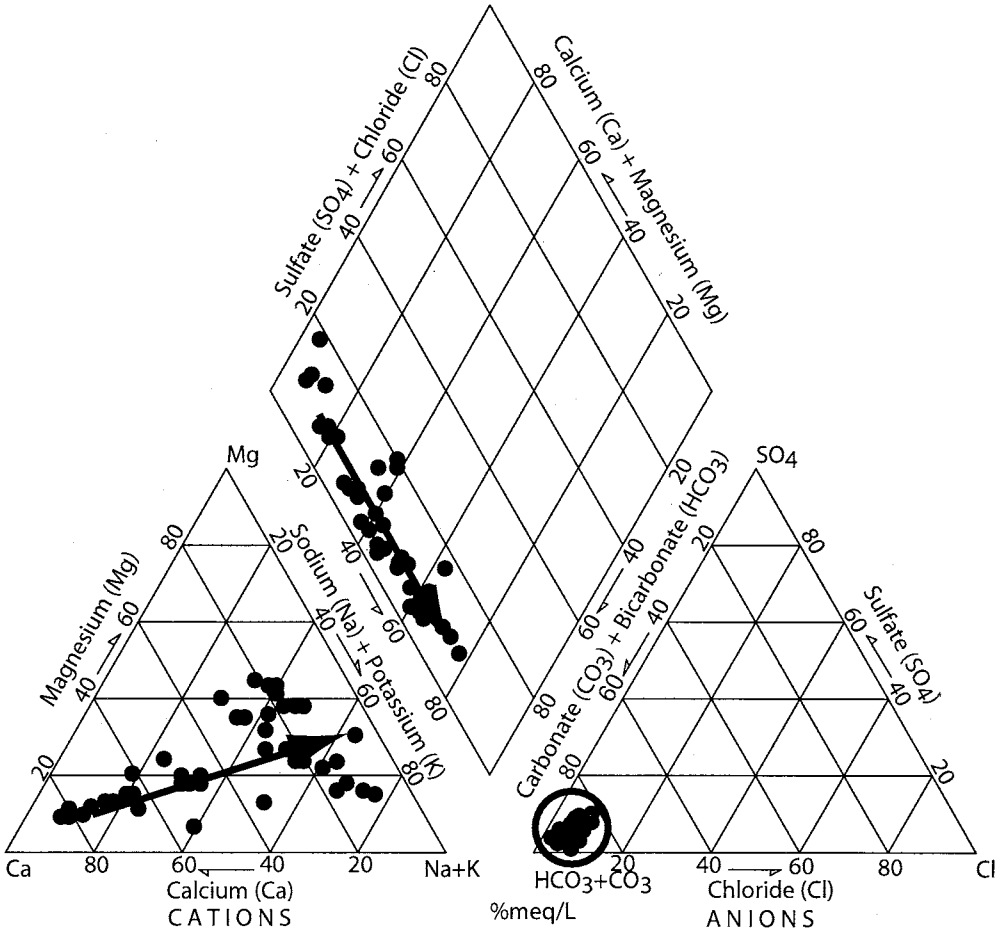

Figure 1-5. Piper diagram showing groundwater chemical evolution in the San Bernardino Valley.

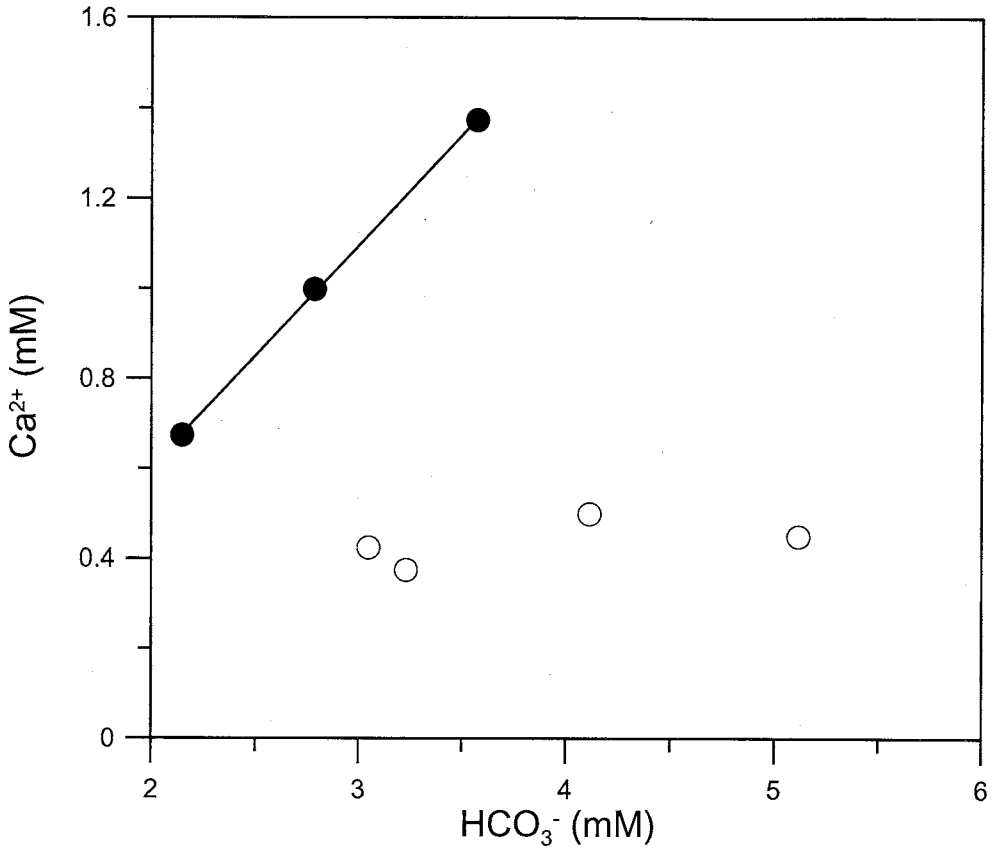

Figure 1-6. Calcium concentration in wells on the flowpath approximation as a function of bicarbonate concentration. Solid symbols represent the first three wells on the flowpath, hollow symbols represent the final four wells on the flowpath.

make up a significant portion of the fill. On the initial portion of the flowpath, the alluvial sediment in the basin fill contains a significant portion of carbonate minerals; on the latter portion of the flowpath, the alluvial sediments are dominated by material derived from rhyolitic tuffs. On the initial portion of the flowpath, where basalts are absent and carbonate minerals are common in the alluvium, incongruent dissolution of calcite and dolomite (producing Ca^{2+}, Mg^{2+}, and HCO_3^-) is the dominant control on water chemistry. For the latter portion of the flowpath, the lithologic makeup (sediments derived from rhyolitic rocks; basalts) suggests that silicate mineral weathering is a major control on chemical evolution (Bowser and Jones, 2002). Indeed, silicate mineral hydrolysis exerts some control on the chemical evolution in the latter portion of the flowpath, but another process (discussed below) acts as an independent control on water chemistry and also promotes the silicate mineral hydrolysis (see Chapter 2).

The relationship between helium isotope ratios in dissolved gas from San Bernardino groundwaters and HCO_3^- concentration is shown in Figure 1-7. The value "R" represents the ratio of ^3He to ^4He for the dissolved gas extracted from a given water sample, and "R_a" is the $^3He/^4He$ ratio of the atmosphere. High values of the ratio R/R_a for $^3He/^4He$ are diagnostic of injection of mantle He (Oxburgh *et alii*, 1986). The observed increase in R/R_a values along the flowpath (Table 1-1) is direct evidence that magmatic gas is being added to the aquifer; CO_2, like He, is commonly associated with magmatic outgassing (Mao *et alii*, 2002; White and Waring, 1963). Input of magmatic CO_2 causes HCO_3^- concentration to increase via two mechanisms—the dissolution of CO_2 followed by conversion to HCO_3^-, and by providing a needed reactant for silicate hydrolysis. The chemical evolution of water in the basin suggests that the rate of weathering increases as PCO_2 increases (see Chapter 2).

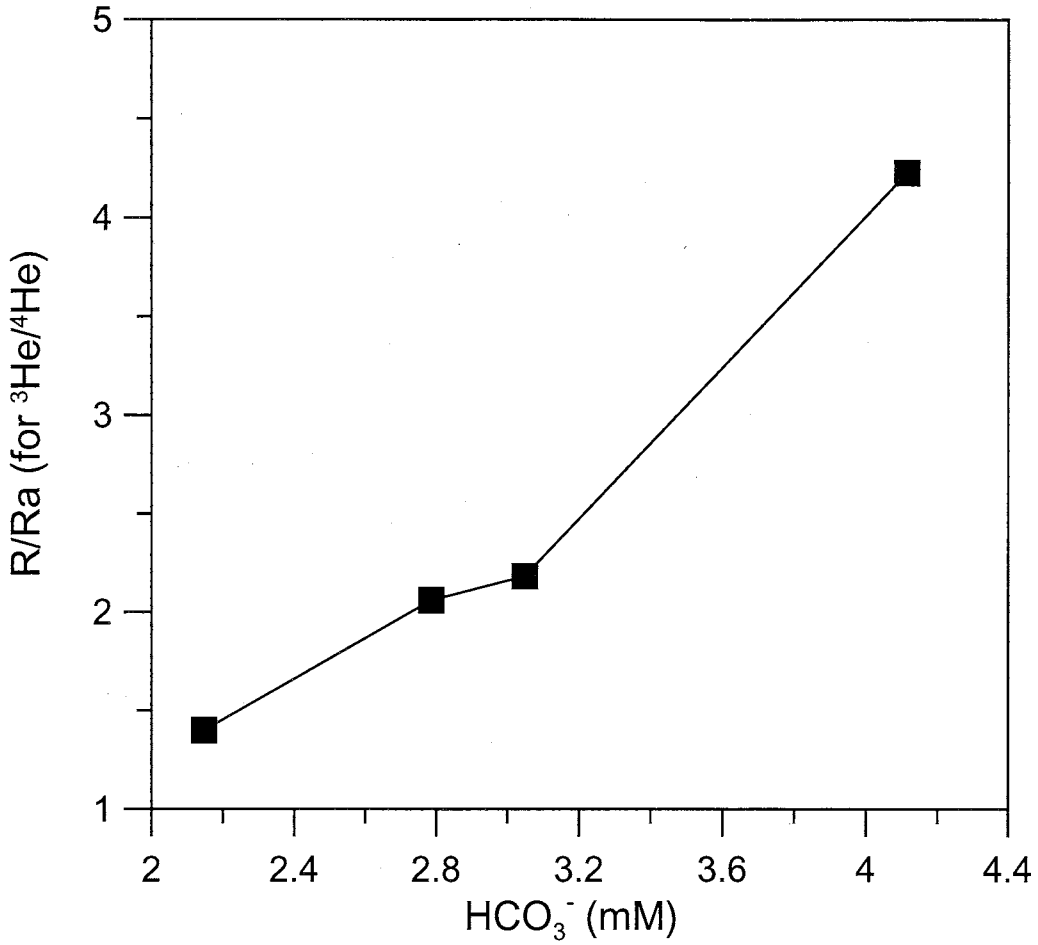

Figure 1-7. Bicarbonate concentration in wells on the flowpath approximation as a function of R/R_a for $^3He/^4He$.

The processes dominating the evolution of water chemistry on both portions of the flowpath act to keep HCO_3^- as the dominant anion. Dissolution of carbonate minerals will increase HCO_3^- concentration without significant increases in other anions, as will silicate hydrolysis (Jones, 1966). Given the pHs of San Bernardino waters, nearly all magmatic CO_2 that dissolves will be converted to HCO_3^-.

Although spring waters have undergone the same processes as well waters, they have elevated concentrations of Mg^{2+} due to contact with valley basalts. Valley-floor springs are present only in the area near the center of the basin. In this area, basalts are present only at relatively shallow depths; the wells in this area yield water from below the depths basalts are present, but spring waters must either have flowed through fractures in the basalts or in close contact with basalts.

Hydraulic conductivity

Hydraulic conductivity values for the San Bernardino aquifer were estimated using several methods, including pumping tests, application of Darcy's Law, and air minipermeametry.

Pumping tests were carried out near the basin center using several flowing artesian wells as "pumping" wells, and observing the changes in head experienced by neighboring wells (Earman *et alii*, 2003). Both drawdown and recovery data were analyzed with AQTESOLV software (HydroSOLVE Inc., 2000) using the Theis method (Batu, 1998). Transmissivity values obtained from analysis of seven pumping tests ranged from 5.3×10^{-4} to 3.6×10^{-3} m^2/s, with an average value of 2.5×10^{-3} m^2/s, and all but one value falling between 1.8×10^{-3} and 3.6×10^{-3} m^2/s. By using an estimated value for aquifer thickness of 275 m (there are no fully-penetrating wells in the area that could be used to obtain an actual value for aquifer thickness; our estimate was based on our structural model of the basin), these values were converted to hydraulic conductivities ranging from 1.9×10^{-6} to 1.3×10^{-5} m/s, with a mean value

of 9.1 x 10^{-6} m/s. Slug tests in the local aquifer in the basin center were conducted by Davis *et alii* (1997), yielding an average conductivity value of 4.9 x 10^{-6} m/s, with low and high values of 5.0 x 10^{-7} and 2.7 x 10^{-5} m/s.

The groundwater ages for the wells along the flowpath approximation were used to determine travel time between pairs of neighboring wells. By assuming a porosity value of 0.25 and the using calculated travel times and the known distances between wells to estimate groundwater velocity, a form of Darcy's Law could be solved for *K*. Values obtained using this method range from 2 x 10^{-6} to 2 x 10^{-4} m/s, with a mean value of 2 x 10^{-5} m/s.

Air minipermeametry (Davis *et alii*, 1994) was performed at several sites in the basin. For each measurement, hydraulic conductivity of the interrogated sediments calculated using the measured permeability, atmospheric conditions at the time of measurement, and the properties of water. Values obtained for *K* range from 5.8 x 10^{-5} to 1.5 x 10^{-3} m/s, with a mean value of 3.0 x 10^{-4} m/s (Earman *et alii*, 2003).

With the exception of the air minipermeameter data, the various methods yield similar values for *K*. There are two likely explanations for the anomalously high values obtained via air minipermeametry. The only known outcrops in the basin that could be tested with the air minipermeameter were either basalts (*K* values too low to be accurately tested) or streamcuts. The fluvial sediments exposed in streamcuts are likely the most permeable deposits in the basin fill. In addition, these surficial deposits have not undergone the compaction and cementation that deeper sediments tested with the other methods have experienced.

Basin hydrogeologic synthesis

Groundwater flux

Darcy's Law was used to calculate groundwater flux across the international border through the main aquifer. The mean transmissivity value from the pumping

tests (2.1 x 10^{-3} m^2/s) was used to account for both the *K* term and the aquifer thickness; the width of the aquifer at the international border (8420 m) and the hydraulic gradient calculated from wells in the border vicinity (3.32 x 10^{-3}, based on a head difference of 7.7 m, and a horizontal separation of 2321 m) were also used. The flux was calculated to be 2 x 10^5 m^3/yr, reasonably comparable to the two known prior estimates of 6.8 x 10^6 and 6.2 x 10^5 m^3/yr (Anderson *et alii*, 1992; Hawley *et alii*, 2000). Upward flux from the main aquifer to the local aquifer across the local confining unit is estimated to be 4 x 10^3 m^3/yr, based on an area of 9.8 x 10^7 m for the confining clays, a measured hydraulic gradient of 0.25 between the main aquifer and the local aquifer, and a confining unit hydraulic conductivity of 5 x 10^{-12} m/s (the modal conductivity value for clay reported by Freeze and Cherry, 1979). No attempt was made to estimate discharge via wells or springs, but the sparse population and limited use of most wells in the basin and the low discharge of most springs suggests that this value is small compared to the trans-boundary discharge. As a result, the trans-boundary flux represents a low-end estimate of annual recharge for the basin.

Groundwater recharge areas

A mass-balance calculation (described in Appendix 4) was used to estimate the proportion of groundwater derived from the Chiricahuas and the other bounding ranges, assuming the San Bernardino groundwater was composed of a mix of precipitation from the Chiricahuas and the other bounding ranges. The mean $\delta^{18}O$ of the Chiricahua groundwaters (-9.97 ‰) was used as one end member of the mix. A $\delta^{18}O$ of -7.99 ‰ was used for the other ranges. This value was based on the intersection of the evaporation line for the Peloncillo groundwaters with the global meteoric water line. Due to dry conditions during field work, only one sample from the Perilla and Pedregosa ranges was obtained; this sample appears to have undergone significant evaporation, and may also have been affected by fractionation due to

freezing. Because reliable values from the other ranges were not available, and these ranges have are essentially the same elevation as the Peloncillos, the Peloncillo value was used as representative for all three ranges. Given the mean $\delta^{18}O$ value of San Bernardino groundwaters (-9.29 ‰), mass balance calculations suggest that 66 % of the recharge to the main aquifer is derived from the Chiricahua Mountains, with the other ranges providing 34 %. Valley-floor precipitation appears to be of importance only in limited zones of the basin where focused recharge can occur; even in these zones, it is less important than water that originated as precipitation falling on the bounding mountain ranges.

Groundwater recharge elevations and sources

Stable isotope data indicate that the Chiricahuas are the main recharge area for the San Bernardino aquifer. Comparing stable isotope content of spring water to the spring orifice elevation yielded a general trend of isotopically-lighter waters at higher elevations, but the correlation was poor ($r^2 = 0.18$). As shown in Figure 1-8 (values represented in the plot are provided in Appendix 5), comparing the stable isotope content of spring water to the maximum recharge elevation for that spring (the highest elevation in the surface drainage in which the spring is located) and removing three 'outlier' values from the original data set ($n = 23$) yielded a much better correlation ($r^2 = 0.68$). As indicated by the elevation associated with the mean Chiricahua groundwater of -9.29 ‰ on the best-fit line in Figure 1-8, San Bernardino groundwater signatures to this isotope-elevation relationship would suggest that precipitation that falls at about 2300 m is the main source of recharge for the basin waters. However, groundwater in the basin is derived not only from the Chiricahuas, but the other bounding ranges, which yield water with heavier isotope signatures due to their relatively elevation. In addition, most basin groundwaters appear to have been influenced by evaporation at some point prior to sampling, possibly during

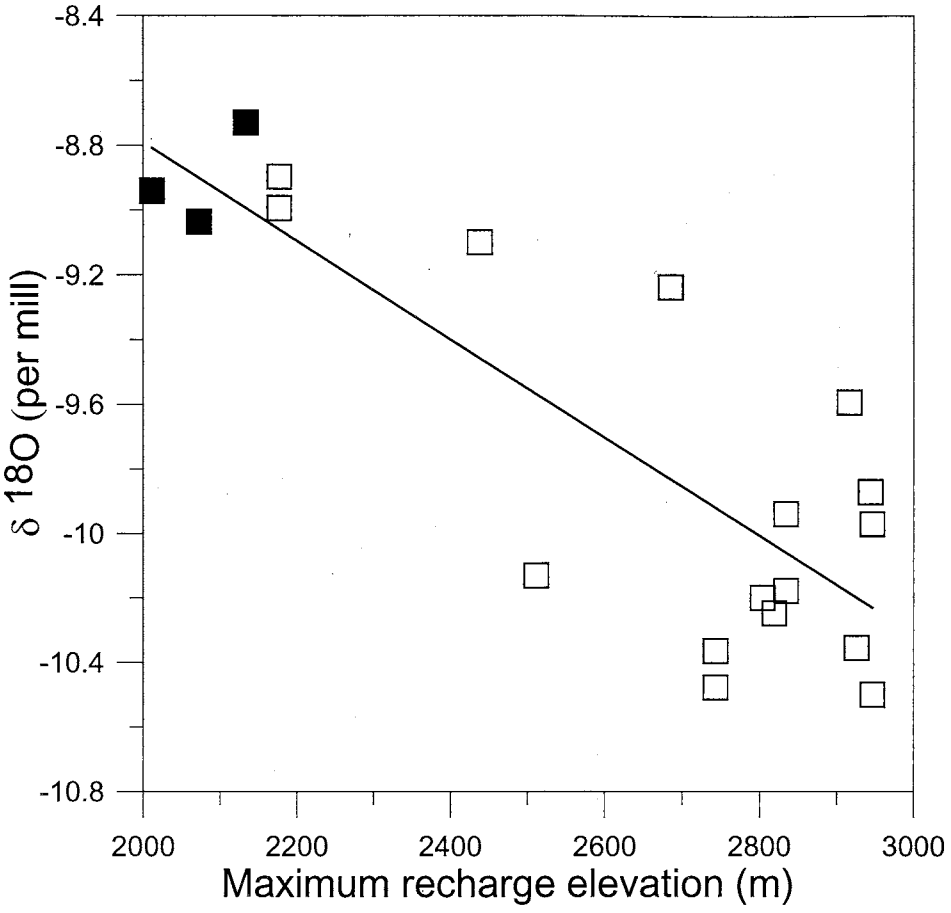

Figure 1-8. $\delta\ ^{18}O$ as a function of recharge elevation for springs in the Chiricahua Mountains. Cottonwood Corral, Krentz, and Sycamore Springs are represented with filled symbols, springs not showing a distinct evaporative signature are represented with open symbols.

the "re-recharge" process, whereby groundwater recharges at high elevation in the range, discharges at some point, experiences evaporation during overland flow, and subsequently infiltrates and becomes recharge (see Chapter 3). These facts suggest that the value of 2100 m is a minimum, as most water supplied from the Chiricahuas probably falls at higher elevations.

The relationship between season and isotope content of precipitation at a given location is well recognized, and has been used often been used to estimate the proportion of recharge derived from snowmelt and rain (e.g. Mariner and Nimz, 2000; Maulé *et alii*, 1994). Using snow and rain isotope compositions (Figure 1-9; the $\delta\ ^{18}O$ of the fresh snow ellipse centroid is -13.85 ‰, the $\delta\ ^{18}O$ of the fresh rain ellipse centroid is -7.35 ‰) as end members for a two-component mixing model suggests that groundwater in the San Bernardino aquifer (mean $\delta\ ^{18}O$ of -9.29 ‰) is composed of approximately 30 % snowmelt and 70 % rain. Although this proportion may seem reasonable in light of the proportions of water-equivalent that fall as rain and snow at 2700 m in the Chiricahuas (approximately 25 % snow and 75 % rain, assuming 10 % water equivalent for snow), snowmelt is probably more important to the recharge process than the proportion of precipitation composed of snow suggests. Most rain in this area falls in relatively brief but intense monsoonal storms during the summer, while infiltration from snowmelt occurs as a fairly uniform pulse in the spring. This allows wetting of the soil to be followed by further infiltration in the case of snowmelt, while the soil will dry between rain events. In addition, the input of water from snowmelt occurs when potential evapotranspiration is low, because temperatures are cool and vegetation is dormant; rainfall occurs when temperatures are high and vegetation is active, leading to high potential evapotranspiration. The reason that the mass balance calculation using fresh snow and fresh rain for end members suggests a relatively low proportion of snowmelt in groundwater recharge is that it does not take

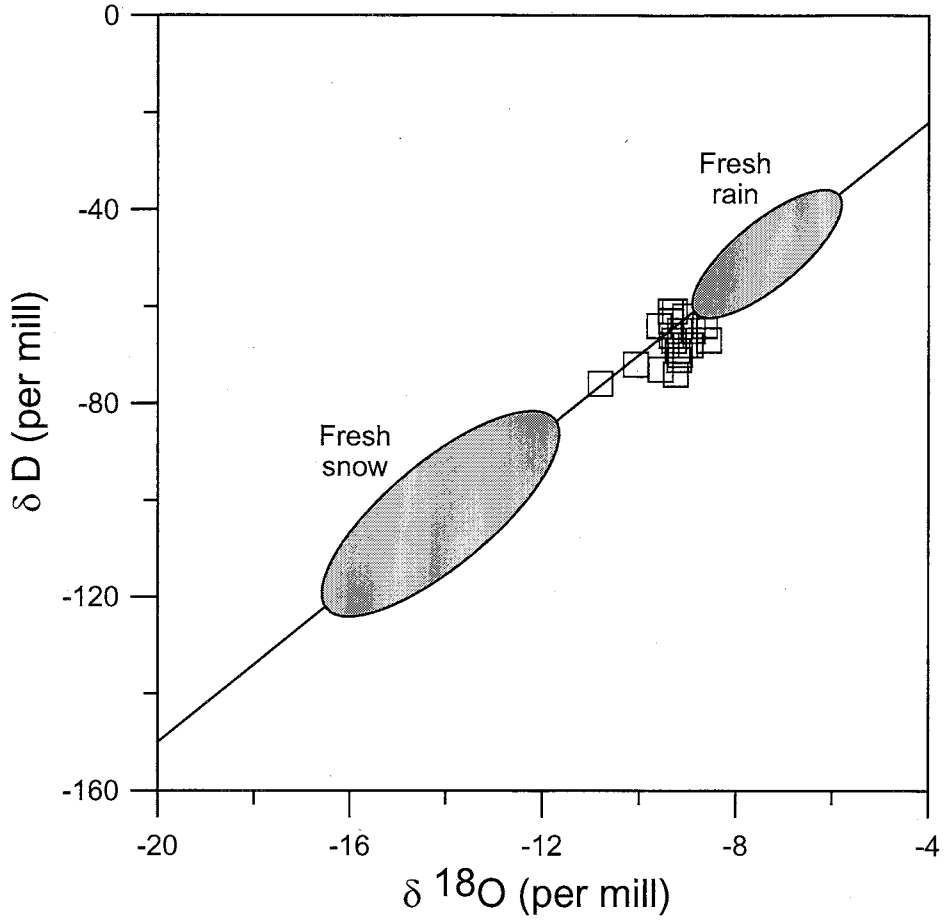

Figure 1-9. Stable isotope values of spring waters from the Chiricahua Mountains, shown with the global meteoric water line. Ellipses represent ranges of values for of fresh snow and fresh rain near the crest of the range during the study period.

into account the isotopic alteration of snow prior to and during melt. As described in Chapter 4, this alteration makes the bulk melt water isotopically heavier than the snow from which it is derived, and accounting for this alteration can lead to significant increases in the proportion of snowmelt in groundwater recharge. Based on samples of altered snow collected during this study, the proportion of snowmelt in the San Bernardino recharge appears to be about 60 %, with rain accounting for the remaining 40 % (see Chapter 4).

IMPLICATIONS

The San Bernardino Valley has four neighboring basins in the USA (Figure 1-1). These basins were all formed by Basin-and-Range extension, and the highlands bounding them are mineralogically similar to those bounding the San Bernardino Valley. Based on the similar modes of formation, ages, and source materials for the basins' fill, one might expect groundwater quality and chemical evolution to be similar in the San Bernardino Valley and its neighboring basins. In fact, while groundwater chemical evolution in the four neighboring basins is similar, the chemical evolution of San Bernardino groundwater is distinct (Figure 1-10). The major differences are related to tectonics and the presence of the accommodation zone in the San Bernardino Valley (none of the neighboring basins contain an accommodation zone). These differences and their relation to the accommodation zone are discussed below.

Influence of basin-fill thickness

The thickness of basin fill in the San Bernardino Valley is low compared to that in neighboring basins—the maximum thickness of basin fill in the San Bernardino Valley is 781 m, while the average thickness of basin fill in southeastern Arizona is 1600 m (Scarborough and Peirce, 1978). The thin basin fill in the San Bernardino Valley is the result of crustal buoyancy produced by magmatism associated with the accommodation zone. While the neighboring basins experienced significant

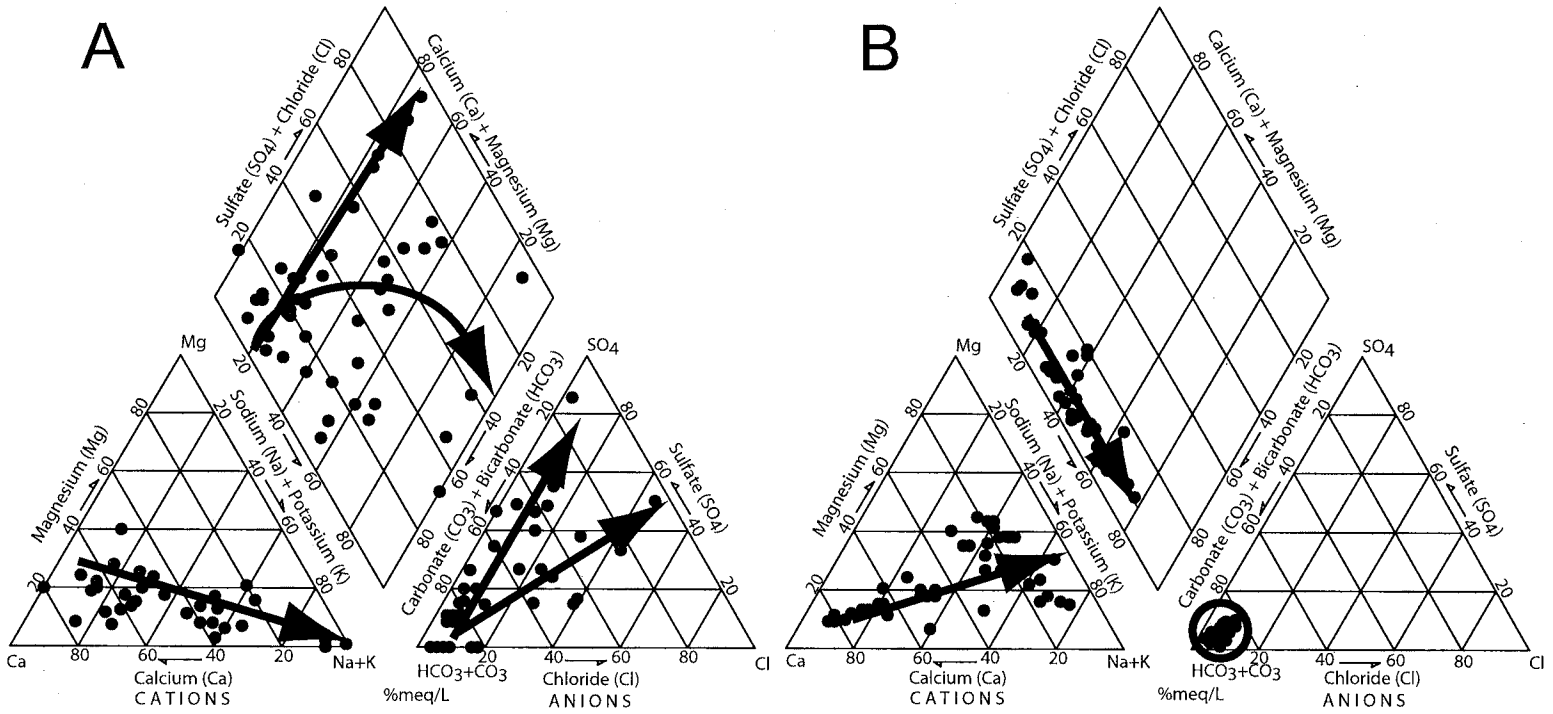

Figure 1-10. Piper diagrams showing the chemical evolution of waters in the neighboring basins (plot A) and the San Bernardino Valley (plot B).

subsidence and infilling during the Oligocene and early/mid-Miocene (Drewes, 1981), this buoyancy inhibited subsidence in the San Bernardino Valley.

Thick basin fill allows deep groundwater circulation; water moving along a deep flowpath typically has a longer aquifer residence time than water moving along a shallow flowpath. Increased residence time allows for increased water-rock interaction, and thus higher levels of dissolved solids. Although values of total dissolved solids (TDS) content of groundwaters are not available for all the neighboring basins, electrical conductivity (EC) is typically representative of TDS, and EC values are available. The maximum value measured in the San Bernardino Valley (1410 μS/cm) is significantly lower than the maximum values measured in neighboring basins, which range from 2380 to 7800 μS/cm (Barnes, 1991; Hawley *et alii*, 2000; Oram III, 1993; Rascona, 1993; Schwab, 1992).

Although dissolution of evaporites is a contributing factor to elevated ECs in the neighboring basins, evidence supports the concept that long residence times are a significant factor in controlling the ECs of groundwaters in the neighboring basins. Groundwater ages for the San Bernardino Valley show that waters in the basin center are approximately 6500 yr old. For basins in southeastern Arizona with fill depth similar to the neighboring basins, reported maximum ages range from "greater than 12,000 years" (Robertson, 1991) to 14 600 yr (Campana, 1987). Smalley (1983) reports ^{14}C values for groundwater in the Gila sub-basin of the Safford Basin, but does not report ages based on these data. The data were analyzed using the method of Fontes and Garnier (1979), and found the maximum groundwater age was in excess of 20000 yr. In general, groundwater in alluvial aquifers of southeastern Arizona basins is of the same age range seen in the San Bernardino Valley if the water has experienced only shallow circulation; waters that have experienced deep circulation are older (Eastoe, C., University of Arizona, personal communication, 2003).

Influence of recent tectonic activity

Although crustal buoyancy due to magmatism associated with the accommodation zone kept subsidence to a minimum in the San Bernardino Valley during the Oligocene and early/mid-Miocene, tectonic activity has since increased, and the basin is more tectonically active than the neighboring basins. The most dramatic evidence is an 1887 earthquake (estimated Richter magnitude 7.2) along the Pitaycachi fault on the eastern margin of the basin in Mexico (DuBois and Smith, 1980). Lynch's (1972) observations of trenched alluvial fan deposits in the Chiricahuas are evidence of present-day uplift along the mountain-front fault in the USA portion of the basin; Pearthree (1986) indicates that the San Bernardino Valley has been among the most tectonically active in southeastern Arizona during the late Quaternary, and describes significant fault scarps in the Chiricahuas as being between three and ten thousand years old.

The vast majority of subsidence in the San Bernardino Valley has taken place within the last 10 Myr, a period in which the neighboring basins have been relatively inactive (Morrison, 1991). Due to this tectonic activity, stream downcutting appears to have been more active in the San Bernardino Valley in recent geologic time than in the neighboring basins. The neighboring basins all had lakes during the last glacial maximum (LGM) (Barnes, 1991; Coates and Cushman, 1955; Long, 1966; Waters, 1989), but detailed mapping in the San Bernardino Valley (Biggs *et alii*, 1999) shows no evidence of a lake being present during that time (lithologic logs suggest the presence of a lake or lakes prior to the LGM).

All of the neighboring basins contain evaporite deposits (Coates and Cushman, 1955; Cushman *et alii*, 1947; Schreiber, 1978; Spiegel, 1957). The San Bernardino Valley has no known evaporites, as indicated by the mapping of Biggs *et alii* (1999) and borehole lithologic data. This difference in the types of minerals present affects

water chemistry. Waters in the San Bernardino Valley, where no evaporites are found, have HCO_3^- as the dominant anion in all parts of the basin (in part due to the injection of magmatic CO_2 described earlier, but also due to the absence of any significant contributor of Cl^- or SO_4^{2-}). In the neighboring basins, HCO_3^- loses dominance to some combination of Cl^- and SO_4^{2-} as water interacts with halite and gypsum (Figure 1-10).

Presence of basalts as a major component of basin fill

Basalts associated with the accommodation zone are ubiquitous in the basin fill of the northern portion of the San Bernardino Valley, but are not significant components of the fill in neighboring basins. This is important to groundwater quality because basalts are a significant source of magnesium. The alluvial fill material in neighboring basins is mineralogically similar to that interbedded with the basalts in the San Bernardino Valley—it is derived from mountain ranges that are predominantly composed of rhyolitic/granitic rocks and some sedimentary units. These sedimentary rocks do contain some dolomites (which could provide Mg^{2+}), but dolomites are a minor component compared to limestone, sandstone, and siltstone. As a result, neighboring basins do not have large magnesium sources in their basin fill.

Groundwaters in the neighboring basins tend to develop cation signatures dominated by Na^+, with little discernable influence from Mg^{2+} (Figure 1-10). As groundwater moves through the San Bernardino Valley, Na^+ increases, but Mg^{2+} exerts a strong influence on the cation signature.

Injection of magmatic CO_2

As described earlier, groundwater chemistry in the San Bernardino Valley is influenced by the injection of magmatic CO_2 associated with the accommodation zone. In addition to affecting the present-day water chemistry, this has implications for the types of evaporite minerals formed. If evaporated, groundwaters from the center of the San Bernardino Valley will yield a suite of minerals dominated by Na-CO_3 minerals

(mainly trona), while groundwaters from the centers of the neighboring basins would yield more typical evaporite mineral assemblages, dominated by some combination of carbonates, gypsum, and sulfate (see Chapter 2).

The difference in evaporite minerals can be explained using the Hardie-Eugster model of evaporite formation (Hardie and Eugster, 1970). Calcite is typically the first mineral to form upon evaporation, and it will precipitate until the supply of either Ca^{2+} or $CO_3^{2-}{}_{TOT}$ (the sum of concentrations of $H_2CO_3^*$, HCO_3^-, and CO_3^{2-}), is exhausted. The termination of calcite precipitation is referred to as a 'chemical divide,' because which of the two components of calcite is depleted will influence the types of minerals that will form upon subsequent evaporation. If, for instance, Ca^{2+} is depleted from the water, subsequent precipitation of gypsum is not possible. Conversely, if $CO_3^{2-}{}_{TOT}$ is depleted, Na-CO_3 minerals will not form.

The ratio of calcium to carbonate in the groundwaters is the difference between the San Bernardino Valley and its neighboring basins—San Bernardino groundwaters have a 'surplus' of HCO_3^- compared to those found in the neighboring basins. This surplus is partly due to dissolution of magmatic CO_2, and partly due to silicate hydrolysis, which appears to increase in importance as PCO_2 is increased by magmatic CO_2 input (see Chapter 2).

Other influences of tectonic processes

Tectonic processes have likely affected other aspects of groundwater flow in the San Bernardino Valley that may not manifest themselves geochemically. Fundamental differences in basin hydraulics are likely to result from different tectonic regimes. One physical difference between the San Bernardino Valley and the neighboring basins that has already been mentioned is the different depths of circulation related to different basin thicknesses. In addition to affecting water

residence time, the thin basin fill in San Bernardino Valley means its aquifer has lower storativity than those in the neighboring basins (assuming similar porosities).

Another apparent difference is the average value of hydraulic conductivity in the basins. While the San Bernardino Valley does have a zone in the basin center with finer-sized particles than the surrounding fill, the clay units present are relatively thin compared to those in the centers of the neighboring basins, and not as large in area (Coates and Cushman, 1955; Cushman *et alii*, 1947; Schwennesen, 1919). The alluvial aquifer of the San Bernardino Valley, with a relatively small amount of fine-grained material in the basin center likely has higher average hydraulic conductivity than the neighboring basins which contain large, thick packages of fines.

CONCLUSIONS

Several major hydrologic properties (including chemical evolution of water, dissolved-ion concentration, storativity, and water residence time) of the San Bernardino Valley aquifer differ markedly from those of its neighboring basins, even though all the basins have common ages and modes of formation, and are bounded by highlands of similar lithology. The San Bernardino Valley has hydrologic properties distinct from those of its neighboring basins because its geology is unique when compared to that of the neighboring basins; all the major geologic differences are due to the presence of a magmatically-active accommodation zone. Important influences associated with the accommodation zone include extensive basaltic volcanism, thin basin fill due to crustal buoyancy, and recent tectonic activity increasing stream downcutting, making San Bernardino an externally-drained basin. These facts lead us to propose that other basins with magmatically-active regional segmentation boundaries may have hydrologic properties distinct from their neighbors, and that resultant differences in water chemistry can drive the formation of different evaporite minerals. The geological differences and the resultant chemical differences between

the San Bernardino Valley and its neighboring basins may serve as a model for how chemical evolution of groundwater in other magmatically-active accommodation-zone basins differs from that of their neighbors.

Chapter 2: The role of "excess" CO_2 in the formation of trona deposits

INTRODUCTION

Deposits of trona [$Na_3(CO_3)(HCO_3)\cdot 2(H_2O)$, a non-marine evaporite mineral] are relatively uncommon compared to many other evaporites, such as gypsum and halite. For instance, in Nevada, there are 26 significant deposits of gypsum and 15 of halite, but only two that yield trona (a third yields gaylussite [$Na_2CO_3CaCO_3\cdot 5(H_2O)$](Papke, 1976; Papke, 1987). Smoot and Lowenstein's (Smoot and Lowenstein, 1991) compilation of non-marine evaporite deposits and brine lakes confirms that trona deposits and lakes that would yield trona upon evaporation are relatively rare throughout the world. The prevailing theory for the formation of trona deposits is the evaporative concentration of waters that have high proportions of Na^+ and HCO_3^-; these waters are assumed to have derived high Na^+ and HCO_3^- due to silicate hydrolysis of high-Na^+ granitic/rhyolitic rocks (or sediments derived from these rocks) (Jones, 1966).

The critical control on the precipitation of trona is the relative amount of Ca^{2+} and $CO_3^{2-}{}_{TOT}$ ($[CO_3^{2-}] + [HCO_3^-] + [H_2CO_3^*]$, where bracketed symbols refer to concentration) in the water to be evaporated. According to the Hardie-Eugster model of evaporite formation (Hardie and Eugster, 1970), the first mineral to form from an evaporating water is calcite, and calcite precipitation continues until either Ca^{2+} or CO_3^{2-} is exhausted. Waters with a low proportion of $CO_3^{2-}{}_{TOT}$ relative to Ca^{2+} will be carbonate-depleted after calcite formation, and will thus not yield sodium carbonate minerals upon further evaporation, so a high proportion of $CO_3^{2-}{}_{TOT}$ relative to Ca^{2+} is a major requirement for the formation of significant quantities of sodium carbonate minerals.

Differences in ionic composition of water between different drainage basins are usually ascribed to differences in basin lithology. Weathering reactions release different proportions of the major ions when acting on differing mineral assemblages.

Weathering reactions on granitic/rhyolitic rocks are typically invoked as the pre-condition for trona deposition because of the low ratio of Ca^{2+} to $CO_3^{2-}{}_{TOT}$ that they produce. Silicate hydrolysis (described in greater detail in a later section), a weathering processes that acts on silicate minerals, has products that include HCO_3^- and cations. The cations produced in a silicate hydrolysis reaction depend on the cations in the mineral being weathered. For instance, minerals with high Na content would tend to yield Na^+ when subjected to hydrolysis. Granitic and rhyolitic rocks are composed primarily of K-feldspar, quartz, and Na-plagioclase, with generally little calcium. Therefore, hydrolysis of granitic and rhyolitic rocks will yield HCO_3^-, Na^+, and K^+, but little or no Ca^{2+}. As a result, waters that have their chemistry controlled by silicate hydrolysis of granitic/rhyolitic rocks will have $HCO_3^- >> Ca^{2+}$.

Given the relative frequency of the conditions necessary for trona deposition according to the generally-accepted model (closed drainage basins dominated by granitic/rhyolitic lithology), the uncommonness of trona-forming lakes and trona deposits (Smoot and Lowenstein, 1991) is surprising. During an investigation of groundwater in southeastern Arizona, it was determined that water in the San Bernardino Basin (Figure 2-1) would produce evaporites dominated by sodium carbonate minerals. Surrounding basins, however, would produce evaporites dominated by the much more common calcite, halite, and gypsum. The observation that the San Bernardino Basin does not contain significantly more granitic/rhyolitic rocks than the surrounding basins makes the unusual (calculated) evaporite assemblage even more anomalous. Therefore, the geochemical evolution of groundwater in the

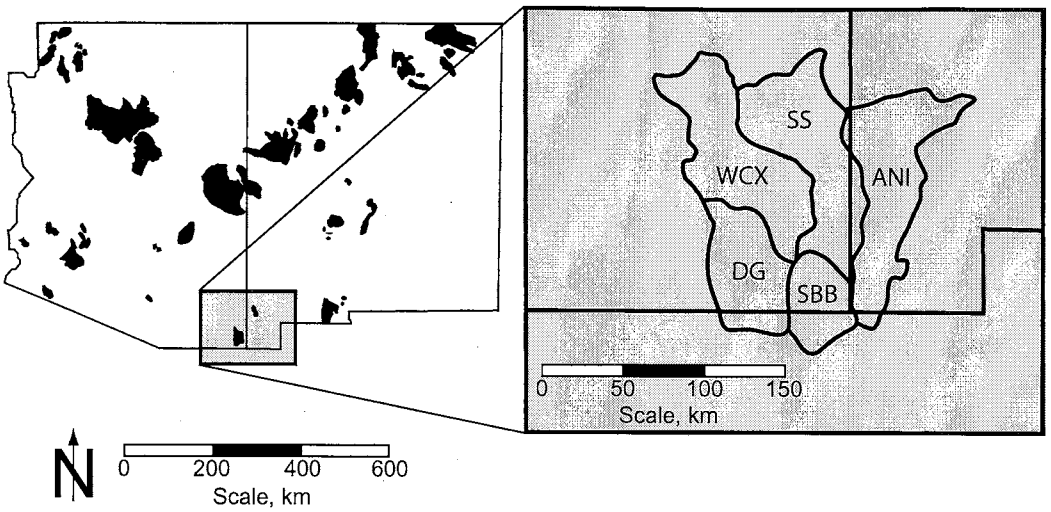

Figure 2-1. Location of the San Bernardino Basin and neighboring basins in Arizona and New Mexico, USA and Sonora, Mexico. SBB: San Bernardino Basin; DG: Douglas Basin; WCX: Willcox Basin; SS: San Simon sub-basin of the Safford Basin; ANI: Animas Basin. Areas of significant Cenozoic volcanism are shown in black on the index map (after Aldrich and Laughlin, 1984).

San Bernardino Basin should be examined in detail to determine if it can yield clues to the more general conditions necessary for trona deposition.

General geologic setting

The San Bernardino Basin is surrounded by four neighboring basins in the USA: the Douglas, Willcox, San Simon, and Animas Basins (Figure 2-1). These five basins all formed due to extension associated with Basin and Range tectonism beginning in the early Oligocene (Drewes, 1981), with intermittent activity continuing through the present (Lynch, 1972). The bounding ranges of the San Bernardino Basin are predominantly composed of rhyolitic rocks, but also contain sedimentary rock (mostly carbonates, but also siltstones and sandstones) (Drewes, 1980). The neighboring basins are bounded by highlands with mineral assemblages similar to that of the San Bernardino Basin (in some cases, the basin-bounding ranges contain granite instead of rhyolitic tuff or rhyolite, but there is always a mix of rhyolitic tuff/rhyolite/ granite and sedimentary units that are primarily composed of carbonates) (Figure 2-2). The majority of the San Bernardino Basin's surface north of the international border is covered by the basalts of the Geronimo volcanic field (Kempton and Dungan, 1989; Lynch, 1972), and basalt interbeds are a major part of the basin fill, the remainder of which is composed of sediments derived from the surrounding highlands. Over most of the USA portion of the basin, the San Bernardino alluvium contains one (unconfined) aquifer. Near the center of the basin, the main aquifer is confined by a clay unit, atop which a local (unconfined) aquifer exists. In this report, all references to the San Bernardino aquifer and water contained therein will deal with the main aquifer.

Based on similarities in age, mode of formation, geographical location, and source material for basin fill, one might expect water quality (and thus the suite of evaporite minerals that would form via evaporation of this water) in all five basins to

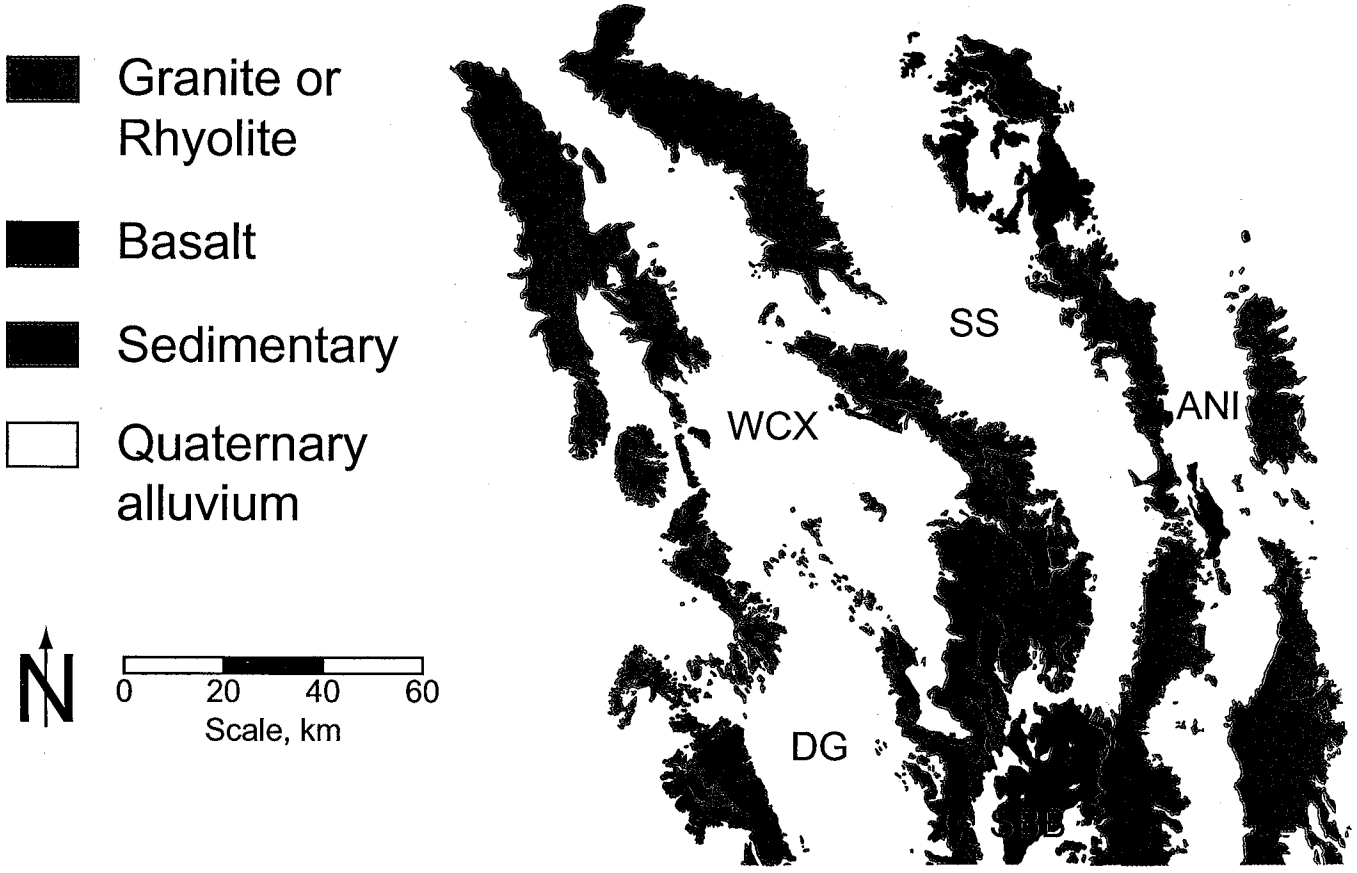

Figure 2-2. Generalized geologic map showing lithology of the San Bernardino Basin, its neighboring basins, and their bounding ranges (after Anderson *et alii*, 1997; Hirschberg and Pitts, 2000). The area covered by the map is bounded by latitudes 31° 40' N and 33° N and longitudes 108° 30' W and 111° W.

be similar. In fact, while the first four traits are similar for the San Bernardino Basin and its neighboring basins, the San Bernardino Basin's groundwater chemistry and potential evaporite mineral suites are distinct.

One significant difference between the San Bernardino Basin and the neighboring basins is that the San Bernardino Basin experienced significant basaltic volcanism in the Cenozoic, while the neighboring basins either have no basalts present or contain small amounts of basalt relative to the San Bernardino Basin. The Douglas and Animas Basins both contain small amounts of basalt; those in the Animas Basin appear to be related to those in the San Bernardino Basin based on age and chemical composition, but the Douglas basalts appear to be unrelated (Lynch, 1972).

Evaporite mineral suites

The computer code SNORM (Bodine and Jones, 1986) was used to determine what minerals would be formed if groundwaters from San Bernardino and its neighboring basins were evaporated. SNORM calculates the normative equilibrium mineral assemblage that would precipitate from an aqueous solution due to complete evaporation at atmospheric partial pressure of CO_2 and standard temperature and pressure. SNORM does not directly simulate the evaporation process, which would involve simulating the removal of pure water (and thus raise issues such as estimating ion activity at extremely high concentrations, and accounting for a number of possible brine-solid interactions). Instead, SNORM calculates the evaporite mineral assemblage that would form upon evaporation based on the observed solute concentrations of a water sample, distributing the solutes into the correct liquid-free mineral assemblage. The distribution is based on observed low-temperature mineral groups, the Gibbs Phase Rule, and available free energy values (Bodine and Jones, 1986). Chemical data from a representative well near the center of San Bernardino and each of its neighboring basins were used as input (Table 2-1); no other data are

Ion	Animas	Douglas	San Simon	San Bernardino	Willcox
Mg^{2+}	19.0	212.0	48.6	14.0	15.0
Ca^{2+}	32	380	361	18	180
Na^{+}	145	960	570	71	160
K^{+}	7.0	6.0	5.0	6.2	3.8
F^{-}	1.90	0.80	NR	0.44	NR
Cl^{-}	49.0	1790	425	6.2	44.0
NO_3^{-}	2.4	4.2	3.0	11.0	12.0
HCO_3^{-}	209	249	366	312	320
SO_4^{2-}	231	1140	1585	11	490

Table 2-1. Concentrations of major ions in representative wells near the centers of San Bernardino Basin and its neighboring basins. All values are in units of mg/L; NR = not reported. Data for basins other than San Bernardino are from Coates and Cushman (1955), Barnes (1991), Reeder (1957), and Towne and Freark (2001).

needed for SNORM to function. For San Bernardino, data from our study were used; for the neighboring basins, values from the literature were used. The results (Figure 2-3; values shown in the plot are provided in Appendix 6) show that waters from the center of the San Bernardino Basin would yield an evaporite assemblage dominated by trona (approximately 60 % trona and 3 % burkeite [$Na_6(CO_3)(SO_4)_2$] by mass); representative waters from the neighboring basins would yield some combination of calcite/dolomite, halite, and gypsum/anhydrite. Of the neighboring basins, only some Animas waters would yield any Na-CO_3 minerals (other waters from near the basin center would not yield Na-CO_3 minerals), but no trona. The combined proportion of burkeite and pirssonite [$Na_2Ca(CO_3)_2 \cdot 2(H_2O)$] in the evaporite mineral assemblage for Animas (a maximum of seven percent by mass, shown in Figure 2-3) is far less than in San Bernardino; the Animas assemblage is, as with the other neighboring basins, dominated by calcite, halite, and gypsum.

To examine what drives the difference in potential evaporite assemblages, the conceptual model of Hardie and Eugster (1970) was applied. It suggests the difference is because of conditions at the first chemical divide encountered during evaporation (Figure 2-4). Because San Bernardino waters meet the condition alkalinity > $2m_{Ca^{2+}}$ (alkalinity = 5.69 x $m_{Ca^{2+}}$), Ca^{2+} will be depleted during precipitation of calcite. In the San Simon, Douglas, and Willcox Basins, waters meet the condition $2m_{Ca^{2+}}$ > alkalinity ($2m_{Ca^{2+}}$ = 1.33 x alkalinity to 4.65 x alkalinity), therefore $CO_3^{2-}{}_T$ is depleted. In the Animas Basin, some basin-center waters meet the condition (alkalinity > $2m_{Ca^{2+}}$), but others do not. For those with (alkalinity > $2m_{Ca^{2+}}$), the ratio of alkalinity:$2m_{Ca^{2+}}$ tends to be less than half that observed in San Bernardino Basin waters. The significantly elevated alkalinity:$2m_{Ca^{2+}}$ ratio in San Bernardino waters causes them to move along a separate path in the Hardie-Eugster model than that followed by waters from the neighboring basins, thus forming different evaporites.

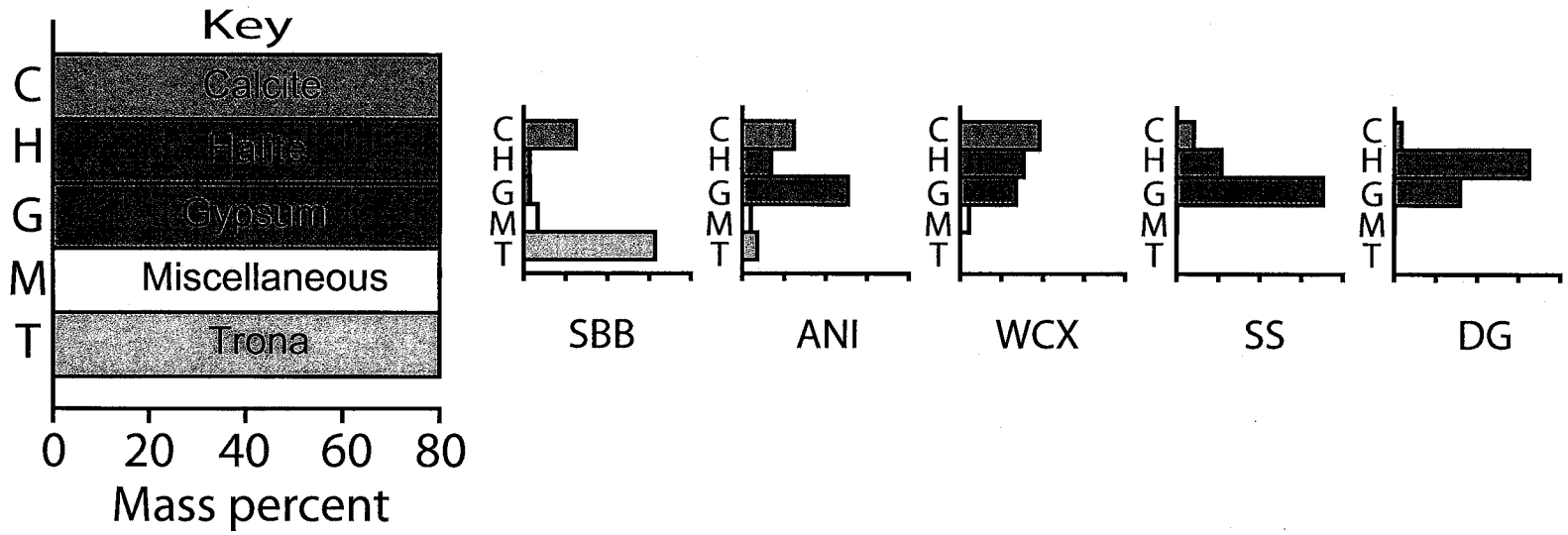

Figure 2-3. Plots showing types of salts that would form from evaporating representative groundwaters from the San Bernardino Basin and its neighboring basins. Large graph shows major salt type corresponding to each bar in small plots. Small plots show salt types for the San Bernardino Basin and its neighboring basins (abbreviations are those used in Figure 1) as mass percents of the total salt assemblage; x-axis tick marks represent 20 percent increments. The mineral names used in the key are representative of mineral families; e.g. 'calcite' includes calcite and dolomite; 'gypsum' includes gypsum and anhydrite; 'trona' includes trona and all other sodium carbonate minerals. The SBB salt assemblage is distinct due to the large proportion (63 %) of Na-CO_3 minerals; water from the Animas Basin would yield a maximum of 7 % total of Na-CO_3-SO_4 and Na-Ca-CO_3 minerals, the remaining neighboring basins would yield none.

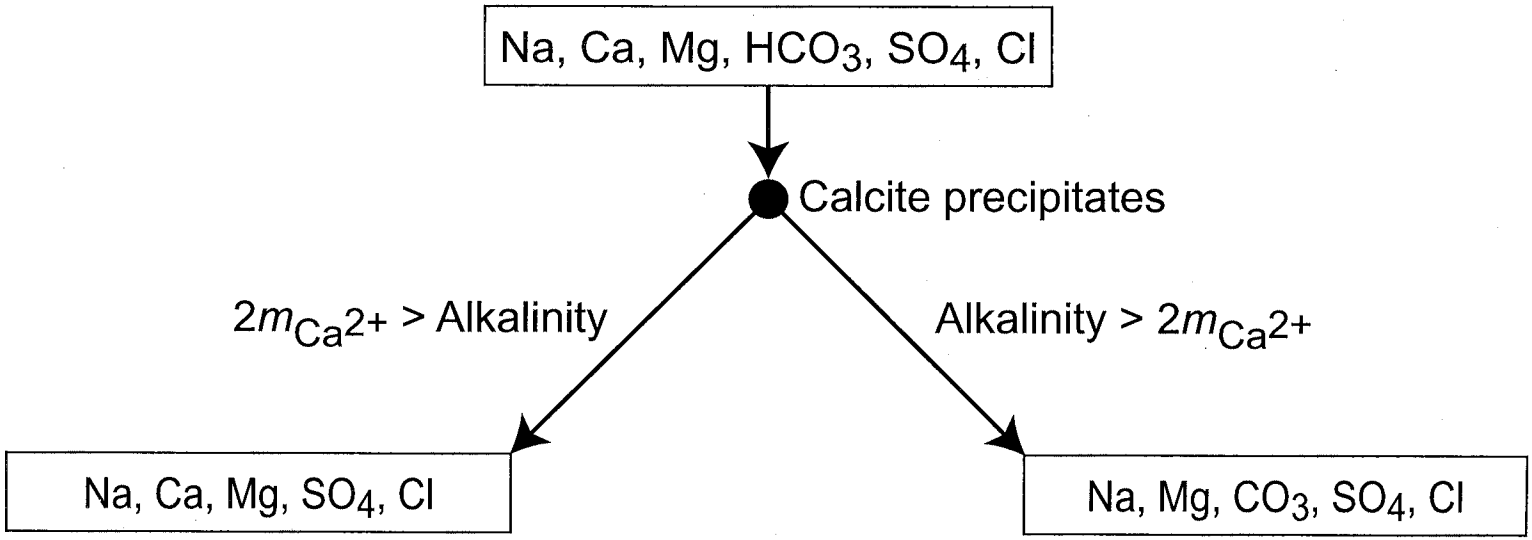

Figure 2-4. Flowchart representation of the first portion of the Hardie-Eugster model for evaporite formation (after Drever, 1997).

Because the ratio of alkalinity to [Ca^{2+}] controls the types of evaporite minerals formed, the chemical evolution of groundwater in the San Bernardino Basin will be examined. The main goal will be to determine the source of the 'excess' HCO_3^- (given that typical San Bernardino water pHs fall between 7.6 and 8.3 from a).

Chemical evolution of groundwater in the San Bernardino Basin

Wells used to approximate a flowpath through San Bernardino Basin

A set of seven wells was selected to approximate a flowpath from the San Bernardino Basin's main recharge area to the basin center (Figure 2-5). Because existing wells were used for sampling, the wells deviate from a true flowpath in the x, y, and z-planes; nonetheless, trends in water chemistry that are consistent with the subsurface conditions are evident along the flowpath approximation. As a result, although it differs from a strictly defined flowpath, for the sake of simplicity, the flowpath approximation will be referred to as 'the flowpath'. Samples from the flowpath wells were analyzed to determine major ion chemistry, ^{14}C activity, $\delta\ ^{13}C$, and ^{3}H concentration (Table 2-2; descriptions of sample collection and analysis are provided in the "Hydrogeology" section of Chapter 1). Four of the flowpath wells were sampled for dissolved gas content, as described in the "Dissolved-gas methods and results" section of Chapter 3. The first three wells on the flowpath are north of the area where basalts are present at the surface, and, although lithologic logs are not available for these wells, logs from other wells in the vicinity show that basalts are absent in the subsurface. The portion of the basin in which these three wells are located is adjacent to one of the major sedimentary outcrops in the bounding ranges, and thus contains a high proportion of carbonate minerals in the alluvial fill compared to other parts of the basin. The final four wells on the flowpath are all in the area containing basalts in the subsurface, with the remainder of the fill dominated by sediments of rhyolitic origin. When discussing the flowpath, the 'initial portion' will

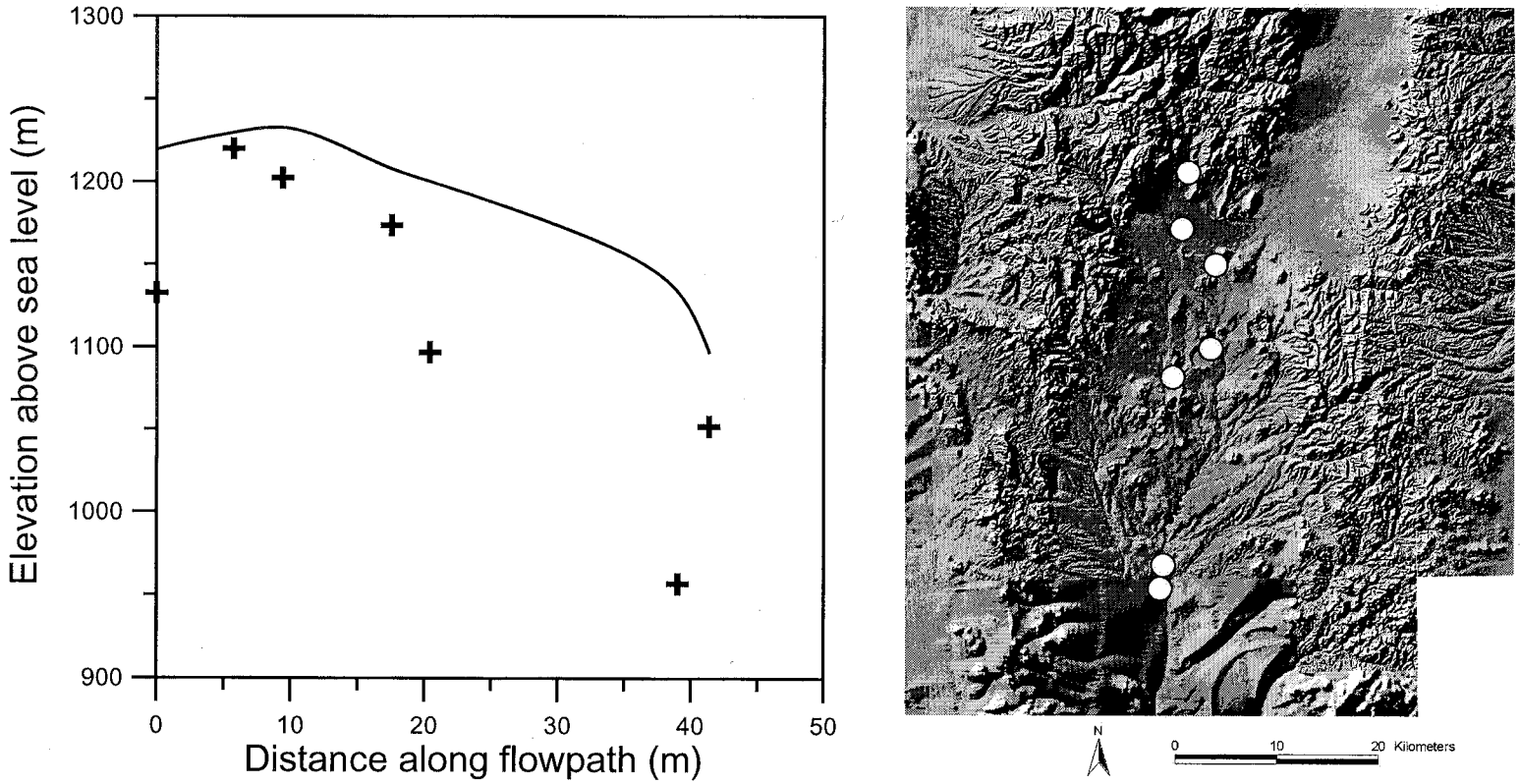

Figure 2-5. Plot showing water table/potentiometric surface (line) and well-bottom elevations of flowpath wells (crosses) as a function of distance along the flowpath (left), along with a map of flowpath well locations (right). The predominant direction of groundwater flow in the basin is from north to south, so the northernmost well is at distance zero on the flowpath.

Ion/ parameter	Anderson Well	Gibbons Well	Ashurst Well	Krentz Well	Ranchita Well	Cotton-wood Well	Austin Well
HCO_3^-	2.148	3.574	2.787	3.230	3.049	4.115	5.116
Cl^-	0.124	0.167	0.164	0.141	0.172	0.161	0.175
SO_4^{2-}	0.095	0.083	0.060	0.048	0.050	0.115	0.115
NO_3^-	0.100	0.150	0.329	0.407	0.521	0.271	0.336
F^-	0.163	0.111	0.051	0.033	0.021	0.019	0.023
Ca^{2+}	0.674	1.373	0.998	0.374	0.424	0.499	0.449
Mg^{2+}	0.082	0.263	0.239	0.453	0.535	0.535	0.576
K^+	0.072	0.097	0.146	0.182	0.194	0.067	0.159
Na^+	0.914	0.609	0.522	1.610	1.262	2.350	3.090
SiO_2	1.865	1.565	1.582	0.916	1.082	1.282	1.066
R/R_a	1.401	-	2.061	-	2.183	4.227	-
DO (mg/L)	1.98	5.12	5.89	2.6	4.87	3.98	4.51
PCO_2 (matm)	3.790	4.110	2.510	0.964	1.330	2.870	4.390
$\delta\ ^{13}C$ (‰)	-10.7	-9.6	-8.6	-8.3	-7.6	-8.3	-7.4
pH	7.55	7.75	7.82	8.31	8.13	7.90	7.86

Table 2-2. Values for groundwater quality parameters for wells on the flowpath (progression from recharge area to basin center is indicated by left-to-right position in the table) through the San Bernardino aquifer. pH and R/R_a are unitless; unless otherwise noted, all other values are in units of mM/L; dashes indicate values not measured.

refer to the zone prior to encountering basalts, and the 'latter portion' will refer to the zone where basalts are a significant portion of the basin fill.

Potential process affecting [HCO_3^-] in the San Bernardino Basin

The concentrations of some of the chemical constituents in the San Bernardino Basin as a function of distance along the flowpath are shown in Figure 2-6. Because the formation of trona is the subject of interest, it is important to find the cause(s) of the high [HCO_3^-] relative to [Ca^{2+}]. Since silicate hydrolysis is the typically-invoked explanation for trona formation, and the San Bernardino aquifer matrix is composed primarily of alluvial fill derived from rhyolitic rocks, it is tempting to assume that this process is controlling the water chemistry; the increase in [Na^+] along the flowpath seems to support silicate hydrolysis as the causative factor. However, PCO_2 also increases along the flowpath. As silicate hydrolysis is a process that consumes CO_2, it appears that a more detailed examination of the chemical evolution is necessary.

There are a number of processes that can affect the concentration of HCO_3^- in groundwater by adding or removing CO_3^{2-} or CO_2 to or from the groundwater. Given the pHs of waters in the San Bernardino Basin (7.6 to 8.3 for the flowpath wells) and its neighboring basins, nearly all CO_3^{2-} or H_2CO_3 introduced will form HCO_3^-. Langmuir (1997) describes in detail processes that affect the $HCO_3^-/CO_3^{2-}/H_2CO_3$ system. Examining the evolution of [HCO_3^-] along the flowpath will show which processes are important controls on the concentration of HCO_3^- in the San Bernardino Basin's basin fill aquifer.

Dissolution or precipitation of carbonate minerals is a common control on [HCO_3^-] in groundwaters. The relationship between [Ca^{2+}] and [HCO_3^-] in the flowpath waters is shown in Figure 2-7. While [Ca^{2+}] and [HCO_3^-] are covariant in the initial portion of the flowpath, [HCO_3^-] increases in the latter portion with almost no change in [Ca^{2+}]. This suggests that carbonate mineral dissolution/precipitation

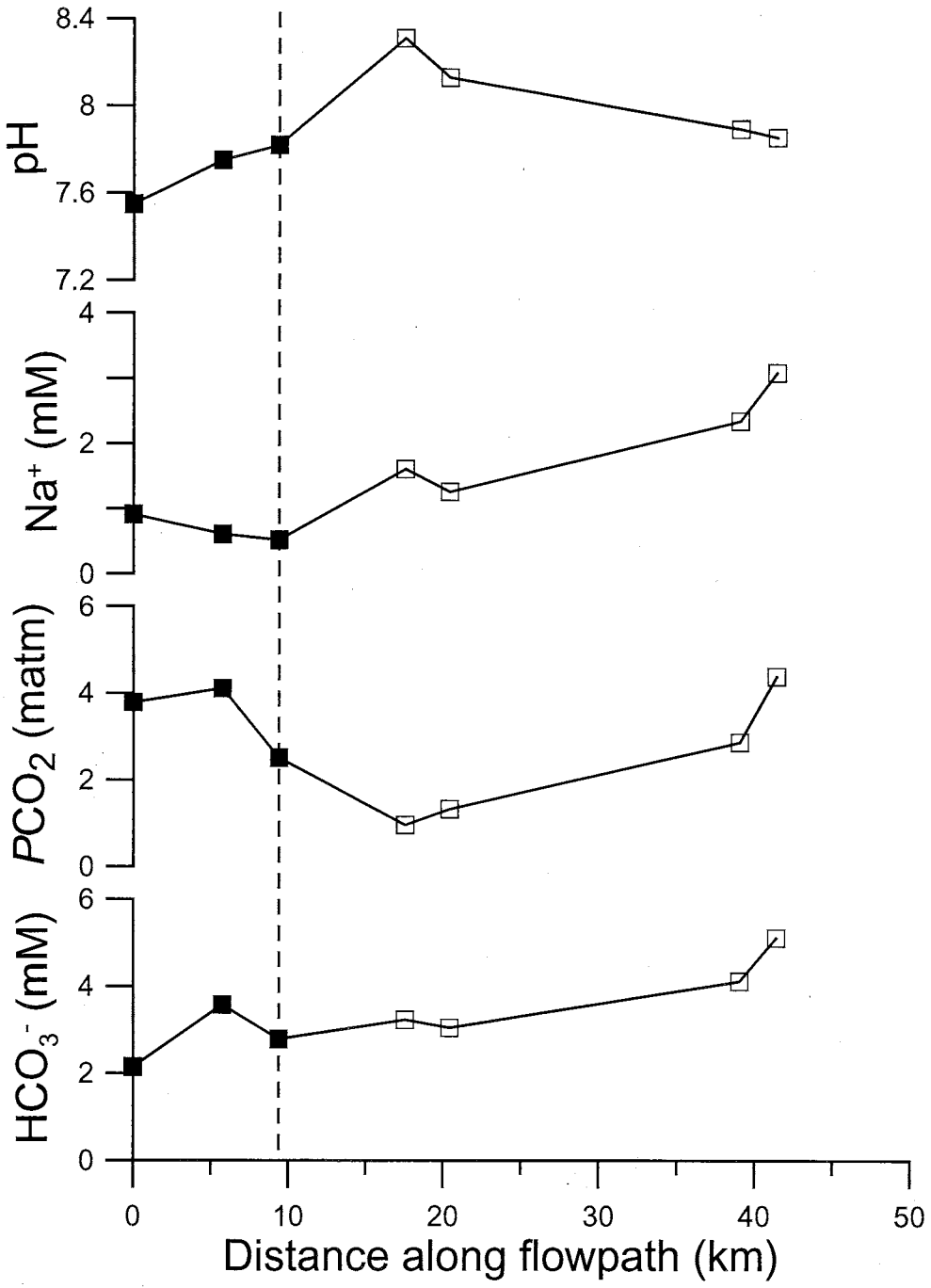

Figure 2-6. Concentrations of bicarbonate and sodium and values for partial pressure of CO_2 and pH as a function of distance along the flowpath. Open symbols represent wells on the initial portion of the flowpath, solid symbols represent wells on the latter portion of the flowpath. Dashed line indicates the position of the boundary between the initial and latter portions of the flowpath.

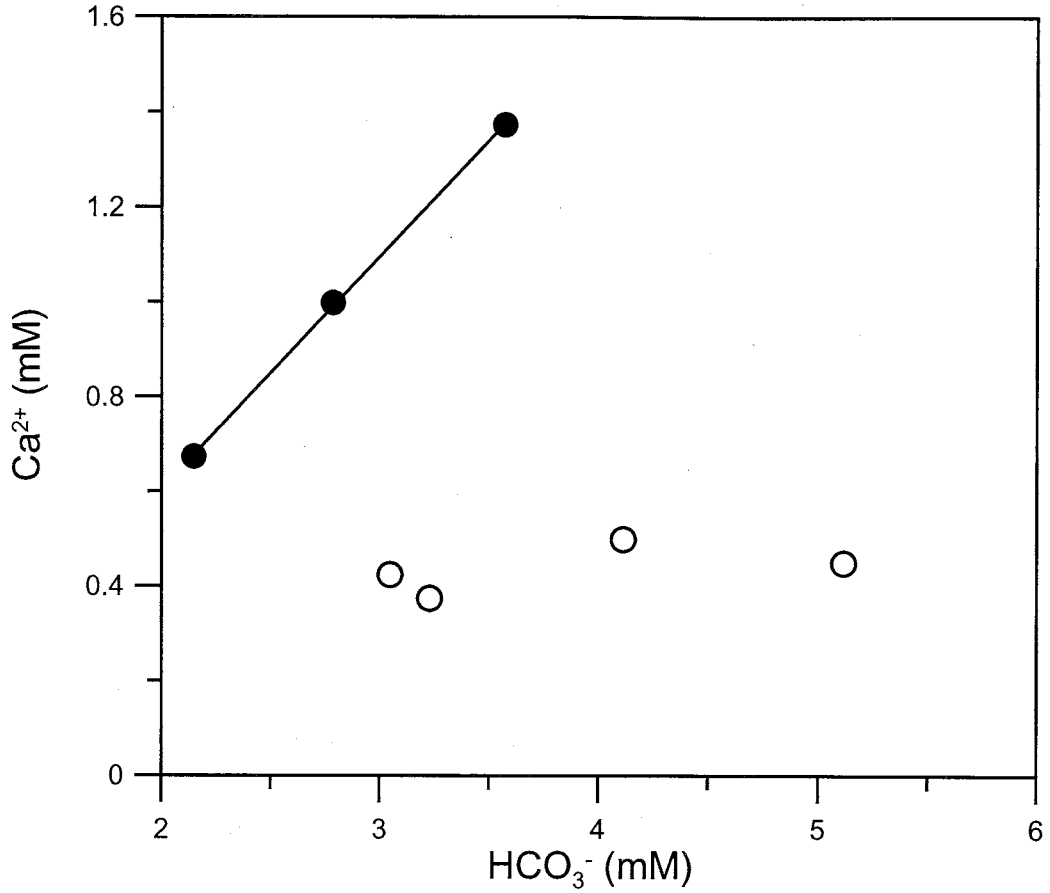

Figure 2-7. Calcium concentration versus bicarbonate concentration for groundwaters on the flowpath through the San Bernardino aquifer. Solid symbols represent points on the initial portion of the flowpath, hollow symbols represent points on the latter portion of the flowpath.

reactions are an important control on [HCO_3^-] in the initial portion, but they are unlikely to be important in the latter portion. As the initial portion of the flowpath is in an area in which the alluvial fill contains a significant portion of carbonate minerals, but the latter is not, the distinction in chemical processes makes sense in the context of the basin's lithology. The slope of the best fit line connecting the points on the initial portion is 0.5 (Figure 2-7), which suggests that simple calcite dissolution is not controlling [HCO_3^-] in the initial portion of the flowpath. Modeling using the computer code NETPATH (Plummer *et alii*, 1991) suggests that waters are initially dissolving both calcite and dolomite, but quickly begin incongruent dissolution with dolomite dissolving and calcite precipitating; incongruent dissolution of calcite and dolomite would account for the initial best-fit-line slope of 0.5 in Figure 2-7.

Chemical weathering of silicates is another major influence on [HCO_3^-] in groundwaters. In many natural waters, silicate hydrolysis is the main control on chemical composition (Bowser and Jones, 2002). Although the stoichiometry of any given silicate hydrolysis reaction is dependent on the composition of the silicate mineral being weathered, a generic reaction can be written as follows (modified from Jones, 1966; Jones *et alii*, 1977):

$$\text{primary silicate} + H_2O + CO_2 = \text{clay} + \text{cations} + HCO_3^- + SiO_{2\,(aq)} \qquad (1)$$

In the initial portion of the flowpath, alluvial fill is derived from both carbonates and rhyolitic rocks, but no basalts are present. Based on average values for mass percents of various oxides in volcanics in the Chiricahuas that could have contributed to the San Bernardino fill (calculated using data from du Bray and Pallister, 1995), the mass ratios of Na_2O and K_2O to MgO are 10:1 and 21:1 (respectively), and the mass ratios of Na_2O and K_2O to CaO are 6:1 and 13:1 (respectively). As a result, the cations produced by silicate hydrolysis in the initial portion of the flowpath should consist almost exclusively of Na^+ and K^+, with only trace amounts of Ca^{2+}. The concentration

of Na^+ shows little correlation with that of HCO_3^- in the initial portion of the flowpath, and the weak correlation is negative, with $[Na^+]$ decreasing as $[HCO_3^-]$ increases (Figure 2-8). This strongly suggests that silicate mineral hydrolysis is not a major control on groundwater chemistry in the initial portion of the flowpath; however, the strong correlation between $[Na^+]$ and $[HCO_3^-]$ (Figure 2-8) on the latter part of the flowpath suggests that silicate mineral hydrolysis is an important control in that zone. In the initial portion of the flowpath, carbonate minerals are buffering the pH, so CO_2 in the system is used for carbonate dissolution, and thus unavailable to participate in hydrolysis reactions. On the latter portion of the flowpath, where carbonates are not present in significant quantities, CO_2 in the system is available as a reactant for hydrolysis.

In the initial part of the flowpath, silicate mineral hydrolysis has only one significant target—the sediments derived from rhyolitic tuff in the basin fill. In the latter part of the flowpath, basalts are present as well. If basalts become a major target of weathering reactions in the latter portion of the flowpath, correlations between $[HCO_3^-]$ and $[Ca^{2+}]$ and $[HCO_3^-]$ and $[Mg^{2+}]$ should be evident. Changes in $[HCO_3^-]$ appear independent of changes in $[Ca^{2+}]$ on the latter part of the flowpath (Figure 2-7). There is only a weak correlation ($r^2 = 0.50$) between $[Mg^{2+}]$ and $[HCO_3^-]$ (Figure 2-9A). There is an initial increase in $[Mg^{2+}]$ as water enters the latter part of the flowpath, but subsequent increases are relatively minor (Figure 2-9B). According to Jones (1966), silicate hydrolysis will preferentially affect materials with high Si/Al ratios. The basalts in the basin fill typically contain 45 to 49 % SiO_2 and 15 to 16 % Al_2O_3 by mass (Lynch, 1978). While typical rhyolitic sediments in the basin contain about the same amount of aluminum (10 to 17 % Al_2O_3 by mass) as the basalts, they are much richer in silica (typically from 60 to 80 % mass percent SiO_2) (du Bray and Pallister, 1995). Major ion concentrations in the groundwater show that, as predicted

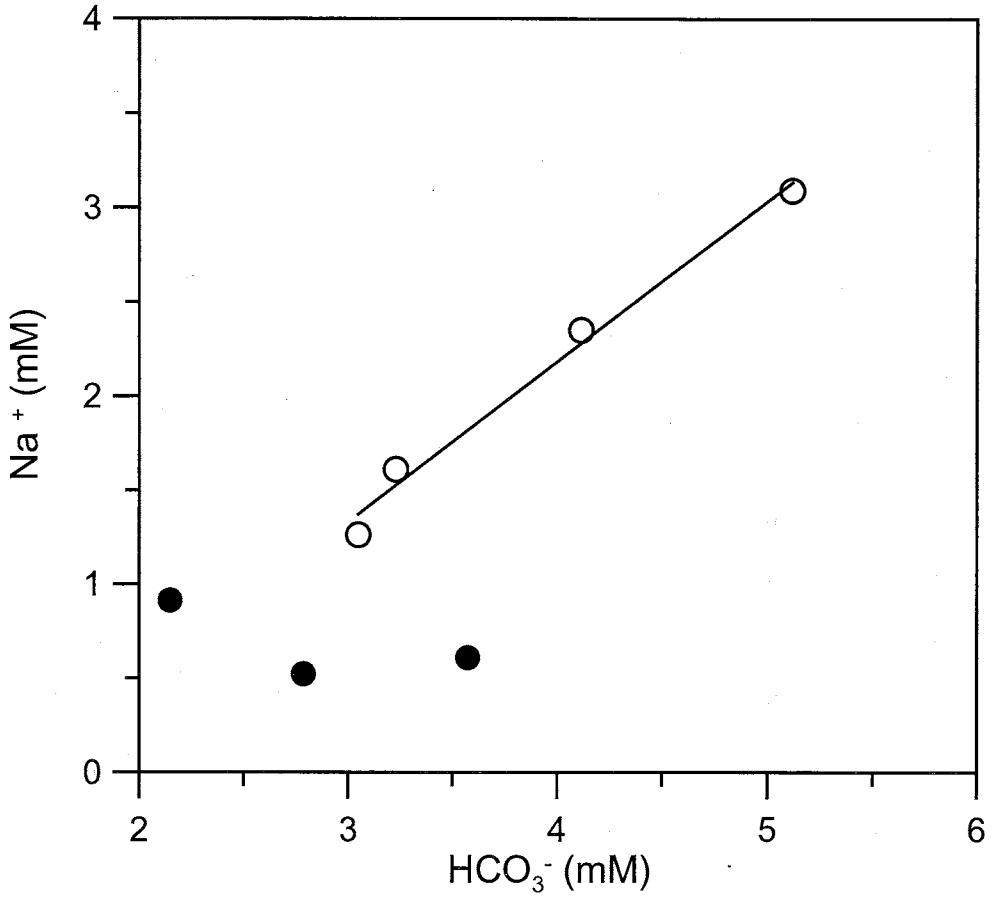

Figure 2-8. Sodium concentration versus bicarbonate concentration for groundwaters on the flowpath through the San Bernardino aquifer. Solid symbols represent points on the initial portion of the flowpath, hollow symbols represent points on the latter portion of the flowpath.

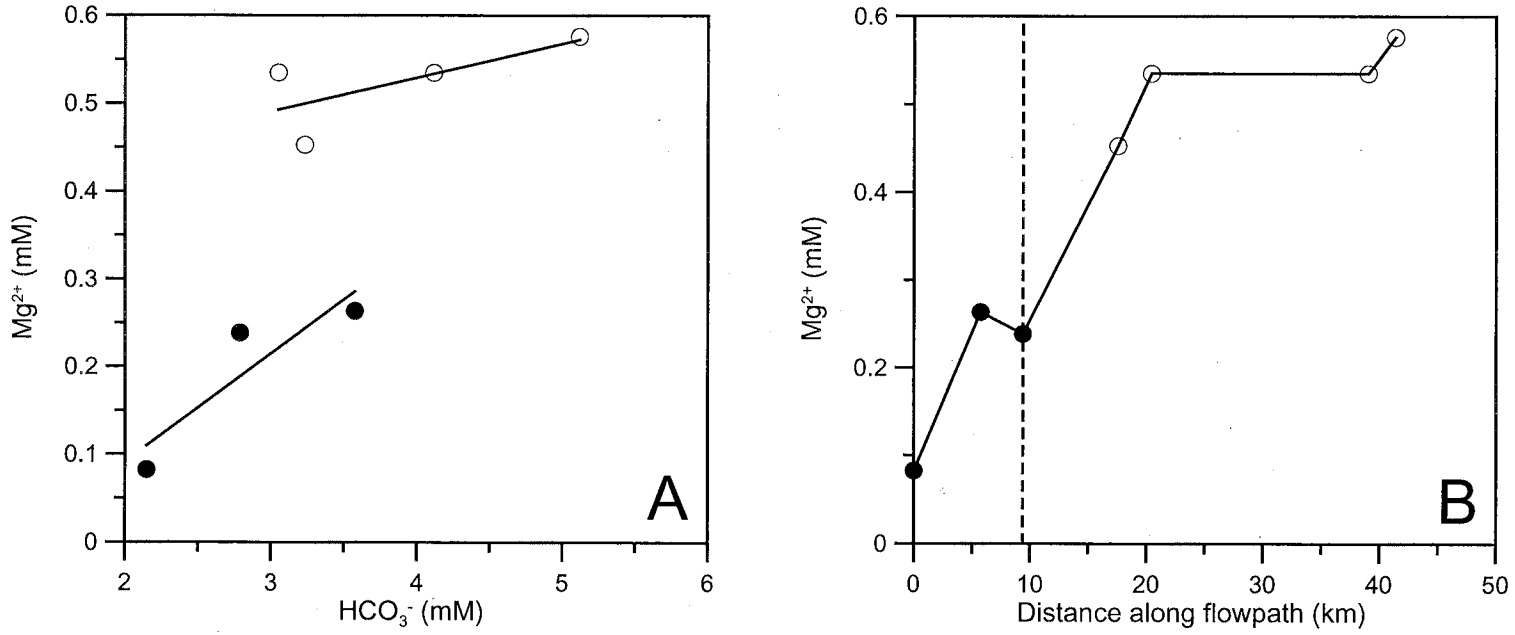

Figure 2-9. A. Magnesium concentration versus bicarbonate concentration for groundwaters on the flowpath through the San Bernardino aquifer. Solid symbols represent points on the initial portion of the flowpath, hollow symbols represent points on the latter portion of the flowpath. **B.** Magnesium concentration as a function of distance along the flowpath. Solid symbols represent points on the initial portion of the flowpath, hollow symbols represent points on the latter portion of the flowpath. Dashed line indicates initial/latter divide on the flowpath.

by the Si/Al ratios, silicate hydrolysis does operate on the basalts (accounting for the jump in $[Mg^{2+}]$ as water enters the latter portion of the flowpath), but to a much smaller extent than it affects the rhyolitic sediments.

Redox reactions are another possible control on $[HCO_3^-]$, especially the reduction of NO_3^- to NH_4^+ and SO_4^{2-} to HS^-, both of which produce CO_2. Although Eh was not measured in any of the waters, evidence suggests that these reduction reactions are not likely to be occurring. Dissolved oxygen values for waters on the flowpath range from 1.98 to 5.89 mg/L (with the lowest value corresponding to the deepest well), suggesting that reducing conditions are not present in the basin fill aquifer (the dissolved oxygen concentrations also suggest that anaerobic decay, which also produces CO_2, is not occurring). Another line of evidence against NO_3^-/SO_4^{2-} reduction is the concentration of nitrate in water as a function of distance along the flowpath (Figure 2-10). With one exception, $[NO_3^-]$ increases between each successive pair of wells. Not only does the trend of increasing $[NO_3^-]$ argue against nitrate reduction (and also denitrification, another CO_2-producing reaction), but, as NO_3^- is reduced at higher Eh values than SO_4^{2-} (Langmuir, 1997), it also argues against sulfate reduction.

Microbial respiration or aerobic decay are other potential sources of CO_2, which could be converted to HCO_3^-. There are no known measurements that can explicitly rule out these processes. However, it appears unlikely that these processes exert a significant control on the San Bernardino groundwater chemistry. Given the combination of relatively arid climate and basalt flows that cover much of the valley floor, and are present throughout the majority of the subsurface on the latter part of the flowpath, it is unlikely that a significant amount of organic matter was able to accumulate during basin development. No well logs from the basin suggest the presence of material (such as peat or coal) that would indicate large accumulations

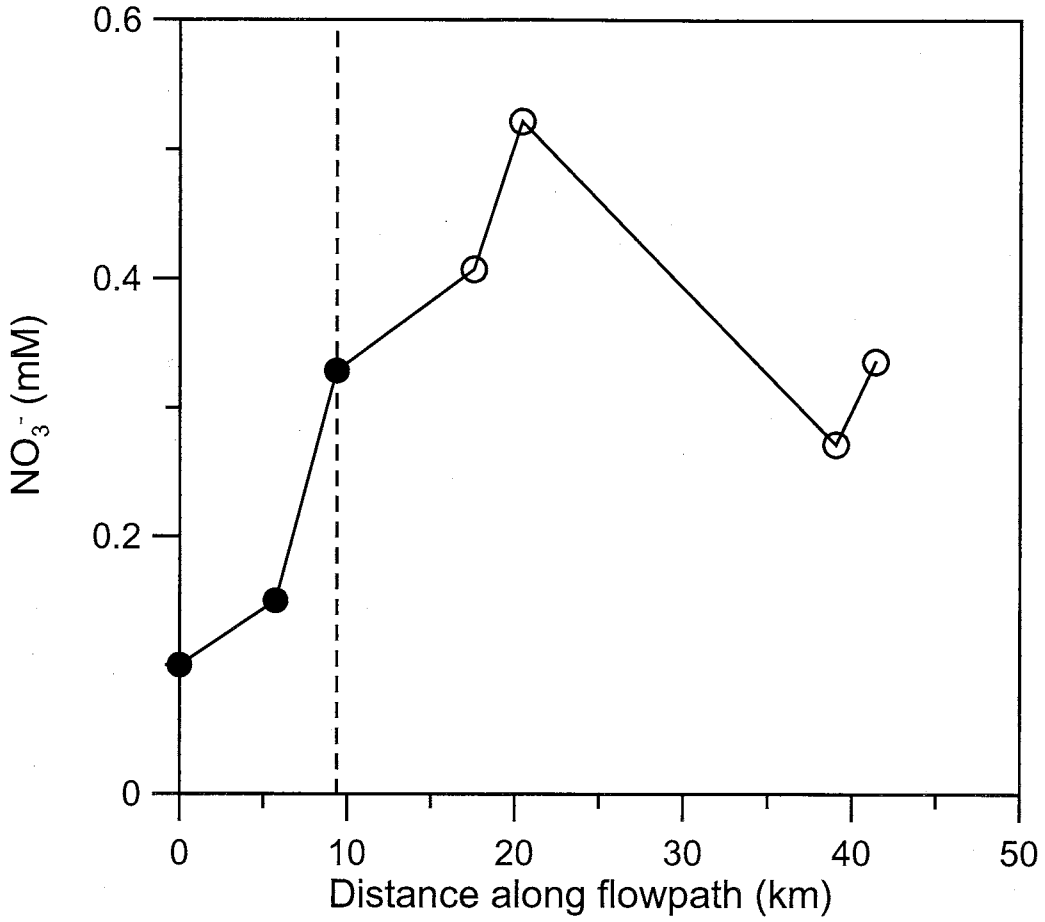

Figure 2-10. Nitrate concentration as a function of distance along the flowpath. Solid symbols represent points on the initial portion of the flowpath, hollow symbols represent points on the latter portion of the flowpath. Dashed line indicates initial/ latter divide on the flowpath.

of organic matter. Some petroleum exploration wells were drilled in the basin, but none were completed due to lack of hydrocarbons. In the records for one well, it is noted that "No indications of hydrocarbons of any kind were encountered in this well" (Arizona Oil and Gas Commission petroleum exploration well archives, well record #564).

The final major reaction that could influence [HCO_3^-] in the aquifer is the conversion of CO_2 from some source other than those discussed previously to HCO_3^-. Any such added CO_2 would be converted to HCO_3^-, either via dissolution and interaction with H^+ or through silicate hydrolysis. With the exception of the zone from 10 to 20 km along the flowpath, PCO_2 and [HCO_3^-] are covariant, and the most dramatic increases in both values occurs over the last 25 km of the flowpath (Figure 2-6). Although silicate hydrolysis appears to be occurring in the latter part of the flowpath, it does not appear to be the sole control on [HCO_3^-] because that would cause PCO_2 to decline as [HCO_3^-] increased. Based on this evidence, there must be injection of CO_2 into the aquifer. As this CO_2 appears to play an important role in creating the conditions necessary for trona formation, identification of its source is important to understanding trona formation.

Sources of CO_2

Although the basin fill aquifer is unconfined for most of its areal extent, it is confined near the center of the basin, including the area where the increases in PCO_2 and [HCO_3^-] are the most rapid, meaning that input of atmospheric/soil CO_2 is not a reasonable source. The PCO_2 values for San Bernardino waters are all higher than the atmospheric value of $10^{-3.5}$ atm; three of the seven are within the range of values for soil of $10^{-2.5}$ to $10^{-1.5}$ atm (Drever, 1997). It is important to note that these high PCO_2 values are not simply found near the recharge zone. In fact, the highest value is from the last well on the flowpath, at which point the aquifer is confined, and the

water has moved over 40 km in the subsurface, with CO_2 being consumed in carbonate dissolution and silicate weathering reactions on its travels. The value of the ratio R/R_a for the isotopes ^3He and ^4He (where R is the $^3He/^4He$ ratio of a water sample, and R_a is the $^3He/^4He$ ratio of the atmosphere) as a function of distance along the flowpath is shown in Figure 2-11 (these values were derived from dissolved-gas samples, for which the sampling and analysis is discussed in Chapter 3). High values of R/R_a are diagnostic of incorporation of mantle He (Oxburgh *et alii*, 1986) due to the fact that the mantle helium has an R value distinct from that of helium derived from other reservoirs (Solomon, 2000). Clark and Fritz (1997) describe $^3He/^4He$ R/R_a values of surface waters as being close to 1, those of crustal fluids ranging from 0.007 to 0.022, and those of mantle He falling between 7 and 21. Although this increase in the aquifer R/R_a value is not direct proof of magmatic CO_2 input, it is direct evidence that gas is being added to the aquifer; CO_2, like He, is virtually always associated with mantle outgassing (Mao *et alii*, 2002; White and Waring, 1963). The presence of extensive basalt in the basin indicates that such inputs are plausible. Basalt covers much of the valley floor (Figure 2-2); they are also common in the basin fill in the zones where they occur at the surface. Basaltic volcanism was active in the basin from at least 4.7 Myr to 0.26 Myr ago, and eruptions may have occurred as long as 9.2 Myr ago (Kempton, 1984; Kempton and Dungan, 1989; Lynch, 1972). The basalts contain xenoliths such as lherzolite that confirm that they originated in the mantle (Evans, 1978).

The common trends in $[Na^+]$, PCO_2, and $[HCO_3^-]$ after the 17.5 km point on the flowpath (Figure 2-6) suggest that silicate mineral hydrolysis driven by injection of magmatic CO_2 is acting to control the concentration of HCO_3^- in the basin fill aquifer.

The relationship between PCO_2 and the rate at which silicate weathering reactions proceed is difficult to quantify, as many studies have been performed under

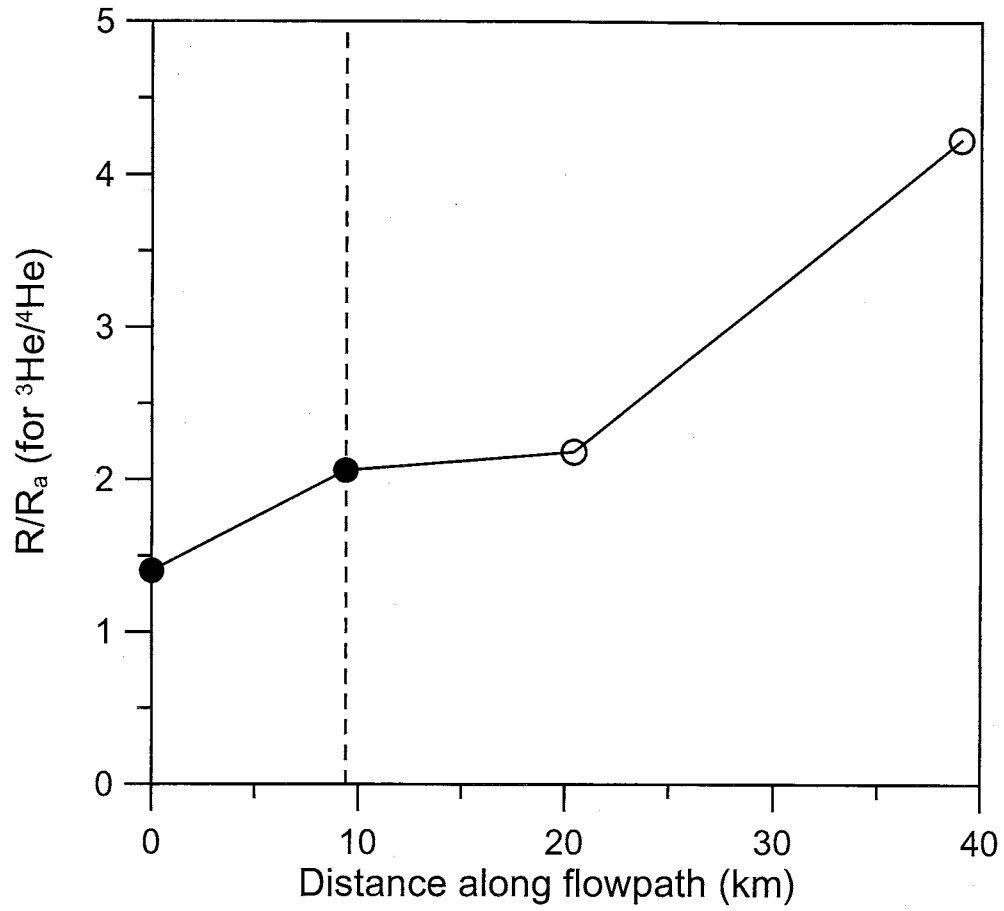

Figure 2-11. R/R_a for $^3He/^4He$ as a function of distance along the flowpath. Solid symbols represent points on the initial portion of the flowpath, hollow symbols represent points on the latter portion of the flowpath. Dashed line indicates initial/ latter divide on the flowpath.

conditions that make it difficult to apply the results to "normal" aquifers, such as temperatures above 100 °C, pressures as high as 20 atm, and/or very basic or acidic pH (for a summary of hydrolysis studies, see Stephens, 2002). However, a number of studies have tied increased silicate weathering rates to increased PCO_2, consistent with the behavior inferred based on the San Bernardino chemical data.

Additional evidence that magmatic CO_2 is influencing the water chemistry in the San Bernardino Basin comes from values of $\delta^{13}C$ (Figure 2-12). Rose and Davisson (1996) show that input of magmatic CO_2 can influence both $\delta^{13}C$ and the activity of ^{14}C in groundwater. Values of $\delta^{13}C$ along the flowpath in the San Bernardino Basin do not follow a uniform trend due to differing depths of wells, but a general trend of decrease is evident as water moves through the basin. In the initial portion of the flowpath, changes in $\delta^{13}C$ and ^{14}C activity are apparently affected only by interactions with carbonate minerals. In the latter portion of the flowpath, the influence appears to be from direct solution of magmatic CO_2 gas. To test these concepts, several scenarios for alteration of the $\delta^{13}C$ over the course of the flowpath were modeled. The mixing calculations used for these models are described in Appendix 4.

First, it was assumed that changes in groundwater $\delta^{13}C$ along the entire flowpath were driven solely by dissolution reactions with carbonate minerals having $\delta^{13}C$ of 0 ‰ (actual values for local carbonates were not measured, so the 'standard' marine carbonate value of 0 ‰, which is also the approximate median of the range of values for $\delta^{13}C$ for marine limestone given by Clark and Fritz (1997) was assumed to apply). Based on the change in $[HCO_3^-]$ from the beginning to the end of the flowpath (3.0 mM/L; see Table 1-1) and the initial $\delta^{13}C$ value of -10.7, this scenario would yield a $\delta^{13}C$ of about -3.5 ‰ at the end of the flowpath, significantly enriched compared to the observed value of ~-7.5 ‰ (Figure 2-13). The next model assumed that the

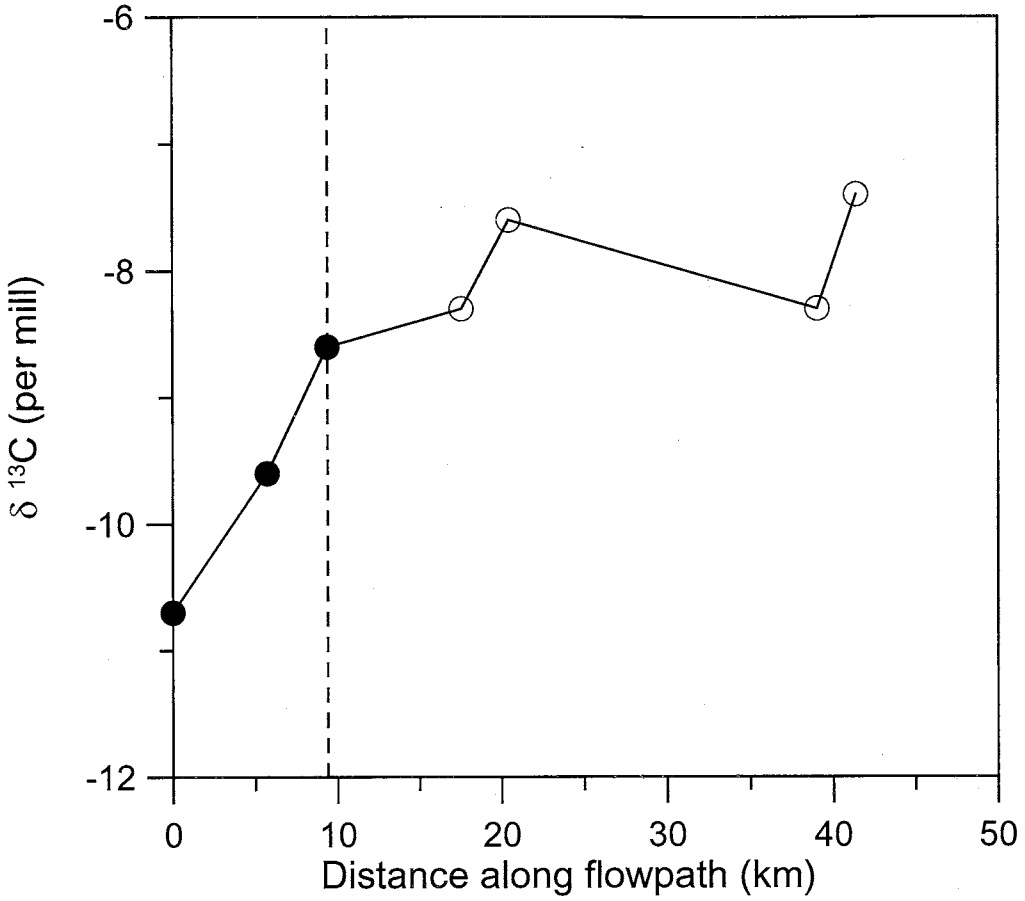

Figure 2-12. Plot showing $\delta\ ^{13}C$ as a function of distance along the flowpath.

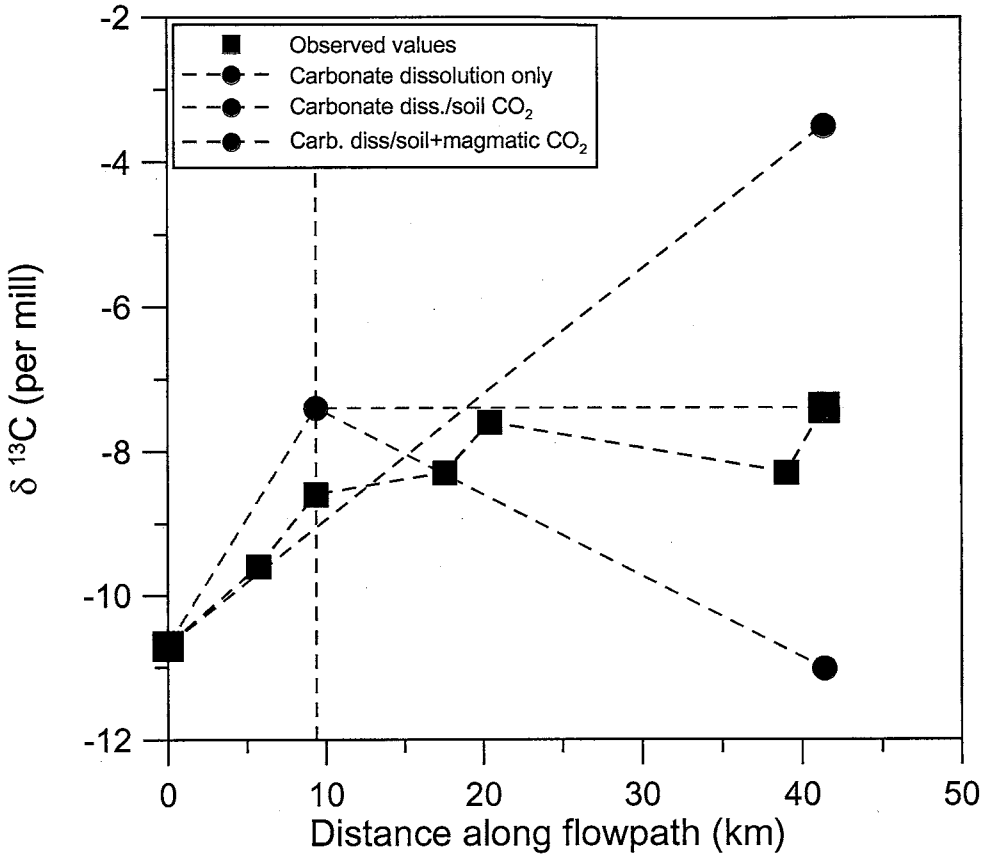

Figure 2-13. Diagram showing the results of the mixing models used to investigate the change in $\delta\ ^{13}C$ observed from the initial point to the end point of the flowpath. Red squares represent the observed initial and final values; the blue circle represents the value that water at the end of the flowpath would have if the change in HCO_3^- from the initial well to the end point was due entirely to dissolution of carbonate minerals with $\delta\ ^{13}C$ of 0 ‰; the green circles represent the values predicted for $\delta\ ^{13}C$ at the initial-latter portion boundary (vertical dashed line) and the end of the flowpath assuming that the change in HCO_3^- over the initial portion of the flowpath was due entirely to dissolution of carbonate minerals with $\delta\ ^{13}C$ of 0 ‰, but the change over the latter portion of the flowpath were due entirely to dissolution of soil CO_2 with $\delta\ ^{13}C$ of -20 ‰; the purple circle represents the predicted $\delta\ ^{13}C$ at the end of the flowpath if the the change in HCO_3^- over the initial portion of the flowpath was due entirely to dissolution of carbonate minerals with $\delta\ ^{13}C$ of 0 ‰, but the change over the latter portion of the flowpath was due to dissolution of CO_2 that is a mix of 60% magmatic gas with $\delta\ ^{13}C$ of -9.5 ‰ and 40% soil CO_2 with $\delta\ ^{13}C$ of -20 ‰.

change in $\delta^{13}C$ over the initial portion of the flowpath was controlled by carbonate minerals having $\delta^{13}C$ of 0 ‰, but input of soil CO_2 (either by direct dissolution or via silicate hydrolysis) was the controlling process over the latter portion of the flowpath. In this case, the change in $[HCO_3^-]$ over the initial portion of the flowpath was used to modify the initial $\delta^{13}C$ value in the same manner as the model described above; the modeled $\delta^{13}C$ at the end of the initial portion of the flowpath was then used as the initial value for $\delta^{13}C$ on the latter portion of the flowpath, and the change in $[HCO_3^-]$ over the latter portion of the flowpath was used to predict the final $\delta^{13}C$ value (a $\delta^{13}C$ of -20 ‰ was assumed for the soil CO_2, based on the value of -20.1 ± 1.6 ‰ reported by Kalin (2000) for average soil CO_2 in the Tucson Basin (approximately 180 km to the northwest of San Bernardino Basin)). This model yielded an end-of-flowpath $\delta^{13}C$ value of about -11 ‰, significantly depleted compared to the observed value of ~-7.5 ‰ (Figure 2-13) (this and all other mass balance calculations involving gas dissolution use a fractionation factor based on Wigley *et alii* (1978) adjusted for the temperature and pH at which dissolution occurs in the San Bernardino aquifer). Because chemical and isotope data both point to carbonate minerals as the main control on the initial portion of the flowpath, a mixing model (Appendix 4) was used to estimate the $\delta^{13}C$ of C input into the aquifer over the latter portion of the flowpath based on the change in $[HCO_3^-]$ over the latter portion of the flowpath and the estimated $\delta^{13}C$ at the start of the latter portion (from the previous model). This model suggests that average $\delta^{13}C$ input over the latter portion of the flowpath is about -13.8 ‰. Mantle CO_2 tends to have $\delta^{13}C$ values above -10 ‰ (Clark and Fritz, 1997), implying it alone is too enriched in $\delta^{13}C$ to be the sole source of HCO_3^-. The increasing $[HCO_3^-]$ in the latter portion of the flowpath thus appears to be due to input of some combination of mantle CO_2 and soil CO_2. Mass balance using $\delta^{13}C$ of -20 ‰ for soil CO_2 and -9.5 ‰ for magmatic CO_2 (Rose and Davisson, 1996) suggests that magmatic CO_2 is responsible for 60 %

of the input, and soil CO_2 for 40 %. Note that this proportion accounts for the entire length of the latter portion of the flowpath. Although new soil CO_2 is not likely to be added to the aquifer where it is confined, it is the main source of dissolved CO_2 at the time of groundwater recharge. As addition of magmatic CO_2 appears to take place along the entire flowpath (although the gas is likely added to the aquifer through discrete fractures, at the spatial resolution of the observations, determining exact input zones is not possible), the CO_2 dissolved in the water has some combination of soil and magmatic origin, depending on location. This shows that, whether through direct dissolution, or serving as a reactant in silicate weathering reactions, magmatic CO_2 plays a significant role in driving the chemical evolution of waters in the San Bernardino aquifer. The resulting increase in total CO_3^{2-} is a controlling factor in the types of minerals that would form if San Bernardino waters were evaporated.

IMPLICATIONS

The mineral suite that would be formed by evaporating San Bernardino Basin groundwater is markedly different from those that would be formed by evaporating groundwaters from the neighboring basins. The major difference between the San Bernardino Basin and its neighboring basins is the degree of Cenozoic volcanism; in the San Bernardino Basin, there is evidence for contemporary CO_2 injection related to the Geronimo volcanic field. As shown by the Hardie-Eugster model, input of CO_2 without associated input of Ca^{2+} has the potential to alter the types of minerals formed during evaporation. In addition to the direct impact of CO_2 injection on evaporite mineralogy, increased PCO_2 also appears to increase the rate of silicate weathering. The only neighboring basin that would yield any Na-CO_3 minerals via evaporation is Animas, which experienced relatively minor basaltic volcanism associated with the Geronimo volcanic field (note that Animas groundwater would not form trona but burkeite and pirssonite). This volcanism has produced a contemporary zone of

hydrothermal activity (Elston *et alii*, 1983). The limited distribution of the basalts (and associated hydrothermal waters) in the Animas Basin suggest that fewer conduits for gas migration are available than in the San Bernardino Basin. The relatively low flux of deep-source CO_2 leads to a significantly lower proportion of Na-CO_3 minerals in the suite of potential evaporites, and the lack of trona deposition.

To our knowledge, input of deep-source CO_2 to aquifers has not previously been considered to play a significant role in trona formation, but our analysis above indicates it plays a critical role in the production of trona-precipitating groundwater in the San Bernardino Basin. Jones (1966) does mention that "some" carbon dioxide may derived from sources such as "deep circulation from some fault zones or thermal areas," but that the CO_2 for hydrolysis is "derived primarily within soils which support a P_{CO_2} significantly above that of the atmosphere because of biotic activity," and states that carbonate brines in the western USA "derive their carbonate content from silicate hydrolysis at the normal temperatures of weathering." The association of several deposits of trona with oil shales has led to the proposal that, in addition to the presence of high-Na rocks, input of CO_2 from decaying organic matter can help drive trona formation (Youxun, 1985). For some deposits, secondary processes such as sulfate reduction are also invoked (e.g. Dyni, 1998), but these processes are not considered important in driving the formation of trona, only for producing extremely pure deposits. If deep-source CO_2 input is a key factor in driving the San Bernardino waters toward forming trona upon evaporation, it is possible that it is also doing so in other modern basins, and has been a factor in the formation of trona deposits in the past.

Characteristics of the San Bernardino Basin that may lead to trona formation

Faulting and magmatism are two phenomena that can form conduits for the transfer of deep-source CO_2 to aquifers. In the USA, evaporite deposits are

relatively common in the Basin and Range physiographic province due to closed-basin topography that has led to the formation and desiccation of large lakes in the geologically-recent past. Because the Basin and Range is a region of crustal extension, faults are common, and numerous basins have experienced magmatism; however Na-CO_3 minerals are relatively rare among the evaporites that are present. As a result, it would be desirable to identify some less-generalized trait or traits of the San Bernardino Basin that could be associated with the CO_2 input.

The major geologic uniqueness of the San Bernardino Basin (compared to its neighboring basins) is the presence of the magmatically-active accommodation zone and the associated significant Late Tertiary and Quaternary basaltic volcanism. Based on our analysis of the basin geology (Earman *et alii*, 2003), it appears that the basalts are associated with a regional tectonic segmentation boundary that can be classified as an oblique, antithetic, anticlinal accommodation zone, a structure that "accommodate[s] the transfer of strain between overlapping zones or systems of normal faults" (Faulds and Varga, 1998). Such structures cause crustal thinning, and are often associated with magmatism, thus increasing the potential for CO_2 injection.

Papke (1976) describes the occurrence of evaporites in Nevada. The three major deposits of Na-CO_3 minerals (trona and gaylussite) discussed in the report appear to be associated with zones of accommodation or attenuation (both of which cause crustal thinning) that have experienced basaltic magmatism (Faulds and Varga, 1998; Francis and Walker, 2001; Maurer and Welch, 2001; McIntyre, 1990). In basins adjacent to those containing the three Na-CO_3 deposits, salts are dominated by gypsum or barite (Papke and Castor, 2003), supporting the concept that basins with tectonic boundaries that cause crustal thinning can have distinct groundwater chemistry that favors Na-CO_3 mineral formation. Other Na-CO_3 deposits in the USA are found in

association with the Columbia River flood basalts; these basalts are associated with crustal rifting (Hooper, 1990).

Smoot and Lowenstein (1991) list the major sodium carbonate deposits in the world: the Green River Formation (Wyoming, Colorado and Utah, USA), the Wucheng Basin (China), and Searles Lake (California, USA); present-day lakes described as having the potential to precipitate sodium carbonate minerals are Mono Lake (California, USA), Owens Lake (California, USA), Deep Springs Lake (California, USA), Abert Lake (Oregon, USA), Lake Magadi (Kenya), and Lake Chad (Chad and Cameroon).

Review of ancient trona deposits

The Green River Formation is the largest known deposit of trona in the world (Dyni, 1996). There is evidence that volcanism was active at the time of deposition, as "significant quantities of dacitic ash" were added to the lakes from which the trona formed (Dyni, 1991), but the deposit does not appear to be related to basaltic volcanism and/or significant crustal thinning (Bradley, 1964). However, the size of the trona deposits of the Green River Formation is not their only unique feature. The Green River tronas are one of only two known Eocene deposits; the other such formation is the Wucheng deposit in Henan, China (Youxun, 1985). Other similarities between the Green River and Wucheng tronas are that they are both associated with oil shales, and that neither is located near an area of basaltic magmatism (Bradley, 1964; Youxun, 1985). As described by Youxun (1985), an abundant supply of CO_2 is needed to form trona; such a supply of CO_2 could easily be produced by decomposition of the remains of planktonic organisms associated with the oil shales present in both the Green River and Wucheng deposits. Na^+ must also be present in abundant quantities—the presence of the silicic volcanic ash associated with the Green River deposit and granitic/rhyolitic metamorphic and igneous rocks associated with the Wucheng deposit

(Youxun, 1985) account for this—silicate hydrolysis of the minerals in these rocks readily explains the high ratio of sodium to other cations. A large trona deposit in Turkey is accompanied by bituminous shale (Helvaci, 1998), and Dyni (1998) notes that many of the known buried trona deposits have been discovered accidentally during exploratory drilling for fossil fuels.

Review of recent trona deposits and present-day Na-CO_3-type lakes

The Searles Lake evaporites (Eugster and Smith, 1965) are a significant evaporite deposit that is rich in trona. The evaporites found today were formed from a Pleistocene lake that was fed with water from Owens Lake; the Owens River, which flows into Owens Lake, is supplied primarily from tributaries originating in the Sierra Nevada, a range that is predominantly composed of granitoids (quartz and feldspar-dominated phaneritic igneous rocks). The Owens River has several tributary streams that drain the Long Valley caldera, which has been active for at least 200 kyr (Sorey *et alii*, 1998), and as long as 740 kyr, based on the age of the associated Bishop Tuff. The Long Valley caldera is currently emitting large amounts of gas with helium R/R_a values of about 4 to 5 and CO_2 concentrations typically in excess of 97 % (Hilton, 1996). As previously described, Owens Lake receives inflow from the Owens River, which has several tributary streams that drain the Long Valley caldera; the lake itself is located along an accommodation zone (Stewart *et alii*, 1998) that may be a source of additional CO_2. Mono Lake is located adjacent to the Long Valley caldera, and samples of gas collected at the shoreline of the lake have R/R_a values of about five and contain in excess of 98 % CO_2 (Hilton, 1996), giving direct evidence of magmatic CO_2 input. Deep Springs Lake is a "fault trough pond" (Jones, 1966) formed by the Deep Springs fault which has experienced significant activity (Lee *et alii*, 2000; Schroeder *et alii*, 2002); Deep Springs Valley also contains Late Pleistocene basalt flows. Abert Lake and the nearby Alkali Lake (also a carbonate-type water) are in an area

identified by Stewart *et alii* (1998) as a synclinal accommodation zone and described by Pezzopane and Weldon (1990) as a zone of active shear. Lake Magadi is located in the East African rift (Jones *et alii*, 1977). Lake Chad is located at the intersection of the Termit and Bornu rift basins of the West African rift system, where faulting has been active during the Cenozoic (Genik, 1993; Pouclet and Durand, 1984); a number of oil and gas discoveries have been made nearby (Genik, 1993). In addition to the opportunities for CO_2 injection, there are granitic/rhyolitic rocks present in all the settings described above, and active Quaternary basic and intermediate volcanism (Jones, 1965; McConnell, 1967; Pretti and Stewart, 2002; Sherlock *et alii*, 1988; Vicat *et alii*, 2002).

Trona precipitation by waters in the Owens River Basin

To test the theory that injection of CO_2 is an important factor contributing to trona formation, SNORM was used to determine the minerals that would form from a number of stream waters draining a granitoid terrane. Pretti and Stewart (2002) report the chemical compositions of 20 streams in the Sierra Nevada. One stream flows mostly through Pre-Mesozoic sedimentary rocks; the rest flow either mostly or entirely through Mesozoic granitoids. Three of the streams drain the Long Valley caldera; the remainder do not. Sorey (1985) describes the chemistry of waters from eight springs and one well in the Long Valley caldera. Data for the 27 samples from these two studies which had complete major-ion analyses reported were entered into SNORM (Table 2-3). The results (Figure 2-14) show that eight of the 10 samples from Long Valley caldera would yield trona under evaporation, and seven would also yield burkeite. Of the 17 samples not associated with the caldera, nine would not yield any $Na\text{-}CO_3$ minerals; the remaining eight streams would yield some pirssonite, and seven would also produce burkeite. None would produce trona. This suggests that simple weathering of granitoid rocks in the Sierra Nevada does not produce a high enough

Sample No.	Name	Source	LVC
1	Deadman Creek	A	yes
2	Hot Creek	A	yes
3	Casa Diablo Well	B	yes
4	Colton Spring	B	yes
5	Hot Creek Gorge Spring	B	yes
6	Little Hot Creek Springs	B	yes
7	Meadow Spring	B	yes
8	Big Springs	B	yes
9	Laurel Spring	B	yes
10	Casa Diablo Hot Springs	B	yes
11	[no sample]	-	-
12	Convict Creek	A	no
13	McGee Creek	A	no
14	Hilton Creek	A	no
15	Rock Creek	A	no
16	Pine Creek	A	no
17	Bishop Creek	A	no
18	Big Pine Creek	A	no
19	Birch Creek	A	no
20	Goodale Creek	A	no
21	Sawmill Creek	A	no
22	Independence Creek	A	no
23	Shepherd Creek	A	no
24	Lone Pine Creek	A	no
25	Cottonwood Creek	A	no
26	Ash Creek	A	no
27	Summit Creek	A	no
28	Nine Mile Canyon Creek	A	no

Table 2-3. Tabulation of information regarding data used in SNORM modeling of Sierra Nevada waters. Samples with source = "A" from Pretti and Stewart (2002), samples with source = "B" from Sorey (1985). "Yes" in LVC column indicates a sample associated with Long Valley caldera, "no" indicates a sample not associated with the caldera.

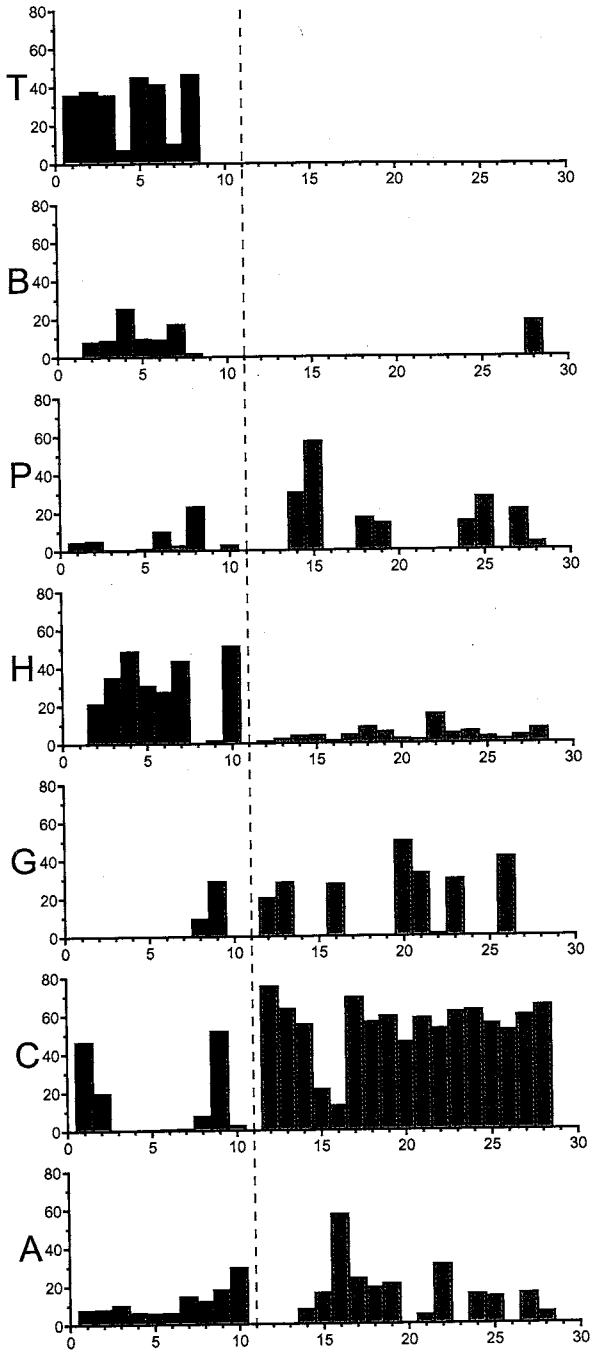

Figure 2-14. Plots showing mass percentages of salts that would form due to evaporating waters from the Sierra Nevada. X-axis values represent sample number, y-axis values represent mass percentages of the salt/salt groups that would form upon evaporation. Samples 1 through 11 are waters from Long Valley caldera; "sample 12" has no data, samples 13 through 27 are waters not associated with Long Valley caldera. Y-axis label abbreviations are as follows: T = trona; B = burkeite; P = pirssonite; H = halite; G = Gypsum + glauberite [$CaNa_2(SO_4)_2$] + syngenite [$CaK_2(SO_4)_2 \cdot H_2O$]; C = calcite + dolomite; A = apthitalite [$K_3Na(SO_4)_2$] + thenardite.

ratio of $CO_3^{2-}{}_{TOT}$ to Ca^{2+} to exhaust Ca^{2+} during calcite precipitation. The result is either no evaporites containing Na and CO_3^{2-} or sodium-calcium carbonate evaporites rather than trona. In contrast, the waters receiving input of CO_2 from the Long Valley caldera typically yield trona. Given that these streams drain mineralogically-similar rocks, this difference is attributable to some combination of direct conversion of CO_2 to HCO_3^- and increased silicate hydrolysis associated with higher PCO_2.

Trona deposition in Searles Lake

If precipitation of trona from the waters of closed-basin lakes is primarily derived from solutes that are introduced during chemical weathering of silicic igneous rocks, then the deposition rate of the trona should be roughly constant over long periods of time, since chemical weathering is a continuous process. This inference can be tested at Searles Lake, California, the terminus for the Owens River during most of the Pleistocene and one of the most important trona deposits in the western USA (the town associated with mineral extraction from the lake deposits is named Trona).

A nearly continuous record of deposition in Searles Lake for the past 3.2 Myr is provided by the deep core KM-3 (Smith, 1983). The mineralogical analysis of this core shows that trona deposition was episodic, with the evaporates deposited in the intervals ~350 to ~250 ka and 40 to 10 ka dominated by a trona/halite assemblage and the intervening periods dominated by the assemblage pirssonite (and its thermal polymorph gaylussite)/dolomite/thenardite (Jannik *et alii*, 1991; Smith, 1983). These assemblages are very similar to those calculated by SNORM for waters from the Owens River tributaries. Those tributaries affected by magmatic CO_2 addition (the ones draining Long Valley) produced normative salt assemblages dominated by trona/ halite/burkeite and the remaining tributaries, dominated by weathering of granitic rocks, produced pirssonite/gypsum/glauberite/syngenite/calcite/dolomite/apthitalite /thenardite assemblages (Figure 2-14).

The variation of evaporite mineral deposition with time suggests the Owens River experienced intervals during which the river chemistry was dominated by magmatic CO_2 injection and accompanying geothermal activity, with the river chemistry during the remainder of the time dominated by weathering-derived solutes. Similar conclusions have previously been drawn by Smith (1976) regarding the sources of lithium and boron in Searles Lake. Discharge of CO_2 and geothermal activity has been observed to vary dramatically during the period of human record (Farrar *et alii*, 1995), thus it is not improbable that it has also varied over longer time periods. In summary, the temporal variation of trona deposition in Searles Lake, and the nature of the evaporite mineral assemblages that are associated with this variation, strongly support the hypothesis that "excess" CO_2 injection is a prerequisite for deposition of trona.

CONCLUSIONS

Our work in the San Bernardino Basin shows that input of magmatic CO_2 can influence water chemistry such that trona would precipitate upon evaporation. The fact that the San Bernardino's neighboring basins (which are mineralogically similar) would not yield trona contradicts the standard theory that trona formation is caused solely by silicate hydrolysis of granitic/rhyolitic rocks in closed basins.

Given the number of basins in the world dominated by granitic/rhyolitic rock, deposits of sodium carbonate minerals are much less common than one would expect based on the standard theory for their origin. Groundwater in the San Bernardino Basin would form trona upon evaporation, and while hydrolysis of silicates in rhyolitic tuff does influence chemical evolution of the basin's water, injection of magmatic CO_2 is a significant control on the water chemistry. For all the major deposits of trona and present-day Na-CO_3 lakes, there is either direct evidence of CO_2 injection or a geologic setting such that CO_2 injection appears plausible. Based on this evidence, it appears

that along with the presence of granitic/rhyolitic rock, the addition of "excess" CO_2 (from the mantle, microbial respiration, or some other source) is an important condition for the formation of trona. Our analysis of streams draining the Sierra Nevada supports this hypothesis, showing that those which have chemistry resulting from simple weathering of granitoids yield either no sodium carbonates or Na-Ca-CO_3 minerals, while those also receiving CO_2 injection yield trona. The intermittent nature of trona deposition in Searles Lake also supports the hypothesis, showing that granitoid weathering alone does not appear to drive trona formation. The association of Na-CO_3 deposits with CO_2 injection could help explain the distribution of sodium carbonate minerals and be useful as a prospecting tool.

Chapter 3: Groundwater recharge in the Chiricahua Mountains (Arizona, USA) and transfer to an adjacent alluvial basin

INTRODUCTION

In the southwestern USA (hereafter referred to as 'the Southwest'), most groundwater is obtained from alluvial aquifers in extensional basins. In today's climatic regime, opportunities for groundwater recharge are limited. Average annual precipitation is relatively low in low-elevation valley floors, but often two to three times higher in the adjacent mountain ranges. As a result, there may be no diffuse infiltration through valley floors (Phillips, 1994; Walvoord *et alii*, 2002), and groundwater replenishment through the valley floors may only occur where 'focused recharge' is possible, such as the zones under drainage channels (Blasch *et alii*, 2004; Goodrich *et alii*, 2004).

The idea that precipitation falling on mountain ranges is an important source of water for Southwestern basin aquifers was recognized prior to the 1900s (Barker, 1898). In the first half of the 20th century, the means of water transfer from mountains to basin aquifers was conceptualized in the "mountain-front recharge" scenario. In the early applications of this scenario, mountain blocks were considered to be impermeable (or of negligible permeability), so at most a negligible portion of rainfall or snowmelt would infiltrate and possibly become recharge in a mountain block. The water would instead flow downslope in stream channels until reaching the permeable alluvial material at the base of the mountain block; at this point, infiltration would commence, with some portion of the infiltration becoming recharge to the basin aquifer.

While this form of recharge likely accounts for a significant proportion of recharge in nearly all Southwestern ranges, observation of mountain systems exposes flaws in the 'traditional' mountain-front recharge scenario. In many mountain ranges,

there are numerous springs present, indicating that groundwater recharge and flow occur in the supposedly-impermeable mountain block. Additional evidence for groundwater recharge and movement in mountain blocks comes from numerous reports of groundwater inflow into tunnels made in mountains for mineral extraction or transportation purposes. For example, a 2.7-km-long tunnel into the Wasatch Mountains (Utah, USA) at 2500 m above sea level has an annual discharge of approximately 4.5×10^5 m^3 (Parry *et alii*, 2000); four mountain tunnels in southern California (USA) described by Feth (1963) have annual discharges ranging from 3×10^5 to 2×10^6 m^3. Most large mountain ranges have perennial streams; observation of one such stream during this study shows that it flows even when there has been no measurable precipitation for two months, and the only snow remaining in the range is found in small (less than 0.5 m^2 in area and less than 5 cm in depth), isolated patches in shaded areas. If the theory that no groundwater is present in the mountain block and overland flow is generated only by rainfall or snowmelt is correct, the streamflow described above would be impossible.

The realization that the traditional conceptual model for mountain-front recharge is flawed is not new. In the early 1960s, J. H. Feth (1963) published a paper in which he stated:

> Information accumulated by many people in the past 10 to 15 years no longer permits unvarying acceptance of the concept that ground-water basin margins can be drawn at the contact between alluvium and consolidated rock, or indeed that mountain ranges are necessarily barriers between ground-water basins. In some places, at least in the semi-arid West, the mountains must be considered major sources of what is here termed "hidden recharge," which is defined as subsurface percolation of water from basin-margin mountains directly into aquifers in the valley basins.

Feth (1963) went on to provide several examples of basin aquifers where the traditional mountain-front recharge model failed to explain observed conditions. In these systems, the traditional model produced imbalanced continuity equations, and/or could not produce reasonable explanations of observed chemical content and piezometric surfaces.

Today, many researchers recognize the fact that mountain blocks can transmit significant quantities of water to basin aquifers. In recent years, a number of authors have used the term 'mountain-front recharge' to describe both downward infiltration from overland flow into a basin aquifer and subsurface transfer of water from the mountain block to the aquifer (e.g. Anderholm, 2001; Manning and Solomon, 2003; Wilson and Guan, 2004; Wilson *et alii*, 1980). Other authors who realize that the traditional mountain-front recharge concept is not correct continue to honor the traditional meaning of term, and describe water transfer from mountains to a basin aquifer as a combination of mountain-front recharge and 'mountain block recharge' (e.g. Hevesi and Flint, 2000; Jacobson *et alii*, 2000).

Although contradictions to the traditional mountain-front recharge model are available through direct observation and sources such as Feth (1963), the concept has not been abandoned. Recent research often considers mountain blocks to be capable of transmitting only negligible quantities of water. Examples include constructing groundwater flow models in which mountain ranges are represented by "impermeable walls" that form "no flow boundaries" (Bakker *et alii*, 1999), although they are highly fractured (Labotka and Albee, 1990; McKenna *et alii*, 1998; Sears, 1955); statements such as "The aquifer systems are bounded below and along the mountain fronts by consolidated bedrock that forms a relatively impermeable boundary to ground-water flow" (Hanson *et alii*, 2003); and the development of a conceptual model for the Great Basin (USA) "to constrain the distribution of recharge in regional models that include

or are surrounded by high mountainous areas producing runoff with subsequent infiltration at lower elevations…[with] the concept and method…applicable to any region where excess precipitation in upland areas is conveyed to lower elevations before it infiltrates" (Stone *et alii*, 2001). Examples such as these show that in many cases, mountain blocks are simply considered impermeable, without examination of the system in question as to the viability of infiltration, recharge, and groundwater transmission.

Wilson *et alii* (1980) recognized that the permeabilities of the soils and bedrock making up a given range will affect the proportions of recharge to an adjacent alluvial aquifer from these two processes. In other words, each mountain-basin system can be expected to have a unique ratio of water transfer via mountain-front and mountain block recharge, based on the geology and climate. Anderson *et alii* (1992) quoted Wilson *et alii* (1980) on this matter, but went on to state that, although a subsurface supply of water from the mountain block may be an important control on recharge to alluvial aquifers, "supporting information" was lacking. In the most recent work dealing mountain-basin water transfer, Wilson and Guan (2004) state that "Hydrologic science above the mountain front, incorporating a full view of the entire mountain block system…is an area ripe for significant advancement." The works of Anderson *et alii* (1992) and Wilson and Guan (2004) show that, although 30 years have elapsed since Feth (1963) demonstrated the that subsurface transfer from mountain blocks is an important source of water for basin aquifers, groundwater recharge and movement in mountains has been the object of little attention.

The majority of studies that deal with mountain-basin water transfer deal only tangentially with the mountain block itself. These studies (e.g. Anderholm, 2001; D'Agnese *et alii*, 1994; Lichty and McKinley, 1995) are designed to estimate the volume transferred to a basin aquifer each year, and use of one or more of the

following methods: solving a water-balance equation for the basin; application of the Maxey-Eakin method (Avon and Durbin, 1994), in which the amount of precipitation received is scaled by empirical coëfficients to determine the amount of recharge; or the method of Dettinger (1989), which scales precipitation amounts by using chloride mass balance to estimate the degree of evapotranspirative loss prior to recharge. Chavez *et alii* (1994) estimate water transfer by using a variation of the Maxey-Eakin method in which input variables are viewed as stochastic.

Other investigations have included closer examination of the hydrogeology of a mountain range. Manning (2002) uses a numerical model incorporating dissolved gases in water, water temperatures, water ages, and range geology to determine the proportion of groundwater in a basin aquifer derived from mountain-block recharge, and to constrain groundwater circulation paths. Cunningham *et alii* (1998), Olson (1982) and Mohrbacher (1984) investigate movement of water from the Santa Catalina Mountains (Arizona, USA) to an adjacent basin. Olson (1982) and Mohrbacher (1984) use major ion chemistry, stable isotopes of hydrogen and oxygen, and geology to examine groundwater flowpaths; Cunningham *et alii* (1998) use tritium, deuterium, and ^{18}O in waters along with range geology to examine water residence times and flowpaths, and they show that waters transferred to the basin via stream infiltration have tracer signatures distinct from those transferred via fractures in the mountain block. Winograd *et alii* (1998) and Abbott *et alii* (2000) use deuterium, and ^{18}O to determine the seasonality of recharge in mountains; Abbott *et alii*(2000) also use the data to estimate zones of groundwater recharge. Caine and Tomusiak (2003) use detailed mapping of geology (including fractures) to estimate permeability, developing a conceptual model of groundwater flow and storage in the Front Range (Colorado, USA). Summers *et alii* (1972) create a water-table map for the Magdalena Mountains (New Mexico, USA) using data from wells, springs, and mine excavations, and

relate observed differences in dissolved-ion chemistry to geologic units in the range. Szecsody *et alii* (1983) and LeFevre (1999) combine geology, major-ion chemistry, groundwater ages, and deuterium and ^{18}O to trace water movement from mountains to adjacent basins and estimate recharge rates.

Given the importance of groundwater in the Southwest and the major role played by mountains in providing water to basin aquifers, Wilson and Guan (2004) appear correct in their assessment that more research regarding groundwater in mountain blocks is called for. One area that is especially in need of study is the delineation of groundwater recharge zones in mountains. With the notable exception of Manning's (2002) work, delineation of recharge zones in mountain ranges has been typically performed using deuterium and ^{18}O, but this method allows determination a maximum recharge elevation, not a definitive value (this issue will be discussed in more depth in a later section). A related topic also deserving of research is determining if high-elevation springs are hydraulically linked to lower-elevation groundwater in the ranges and adjacent basins. High elevation springs are often assumed to be part of "local systems that are not connected to surrounding and underlying groundwater" (Prudic *et alii*, 1995).

This investigations described in this paper were conducted as part of a study of groundwater in a Southwestern basin aquifer (the San Bernardino Valley, Arizona, USA, and Sonora, Mexico). Descriptions of the basin hydrogeology are provided in Chapters 1 and 2. Because the San Bernardino aquifer appears to receive at least 70 % of its water from one of its bounding ranges (the Chiricahua Mountains, Arizona, USA) (Figure 3-1). This paper will focus on the hydrogeology of the Chiricahuas and transfer of water from the Chiricahuas to the San Bernardino aquifer, extending the study conducted earlier from the alluvial basin margin to the crest of the range responsible for the majority of its recharge. Although a case study, given the limited

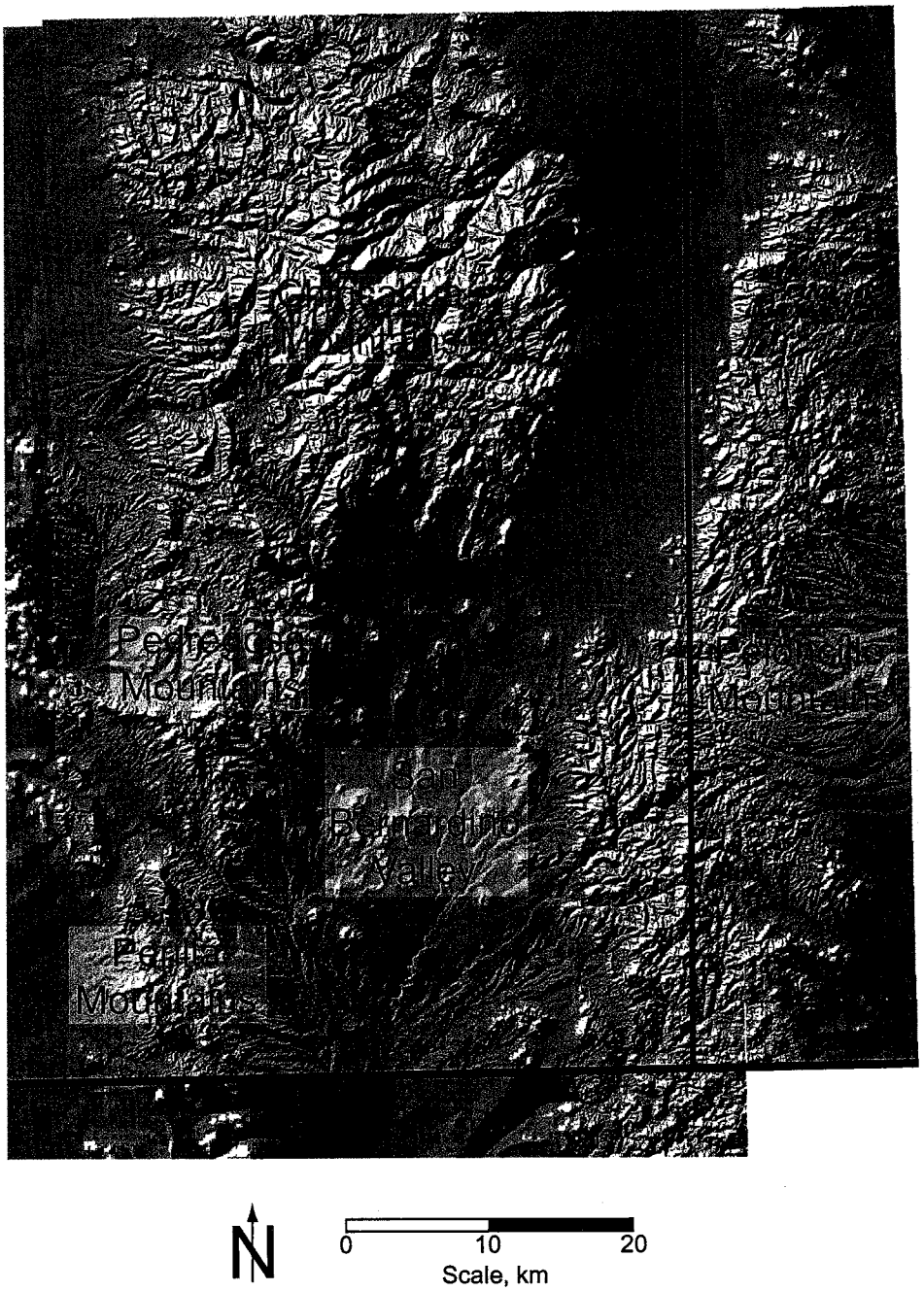

Figure 3-1. A. Locations of the Chiricahua Mountains and San Bernardino Valley, and nearby mountain ranges, southeastern Arizona, USA.

Figure 3-1 (continued) B. Locations of springs and wells described in this report. Sites are identified by numerals as follows: 1: Welch Seep, 2: Lower Rustler Spring, 3: Tub Spring, 4: Ash Spring, 5: Sulphur Spring, 6: Sycamore Spring, 7: Cottonwood Corral Spring, 8: Krentz Spring, 9: Anderson Well, 10: Ashurst Well, 11: Ranchita Well, 12: Twin II Well.

body of mountain groundwater research, additional case studies can provide insights into hydrogeologic regimes that have not yet been examined; in addition, comparison of case study results can lead to new generalizations applicable on a much broader scale. In addition to providing a mountain-centered study as called for by Wilson and Guan (2004), mountain recharge areas will be delineated, as will the potential hydraulic connectivity of mountain springs to basin aquifers. The study will utilize geology, major-ion chemistry, dissolved gases in groundwater, deuterium and ^{18}O in groundwater, hydraulics, thus utilizing a much broader spectrum of techniques than most existing studies of mountain groundwater.

A note on terminology: by strict definition, "groundwater recharge" refers to downward movement of water across the water table (Freeze and Cherry, 1979); but recent works also use the term to describe the non-vertical addition of fresh water to an alluvial aquifer from a mountain block (e.g. Anderson *et alii*, 1992; Wilson and Guan, 2004; Wilson *et alii*, 1980). For clarity, 'recharge' will be used in its strict sense, and the addition of fresh water to an alluvial aquifer from a mountain block will be called 'replenishment.'

BACKGROUND

Location

The Chiricahua Mountains are located in Southeastern Arizona (Figure 3-1A), approximately 10 km west of New Mexico, and approximately 40 km north of the USA-Mexico border. Locations of springs and wells discussed in this study are shown in Figure 3-1B.

Geology

The Chiricahua Mountains are primarily composed of volcanic rocks associated with the Turkey Creek and Portal calderas, although the range also contains sedimentary rocks that were present prior to caldera development (Bryan, 1989;

Pallister and du Bray, 1989). The development of the range is described by Pallister and du Bray (1997). Until approximately 27 Myr ago, the area now occupied by the Chiricahuas consisted of Paleozoic and Mesozoic sedimentary rocks that were mostly overlain by lava and ash deposits from at least two volcanic fields located outside the immediate area. At that time, a rhyolite magma chamber formed, and buoyancy from the magma caused uplift of the overlying rocks. About 26.9 Myr ago, as the magma made its way toward the surface, producing a number of large volcanic eruptions that covered the surface of the region with at least 500 m of ash. Emptying of the magma chamber led to collapse of its roof, forming the Turkey Creek caldera. Over the next 300 kyr, an upwelling dacite magma uplifted the center of the caldera, and emerged to form a moat deposit (between the caldera wall and the uplifted central portion of the caldera). Toward the end of this period, rhyolitic volcanos erupted, producing both ash and lava deposits. The development of the Portal caldera took place at about the same time as the Turkey Creek caldera, and followed essentially the same sequence of events, with the resurgence of the Turkey Creek caldera apparently causing the resurgence in the Portal caldera (Bryan, 1989). In the last 25.2 Myr, the Chiricahuas have been volcanically inactive, with the exception of minor basaltic eruptions on the eastern flank of the range associated with the Geronimo volcanic field of the San Bernardino Valley. The area is still active tectonically (Lynch, 1972; Pearthree, 1986). Basin-and-Range faulting has raised the Chiricahuas relative to its surroundings, and erosion has led to further development of topography.

Climate

The Chiricahuas are known as a "sky island" because the climate in the range is significantly different from that of the surrounding lowlands (Heald, 1975). Although there are no meteorological stations operating above 1655 m (the high point of the range is 2975 m), the biomes present at various elevations in the range

can provide constraints on temperature and precipitation amounts. In addition, the relationship between climate and elevation in southeastern Arizona (the region does include several high-elevation monitoring points) can be used to estimate conditions at elevations above the highest monitoring point in the Chiricahuas.

The lower portions of the range typically receive about 400 to 500 mm of precipitation a year, while the higher elevations receive over 900 mm (Western Regional Climate Center <http://www.wrcc.dri.edu>). Precipitation depths are available for both snow and rain. Assuming that water produced by melting snow would have a depth equal to 10 % of the snow depth (Jim Ashby, Western Regional Climate Center, personal communication, 2003), the precipitation at the base of the range is about 7 % snow; interpolation based on the proportion of snow in precipitation in southeastern Arizona as a function of elevation suggests that approximately 27 % of the precipitation at the crest falls in the form of snow (Western Regional Climate Center <http://www.wrcc.dri.edu>).

Local temperature data show that mean annual temperatures near the base of the Chiricahuas (1500 to 1650 m) are about 12 to 15 °C, depending on location. Interpolation based on the local lapse rate suggests that the mean annual temperature at the highest point in the range is about 2 °C (temperature and elevation data are provided in Appendix 7).

INVESTIGATIONS OF GROUNDWATER RECHARGE AND MOVEMENT

Several methods were used to determine the zones responsible for groundwater recharge in the Chiricahuas and transfer of water from the Chiricahuas to the San Bernardino aquifer. The characteristics of the rock units in the range were examined to determine their propensity for transmitting water; similarly, the locations of groundwater discharge in the range were examined in order to determine how the juxtapositions of the various adjacent units affect groundwater flow. Stable isotopes

of oxygen and hydrogen were used to investigate the proportions of rain and snow in recharge and to determine the altitude zone(s) in which precipitation important for recharge falls. Gases dissolved in groundwater were used to determine the elevations at which recharge takes place. Major-ion content of water was used to determine how interaction with various geologic formations affects the chemical signature of groundwater, and then to determine through which units water in the San Bernardino aquifer has flowed.

Geologic controls on groundwater recharge and movement

The geology of the Chiricahuas has been mapped most recently and in the most detail by du Bray *et alii* (1997). A generalized version of their map is shown in Figure 3-2A. This map shows hydrostratigraphic units (Seaber, 1998); in some cases, these are identical to geologic units, but many of the hydrostratigraphic units combine two or more geologic units. The topography of the Chiricahuas is shown along with the hydrostratigraphic units in Figure 3-2B so that the elevation zones of outcrops can be observed.

Unit 1 is made up of intracaldera tuffs that are platy and have significant primary porosity. Unit 2 is composed of resurgent intrusion and ring-dike rocks that are massive and have low primary porosity, but are highly jointed, and likely able to conduct water due to their secondary porosity. Unit 3 is a combination of two lava deposits that differ lithologically (dacite/monzonite versus rhyolite), but are grouped together here because they are both extrusive deposits that have low primary porosity and contain few faults or joints that could impart significant secondary porosity. Unit 4 is a mix of tuff and lava deposits; it is fractured in some areas, and has potential to transmit water through the tuff zones and fractured areas. Unit 5 has lavas, tuffs, and volcaniclastic sedimentary rocks. In some areas it is well fractured. Unit 6 is made up of sedimentary rocks (primarily Cretaceous and Jurassic in age) that are highly

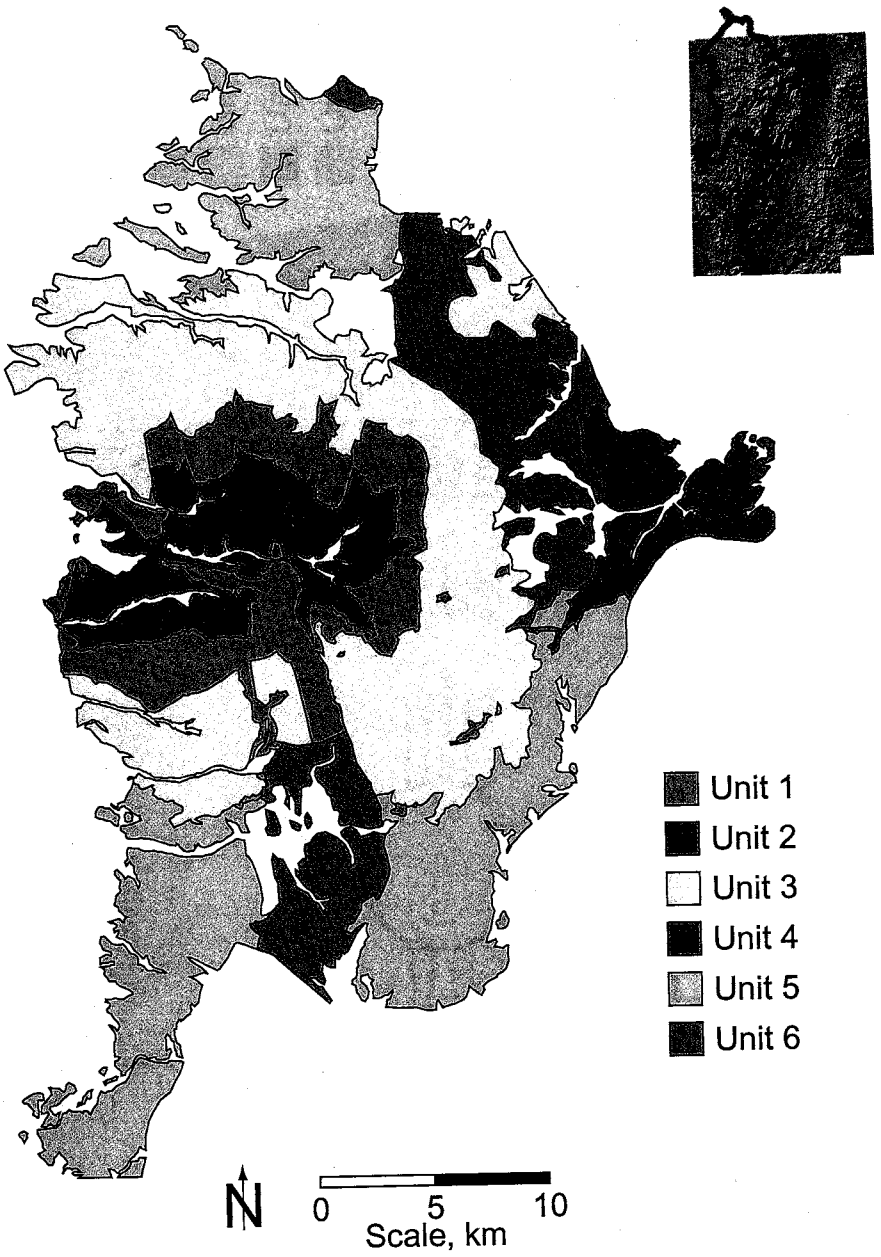

Figure 3-2. A. Generalized geology of the Chiricahua Mountains, after du Bray *et alii* (1997). Inset base map covers the same area as Figure 3-1, the highlighted area on the inset shows the region covered by the geologic map. Brief hydrostratigraphic unit descriptions are as follows (more complete descriptions are given in the text): Unit 1: intracaldera tuffs, Unit 2: resurgent intrusion and ring dike rocks, Unit 3: lava deposits, Unit 4: tuff and lava deposits, Unit 5: lavas, tuffs, and volcaniclastics, Unit 6: sedimentary rocks.

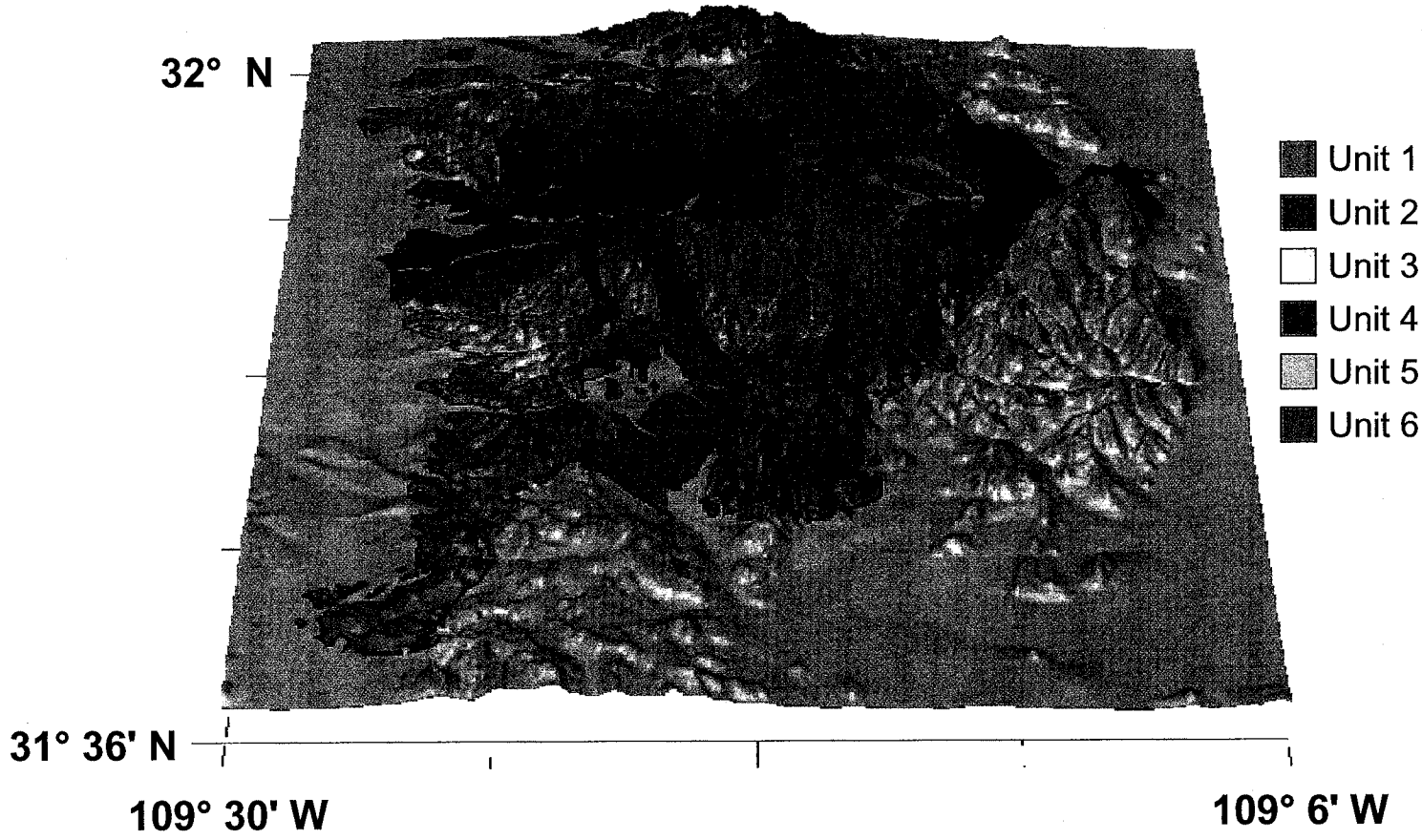

Figure 3-2. (continued) B. Generalized geology (after du Bray et al., 1997) superposed on topography.

fractured and transmissive. Although not given a unit number, Quaternary alluvium is present in drainage channels and at lower elevations in the range.

Based on the characteristics of the rocks in the range, it seems likely that Units 1 and 6 are the primary transmitters of water, with some contribution from Units 2, 4, and 5. Areas where Unit 1 or Unit 6 are present at the surface are likely to be more conducive to infiltration and recharge than other zones. The areas where Unit 3 is present do not appear to be likely zones of significant groundwater movement at or near the surface, but underlying units may transmit water in the subsurface. Overland flow atop Unit 3 may be a significant means of transferring water to lower portions of the range; this issue will be discussed in a later section.

Unit 1, which has relatively high transmissivity, has a significant area of outcrop near the top of the range, but the rest of the high-elevation zone is occupied by outcrops of Unit 3, which is relatively impermeable (Figure 3-2B). Unit 6, which, along with Unit 1, has a high transmissivity, crops out only at relatively low elevations.

Unit 1 is also found in several areas away from the crest. Unit 1 has two 'fingers' extending down from the crest toward San Bernardino Valley (indicated by the solid black ellipses in Figure 3-3), which terminate against Unit 6. In addition, Unit 1 crops out in several locations in the eastern and southeastern portions of the range (indicated by the alternating black-brown ellipses in Figure 3-3). Unit 1 predates Unit 3 (in which the outcrops and fingers of Unit 1 are present), it is known to underlie some of the formations that make up Unit 3 (du Bray *et alii*, 1997); the relationship of these two units in the model of caldera formation (du Bray and Pallister, 1991) suggests that Unit 3 was deposited atop Unit 1, and Unit 1 is observed to underlie Unit 3 . These facts suggest that Unit 1 is most likely laterally continuous in the subsurface between the crest and the lower-elevation outcrops, providing a continuous conduit for water flow.

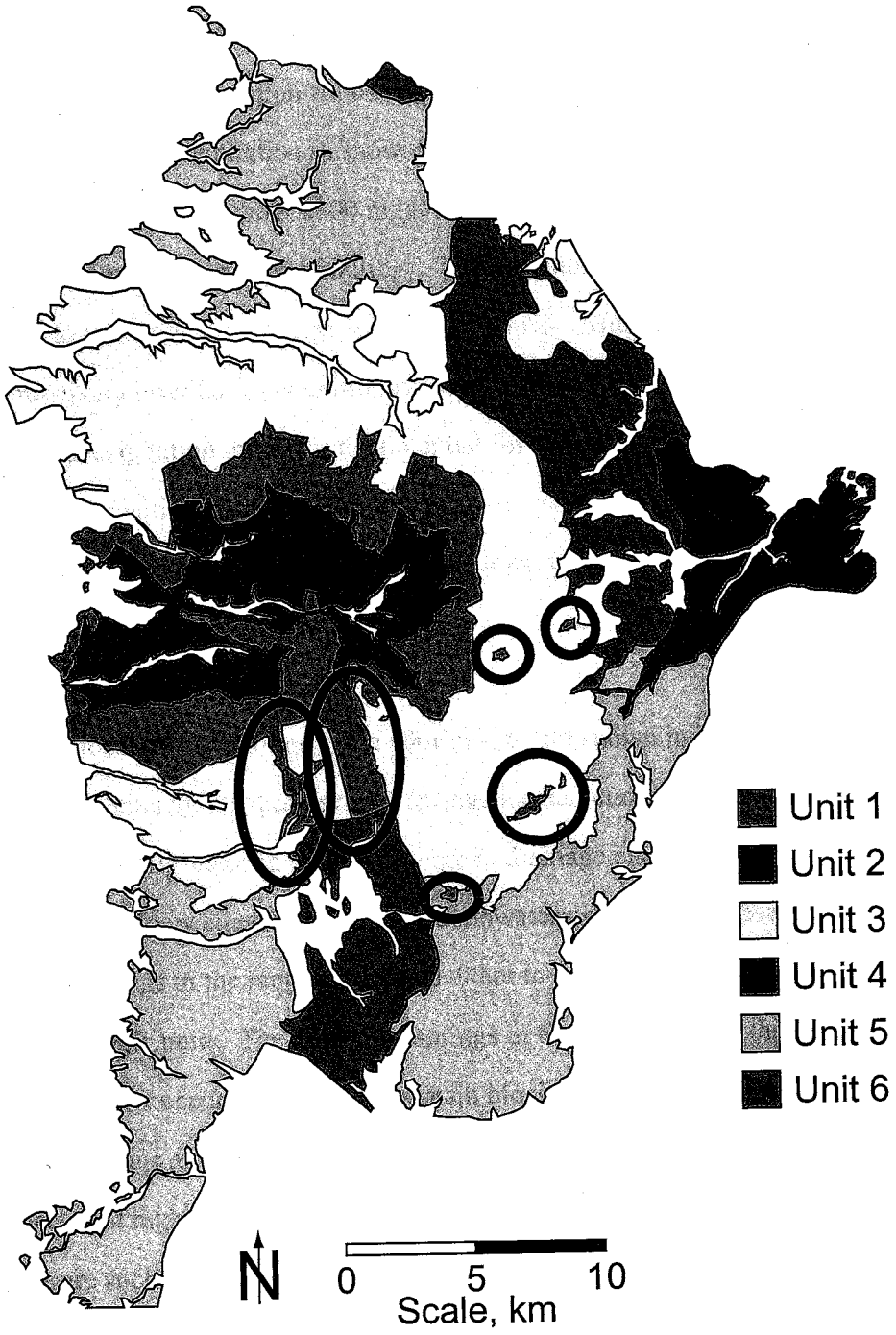

Figure 3-3. Locations of "fingers" (highlighted with solid black ellipses) and outcrops (highlighted by alternating black-brown ellipses) of Unit 1 (after du Bray *et alii*, 1997).

The elevations at which these units are present is important because of several characteristics of precipitation in the Chiricahuas. High-elevation zones receive more precipitation than low-elevation zones; high-elevation zones will receive a higher percentage of total precipitation as snow; and snowpack typically only accumulates in the Chiricahuas above about 2300 m (at lower elevations snow will typically be melted within one to four days of falling). The accumulation of snow is particularly important to groundwater recharge in the Chiricahuas. Much of the rainfall arrives during relatively brief but intense monsoonal storms in the summer. The high intensity of summer precipitation increases the potential for exceeding the infiltration capacity and triggering overland flow; in addition, evapotranspiration (ET) is at its peak in the summer. In contrast, snowmelt provides a long, relatively low-intensity pulse of infiltration during a season when ET is low.

Hydraulics

The locations of springs in the Chiricahuas are shown in Figure 3-4. In addition to previously-mapped springs, springs located during this study are shown. Nearly all the newly-mapped springs emerge in drainage channels, and were identified during periods of low streamflow when groundwater discharge was evident. The vast majority of springs in the range are related either to fractures or contacts between different geologic units. The numerous springs in the range support the idea that groundwater flow occurs within the mountain block.

No springs are present in Unit 1, but the greatest concentration of springs in the range occurs at high elevation along the Unit 1/Unit 3 contact. The dip and foliation of Unit 1 are such that groundwater (including that on the western-sloping west flank of the range) will flow to the east, so the line of springs at the Unit 1/Unit 3 contact is indicative of groundwater moving to the surface as it encounters the low-permeability Unit 3 after flowing through the high-permeability Unit 1. A spring at the downslope

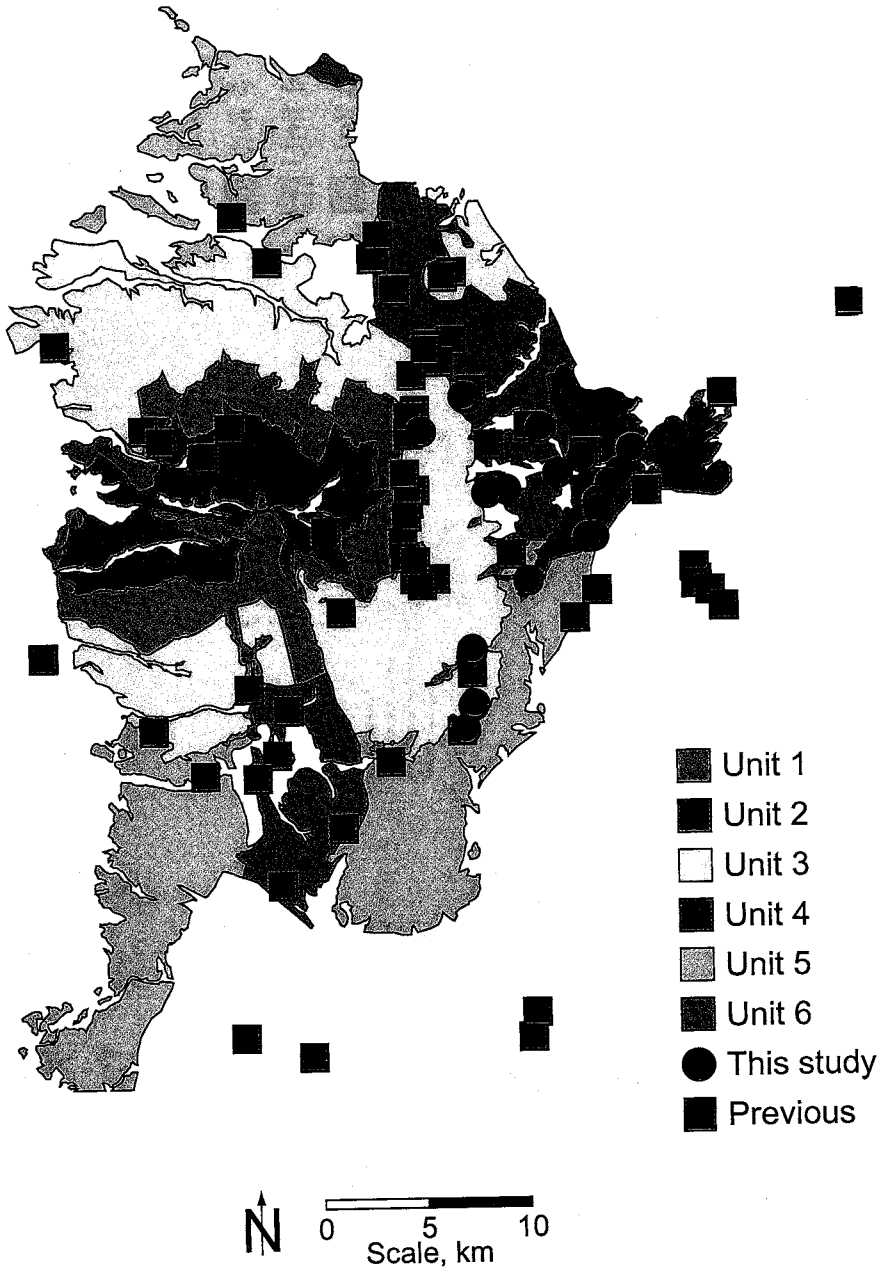

Figure 3-4. Locations of previously mapped springs (green squares) and springs mapped during this study (blue circles) in the Chiricahua Mountains **A.** Map view.

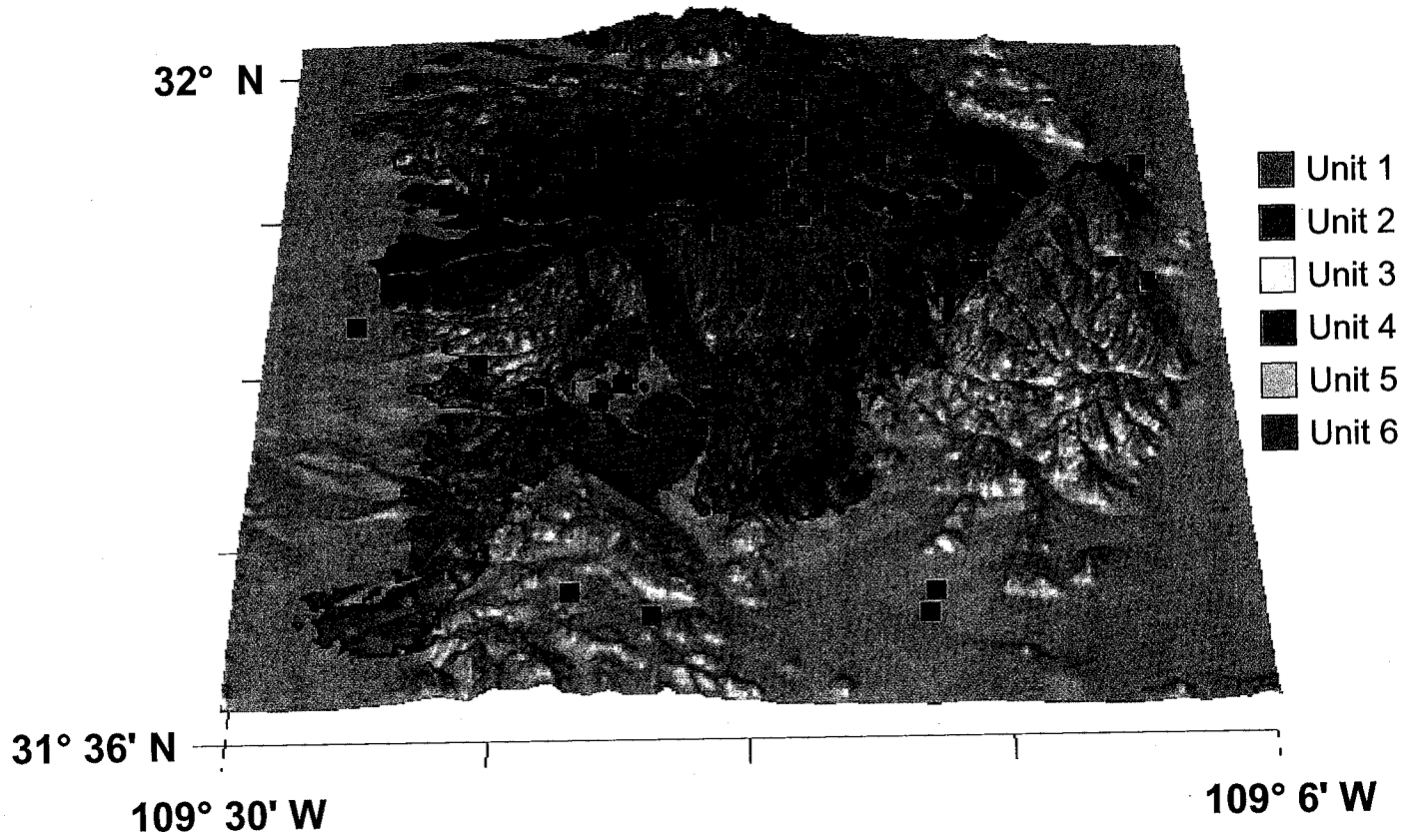

Figure 3-4 (continued) B. Spring and inflow locations superposed on topography.

contact of the small outcrop of Unit 1 and the surrounding Unit 3 (Figure 3-3) supports the continuity of Unit 1 in the subsurface and its importance for transmitting water to the southeast.

Many springs are located in Unit 6 or at a contact between Unit 6 and Quaternary alluvium. Because the alluvium has high permeability, it can readily transmit water that has been carried carried through the range by Unit 6; this water tends to emerge as springflow when encountering a fault or a local topographic low. The outflow from Unit 6/alluvium contacts supports the concept that Unit 6 is, along with Unit 1, responsible for transmitting a significant proportion of the groundwater in the Chiricahuas.

Major Ion Chemistry

For most groundwaters, the dissolved ion composition is controlled by interaction between the water and the rock through which it is/has been flowing. Because different rocks impart different chemical signatures to groundwater, the evolution of water chemistry can yield significant information regarding the rocks with which the water has been in contact.

Water samples were collected and analyzed as described in the "Hydrogeology" section of Chapter 1. A Piper diagram showing water chemistry from the Chiricahua Mountains and the portion of the San Bernardino Valley closest to the Chiricahuas is shown in Figure 3-5A (for detailed discussions of the chemical evolution of water as it flows through the basin, see Chapters 1 and 2; data represented in Figure 3-5A are provided in Appendix 8). The locations of the waters represented in Figure 3-5A are shown in Figure 3-5B.

Springs near the crest of the range discharge water that is dilute (total dissolved solids content is typically less than 50 mg/L), and are predominantly Ca^{2+}-Na^{+}/SO_4^{2-} -type waters. As these waters have only flowed through rhyolitic rocks which have

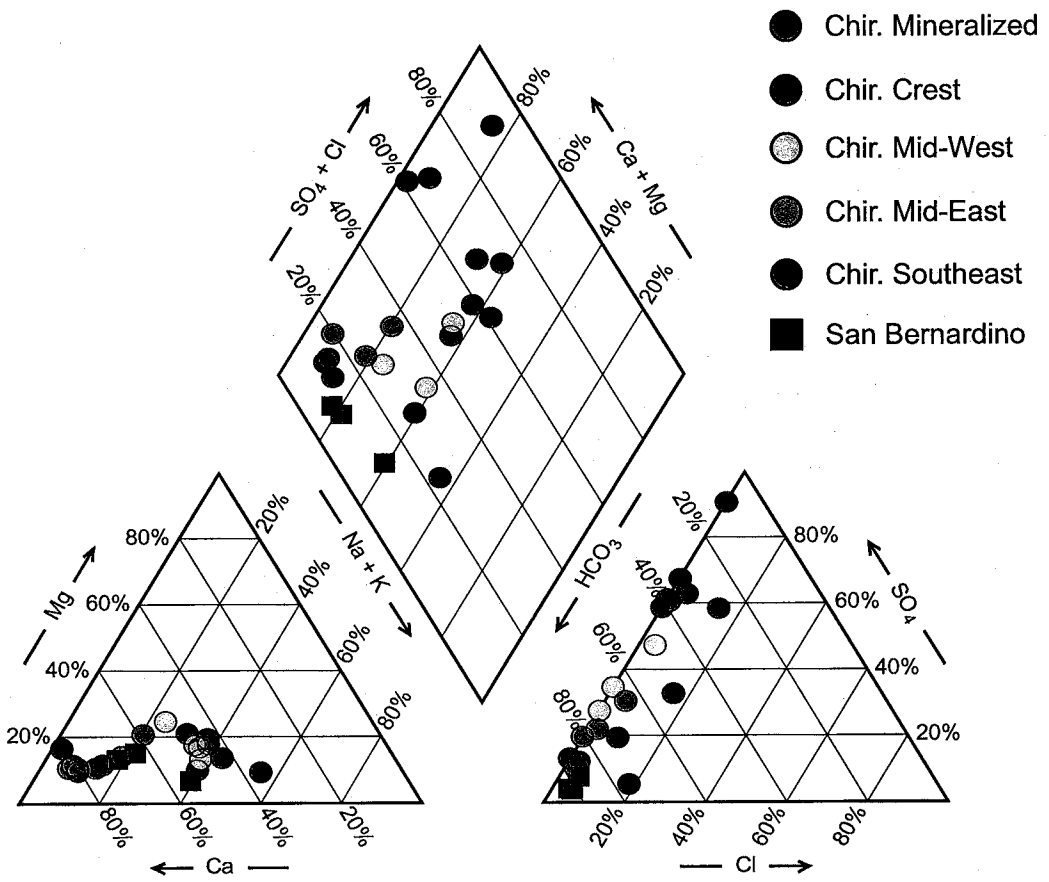

Figure 3-5. A. Piper diagram showing water chemistry of samples from the Chiricahua Mountains and northern San Bernardino Valley.

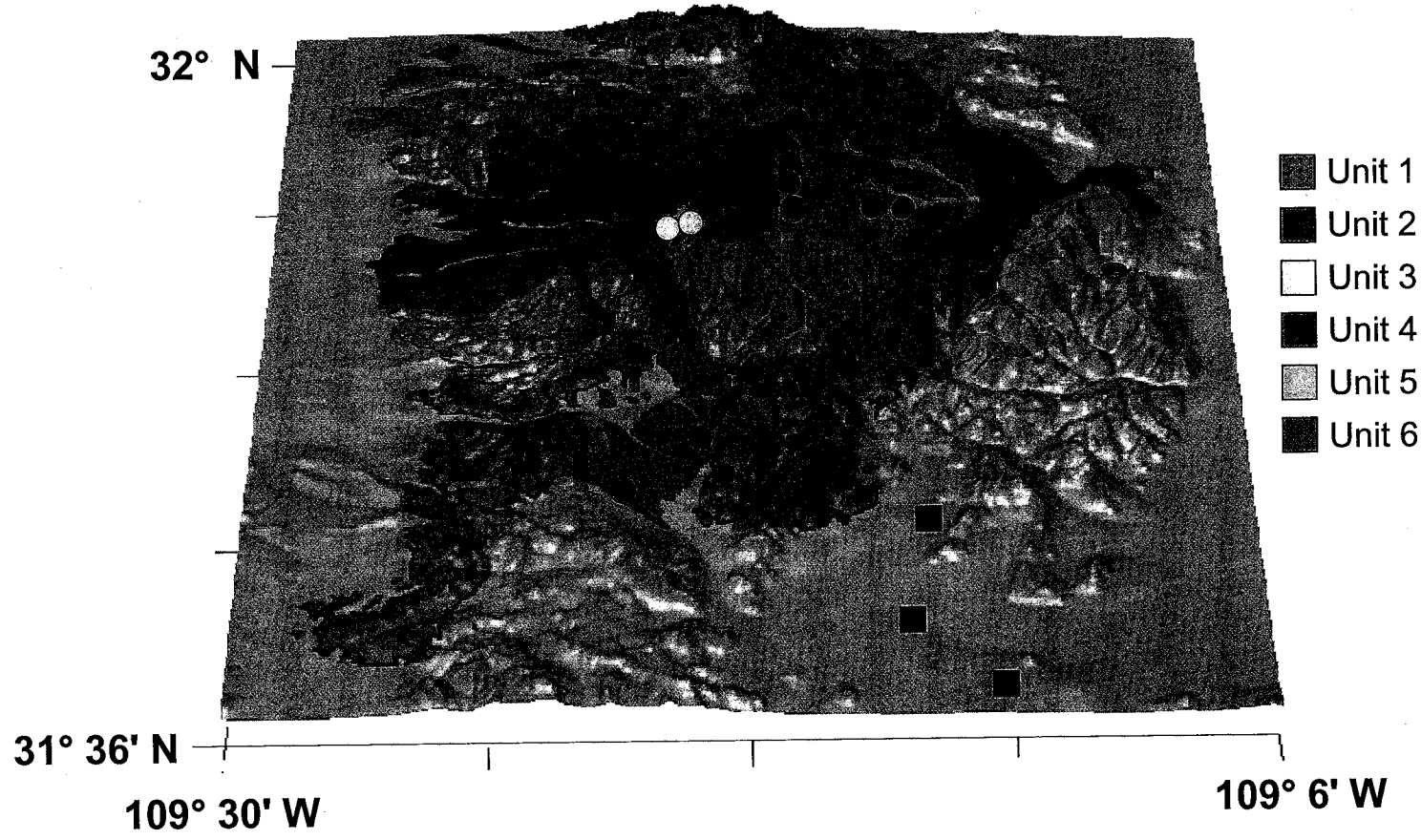

Figure 3-5 (continued). B. Map showing locations of samples represented in Figure 3-5A.

low calcium content and contain no sulfide minerals (du Bray and Pallister, 1995), the presence of such high proportions of calcium and sulfate is unusual. The most likely explanation is incorporation of airborne gypsum during the precipitation and infiltration/recharge processes. Thomas *et alii* (1996) state that airborne deposition of gypsum is common in desert uplands, and that in some areas of the Southwest, gypsum is the dominant component of dust. The presence of playas with gypsum deposits in adjacent basins (Coates and Cushman, 1955; Schreiber, 1978) provides a ready source nearby. Additional sulfur may be deposited in the area due to the presence of a coal-burning power plant and copper smelters in adjacent basins. The crest spring waters also contain significant bicarbonate. Much of the HCO_3^- is probably derived by equilibration with vadose-zone air that contains a high proportion of CO_2 due to plant and microbe respiration. Silicate weathering reactions are another source of HCO_3^-, and are also the most reasonable source for the Na^+ in the waters.

With the exception of springs that have encountered local zones of pyrite mineralization in Unit 6, waters from springs at lower elevations are predominantly Ca^{2+}/HCO_3^--type, but exhibit some variation. There are three chemically-distinct groups of waters on the eastern side of the range.

Some waters in the northeastern portion of the range become much more concentrated (total dissolved solids of 700 to 1200 mg/L), and develop a strong Ca^{2+}/SO_4^{2-} signature. These waters have flowed through Unit 6; some parts of this unit have significant pyrite veining (E. A. du Bray, U. S. Geological Survey, personal communication, 2001). Waters from springs with Ca^{2+}/SO_4^{2-} signatures have flowed through zones of pyrite mineralization and have elevated SO_4^{2-} due to sulfide mineral oxidation; pH remains near neutral due to carbonate minerals in the formation that provide *in situ* buffering of the acidity produced from the sulfide oxidation. Dissolution of carbonates is responsible for much of the HCO_3^- in these waters.

Waters that have not flowed through zones of pyrite mineralization are more dilute (total dissolved solids of 80 to 600 mg/L). Most of these springs have flowed through Unit 6, and have Ca^{2+}/HCO_3^- signatures due to dissolution of carbonate minerals in the sedimentary rocks of this unit. The two samples that do not discharge from Unit 6 are distinct, with increased proportions of Na^+ and K^+ and lower Ca^{2+} due to domination by silicate mineral hydrolysis rather than the carbonate-mineral dissolution seen in the other waters.

Waters in the northernmost portion of the San Bernardino Valley are similar in chemical composition to low-elevation waters from the southeastern portion of the Chiricahuas. The northernmost well water sampled has a similar chemical signature to waters from the southeastern portion of the Chiricahuas that have not flowed through Unit 6; this well is very close to the mountain front, and Unit 6 is not present in the area. The two other well waters in the northern part of the San Bernardino Valley are more similar chemically to southeastern Chiricahua waters that discharge from Unit 6. The shift to water chemistry more similar to that of Unit 6 waters is due to two factors. First is the mixing of waters supplied from different areas in the Chiricahuas including those where Unit 6 is present; the other process controlling the shift in chemistry is that the basin-fill aquifer in the northern portion of the valley has a significant component of carbonate minerals, and NETPATH (Plummer *et alii*, 1991) modeling shows that carbonate-dissolution-and-precipitation reactions dominate the chemical evolution of groundwater in this zone (see Chapter 1 for further discussion of carbonate chemistry in the San Bernardino Valley and a description of NETPATH).

Waters on the western side of the range (which have moved through Unit 2) have slightly higher SO_4^{2-} and lower HCO_3^- than typical waters from the eastern side of the range. These waters are dilute (total dissolved solids of 45 to 70 mg/L), suggesting that the high proportion of sulfate is due to minimal dilution of the initial SO_4^{2-} from

atmospheric deposition. The dilute nature of these waters compared to waters on the eastern side of the range may be due to fracture flow being more important on the western side of the range (due to the low primary porosity but heavy jointing of Unit 2) leading to less water-rock interaction than on the pore-flow dominated eastern side of the range, or that Unit 2 is more resistant to weathering than the rocks on the eastern side of the range. Because Unit 2 is found only on the western side of the range, and thus not likely to be involved in water transmission to the San Bernardino aquifer, the chemical evolution was not investigated in detail.

Stable Isotopes

Stable isotopes of oxygen and hydrogen in the water molecule are useful in many aspects of hydrogeological studies. In particular, the proportions of isotopes of O and H in precipitation vary as a function of temperature, so summer and winter precipitation from a site will typically have distinct isotope signatures. Likewise, the isotope signature of precipitation at various elevations in the same general geographic area should vary as a function of altitude (Clark and Fritz, 1997).

These attributes of the isotope signature allow it to be used to determine the proportion of snow and rain in groundwater recharge, and to determine the elevation zone within which recharge originated as precipitation.

The methodology for the water sampling and sample analysis is discussed in the "Hydrogeology" section of Chapter 1. Stable isotope data for groundwaters from the Chiricahua Mountains, the San Bernardino Valley, and precipitation amalgamated on the floor of the San Bernardino Valley are shown in Figure 3-6A. Precipitation was collected in reservoirs containing mineral oil to prevent post-fall alteration of the isotope composition. The collectors integrated events for periods of at least five months prior to analysis, so the samples gave weighted mean values for all precipitation events during the sampling period.

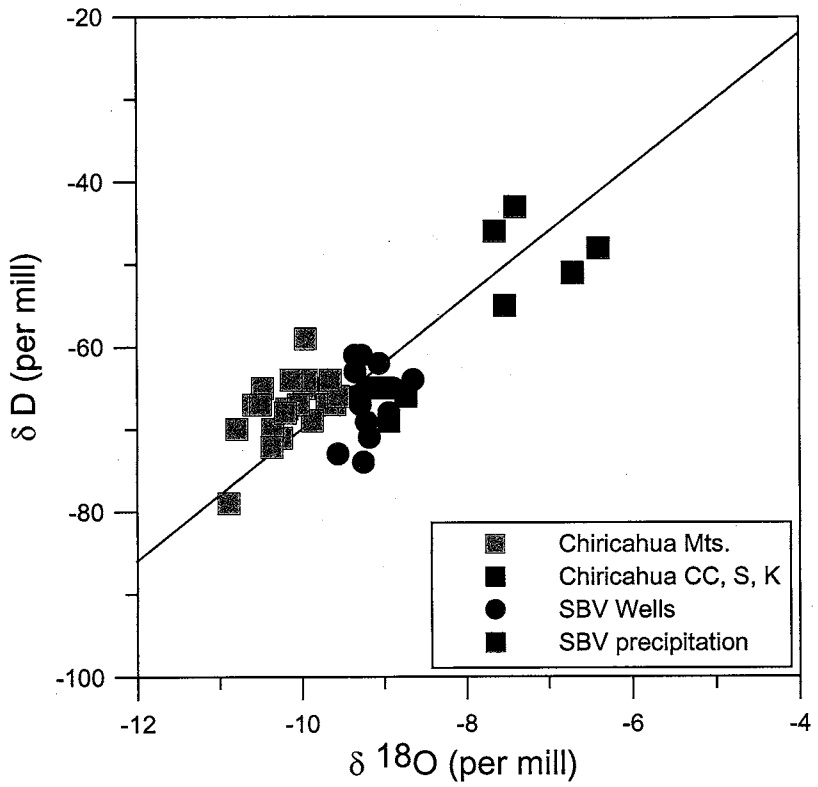

Figure 3-6. A. Stable isotope data from the Chiricahua Mountains and San Bernardino Valley shown with the global meteoric water line.

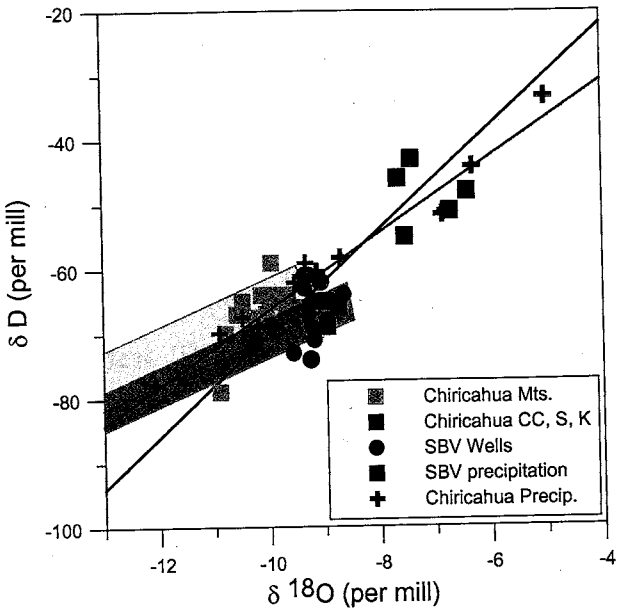

Figure 3-6 (continued) B. Stable isotope data from the Chiricahua Mountains and San Bernardino Valley. The three enriched waters (Cottonwood Corral, Sycamore, and Krentz Springs) from the Chiricahuas are significantly lighter than valley-floor precipitation, but plot to the right of the global meteoric water line (black line). The local meteoric water line (purple line) for the Chiricahuas (based on the 'Chiricahua precip.' data, which represents seasonally-integrated samples from collectors near the crest and the base of the range) has a slope of 5.9, so heavier precipitation does plot to the right of the global line; however, at the δ D and δ ^{18}O values of the three enriched waters, precipitation plots on or to the left of the global line. This shows that unaltered precipitation can not be responsible for the three enriched waters. The two colored boxes are bounded on their upper and lower sides by lines have slopes of 3.9 (the local evaporation slope determined by Earman et al (2003b) using data from the Peloncillo Mountains (Figure 1)). The upper and lower sides of the bottom box (darker blue) bound the three enriched samples, meaning these enriched waters could have been produced by evaporation of any isotopically-lighter water with a composition that plots in bottom box. This shows that evaporation of heavier precipitation or groundwater from the Chiricahuas is a viable mechanism for producing the isotope signature of the three enriched springs. As fresh local precipitation is not capable of producing these signatures, and there is no evidence of inflow from other sources, evaporation is the only reasonable explanation for the formation of these isotope compositions. The upper box (lighter blue) bounds most of the Chiricahua springwaters. As these waters also fall on or near the local meteoric water line, they could represent groundwater that has not experienced any significant post-rainfall evaporation, the product of evaporation of isotopically-lighter precipitation or groundwater that falls within the box, or some combination thereof.

As expected, waters in the Chiricahuas are significantly lighter than valley-floor precipitation. Most of the Chiricahua springs are also slightly lighter than groundwater in the San Bernardino Valley. In part, this is because waters from throughout the San Bernardino Valley are shown, and the Chiricahuas do not supply all the basin groundwater—up to 30 % is derived from the other (lower-elevation) ranges that bound the valley. However, there are three waters from the Chiricahuas that are more enriched than the rest. This appears to be the result of evaporation at some point after precipitation (Figure 3-6B). While local heavier local precipitation does plot to the right of the global line, the three enriched Chiricahua spring samples appear to be too light isotopically to have originated as unevaporated precipitation. The dark blue evaporation box on Figure 3-6B shows that the isotope composition of these three springs could be produced by evaporation of isotopically lighter groundwater or fresh precipitation from the Chiricahuas. The three evaporated waters have the same signature as San Bernardino groundwaters, suggesting that waters such as these are a significant input to the basin-fill aquifer. These waters are all springs (Cottonwood Corral, Sycamore, and Krentz Springs) at relatively low elevation in the southeastern portion of the Chiricahuas.

Relative importance of rain and snow to groundwater recharge

Stable-isotope values for springs in the Chiricahuas and seasonal precipitation from near the crest of the range are shown in Figure 3-7. These data seem to contradict the assumption that snow is a major contributor to groundwater recharge, as the spring samples plot much closer to fresh rain than to the fresh snow. The reason for this apparent discrepancy is that rain typically infiltrates shortly after a precipitation event, but near the crest, the snow does not melt until after it has been exposed on the ground surface for some time. During melt and the period leading up to melt, the isotope signature of snow changes (Cooper, 1998; Rose, 2003; Taylor *et*

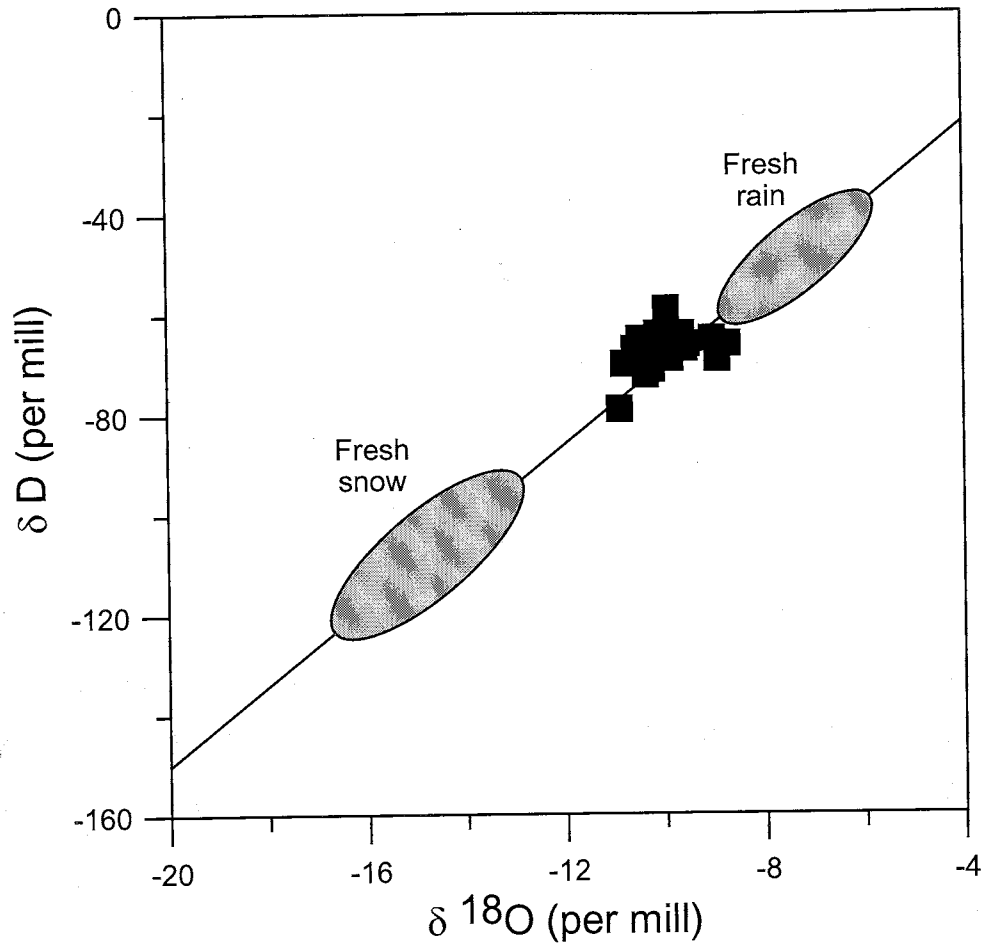

Figure 3-7. Stable isotope values for springwaters in the Chiricahuas and seasonal precipitation from near the crest of the range, shown with the global meteoric water line.

alii, 2001; Unnikrishna *et alii*, 2002). Data from several sites in the southwestern USA (including the Chiricahuas) indicate that the signature of the bulk melt evolves from the fresh snow signature along a line with a slope close to that of the global meteoric water line (see Chapter 4). Mass balance based on samples of altered snow from the Chiricahuas suggests that snow is responsible for about 60 % of the groundwater recharge in the area (see Chapter 4).

Variation of isotope composition with elevation

The isotope signatures of springs in the range as a function of the maximum elevation of the surface-water drainage surrounding the spring are shown in Figure 3-8. This seems to show the elevation effect, with springs which have lower maximum recharge elevations having more enriched signatures, which is typically assumed to result from the precipitation-elevation relationship (Clark and Fritz, 1997). However, the three most enriched spring waters are the same springs that have signatures indicative of significant evaporation. Although most lower-elevation springs do not show distinct evaporative signatures, as do the three most-evaporated springs (Cottonwood Corral, Sycamore, and Krentz Springs) (*id est* they do not plot to the right of the global meteoric water line), an examination of the spring water signatures shows that many of the heavier waters could be the composed of either unevaporated precipitation or water evaporation-afftected (originally lighter) waters from the range (these heavier waters fall within the light blue evaporation band in Figure 3-6B).

Another factor that could be affecting the apparent elevation relationship is the ages of the waters. A number of processes can affect the weighted mean isotope composition of precipitation that falls in any given year or season. One example is year-to year variations in the proportion of precipitation resulting from summer monsoon storms versus winter frontal storms. As described by Heald (1975), summer monsoons in this area originate over the Gulf of Mexico, while winter frontal systems

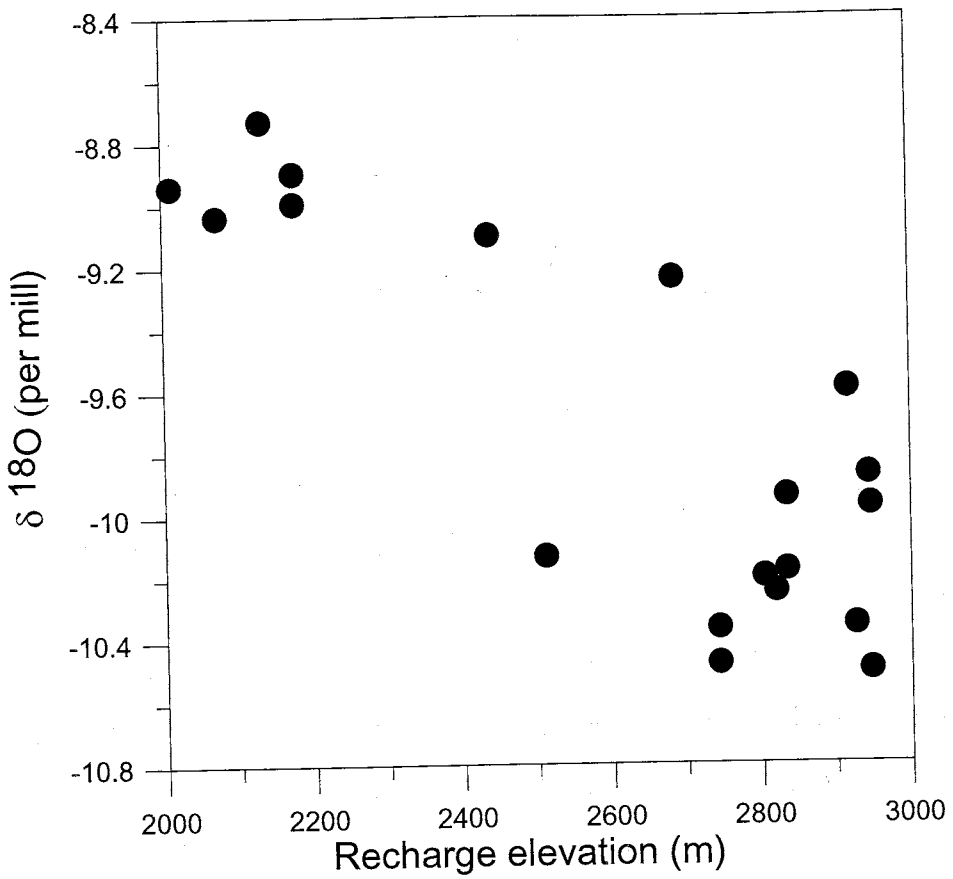

Figure 3-8. δ D of spring waters from the Chiricahuas as a function of the maximum elevation of the surface water drainage in which the spring is located.

originate over the Pacific Ocean; the path traveled by the moisture prior to arrival in the Chiricahuas influences the amount of 'continental effect' experienced by the moisture (heavy isotopes are preferentially removed from clouds during precipitation, so greater distance traveled over land (and thus greater loss of water due to rain/ snowfall) will result in isotopically-lighter water vapor, assuming the same initial composition). Other potential factors include year-to-year variation in the average duration of precipitation events causing different amount effects, and warmer or cooler years affecting both the fractionation during precipitation formation and the amount of in-fall evaporation to which precipitation is subjected. Springs are likely discharging waters that have traveled different distances, depending on the altitudes of recharge and discharge and the flowpaths along which the water have traveled. As a result, they are likely to be discharging waters that were recharged during different years (Ingraham *et alii*, 1991; Newman *et alii*, 2001). Tritium data (Table 3-1) for a subset of the springs suggest that this is the case. Based on the classification scheme of Clark and Fritz (1997), Sulphur Spring is discharging water that was recharged at least 50 yr ago, while Ash and Lower Rustler Springs are discharging water recharged in the past 5 to 10 yr, and Sycamore Spring is discharging a mixture of > 50 yr and < 10 yr-old recharge. Depending on the difference in the ages of the waters in question, and the environmental characteristics particular to the years of recharge, inter-year variation of recharge composition has the potential to mimic an elevation effect or to convolute it.

Because of the factors described above, spring-water isotope compositions do not appear to be ideal for estimating the local elevation effect for precipitation in the range. In an attempt to estimate the local elevation effect for precipitation, samples were collected at multiple elevations for a rain event and a snow event, both of which resulted from winter frontal systems. These samples do not show any distinct variation in isotope composition with altitude (Figure 3-9; the data are provided in Appendix 9).

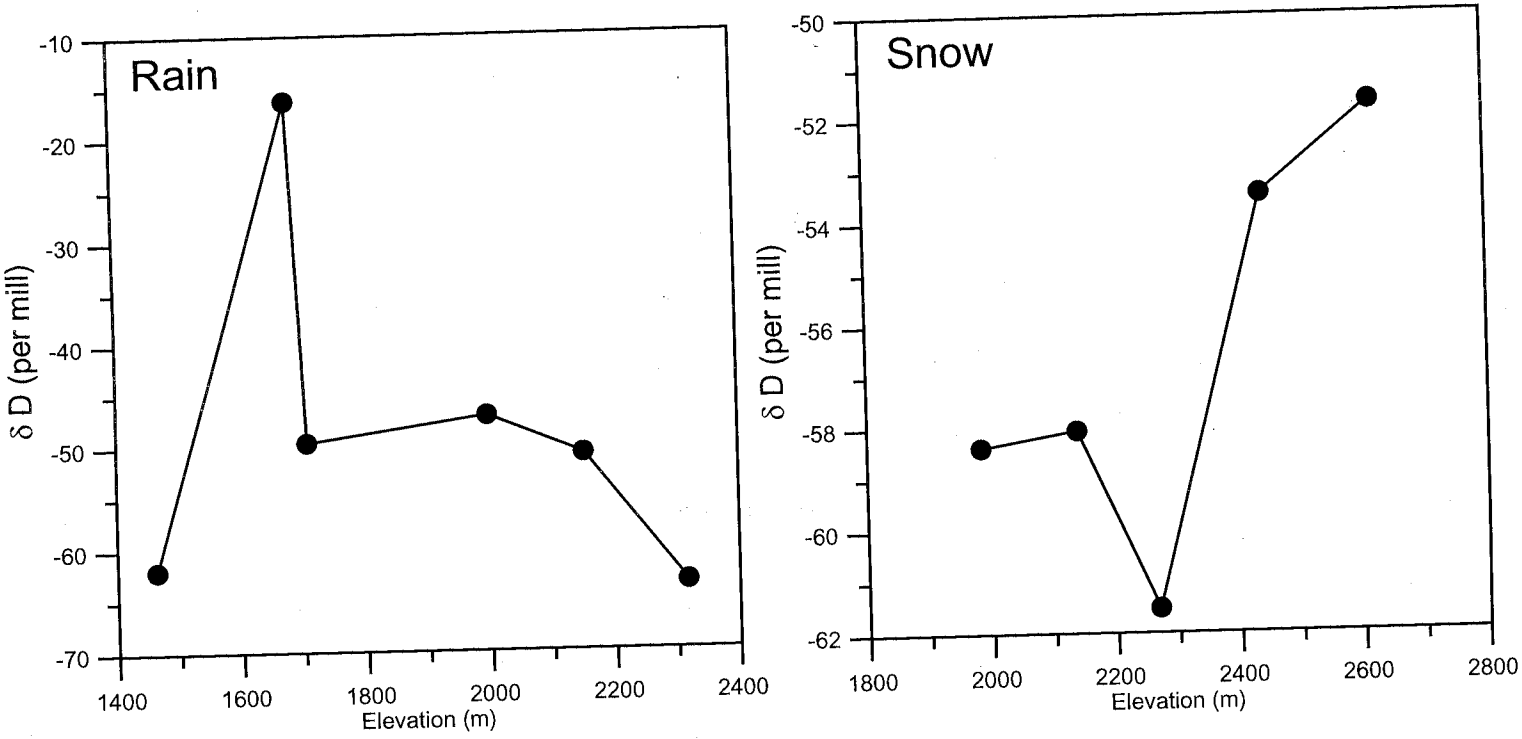

Figure 3-9. Stable isotope values for individual precipitation events, as sampled at a range of altitudes. Note that the typical altitude effect is not seen in either case. Rain and snow samples were collected on 13 February, 2003 and 27 February, 2003 (respectively).

While some studies of precipitation in mountain ranges show a distinct altitude effect, others have found little to no effect (Friedman and Smith, 1970; Niewodniczanski *et alii*, 1981). The lack of an elevation effect in fresh precipitation in mountain ranges has been attributed to factors such as precipitation falling onto elevations of various altitudes from a high horizontal cloud formation (Niewodniczanski *et alii*, 1981) and disruption of the elevation relationship by the turbulence of air masses moving over mountains (Friedman and Smith, 1970).

A sampling of snow from a smaller range of elevations showed a pronounced altitude effect (Figure 3-10; data provided in Appendix 9). Part of the reason may be that these samples were collected while snow was still falling, and thus very fresh; the limited elevation range and the fact that the samples were all collected near the base of the range (thus minimizing the turbulent effects described by Friedman and Smith, 1970). The snow sampling over the wider elevation range took place a day after snowfall, allowing for some isotope alteration to occur. Another possibility is that the factors that convolute the altitude effect when sampling from an individual precipitation event vary in their importance from event to event.

Dissolved Gases In Groundwater

Although stable isotopes can provide information about the elevations at which precipitation contributing to groundwater recharge falls, they do not allow determination of the elevation at which recharge takes place—precipitation will not necessarily become recharge at the same elevation it fell. Given the topography of mountains, it is reasonable to assume that precipitation will not flow uphill prior to infiltration, so the three main possibilities for recharge location are infiltration and recharge at or near the location of fall; infiltration at or near the point of fall followed by interflow some distance downslope of the point of fall, then recharge; and surface

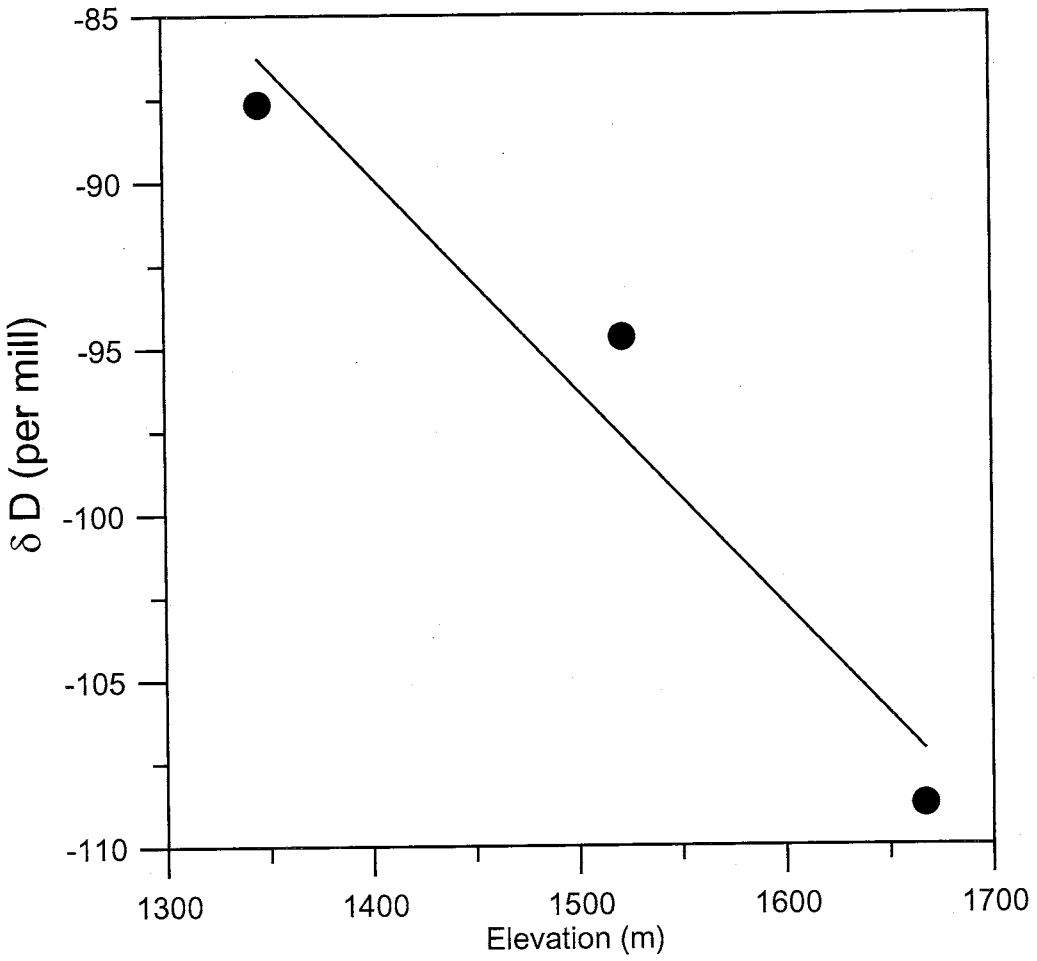

Figure 3-10. δ D of snow samples from an individual event in January, 2001 as a function of altitude. Note that for this sample set, a strong altitude effect is observed.

flow some distance away from the point of fall, then infiltration (possibly followed by interflow) and recharge.

Because the altitude at which recharge takes place in the Chiricahuas was of interest, samples of gases dissolved in groundwaters were collected from several springs in the range and four wells in the San Bernardino Valley. These wells discharge water that is primarily derived from high-altitude precipitation in the Chiricahuas (see Chapter 1).

Various applications of dissolved gases to groundwater studies are discussed by numerous authors (e.g. Aeschbach-Hertig *et alii*, 1999; Ballentine and Hall, 1999; Manning, 2002; Phillips, 1981; Stute and Schlosser, 2000). The analysis of dissolved gases in groundwater can yield information on conditions at the time of groundwater recharge, including the temperature and elevation at which recharge took place. In most cases, the concentration of a gas in water can be assumed to be a function of temperature and elevation at the time of recharge and the amount of 'excess air' incorporated (air added by complete dissolution of bubbles as opposed to air/water equilibration) (Manning, 2002). The specific application of the dissolved-gas method used for this study is that described by Manning (2002), in which dissolved-gas concentrations are used to calculate recharge temperature for a set of assumed recharge elevations. The resultant temperature-elevation pairs are plotted along with the local temperature lapse curve, and the intersection of the lines represents the recharge temperature and elevation of the sample in question. The technique is often referred to as the use of 'noble gases,' but the samples collected for this study were interpreted using concentrations of Ne, Ar, Kr, and N. As nitrogen is not a noble gas, the method will be referred to here as the dissolved-gas method.

Dissolved-gas methods and results

Dissolved gas from each source was collected using passive diffusion samplers which were exposed to flowing source water for a minimum of 48 hr, allowing collection of duplicate gas samples in copper tubing that was sealed using a cold-weld tool. Precautions were taken to avoid atmospheric contamination during sample collection. Samples were analyzed via quadrupole mass spectrometer (for further description of sample collection and analysis procedures, see Manning, 2002). Gas data were input into a Microsoft Excel-based analysis program designed specifically to handle data from gas-diffusion samplers that calculated excess air addition and recharge temperature for a given recharge elevation (Solomon, K., University of Utah, personal communication, 2002). For each sample, recharge temperatures were calculated for a range of potential recharge elevations (typically four or five elevations were used for each sample). For springs in the Chiricahuas, the range of elevations was constrained to lie between the spring orifice and the highest point in the mountain range. For wells in the San Bernardino Valley, the range of elevations was constrained by the elevation of the water table in the valley well nearest to the flank of the Chiricahuas and the highest elevation in the range.

The elevation-temperature pairs for each sample were plotted along with an atmospheric lapse curve for southeastern Arizona. The lapse curve was calculated by plotting mean annual air temperature as a function of elevation for all available weather stations in the area (Western Regional Climate Center, URL <http://www.wrcc.dri.edu>), finding the best-fit line for the data (the data and fit equation are provided in Appendix 7). The sampled water sources produced two types of plots (Figure 3-11; the complete results are provided in Appendix 10)—one in which an intersection between the two curves suggests a unique temperature and elevation of recharge, and the other in which there is no intersection point for the curves. All

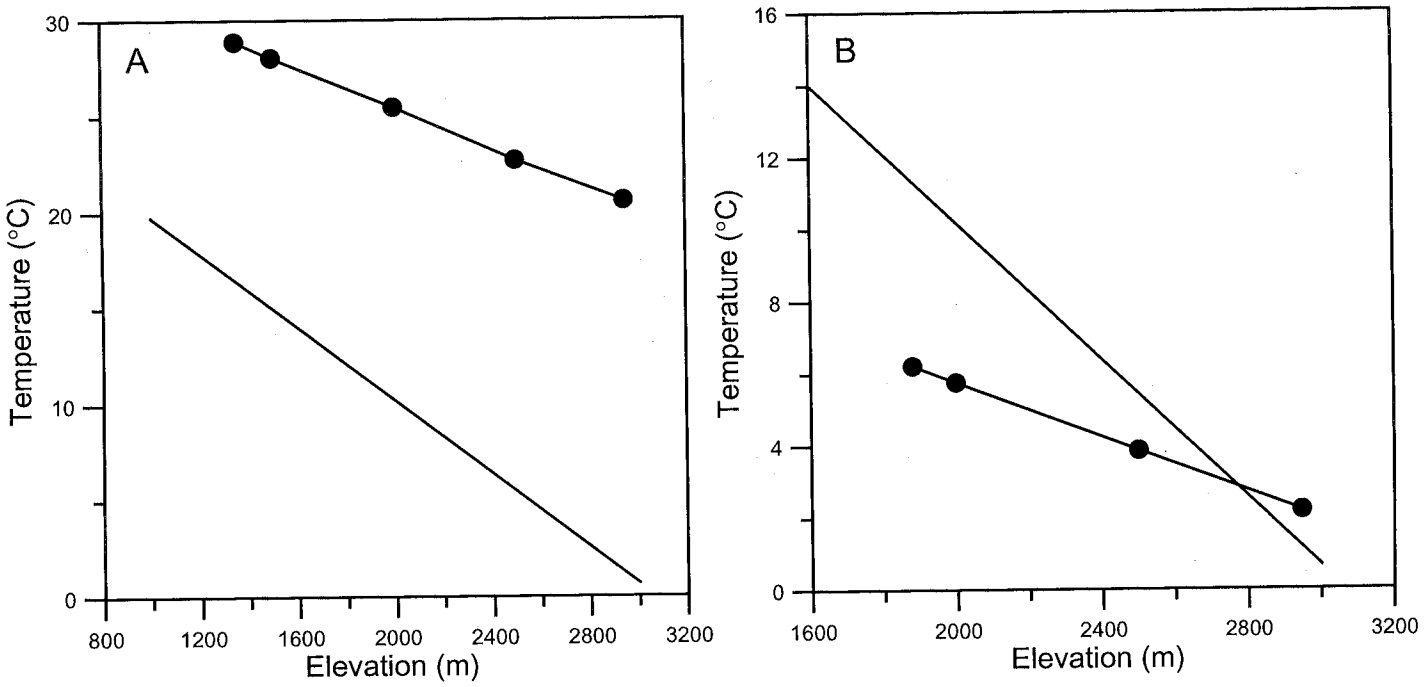

Figure 3-11. Sample plots of recharge temperatures calculated for a set of assumed recharge elevations for a given water source (points connected by line) and the temperature lapse curve for southeastern Arizona (line only). **A.** Ranchita Well; **B.** Ash Spring.

springs in the Chiricahuas produced plots with intersecting curves; these results are shown in Table 1. All the wells in the San Bernardino Valley produced plots with no intersection point, as illustrated by the Ranchita Well plot (Figure 3-11A).

As expected, the two springs nearest the crest of the range (Lower Rustler and Tub) are indicative of high elevation recharge—these samples were collected and analyzed primarily as a validation for the methodology used here, since they had small ranges of potential recharge elevations. Two of the three low-elevation springs showing highly-evaporated stable isotope signatures were sampled for dissolved gases (Sycamore and Cottonwood Corral), and the calculated recharge elevations are fairly close to the spring orifices. These evaporated signatures are suggestive of some combination of infiltration of water that had previously flowed only above ground and "re-recharge," whereby groundwater recharged at high elevations discharges into a stream channel, flows downslope, and recharges again at a lower elevation. One low-elevation spring (Ash Spring, which does not appear to have undergone significant evaporation) shows recharge near the crest of the range, indicating uninterrupted subsurface flow. The remaining two low-elevation springs (Welch Seep and Sulphur Spring) show intermediate recharge elevations. Recharge appears to be taking place at some elevation below the crest of the range, yet still significantly higher than the spring orifice. Given the 100-m uncertainty of the recharge elevation calculations, both these springs appear to be recharged near 2300 m, which is the elevation above which snowpack accumulates and below which snow melts relatively rapidly (Pope, L., U.S. Forest Service, personal communication; and observation during the study).

In the case of the plots with no intersection point, the curves are sub-parallel, and there is significant separation between the two curves, with the predicted recharge temperature for any given elevation being higher than the mean annual temperature

Sample	^{28}N	^{40}Ar	^{84}Kr	^{20}Ne	TDG (atm)	^{3}H (TU)	Spring elevation (m)	Recharge elevation (m)
Sulphur Spring	0.9844	0.0102	8.16E-07	2.19E-05	0.836	0.05	1553	2400
Cottonwood Corral Spring	0.9525	0.0108	7.44E-07	1.86E-05	0.928	-	1832	1900
Sycamore Spring	0.9351	0.0101	8.29E-07	1.70E-05	0.736	4.21	1853	2000
Ash Spring	0.8732	0.0102	7.49E-07	1.67E-05	0.917	5.16	1881	2800
Welch Seep	0.9771	0.0109	7.56E-07	1.91E-05	0.983	-	1975	2300
Lower Rustler Spring	0.8239	0.0097	6.39E-07	1.70E-05	0.894	7.64	2551	2900
Tub Spring	0.8132	0.0078	6.37E-07	1.80E-05	0.894	-	2778	2900

Table 3-1. Data for dissolved gas samples collected from springs in the Chiricahua Mountains, and calculated recharge elevations based on the gas data. Gas concentrations are given as mole fractions. "TDG" = total dissolved gas pressure. Recharge elevations are reported to the nearest 100 m, which is the uncertainty associated with the calculation.

for that elevation. There are several potential explanations for the anomalously high recharge temperatures.

The first possible explanation is mixing of locally-recharged waters with waters having a warmer recharge signature. The most likely mechanism of introduction for the warmer waters is upward migration from depth along range-front faults. The fact that there is continuity of both major-ion chemistry (both types of ions and total dissolved solids content) and stable-isotope content of waters across the mountain/ basin transition is a strong argument against this scenario. Given that calculated recharge temperatures are significantly higher than is reasonable for local waters, the mixing water would need to be introduced in high proportion to the local water, or have equilibrated with the atmosphere at an extremely high temperature. Warming in a deep geothermal system would not be likely to occur in conjunction with atmospheric equilibration that could yield a lower gas recharge signature; exposure to such a system could also be expected to produce a shift in major-ion chemistry due to increased mineral solubilities and dissolution kinetics (Hem, 1992), and could also cause the stable-isotope composition to make a distinct shift to the right of the global meteoric water line due to high-temperature isotope exchange with minerals (Panichi and Gonfiantini, 1981). While long-distance migration of waters with similar isotope content that recharged through a basin floor of low elevation is not impossible, such a long flowpath would allow significant time for water-rock interaction, and a jump in total dissolved solids and/or the ratio of dissolved ions would likely result.

Another possibility is that waters re-equilibrated with the atmosphere at the time of sampling. In such a scenario, water would encounter atmospheric air, and equilibrate at the temperature and pressure conditions present at that time. Because the samples that show anomalously high recharge temperatures were collected at low elevations compared to the "normal" samples, a high-temperature signature would be

imparted. However, significant precautions were taken during sampling to insure that re-equilibration did not take place; these precautions included ensuring that well bores were purged before the diffusion samplers were exposed to the water, maintaining an adequate depth of water above the sampler to prevent the diffusion of atmospheric air into the sampler during the period of emplacement, and maintaining a continuous flow of water over the sampler. If re-equilibration took place in the anomalous samples, the suggested recharge temperature at the elevation of sampling should match the water temperature at the time of sampling. There is no correlation between suggested recharge temperatures and well water temperatures (Figure 3-12; the data are provided in Appendix 10).

Because gas solubility in water decreases as temperature increases, anomalously high recharge temperatures could result from a loss of dissolved gas from water. If degassing occurred, the lower gas levels would suggest recharge at a warmer temperature.

Thomas *et alii* (2003) sampled waters in the Basin and Range province that appeared to have undergone gas loss, causing anomalously-high calculated recharge temperatures. Prior to sampling, these waters, which were supersaturated with CO_2, moved upward, thus experiencing reduced hydrostatic pressure. With this reduction in pressure, CO_2 began to exsolve. As the CO_2 exsolved, it stripped other dissolved gases with it.

Data discussed in Chapter 2 show that groundwater in the San Bernardino aquifer is receiving input of magmatic CO_2, causing high PCO_2 values that could drive the process observed by Thomas *et alii* (2003). In the San Bernardino waters, suggested recharge temperatures increase downgradient, suggesting that exsolution of CO_2 is a continuous process as water flows through the basin. Measurements of helium isotopes in the waters show that the rate of magmatic CO_2 input also increases

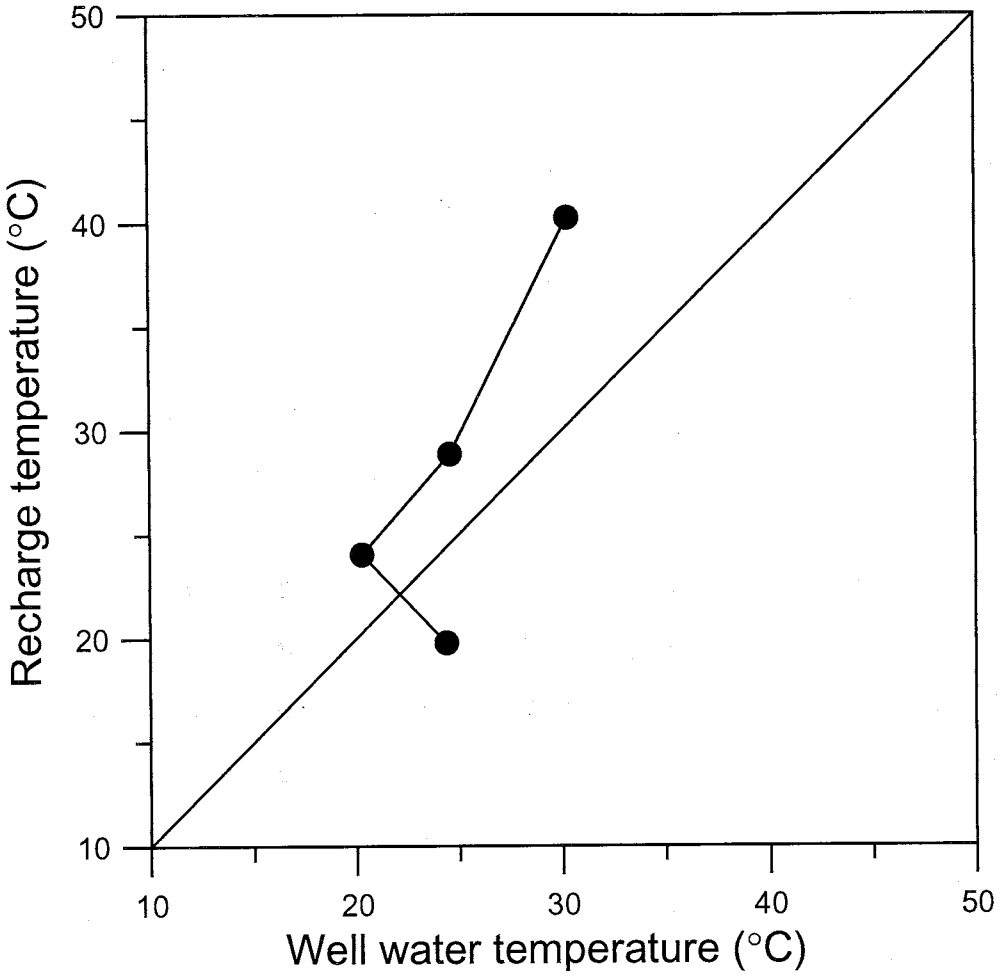

Figure 3-12. Plot of predicted recharge temperature (based on dissolved gas data) as a function of actual water temperature during sampling. Red line shows the 1:1 relationship that would be expected if re-equilibration with the atmosphere was occurring during sampling.

downgradient, indicating that higher inputs of magmatic CO_2 drive more degassing, and thus increasing calculated recharge temperatures. This scenario is the most likely explanation for the anomalously high temperatures suggested by the basin well waters.

SYNTHESIS

The different analyses described in the previous section all give individual indications as to groundwater recharge in the Chiricahuas and replenishment from the Chiricahuas to the San Bernardino Valley, but examining all information together will provide a more robust interpretation of the hydrogeologic system.

Recharge zones

A broad range of evidence points to the region near the crest of the range as the zone responsible for the majority of groundwater recharge in the Chiricahuas. The large number of springs near the crest is evidence that groundwater recharge is active at high elevations. Dissolved-gas data confirm that these springs are being recharged in the crest zone, and show that some springs at lower elevations in the range were recharged near the crest (*exempli gratia* Ash Spring), indicating that high-elevation recharge water can move to low elevations entirely through the subsurface. The presence of the relatively high-permeability Unit 1, the high total precipitation at high elevations, the high proportion of precipitation that falls as snow, and the fact that snowpack develops at these elevations are all *a priori* indications that this zone is conducive to recharge. Much of the lower elevation area of the range is occupied by relatively low-permeability rocks; even when high-permeability rocks (such as Unit 6) are present at lower elevations, the low total precipitation, low proportion of snow, and lack of snowpack development at these altitudes makes recharge less likely.

Although the dissolved-gas data show that some low-elevation springs in the Chiricahuas receive high-elevation recharge, others receive low-elevation recharge. The springs discharging water recharged at low elevations (Sycamore, Cottonwood

Corral) have relatively heavy stable-isotope signatures, but these signatures are consistent with high-elevation water that has undergone evaporation, as opposed to low-elevation precipitation. While some of this water may have moved to lower elevations entirely by overland flow, another phenomenon is likely responsible for some of the low-elevation recharge of high-elevation precipitation. As discussed earlier, a large number of previously-unmapped springs are present in drainage channels (like other springs in the range, these in-channel springs are associated with either unit contacts or fractures). Water which recharged at high elevation and emerges into a channel is subject to evaporation during its period of overland flow. In a permeable unit (such as Unit 6, which is present at lower elevations; the springs with evaporated signatures are all found in this unit), this water has the opportunity to infiltrate and become recharge after its period of surface flow, or become re-recharge.

The high-elevation recharge zone that supplies many of the springs appears to be related to the development of snowpack. The lowest extent of the high-elevation recharge zone appears to be 2300 m; this elevation is also the 'snowpack line' above which snowpack develops and below which snow tends to be melted within a few day of falling. However, no springs sampled for dissolved gases show recharge elevations between 2400 m and 2800 m, although snowpack develops in the entire zone above 2300 m. The cause of the "gap" in recharge elevations (*id est* the fact that recharge does not appear to take place in the entire zone that has snowpack development) is lithologic. The low-permeability Unit 3 is present in a large part of the snowpack zone. The boundary between Unit 3 and the high-permeability Unit 6 on the eastern side of the range is variable, ranging from as low at 2050 m up to about 2450 m. Thus, groundwater recharge appears to take place in two main regions, both of which are in the snowpack zone. The first is the area of outcrop for Unit 1, the second is the zone where the snowpack zone and the area of outcrop of Unit 6 overlap.

Zones of groundwater movement

Although the largest areas of outcrop for Unit 1 are found near the crest of the range, the "finger" pointing to the south/southeast and the outcrops to the southeast (Figure 3-3), along with the depositional relationships of the Unit 1 and Unit 3, suggest that it is laterally continuous in the subsurface. Given the permeability of Unit 1 and the fact that its high-elevation zones receive the vast majority of the high-elevation groundwater recharge, it is reasonable to assume that it serves as a conduit for subsurface flow to lower elevations. As discussed previously, the high-elevation stable-isotope signatures of waters at lower elevations do not necessarily indicate high-elevation recharge, as water could have flowed downslope overland after having fallen, and recharged at a lower elevation. However, the dissolved-gas data showing high-elevation recharge for lower-elevation springs supports this concept. The high concentration of springs downslope of Unit 1 shows that it is transmitting a significant quantity of water. Although some of this water discharges from springs just past the interface with Unit 3, a significant amount may continue to flow through Unit 1 in the subsurface.

Along with Unit 1, Unit 6 has high permeability. Unit 6 is primarily present at lower elevations, so it transmits a combination of water received from Unit 1 via subsurface flow (Unit 6 abuts the two southward-pointing "fingers" of Unit 1) and water recharged in its own outcrop zone. This recharge is derived from a combination of purely overland flow and re-recharge water which originally recharged in Unit 1 near the crest of the range; the rest is recharge from the high-elevation portion of Unit 6 that occupies the snowpack zone.

Unit 1 has high primary porosity and is not extensively fractured, suggesting that flow is predominantly through pores. Although Unit 6 has high primary porosity, it is also highly fractured, so it is a dual-permeability flow system. Observations in

the field show that several springs discharging from Unit 6 (including one that appears to have the highest discharge of any low-elevation spring) emerge from fractures, suggesting that in many parts of that unit, fracture flow is the dominant method of transmission. Although the dissolved-gas data show that waters can move from high elevations to low elevations in the range without atmospheric re-equilibration, this does not necessarily rule out the presence of unsaturated zones in the mountain block. This is because such zones, if present, could be isolated from direct contact with the atmosphere, and over time had their gas signatures set to one indicative of high-elevation recharge due to long-term equilibration with the dissolved gases in the water flowing through. However, there is no direct evidence that such unsaturated zones are present. As a result, out conceptual model of groundwater movement through the range assumes a saturated system.

Although our data do not allow determination of the percentages of low-elevation recharge derived from purely overland flow versus water that is re-recharging, field observations suggest that re-recharge is responsible for a significant proportion. Many of the perennial or semi-perennial streams in the range originate as springs, and seepage into channels via the channel banks has been observed at a number of sites below the high-elevation zone where these major channels originate. The precipitation regime of the region is such that overland flow in channels can be attributed in its entirety to groundwater discharge during much of the year (*exempli gratia* no measurable precipitation in over a month rendering pure overland flow an impossibility, even in the lowest parts of the range). While pure overland flow certainly contributes to streamflow during certain periods, much of total discharge of streams is water that had previously been in the subsurface. Figure 3-13 shows a conceptual model of potential modes of groundwater recharge and movement in the Chiricahuas.

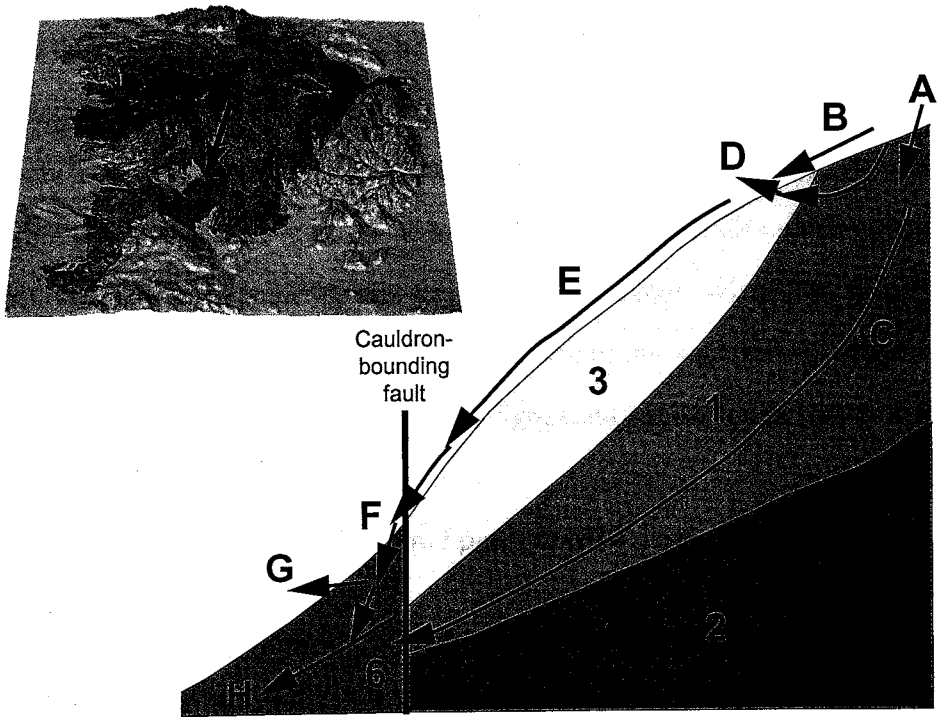

Figure 3-13. Conceptual model of water movement in the Chiricahua Mountains (evapotranspiration is mostly ignored to simplify the model). The transect for which the cross section is drawn is indicated by white-and-black arrow on the map of the range in the figure inset. Numerals on the figure identify the hydrostratigraphic units, arrows indicate water movement. Rainfall or snowmelt high in the range may infiltrate (A) or flow downslope overland (B). Infiltration (A) that becomes recharge may move through the range along a deep flowpath (C) or a shallow flowpath that intersects a low permeability unit and discharges (D). Channel flow on the slopes of the range (E) is made up of some combination of pure overland flow (B) and discharged groundwater (D). Upon encountering high-permeability materials in lower zones, water that is not evapotranspired will eventually infiltrate (F). As near the crest of the range, infiltration that becomes recharge can follow a shallow flowpath, where it may discharge at a unit boundary or fault (G); or a deeper flowpath, flowing into the alluvial aquifer of San Bernardino Valley (H). The subsurface flow into San Bernardino (H) is a combination of low-elevation recharge (F) and deep subsurface flow through the range (C).

Waters flowing through Unit 6 have dissolved ion content that easily distinguishes them from waters that have flowed only through the rhyolitic rocks that make up the majority of the range. The portion of Unit 6 on the southern side of the Chiricahuas does not appear to have any zones of high mineralization that cause the extremely high TDS and SO_4^{2-} seen in some springs on the northeastern side of the range, but the three springs in this zone have Ca^{2+}/HCO_3^- signatures resulting from the dissolution of carbonate minerals that serve as a distinct indicator of flow through the sedimentary rocks of the Chiricahuas. The presence of this signature in well waters of the San Bernardino Valley suggests that a significant amount of this water flowed through Unit 6.

The influence of elevation and seasonal precipitation on recharge in other mountain-basin systems

Abbott *et alii* (2000) found that the upper 500-m elevation zone of a mountainous zone in Vermont (USA) produced groundwater recharge year-round, while the lower elevations had recharge only in the colder months of the year. Manning (2002) found that groundwaters in the Salt Lake Valley, Utah (USA) had apparent recharge elevations of up to 2400 m, even though the long screens on sampled wells made it likely that the samples were a mix of mountain-block recharge and low-elevation recharge (which would cause recharge elevations to appear lower than the true elevation of the mountain-block component). James *et alii* (2000) found recharge elevations for springs in the Cascade Range (Oregon, USA) located at 920 and 597 m to be 2200 and 2500 m (respectively), "consistent with recharge along the Cascade crest," even though lateral distances between the springs and the crest are 30 and 50 km (respectively). Szecsody *et alii* (1983) estimated the percentage of precipitation that becomes recharge in a mountain range in Nevada, using similar methodology to that later described by Dettinger (1989). They found that the percent recharge increased with elevation; however this increase was not linear. From 1830

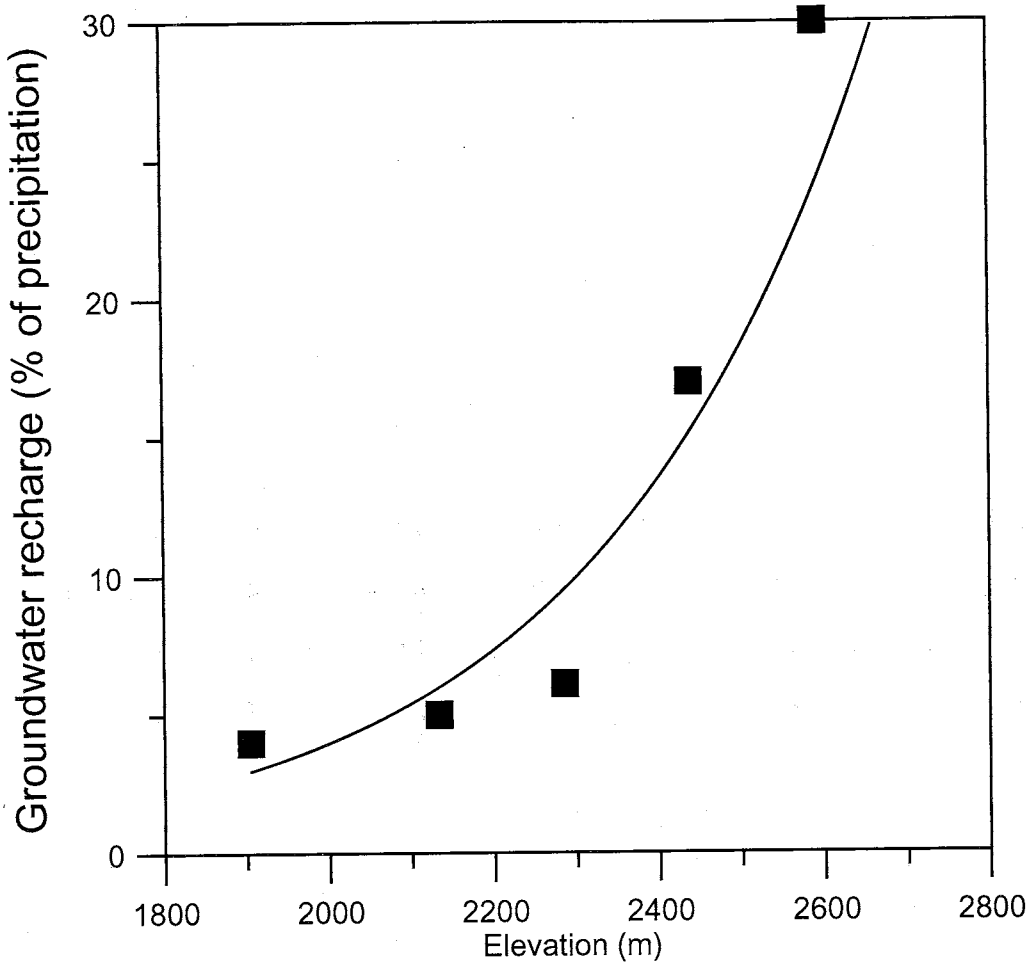

Figure 3-14. Percentage of precipitation in the Eagle Mountains (Nevada, USA) that becomes groundwater recharge at a range of elevations (after Szecsody *et alii*, 1983).

to 2290 m, there were only moderate increases in the percent recharge, but significant increases above 2290 m (Figure 3-14). By calculating the surface area of the range that fell within a series of 150-m elevation zones for which they had determined precipitation amounts and recharge percentages, they were able to estimate the total volume of potential recharge for each zone. Although the area of each successively-high zone is smaller than that of the zone below it, total recharge volume often increased with elevation. The zone with a midpoint elevation of 2590 m contributed the greatest volume of recharge, followed by the 2740-m zone and the 2438-m zone. The relatively small area near the crest of the range (2360 to 2820 m, a 460-m elevation zone with surface area of 16.5 km^2) contributed as much recharge as the low portion of the range (1450 to 2360 m, a 910-m elevation zone with surface area of 95 km^2). This shows that high-elevation zones, although smaller in area that low-elevation zones, can contribute significant amounts of recharge.

Winograd *et alii* (1998) found that summer convective storms, which make up about one-third of the annual precipitation in the Spring Mountains, NV (USA) make up only about 10% of groundwater recharge in the range, while cool-season precipitation is the main contributor. Cunningham *et alii* (1998) found that 50 spring and well waters in the Santa Catalina Mountains (Arizona, USA) had δ D and δ ^{18}O in the same range as winter mountain precipitation, indicating that "winter precipitation is an important water source for springs (and flow in fractures)."

CONCLUSIONS

This study provides adds to the relatively small body of mountain-centered groundwater research in arid/semi-arid regions, and, in combination with work on an adjacent basin (described n Chapters 1 and 2), provides a complete analysis of a mountain-basin system, rather than a basin-centered study that ends at the basin topographic margin. The Chiricahuas are a complicated system, with sedimentary

rocks present in addition to igneous rocks of varied permeability. Due to the complicated nature of the range, any single method of investigation could provide at best a partial picture of the hydrogeology of the range. By applying a range of tools broader than used in most previous studies, including geology, water chemistry (major-ion content), isotopes of O and H in water, dissolved gases in water, hydraulic evidence for groundwater flow, and local climatic conditions, a picture of groundwater flow in the range was developed that is much more complete than possible using fewer lines of investigation.

The zone near the crest of the range appears to be responsible to the majority of groundwater recharge. In addition, even low-elevation recharge near appears to be composed predominantly of water that fell as high-elevation precipitation. The Maxey-Eakin model predicts that recharge increases exponentially with precipitation amount for precipitation rates between 8 and 51 cm/yr, but one might assume that the smaller surface area of the high-precipitation zones would cancel out in increased proportion of recharge, resulting in a relatively uniform volume of water contributed from each elevation zone in a range. In conjunction with the work of Abbott *et alii* (2000), Manning (2002), James *et alii* (2000), and Szecsody *et alii* (1983), this suggests that the conditions (high precipitation amount, high proportion of snow in precipitation, snowpack development, and low evapotranspiration) in high-elevation zones of large ranges in the western USA create more than enough increased potential for recharge to compensate for the smaller surface area of these zones. The association of groundwater recharge with zones that correlate to readily-observable properties (snowpack development, lithology, *et cetera*) suggests that it may be possible to delineate recharge zones using remote sensing methods. This could be done by examining areas of snowpack development along with characteristics such as the

geology, vegetation, evapotranspiration, and topography. Such a method would be of value to water-resources planners.

Some high-elevation recharge in the Chiricahuas travels to low elevations entirely in the subsurface. This contradicts the idea that mountain springs represent isolated perched systems (e.g. Prudic *et alii*, 1995), and shows that aquifer replenishment via the mountain-block can result from groundwater transmission through a significant portion of the range. Other high elevation recharge water emerges from springs at lower elevations, and flows overland. Observation of flows in drainage channels in the Chiricahuas and the relation (or lack thereof) of these flows to recent precipitation events suggests that a significant proportion of low-elevation recharge is the result of "re-recharge," as opposed to infiltration of pure overland flow.

In the Chiricahuas, the zone of high-elevation groundwater recharge appears to overlap almost exactly with the zone of snowpack development, a phenomenon that has not previously been documented. Although the importance of cool-season precipitation in recharge has been noted (e.g. Cunningham *et alii*, 1998; Winograd *et alii*, 1998), this incorporates both snow and rain, and no studies report the elevation cutoff for snowpack development or attempt to associate recharge with snowpack development. If snowpack development is important in driving groundwater recharge in other ranges, the potential for climate change to impact groundwater recharge is high, given that current models for the western USA predict that over the next 50 yr, total precipitation will remain constant, but the proportion of snow will decrease, and snowlines will rise (Hamlet and Lettenmaier, 1999; Leung *et alii*, 2004; Leung and Wigmosta, 1999).

Chapter 4: Determination of the proportion of snowmelt in groundwater recharge, southwestern USA

INTRODUCTION

Groundwater is an important resource in the southwestern USA (referred to hereafter as 'the Southwest'), which has experienced rapid population increases in last several decades. Snowmelt is an important contributor to groundwater recharge in many areas of the world, including the Southwest. In the Southwest, low-lying basin floors are commonly surrounded by mountain ranges. The high elevation of the mountain ranges relative to valley floors results in lower temperatures in the ranges, which produces higher average annual precipitation and also increases the percentage of total precipitation falling as snow.

A basic examination of the potential for groundwater recharge from snowmelt suggests that snow is likely to exert a stronger influence on groundwater recharge than suggested by its contribution to average annual precipitation. Wilson *et alii* (1980) provide a summary of attributes of snow and rain that suggests snowmelt is more likely to become recharge than rainfall. Summer storm events in the Southwest tend to be of high intensity and short duration, which is likely to produce a high percentage of overland flow versus infiltration. In contrast, snowmelt is a process of relatively low intensity but long duration, providing a pulse of water likely to have a relatively high ratio of infiltration to runoff. Summer rains fall when temperatures are high and vegetation is at its most active, meaning potential evapotranspiration is at or near a maximum. Snow melts when vegetation is mostly dormant and temperatures are low, minimizing potential evapotranspiration (the relatively high albedo of snow compared to bare or vegetated ground contributes to this as well). Finally, storms producing snow tend to blanket fairly wide areas, in contrast to summer rains, which can have spotty coverage.

The recent population growth in the Southwest is placing increasing demands on groundwater resources, so sound long-term management of these resources is essential. In turn, good aquifer management requires an understanding of how the aquifer's water is recharged, including the sources of input. Thus, knowledge of the importance of snow (especially mountain snow) in the replenishment of alluvial aquifers is a key to sound water-resources planning.

Isotopic characteristics of snow

The stable-isotope composition of recipitation tends to plot on or near the global meteoric water line (GMWL), but its location on the line is a function of temperature. On the global scale, average annual precipitation from warm areas is isotopically heavier than that from cool areas. On a local scale, areas with distinct seasonality receive rain that is isotopically heavier than snow (Clark and Fritz, 1997). If the isotope compositions of rain, snow, and locally-recharged groundwater from a given area are known, a mixing model can theoretically be used to determine the proportions of rain and snow that contribute to groundwater recharge (Hershey, 1989; Maulé *et alii*, 1994). However, care must be taken in the application of this method, because the isotope composition of snow tends to change with time on the ground.

The physical character of snow changes from the time of its fall to the conclusion of its melt. As described by Colbeck (1987), a process called 'snow metamorphism' affects the physical structure of snow, with snow crystals typically becoming larger and more rounded as time progresses. While rainwater falling on the snowpack can drive snow metamorphism, it is not a necessary condition. This is important because the areas investigated in this study typically receive little or no spring rain, so metamorphism driven by input of liquid water would not be common. Snow metamorphism can result solely from mass transport driven by temperature gradients in snowpacks that result from differing temperatures at the snowpack surface

and base (Colbeck, 1987). In addition to temperature-gradient metamorphism, and rain-on-snow events, snowpacks can potentially be affected by processes such as evaporation/sublimation, partial melt and refreezing, condensation of atmospheric water vapor on the snow surface, and isotope exchange with atmospheric and soil water vapor.

Because physical changes may impart fractionation in stable-isotope systems, processes such as those described above may cause the isotope content of snow to change; these changes tend to be ongoing during exposure and melt (Stichler, 1987). As a result, a composition determined for fresh snow (or determined for a snowpack on one specific day during its exposure) is not necessarily indicative of the composition of the meltwater that will be derived from the snow. Similarly, a sample of meltwater collected on a given day might not be representative of melt from other days, nor of the mean composition of meltwater derived from the snowpack.

Most of the investigations of changes in the isotope composition of snow and snowmelt have focused either on the snow itself (e.g. Sommerfield *et alii*, 1991; Stichler, 1987; Stichler *et alii*, 1981; Unnikrishna *et alii*, 2002), or application of the phenomenon to hydrograph separation (e.g. Hermann *et alii*, 1981; Rodhe, 1981). Relatively few investigations have incorporated isotope effects on snowpack into the determination of snowmelt contributions to groundwater recharge (e.g. Rose, 2003; Winograd *et alii*, 1998).

INVESTIGATIONS OF POTENTIAL METHODS TO DETERMINE BULK STABLE-ISOTOPE INPUT COMPOSITION OF SNOW

Because the stable-isotope composition of snowmelt varies with time, for some surface-water studies, it may be necessary to collect meltwater samples on a frequent basis to get an accurate picture of the input function into the system of interest (Unnikrishna *et alii*, 2002). For groundwater studies, however, it may only be necessary to know a bulk input value. Of course, this depends on the nature of the

system. Water from springs and wells near recharge areas or in fracture-flow or karst systems can display significant variations in chemical and isotopic composition on short time scales. In these cases, a knowledge of isotope input on a fine time scale may be necessary, similar to surface-water systems. In contrast, for many observation points, the stable isotope content of water from springs or wells remains fairly constant over time. If such an observation point is used, then a 'bulk input' value for stable-isotope composition is sufficient to characterize the system, and information regarding short-term variations is not needed (for discussion of variation in springwater stable isotope content, see Ingraham *et alii*, 1991; and Newman *et alii*, 2001).

This study was designed to determine the stable-isotope composition of bulk snowmelt input to groundwater systems, to determine how different this composition is from the fresh-snow composition, and to investigate some of the processes important in driving the shift. Sets of precipitation collectors of different designs were used to determine the bulk-melt composition and its relation to the fresh-snow composition; studies of snowpacks in the field were used to examine the processes important to the isotope evolution.

Determination of the bulk meltwater composition and its difference from the fresh snow composition

Most of the samplers currently in use for determining the stable-isotope composition of precipitation are based on collectors described by Friedman *et alii* (1992), or are similar to one of the collector types they describe. For a study of stable-isotope composition of precipitation in southeastern California, Friedman *et alii* (1992) employed three types of collectors (Figure 4-1). For sites where no snow or only a moderate amount of snow was expected, one of two versions of a 'funnel collector' was emplaced. In both versions, the funnel was supported approximately 1 m off the ground by a stake, and connected by tubing to an underground reservoir containing "hydrocarbon oil." For sites where no snow was expected, a funnel of standard design

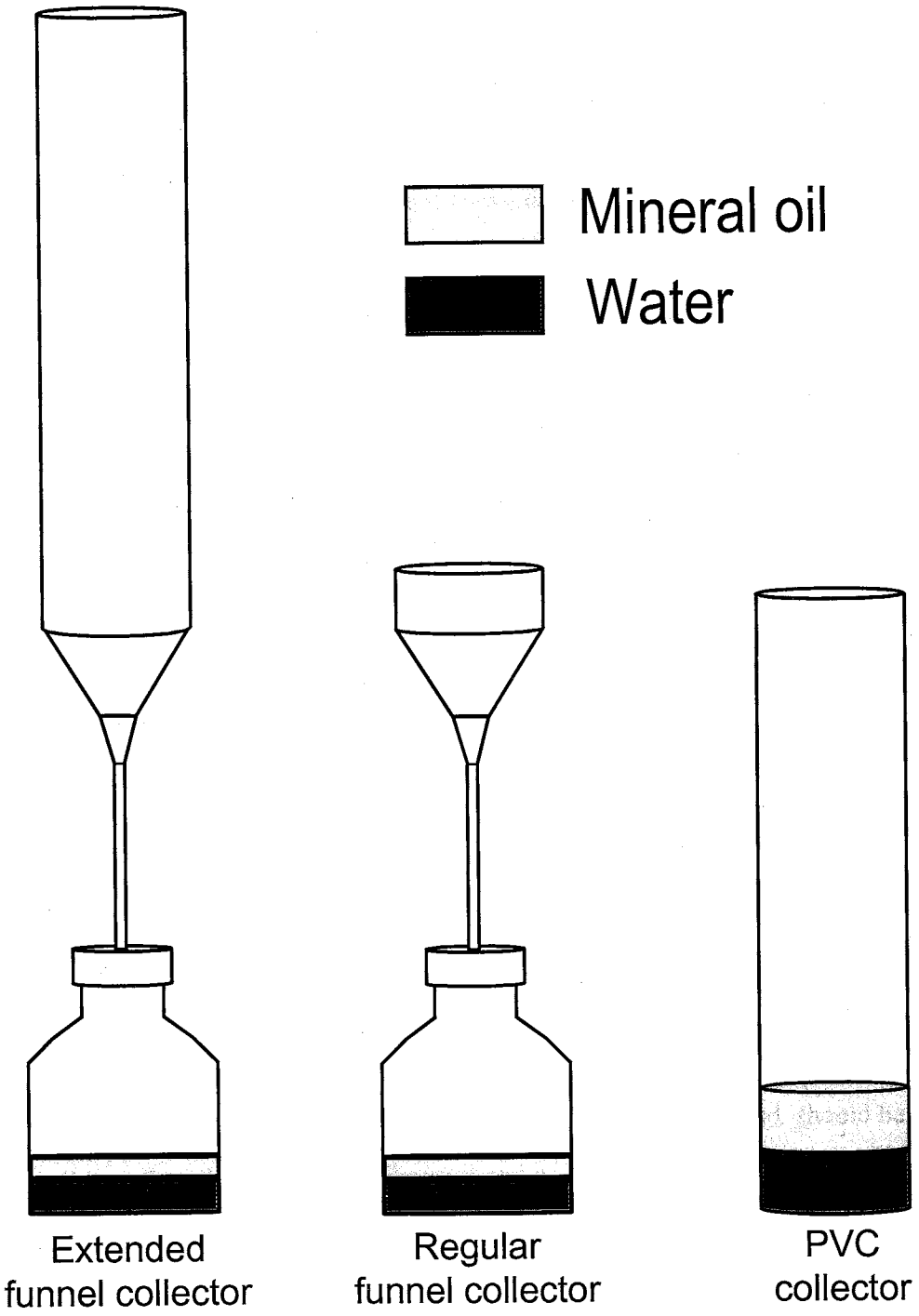

Figure 4-1. Schematic representation of precipitation collectors used in this study, modeled after Friedman *et alii* (1992).

was employed; for sites expected to receive moderate amounts of snow in addition to rain, plastic Büchner funnels were used (these are referred to here as 'regular funnel collectors'). 'Extended funnel collectors' were constructed by removing the porous plates from the Büchner funnels and replacing them with metal screens; the edges of the Büchner funnels extended 7.5 cm above the screens, but some were fitted with 150-cm extension tubes. Finally, at sites where large amounts of snow were expected in addition to rain, a regular funnel collector was employed along with a snow collector (referred to here as a 'PVC collector'). The PVC collector consisted of a 19-cm-diameter plastic pipe, approximately 1.25 m high, sealed at the bottom, and buried about 0.3 m in the ground, with a layer of hydrocarbon oil in the bottom. At the dual-collector sites, the collector used was alternated based on the season. The regular funnel collector was covered during the winter, so samples were only collected in the PVC collector during that time; in the summer, the PVC collector was covered, and samples were collected only in the regular funnel collector.

The size of holes in the metal screens in the Büchner funnels of the collectors used at Friedman *et alii*'s (1992) 'moderate snow' sites is not described, but because the 150-mm extension tubes were fitted in order to "increase the amount of snow that they could hold before melting occurred," it is clear that the screen provided sufficient obstruction to allow the accumulation of snow in the funnel body. As a result, snow falling into the collector would not be protected from metamorphic processes by the hydrocarbon oil until after it had melted. Rain, on the other hand, should have been able to flow through the metal screen and be protected almost instantly by the hydrocarbon oil. The 19-cm diameter of the PVC collector's opening would allow snow to enter immediately, even during heavy events, thus protecting it from alteration.

A new scheme for deploying paired precipitation collectors at a single site to determine the degree of isotope alteration in snow and estimate the isotope composition of bulk infiltration derived from snowmelt

Although Friedman *et alii* (1992) compared data from the funnel collectors and the PVC collectors, it is apparent that the PVC collectors provided immediate protection from metamorphic processes, while the funnel collectors likely allowed metamorphism prior to protection of liquid melt by the hydrocarbon oil. Although a data set that relies on different types of collectors at different sites is not ideal for interpreting spatial variations of stable isotopes in fresh precipitation, using paired collectors at a given site could provide an easy means of determining the degree of isotope metamorphism that snow undergoes and the bulk input signal from snowmelt.

By installing a funnel collector (regular or extended) and a PVC collector at a single site, and allowing both to operate throughout the year, two sets of data can be collected. The PVC collector should maintain the stable-isotope composition of fresh precipitation, regardless of whether it is rain or snow. The funnel collector should maintain the stable isotope composition of fresh rain, but the plate or screen in the Büchner funnel will act as an analog for the ground. Water will flow into the oil-covered reservoir only after snow-melt events, and thus the snow trapped in the funnel body will be subjected to most of the same processes as snowpack on the ground (input of heat from the soil and exchange with soil gas are the only two processes that will be impeded by the funnel collector). The resultant melt should provide a much better approximation of the melt that would infiltrate the ground surface than samples of fresh snowpack.

Sets of precipitation collectors were installed at eight sites (Figure 4-2) in Arizona and New Mexico. A PVC collector was installed at every site, and at least one type of funnel collector was also installed. At some sites, both regular and extended funnel collectors were operated in addition to a PVC collector. In the Chiricahua

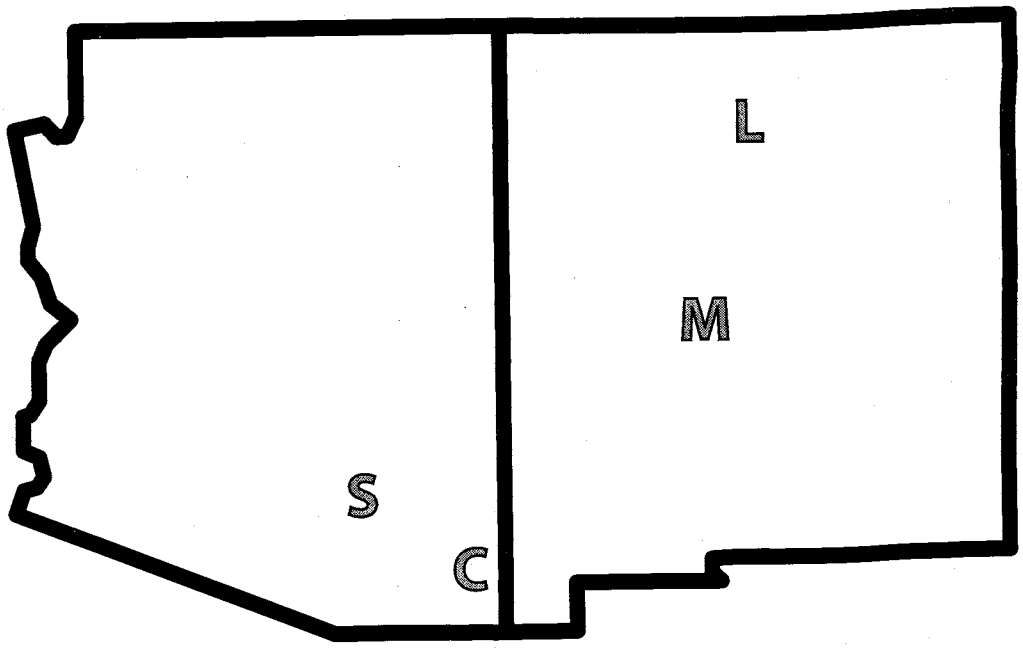

Figure 4-2. Map showing locations of precipitation collector sets in New Mexico and Arizona, USA. Letters on the map correspond to the first letter of each location. Location L (Los Alamos) has two sites—LA Low at 2140 m and LA High at 2682 m. Location M (Magdalena Mountains) has three sites: Mag Low at 2149 m, Mag Mid at 2560 m, and Mag High at 3243 m. Location C (Chiricahua Mountains) has two sites—Chir Low at 1640 m, and Chir High at 3017 m. Location S (Santa Catalina Mountains) has one site (Stew) at 2791 m.

Mountains and Los Alamos, collector sets were installed at high elevations (as close to the crest of the range as reasonably possible given installation and collection logistics) and low elevations. In the Magdalena Mountains, three collector sets were installed, at high, low, and mid-elevations in the range. A single set of collectors was emplaced near the crest of the Santa Catalina Mountains. The collectors were sampled twice a year: once in the spring, yielding integrated samples from the winter season; and once in the fall, yielding integrated samples for the summer season.

INVESTIGATION OF PROCESSES CONTRIBUTING TO ISOTOPE ALTERATION IN SNOW

To investigate the processes responsible for the alteration of the stable-isotope composition of snow, a study area was established in the Magdalena Mountains. The study area consisted of two adjacent sites. At each site, a collection pan rested on the ground. These pans were composed of white plastic in order to mimic the albedo of snow, and prevent the anomalous energy input that would be associated with dark and/or metal pans. The weight of both pans could be measured on site, and they were designed so that meltwater produced from the snow would enter a collection bottle containing a layer of mineral oil. One of the pans could be covered by a shade to block direct energy input from the sun (free circulation of air over the snow still was allowed); the other pan was left exposed to the natural cycle of sunlight and darkness. The shade was emplaced over the first collection pan as soon as feasible after the conclusion of a snow event. In some cases, this was accomplished in the late afternoon, but if snow was still falling at or near dusk, the shade was emplaced as soon as possible the morning after the snowfall. Therefore, although snow in the shaded pan may have received a short period of direct solar energy input, it was kept to a minimum.

The comparison of results from adjacent snows experiencing different energy inputs was considered important because freeze-thaw cycling is recognized as being a

significant control on isotopic metamorphism of snow and ice (Cooper, 1998; Jouzel and Souchez, 1982), and the variation in energy input could also affect the amount of evaporation/sublimation taking place. Sample collection and analysis methods are described in the "Hydrogeology" section of Chapter 1.

Results

Precipitation collectors

The types of collectors deployed at each site for each season are summarized in Table 4-1. Data from the precipitation collectors are shown in Table 4-2 and Figures 4-3 and 4-4. The data shown in Figure 4-3 represents two winter collection seasons and one summer collection season; data collected during the winter 2002-2003 are shown in Figure 4-4. Note that not all stations were activated at the same time, so some sites have no data for a given time period.

Winter 2002-2003 Data

For all sites, water in the reservoirs of the regular-funnel collector was enriched in δ D and δ ^{18}O compared to that in the PVC collector (Figure 4-4). At the LA High site, the water in the extended-funnel collector was enriched compared to that in the regular-funnel collector; the degree of enrichment is similar, but slightly less than the regular funnel-PVC collector enrichment. In all cases, the slope of the lines connecting the samplers for a site is between 5.1 and 7.4. At the two low elevation sites and the Chir High site, the degree of enrichment was relatively small; the LA High and Mag High sites both showed relatively large enrichments.

The amount of enrichment is related to the amount of time the snow was exposed between fall and melt. Because temperature and amount of precipitation are related to elevation, the low-elevation sites tend to receive less snow than the high-elevation sites, and the snow is subjected to higher temperatures, thus speeding melt. The Chir Low site is an exception, as it experienced nearly the same degree of

Site and collector type	Winter 2002-2003	Summer 2003	Winter 2003-2004
C High PVC	X	X	X
C High RF	X	X	X
C Low PVC	X	X	X
C Low RF	X	X	
C Low EF (black)			X
L High PVC	X	X	X
L High RF	X	X	X
L High EF (black)	X	X	X
L Low PVC	X	X	X
L Low RF	X	X	
L Low EF (white)			X
M High PVC	X	X	X
M High RF	X	X	X
M High EF (black)			X
M High EF (white)			X
M Mid PVC		*	X
M Mid RF		X	
M Mid EF (white)			X
M Low PVC		X	X
M Low RF		X	
M Low EF (white)			X
S PVC		X	X
S RF		X	
S EF (white)			X
S EF (black)			X

Table 4-1. Listing of collector types active at the study sites during given time periods. Station abbreviations are as given in Figure 2; PVC = PVC collector, RF = regular funnel collector, EF = extended funnel collector. *A PVC collector was in place at the M Mid site in summer 2003, but the sample was not analyzed due to the presence of a dead animal.

Site/Collector type	Winter 2002-2003		Summer 2003		Winter 2003-2004	
	$\delta^{18}O$ (‰)	δD (‰)	$\delta^{18}O$ (‰)	δD (‰)	$\delta^{18}O$ (‰)	δD (‰)
Chir High PVC	-10.9	-69.9	-9.5	-62.1	-10.3	-71.7
Chir High RF	-10.5	-67.4	-9.3	-59.1	-10.2	-68.9
Chir Low PVC	-9.1	-60.5	-6.9	-51.6	-11.5	-77.5
Chir Low RF	-8.7	-58.3	-6.8	-51.1	X	X
Chir Low EF (black)	X	X	X	X	-12.1	-77.9
LA High PVC	-16.6	-117.7	-8.8	-54.25	-16.1	-110.0
LA High RF	-14.8	-107.0	-8.5	-53.3	-14.1	-102.9
LA High EF (black)	-13.5	-98.2	-8.3	-50.4	-14.1	-102.1
LA Low PVC	-15.0	-111.1	-8.1	-50.1	-15.5	-106.9
LA Low RF	-14.4	-106.6	-7.6	-49.2	X	X
LA Low EF (white)	X	X	X	X	-15.81	-107.8
Mag High PVC	-13.2	-94.6	-9.2	-60.4	-12.1	-83.1
Mag High RF	-11.95	-85.3	-8.2	-56.4	-11.1	-74.7
Mag High EF (black)	X	X	X	X	-11.3	-73.3
Mag High EF (white)	X	X	X	X	-11.2	-74.6
Mag Mid PVC	X	X	X	X	-12.3	-79.3
Mag Mid RF	X	X	-9.2	-64.5	X	X
Mag Mid EF (white)	X	X	X	X	-11.9	-77.9
Mag Low PVC	X	X	-7.8	-55.7	-11.5	-75.6
Mag Low RF	X	X	-8.0	-56.7	-11.4	-75.1
Mag Low EF (white)	X	X	X	X	-11.4	-75.1
Stew PVC	X	X	-7.5	-56.5	-11.4	-72.8
Stew RF	X	X	-7.8	-58.5	X	X
Stew EF (white)	X	X	X	X	-10.7	-73.1
Stew EF (black)	X	X	X	X	-10.8	-73.5

Table 4-2. δ D and $\delta^{18}O$ of samples from precipitation collectors used in this study.

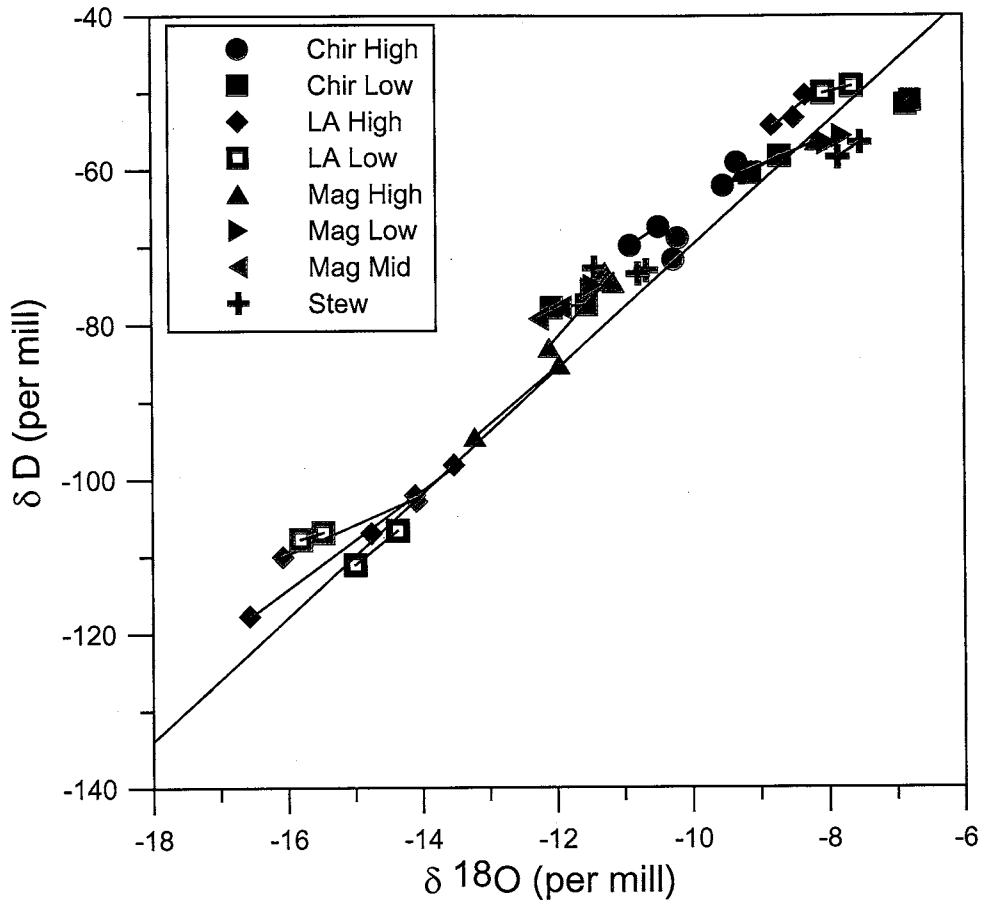

Figure 4-3. Plot of stable isotope data for all samplings of precipitation collectors used in this study. For each station, the open symbol represents winter precipitation from 2002-2003, the solid black symbol represents precipitation from summer 2003, and the grey-filled symbol represents precipitation from winter 2003-2004.

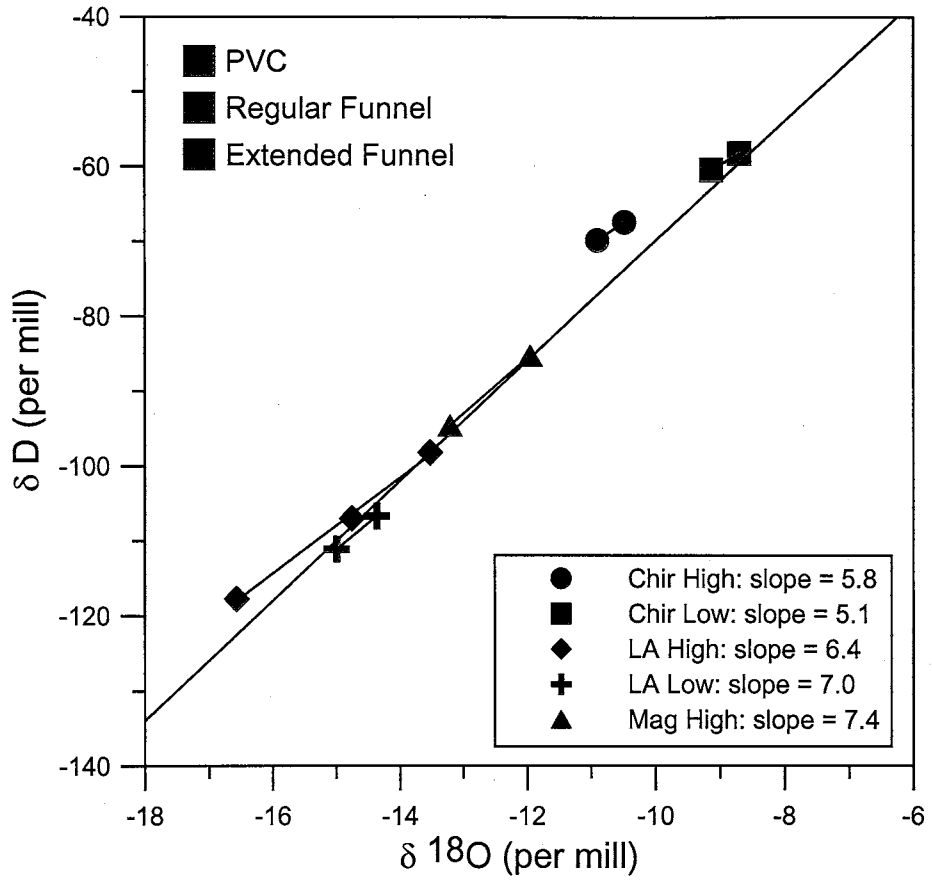

Figure 4-4. Plot of stable isotope data from winter 2002-2003, shown with the global meteoric water line. For each site, the PVC collector is represented by an open symbol; the extended funnel collector is represented by a solid symbol.

enrichment as the Chir High site. The Chiricahua Mountains had an unusually warm and dry winter, and due to its latitude, this site typically has warmer temperatures at a given elevation than the Mag and LA sites. Because little snow fell in the Chiricahuas that winter and temperatures were high, relatively little enrichment occurred, even at high elevation.

Several important findings are illustrated in Figures 4-3 and 4-4. First, if snow makes up a significant proportion of precipitation, different types of precipitation collectors can yield significantly different results at the same site. As a result, comparing isotope compositions from different collector types may not be valid. In addition, certain collector designs appear to preserve an isotope composition other than that of fresh snow. If the goal of a study is to measure the isotope composition of precipitation, collector design should be carefully considered if snow is a significant portion of the precipitation. Finally, even when significant enrichment of the fresh-precipitation compositions takes place, it may not be obvious. Due to the relatively high slopes of the enrichments on a δ D-δ ^{18}O plot, in no case does an enriched point plot far enough to the right of the global line to raise concern about its validity as a fresh precipitation sample. In fact, at four of the five sites, the enriched sample plots closer to the global line than does the fresh precipitation sample.

The observed slopes observed are higher than would be expected if the enrichment process were dominated by a kinetically-influenced process such as evaporation/sublimation. As evaporation/sublimation undoubtedly affected the snow at these sites to some degree (e.g. Lawson, 1997; Leydecker and Melack, 1999), this suggests that some other process or processes are operating as well, and that these processes are not kinetically influenced. This issue will be discussed further in a later section.

All data

The data from all precipitation collectors (Figure 4-3) show that, as expected, the summer precipitation compositions are enriched compared to the winter precipitation compositions. During the summer collection, all precipitation fell as rain, and, as predicted based on collector design, most sites show only minimal differences between collector types. Much of the difference at these sites is attributable to the fact that the different collector types were not at exactly the same elevation above ground surface and had slightly differently-sized openings, so collector efficiency was not identical; analytical error may be responsible for some of the difference. The Mag High site did show a significant difference between the PVC- and regular-funnel-collector samples. At the time of sampling, it was found that the regular funnel collector had been disturbed from its upright orientation. The tilted position may have affected the isotope composition of the collected precipitation in two ways. First, the tilt imposed on the collector may have thinned the layer of mineral oil covering the collected precipitation at the highest point in the reservoir such that evaporation could have taken place. Friedman *et alii* (1992) show that a layer of mineral oil in a collection reservoir will prevent evaporation as long as it is of sufficient thickness; although mineral oil was added in excess of the amount needed to achieve this condition if the collector remained upright, the tilting of the collector may have negated this. Second, the Mag High site is in a treeless area at the crest of a large mountain range, and wind gusts in excess of 160 km/hr have been recorded in the area. If one or more rain events occurred in conjunction with strong winds, the resultant directionality of the rain may have caused greater collection efficiency for a given event or events by one sample versus the other. The minimal differences between collectors for the summer samples at most sites show that the larger variations

observed for the winter 2002-2003 samples are not attributable to differences between the collector types.

The degree of alteration observed for the winter 2003-2004 is typically less than that seen for the previous winter (Figure 4-3). For the two sites that had all three collector types (Mag High and LA High), enrichment was observed for the funnel-collector samples relative to the PVC-collector samples, but there was no enrichment observed between the regular- and extended-funnel-collector samples. This suggests that snow events were such that the extended-funnel collectors did not accumulate more snow than the regular-funnel collectors, and thus did not offer an opportunity for increased exposure time. Two sites (Mag High and Stew) had both black and white extended-funnel collectors to test the hypothesis that more rapid melt in the black collector would yield less enrichment than observed in the white collector. However, the samples from these collectors were nearly identical isotopically. The 2003-2004 winter was unusually warm and dry throughout the study region, so less snow and higher temperatures minimized the alteration at most sites. In addition, while precipitation collected during the winter of 2002-2003 contained only minimal rain, significant amounts of rain were collected in the winter 2003-2004 sampling due to unusual spring rains. Because rainfall puts water of nearly identical isotope composition into both collectors, significant amounts of rain would lessen the difference in isotope content between the collectors that would have been observed had only snow been collected.

GROUNDWATER RECHARGE DERIVED FROM SNOWMELT

The data gathered for this study were used in conjunction with other records of isotopes in precipitation and groundwaters from the study sites (Adams *et alii*, 1995; Blake *et alii*, 1995; Cunningham *et alii*, 1998; Earman *et alii*, 2003; Gross and Wilcox, 1983; Wright, 2001) in order to estimate snowmelt contributions to groundwater

recharge at the four study sites. The results for all sites are shown in Table 4-3; an illustration of the methodology used is provided for the LA High site.

LA High site

Data collected at the LA High site in the winter of 2002-2003 are shown in Figure 4-5A; data from the winter of 2003-2004 are shown in Figure 4-5B. The ellipse labeled "Residual Snow" in Figure 4-5A gives the range of values for the small (< 30 cm in diameter) patches of snow remaining on the ground when melt was nearly concluded, and the vast majority of snowpack was no longer present Samples were collected on 11 April, at the conclusion of the main winter snowpack melt, and on 19 May, at the conclusion of the melt of a late-season snow that fell after the main snowpack had completely melted. Residual snow was not collected in 2004.

The fresh snow from winter 2002-2003 (as sampled in the PVC collector) is heavy compared to the centroid of the ellipse representing the range of winter precipitation values, but still within the observed range. The alteration of the snow in the regular and extended-funnel collectors shifted the isotope composition to a significantly heavier value, much closer to the mean value for groundwater. The values observed for the residual snow indicate that snow continues to become isotopically enriched until melt is complete, and that greater exposure times result in increased enrichment. The continued enrichment follows the same trend as the three precipitation collectors (the fit line for the collectors intersects the residual snow ellipse if extended in that direction). The residual snow is heavier than the mean groundwater, but as it makes up only a relatively small portion of the meltwater contribution, its heavy isotope values are moderated by the lighter material that makes up the majority of melt.

Although no data that would allow direct comparison of collector data to actual infiltration were collected, the extended funnel collector appears to provide a

Site	2002-2003	2003-2004	Long-term	Precip. %
Chiricahua Mts. (C)	-	-	60	30
Los Alamos (L)	54	48	-	41
Magdalena Mts. (M)	51	69	-	49
Santa Catalina Mts. (S)	-	43	-	25

Table 4-3. Values calculated for percentage recharge due to snowmelt at the study sites. "Precip %" values are the proportion of snow in average annual precipitation, assuming snow water equivalence is 10%.

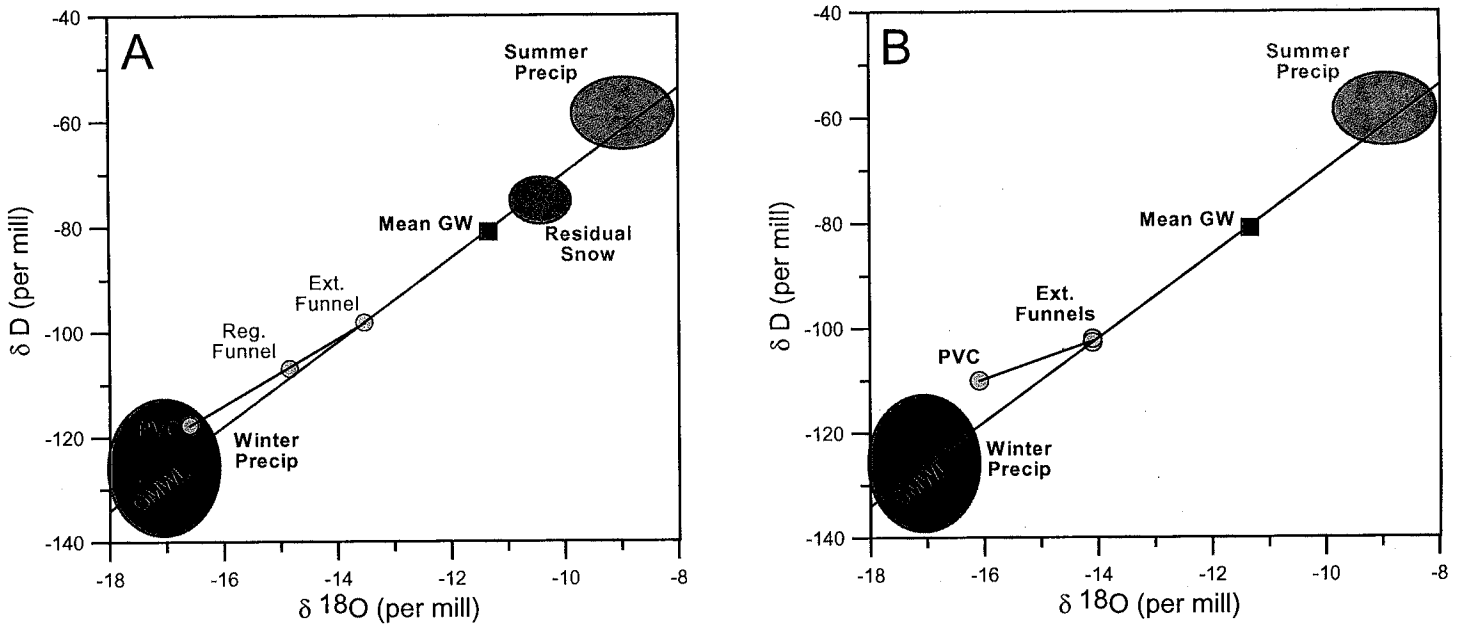

Figure 4-5. Plots showing the isotope composition of samples from the three collectors at the LA High site and the global meteoric water line. Also shown on both figures are the ranges of values for summer and winter precipitation based on long-term monitoring [from *Adams et al.*, 1995], and a mean value for groundwater in the study area [calculated from data in *Blake et al.*, 1995]. PVC = PVC collector, Reg. Funnel = regular funnel collector, Ext. Funnel = extended funnel collector, Mean GW = mean value for groundwater. **A:** data for winter 2002-2003. Also shown is a range of values for 'residual snow' (the last small patches of snow remaining near the conclusion of melt). **B:** data for winter 2003-2004.

more representative value of infiltration water isotope composition than a fresh snow sample. Assuming that the sample from the extended-funnel collector is the best available representative of the bulk meltwater input, it was used as the snowmelt end member of a mixing calculation (described in Appendix 4) to determine the proportion of snowmelt and rain in the groundwater. Using the $\delta^{18}O$ value of the meltwater from the extended funnel collector (-13.5 ‰) as the snowmelt end member, and the value taken from the centroid of the long-term rain ellipse (-8.9 ‰) as the rain end member, the model predicts that snowmelt is responsible for 53% of the groundwater recharge at the study area. In contrast, if a fresh-snow value (as represented by the PVC-collector sample's $\delta^{18}O$ value of -16.6 ‰) is used in place of the altered-snow value, the proportion of snowmelt in groundwater recharge would be only 32%.

As expected due to the warmer temperatures in the winter of 2003-2004, the fresh snow value (PVC collector) is heavier than that of the previous winter, but the lack of enrichment beyond that observed for the regular funnel collector yields a lighter value than the previous winter for the snowmelt input end member. As a result, data from this season suggest a slightly lower proportion (48%) of the recharge is derived from snowmelt (using the $\delta^{18}O$ of -14.1 ‰ from the extended funnel collector in the mixing model described above), and a lower difference between the proportions calculated using the enriched and fresh snow samples (11% rather than 21% for the previous winter).

All sites

The calculated contribution of snowmelt to groundwater recharge at the four study sites ranges from 43% to 69%, depending on the site and the year of data used in the calculations. In all cases, the proportion of snowmelt in recharge is higher than the proportion of snow in average annual precipitation. For the Mag and LA sites, the lower calculated proportions of snowmelt in recharge are only 2% and 7% higher

(respectively) than the proportion of snow in average annual precipitation, while the high calculated values of recharge are 20% and 13% higher (respectively) than the proportion of snow in average annual precipitation. For the Stew and Chir sites, the calculated proportions of snowmelt in recharge are only 22% and 30% higher (respectively) than the proportion of snow in average annual precipitation

Although the estimates from the two years in which data were gathered are comparable for the LA site, the Mag site showed a distinct difference. Unfortunately, there are no longer-term data for stable isotopes in precipitation at the Mag site as there are for the other sites, so it is not known how similar the PVC-collector values observed in this study are to average precipitation at the site. In all cases, long-term monitoring with paired collectors would likely provide a more accurate range of values for recharge derived from snowmelt, and also a mean value based on a more reasonable number of observations.

At the LA site, the relatively heavy isotope composition of fresh snow (compared to the mean groundwater) in a warm year was counteracted by lower enrichment than seen in a cooler year, and a lower amount of snow, resulting in a lower calculated recharge due to snowmelt. Whether this pattern would continue at this site for other warm years is not known. At the Mag site, the degree of alteration remained similar in both years, so isotopically-heavier warm-year snow led to a higher estimate of snowmelt contribution to recharge. Due to the climate regime in effect at the time of the study, no cool years were observed, so it is not known to what degree the relative lightness of fresh snow falling in such a year would be offset by the increased exposure time resulting from greater amounts of snow and cooler temperatures.

Another issue is the degree to which the extended-funnel collector value is representative of actual recharge. While it appears to be a good representation of

the isotope composition of bulk meltwater, no attempt was made to determine what portion of this water infiltrated, or how the proportion of infiltration to runoff might have varied during the continuous enrichment while the snow was exposed. If piston flow is assumed during infiltration, it could be argued that the bulk isotope composition used here to calculate the proportion of snowmelt in recharge is too heavy, as the lighter meltwater emerging from the snow during the initial period of melt will be the first to infiltrate and the first to become recharge, while the heavier meltwater entering the soil during the latter portions of melt is the last to enter the soil, and might not become recharge. However, the applicability of true piston flow to these sites is not known. In an examination of meltwater infiltration, Maulé *et alii* (1994) found that infiltrating meltwater mixed with existing pore water rather than displacing it; a similar scenario could apply to the sites examined in this study, which would imply no early-versus-late melt weighting is needed.

SNOW PLOTS

Data from a snow event monitored for this study are given in Table 4-4, and shown in Figures 4-6, 4-7, and 4-8 (some additional data in the plots but not in Table 4-4 are provided in Appendix 11). Both the shaded and unshaded snow lasted from 20 January until 31 January. In general, progressive enrichment of both the remaining snow and the meltwater took place in both pans; the unshaded pan exhibited greater degrees of enrichment for both the melt and the remaining snow.

Shading affected the mode of mass loss in the snow (Figure 4-6). The shaded snow lost 35% of its mass due to evaporation/sublimation, while the unshaded pan lost only 13% of its mass in this manner. The unshaded snow yielded its first melt a day prior to the shaded pan, and always had higher mass loss due to melt on any given day. Another effect of the shading is evident in the period from 25 January to 27 January, when extremely cold temperatures prevailed. The shaded pan lost no mass because

Sample	δ D (per mill)	δ ^{18}O (per mill)
US Snow 21 January	-109.5	-16.8
US Snow 22 January	-106.3	-16.5
US Snow 23 January	-101.9	-16.7
US Snow 24 January	-93.7	-15.0
US Snow 25 January	-92.3	-14.1
US Snow 27 January	-86.7	-13.1
US Snow 29 January	-85.3	-12.3
S Snow 21 January	-110.8	-17.4
S Snow 22 January	-108.4	-17.2
S Snow 23 January	-103.3	-15.5
S Snow 24 January	-97.0	-14.3
S Snow 25 January	-96.5	-14.2
S Snow 27 January	-95.3	-13.6
S Snow 29 January	-95.5	-13.5
US Snowmelt 23 January	-112.9	-17.7
US Snowmelt 24 January	-103.6	-16.2
US Snowmelt 25 January	-103.6	-16.1
US Snowmelt 27 January	-78.8	-12.6
US Snowmelt 29 January	-79.5	-10.6
US Snowmelt 31 January	-78.6	-11.8
S Snowmelt 24 January	-109.0	-17.1
S Snowmelt 25 January	-107.6	-15.5
S Snowmelt 29 January	-90.8	-13.1
S Snowmelt 31 January	-93.4	-13.4

Table 4-4. Evolution of δ D and δ ^{18}O of snow and meltwater from adjacent plots of shaded ("S") and unshaded ("US") snow and melt derived from the snow plots.

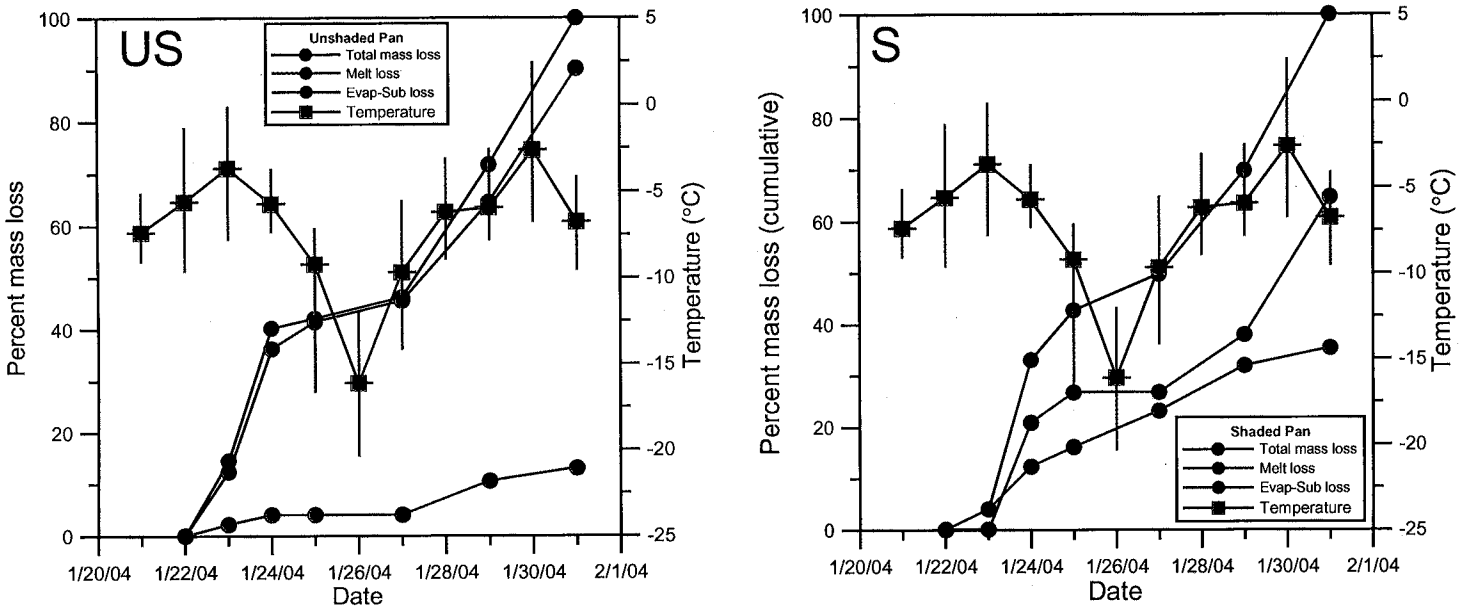

Figure 4-6. Mass loss of adjacent shaded and unshaded snow patches shown with temperature from the nearest meteorological station. **US**: unshaded snow, **S**: shaded snow. The box with a horizontal line through its center represents mean daily temperature, the high and low points of the associated vertical bars represent maximum and minimum temperatures (respectively). Temperature data is from the nearest meteorological station, located in the same mountain range, but approximately 700 m higher in elevation. Although the temperatures from this station are cooler than those experienced at the study site, the correlation of snow behavior with temperature shows that the same temperature trend observed at the meteorological station applies to the study site.

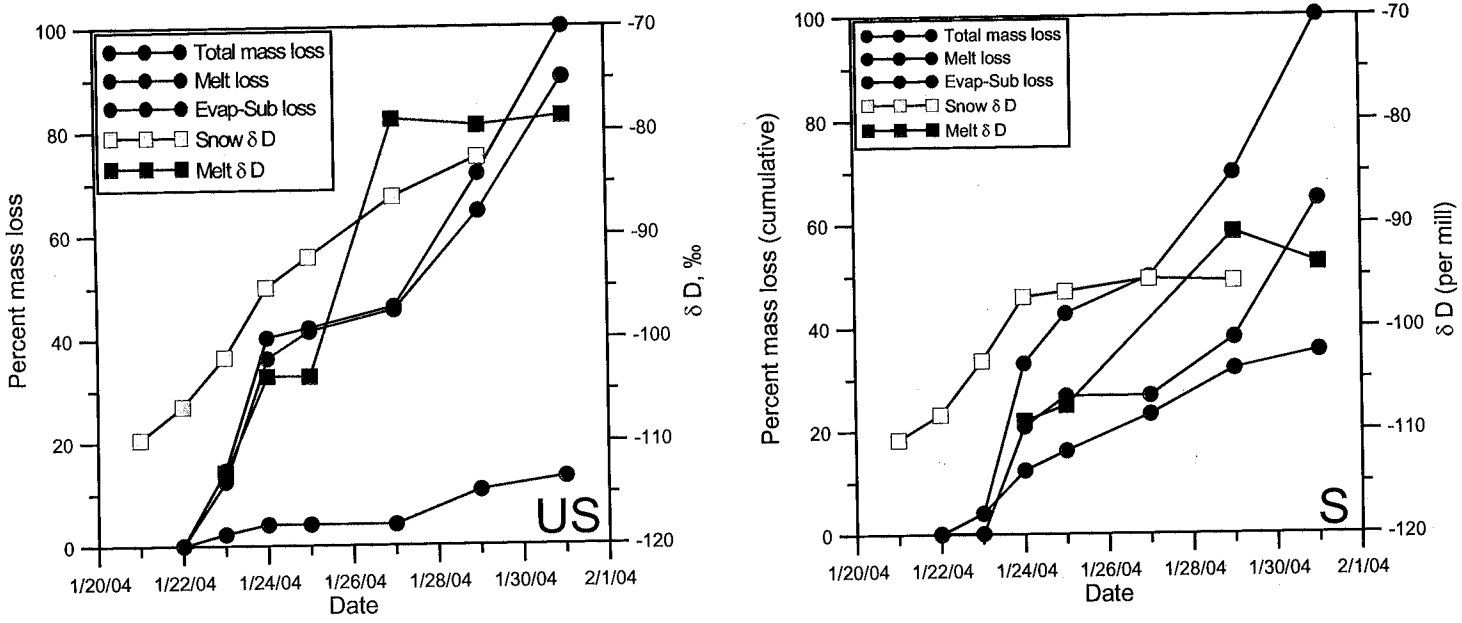

Figure 4-7. Mass loss of adjacent shaded and unshaded snow shown with the δ D of the snow and the meltwater derived from it. Note that the date represents collection date; snow values represent the snow present at the time of sampling, but the melt is that which was produced in the period prior to sampling. **US**: unshaded snow, **S**: shaded snow.

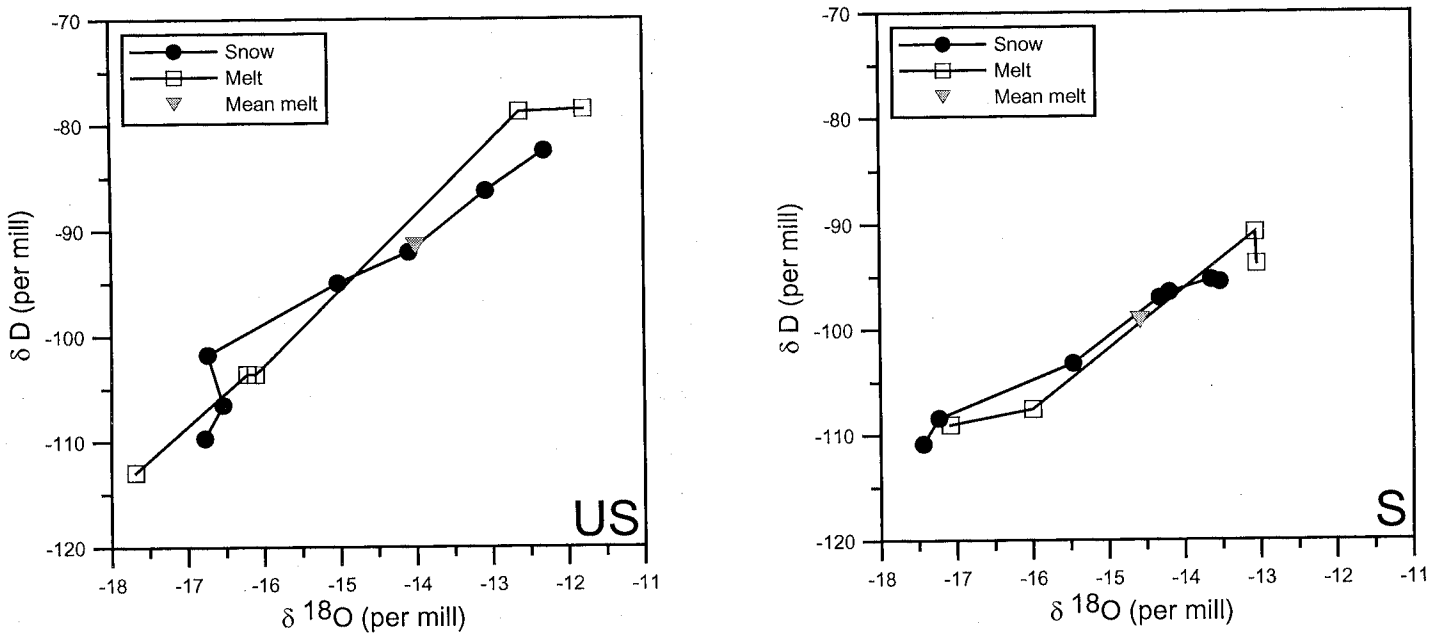

Figure 4-8. δ D versus δ ^{18}O for the snow and melt from adjacent unshaded (**US**) and shaded (**S**) snow patches. The triangles represent the weighted mean of all melt samples. Note that the mean melt is enriched compared to the fresh snow.

of melt in this period, but the unshaded pan experienced melt loss due to the extra energy derived from solar radiation. For both the shaded and the unshaded snow, the two days with the highest temperatures (23 and 30 January) correlate with the highest slopes on the melt loss curves; the shift in slope on the total mass loss curve on these days is more distinct for the shaded pan than the unshaded pan.

Sublimation of snow, being a kinetically-influenced process, tends to drive isotope evolution on a slope similar to that for evaporation on a δ D-δ ^{18}O plot (Stichler *et alii*, 2001). During periods of melt, it is not possible to distinguish the evaporation of meltwater in the snow matrix from sublimation of snow, but the impact on the isotope evolution will be the same. The shaded snow and its meltwater evolve along slopes of 3.8 and 4.4 (respectively), while the unshaded snow and its meltwater evolve along slopes of 5.4 and 6.2 (respectively) (Figure 4-6). Because the shaded snow had more mass loss due to kinetically-influenced processes, this suggests that the slope followed during alteration is a balance between equilibrium processes that mostly cause high slopes and kinetically-influenced processes that cause evolution to move along a lower slope.

From 25 January to 27 January, the shaded snow lost 160 g of mass, but this was almost exclusively due to evaporation/sublimation (less than 0.6% of the mass lost in this period was due to melt). Because the loss due to melt was negligible, processes such as fractionation due to partial melting, melt/snow interaction, and meltwater/atmospheric water-vapor exchange can be ruled out as affecting the isotope composition of the snow. The mechanisms with the potential to drive isotope evolution during this period are sublimation, snow/atmospheric water-vapor exchange, and condensation of atmospheric water vapor on the snow surface. The amount of condensation (if any) on the snow surface was probably minimal compared to the mass loss, so this will be ignored. The equilibrium fractionation factors described

by Majoube (1971a) and Merlivat and Nief (1967) were adjusted for kinetic effects using the method of Gonfiantini (1986) (meteorological data from the crest of the range were modified to account for the lower elevation of the study site, yielding an average temperature of -7.2 °C, and average relative humidity of 0.772 from 25 to 27 January). The adjusted fractionation factors suggest that pure sublimation would cause enrichment to plot on a slope of 5.0 during this period, quite close to the observed slope of 5.3. The difference between the measured and predicted slopes could be explained by two factors. First, the extrapolation of meteorological conditions at the site might have been slightly in error. Second, the estimated fractionation factors could be correct, but an equilibrium process (such as exchange with atmospheric water vapor) could have been active in addition to sublimation, pulling the slope higher. An experiment discussed at the end of this chapter shows that snow kept below freezing can have its isotope composition affected by exchange with atmospheric water vapor. Although the observed and predicted slopes are similar, the magnitude of observed enrichment is much smaller than the predicted enrichment (Figure 4-9). The most likely explanation is that both Majoube (1971a) and Merlivat and Nief (1967) determined vapor/ice equilibrium fractionation factors using experimental systems relying on the instantaneous freezing of water vapor. As described by Moser and Stichler (1980), the vapor/ice transition can be expected to yield "isotope effects close to those demanded by equilibrium conditions," but the ice/vapor transition may not, depending on the configuration of the ice crystals and their surface area/volume ratio.

Another phenomenon of note is that for both snow patches, the melt derived from the snow is isotopically lighter than the remaining snow during the initial period of melt, but becomes heavier than the snow during the latter portion. For both the shaded and unshaded snow, the first samples of melt heavier than the remaining snow were collected when about 70% of the snow's initial mass had been lost. Based on

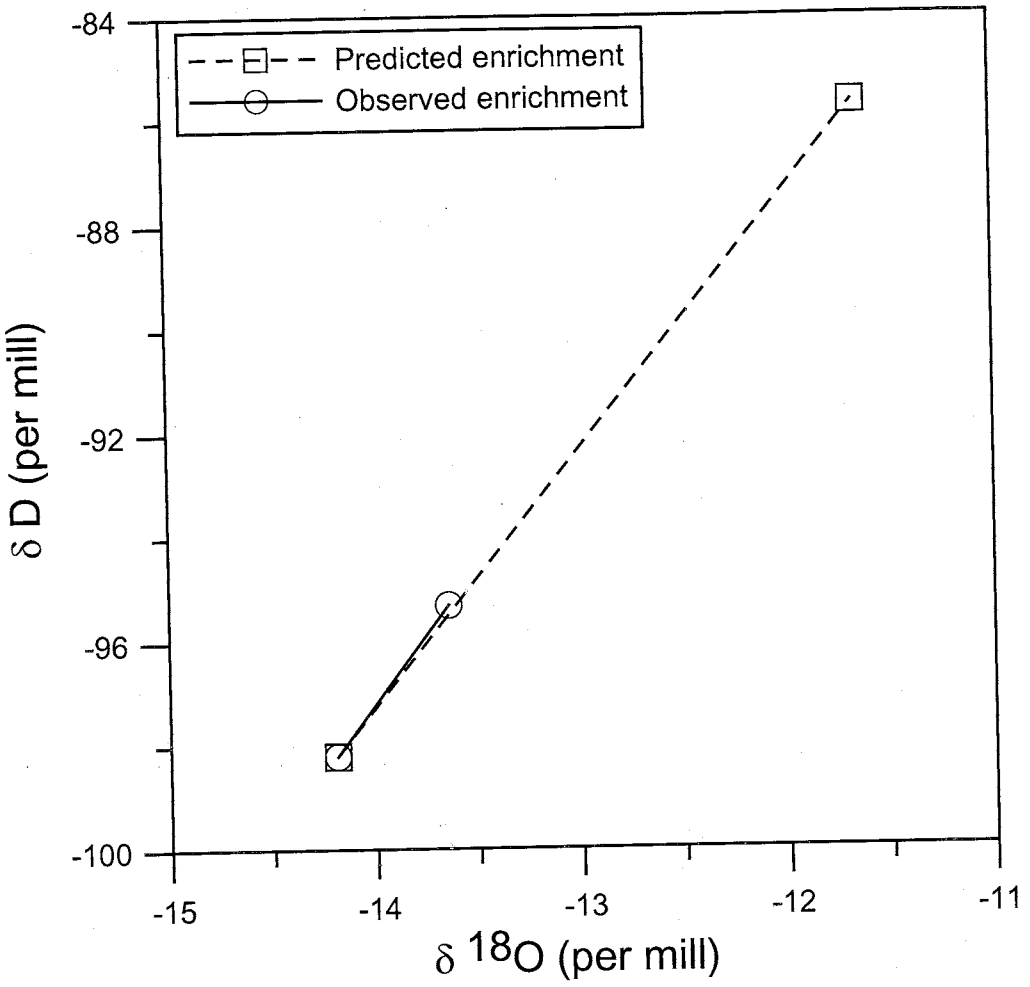

Figure 4-9. Observed enrichment of shaded snow due to sublimation (with possible influence from exchange with atmospheric water vapor) from 25 to 27 January shown with predicted enrichment (based on theoretical values).

laboratory experiments with constant input of thermal energy, Hermann *et alii* (1981) found that for constantly melting snow in the laboratory, initial melt is typically lighter than snow due to fractionation effects, and that the isotope composition of the melt approaches that of the snow as melt progresses; they did not, however, find melt heavier than snow. This suggests that constant melt is not a good approximation of field conditions in which melt occurs only for part of each day. At least two field studies have observed snowmelt heavier than the snow from which it is derived, but no interpretation of the mechanisms was made (Hooper and Shoemaker, 1986; Martinec *et alii*, 1977); possible causes include evaporation of meltwater in the snowpack, and isotope exchange between meltwater and atmospheric water vapor. Hermann *et alii* (1981) conducted a laboratory experiment with alternating freeze-thaw cycles, but data were presented for the meltwater only, so the snow/meltwater relationship is not known.

The isotope evolution of the snow is dependent upon the interplay of a number of processes. The importance of the evaporation/sublimation process is dependant on the incoming solar energy. If the solar energy input is relatively high, melt processes tend to drive most of the isotope evolution, with evaporation/sublimation processes accounting for a relatively small part of the observed enrichment. In cases of relatively low solar energy input, evaporation/sublimation processes are more important in driving the isotope evolution, but are balanced by equilibrium processes, including isotope exchange between snow and meltwater, snow and water vapor, and meltwater and water vapor. We conducted a laboratory experiment to assess the potential significance of isotopic exchange between snow and water vapor to see if it could be a significant contributor to the observed evolution.

Investigation of the potential for isotope exchange between snow and atmospheric water vapor to affect the isotope evolution of snow

Background

In recent years, there has been increased focus on the fact that the stable isotope signature of snow undergoes alteration throughout the period between snowfall and the completion of melting; understanding the magnitude of this alteration and the mechanisms that cause it is essential to achieving correct results from stable isotope studies that deal with snow and/or snowmelt. There are many mechanisms that have the potential to alter the isotope content of snow (either individually or in concert with other mechanisms), including melt, partial melt and refreezing, mass transport due to temperature gradients, rain-on-snow events, isotope exchange between meltwater and atmospheric vapor (or soil vapor), and evaporation/sublimation. Another possible mechanism for alteration is isotope exchange between snow and atmospheric water vapor, but the viability and potential influence of this process on the isotope composition of snow is not universally recognized or accepted.

In the past, it was commonly believed that isotope exchange between snow and water vapor cannot exert a significant influence on the isotope composition of a snowpack due to the slow rate of molecular diffusion in solids such as snow (e.g. Búason, 1972; Hage *et alii*, 1975). The prevalent view now is that snow-vapor exchange can be important. Cooper (1998) states that exchange with atmospheric water vapor can have a significant impact on the isotope content of snow, especially the upper layers of the snowpack, and a number of authors, including Stichler (1987), Friedman *et alii* (1991), Sommerfield *et alii* (1991), and Rose *et alii* (1999), suggest that exchange with atmospheric water vapor could help explain alteration observed during field studies of snowpack. However, studies that suggest snow-vapor exchange is an important process appear to do so based on 'Occam's razor'-type reasoning: observed shifts in snow isotope compositions that are most easily explained if snow-

vapor exchange is invoked. To our knowledge, no experiment has given direct evidence of snow-vapor exchange. Perhaps as a result of this lack of direct evidence, many studies appear to discount the process. For instance, Feng *et alii* (2002) and Taylor *et alii* (2002) state that the two factors controlling isotopic evolution of snow are the rate of meltwater-ice isotopic exchange and the ratio of ice to liquid in the system; and Unnikrishna *et alii* (2002) describe a snowpack surface as being affected by "precipitation, evaporation and condensation, and melt out" but do not mention isotope exchange.

If isotope exchange does occur between snow and atmospheric water vapor, the impact could be significant. In many systems, isotope exchange is the main factor that determines the distribution of stable isotopes (Ingraham and Criss, 1993). The most commonly-known example is Craig *et alii's* (1963) demonstration that exchange with atmospheric water vapor dominates the isotopic evolution of liquid water after an initial period of evaporation influence. Ingraham and Criss (1993) show that two waters in a sealed container with different isotope signatures will undergo isotope exchange with each other via the atmospheric water vapor, eventually reaching a common isotope composition.

A set of experiments was performed to investigate the possibility that isotope exchange between snow and atmospheric water vapor significantly alter the isotope composition of the snow.

Experimental design

Snow was collected from the Magdalena Mountains near Magdalena, NM (USA), and sealed in airtight containers, which were placed in an insulated cooler with ice packs for transport to the laboratory (and stored in a freezer if not used immediately upon return). In the laboratory, an aliquot of the snow (approximately 60 g) was placed on a screen underlain by a pan to collect any melt that might be

generated from the snow. The snow and melt pan were kept in a sealed, temperature-controlled chamber for 10 days. Samples of snow were collected at the beginning and end of each experimental run. To determine if exchange occurs between snow and atmospheric water vapor, two runs were conducted in which the isotope composition of the atmospheric water vapor in the experimental chamber differed significantly.

One run was designed as a control. In this case, the temperature of the experimental chamber was kept below 0 °C, and the water vapor in the chamber air was simply that which was sealed in as part of the ambient atmosphere in the laboratory.

For the second run, the temperature of the experimental chamber was kept below 0 °C, and, in addition to the snow, a pan of water (approximately 200 g) of distinctive isotope composition was placed inside the chamber. The water was maintained in the liquid state by two means: addition of NaCl to suppress the freezing point, and bubbling air through the water with a battery-operated pump. The water was pre-cooled in the chamber prior to the introduction of the snow in order to eliminate the possibility of thermal pumping driving mass movement from the water to the snow. The water was intended to provide a large reservoir compared to the vapor present in the chamber air, and force the isotopic composition of the water vapor to a value unique from that in the control experiment. If snow-vapor exchange is a significant process, the difference in chamber water vapor isotope content during these two runs should cause different isotope evolution of the snowpack.

In both cases, the experimental chamber was an airtight plastic container that was housed inside a larger, temperature-controlled chamber. The inner chamber was not in direct contact with the outer chamber floor or walls. This chamber-in-chamber design was intended to eliminate the 'plating-out' effect observed by Sommerfield *et alii* (1991), in which the freezer walls are a sink for water vapor in the chamber due

to the fact that they are the coldest part of the system during the initial portions of the cooling cycles of the freezer. Although not successful in eliminating plating out, the chamber-in-chamber design reduced it to about 10 to 20 % of what was observed in runs conducted without the inner plastic chamber.

In order to assure that any exchange that took place could be distinguished from other processes (*exempli gratia* evaporation), the water used in the second experiment was distillate produced from Canadian shield brine (CSBD). This brine is isotopically unique because, compared to a water that plots on the global meteoric water line (GMWL), it is significantly enriched in δ D, but not in δ ^{18}O—in other words, it plots 'above' or 'to the left' of the GMWL. Isotope exchange with this water should thus cause a shift in isotope composition of the snow that could not be accounted for via evaporation/sublimation, because the slope of evolution on a δ D-δ ^{18}O plot would be too high.

Results

The results of the experiments are shown in Table 4-5 and Figures 4-10 and 4-11. Because the initial δ values of snow samples used in different runs were not identical, Figure 4-10 shows the change in isotope composition rather than the actual δ values to allow easy comparison. Snow that was alone in the chamber as 'snow without CSBD,' and the snow accompanied in the chamber by the CSBD as 'snow with CSBD.'

For the two main experiments described above, a logging thermometer showed that the snow was maintained at -3 ± 1.5 °C; visual observation confirmed that no liquid water was present at the conclusion of the experiments, and that none appeared to have been produced and subsequently frozen.

Compared to the snow with CSBD, the snow without CSBD experienced greater enrichment (Figure 4-10), with the shift in isotope composition characterized

Sample	Inititial δ D (‰)	Final δ D (‰)	Initial $\delta^{18}O$ (‰)	Final $\delta^{18}O$ (‰)	Initial Mass (g)	Final mass (g)
Snow with CSBD	-104.3	-99.5	-15.34	-14.95	55.7	51.9
CSBD	-74.6	-71.5	-15.92	-15.26	193.8	190.5
Snow without CSBD	-104.7	-97.7	-16.78	-14.86	56	49.7

Table 4-5. Values for isotope composition and mass of the CSBD, snow with CSBD, and snow without CSBD.

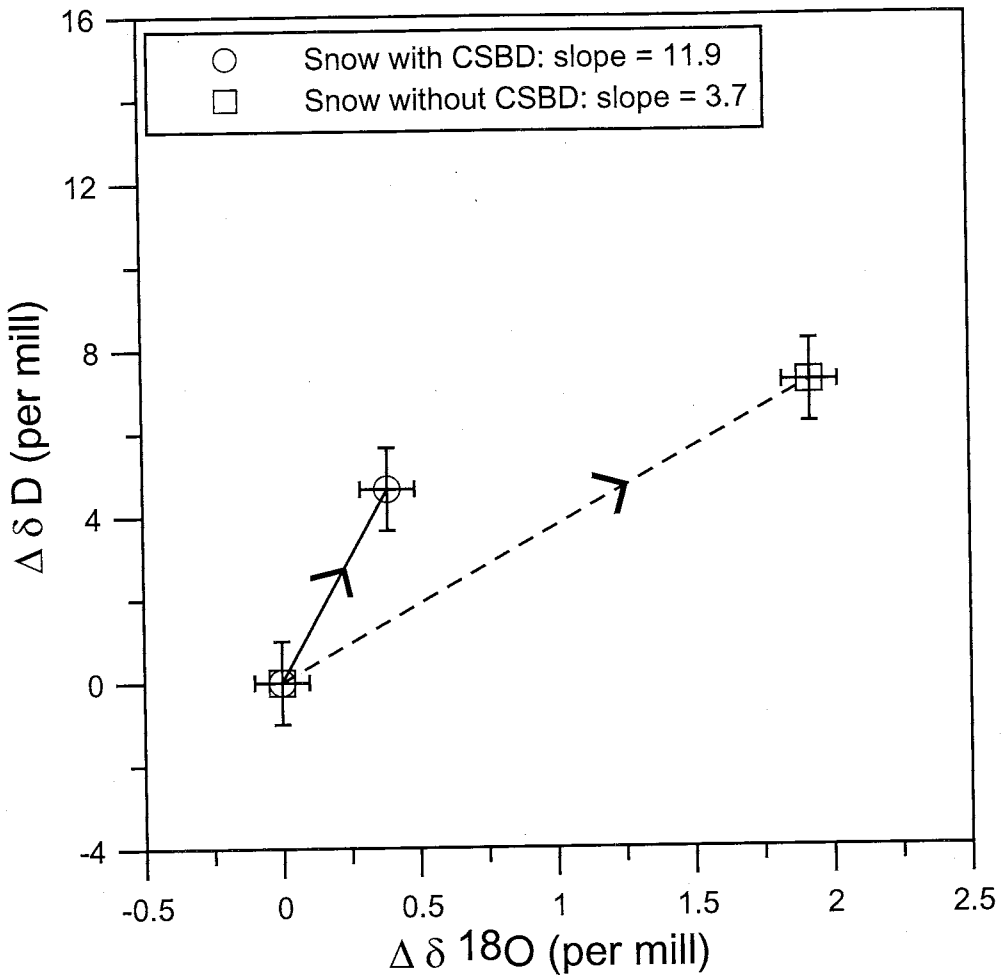

Figure 4-10. Plot showing the shift in isotope composition for snow with CSBD and snow without CSBD during their 10-day experimental runs. Error bars on the plot indicate the analytical uncertainty associated with the data.

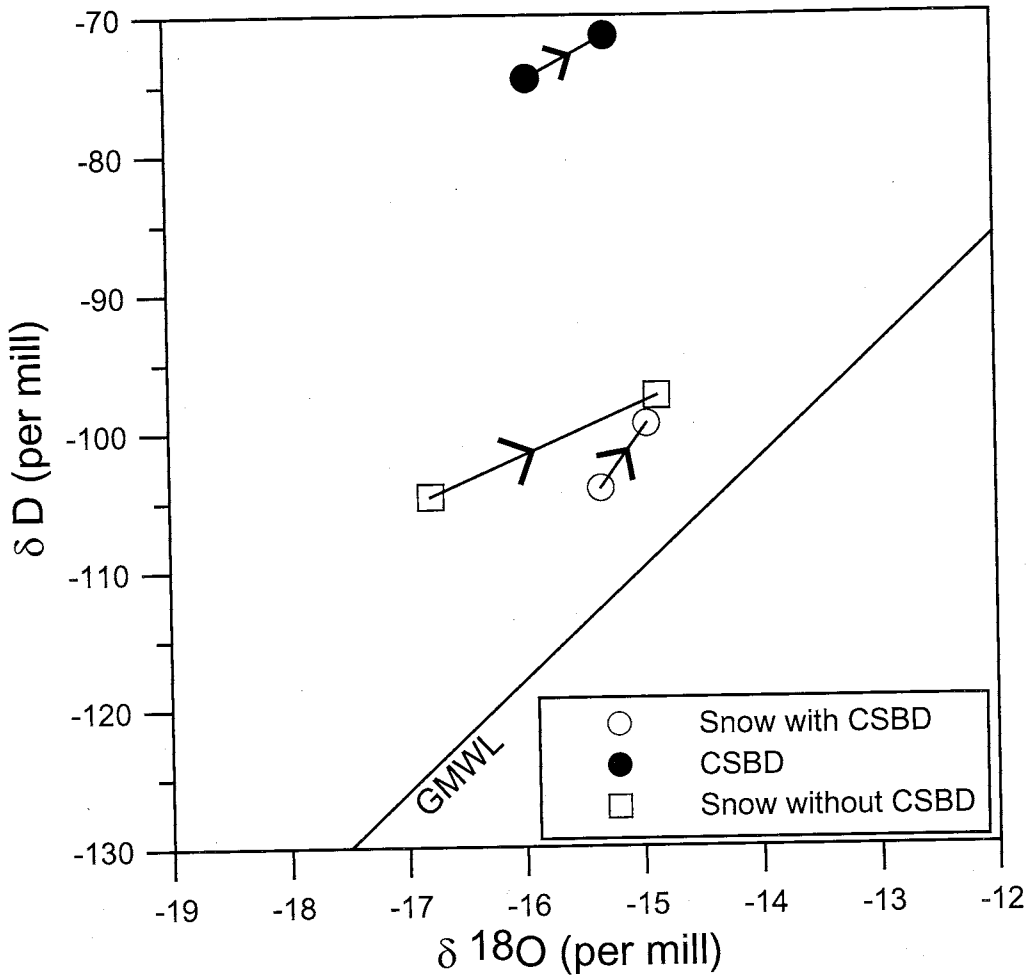

Figure 4-11. Plot showing the non-normalized values for the CSBD, snow with CSBD, and snow without CSBD before and after the experimental runs, along with the global meteoric water line (GMWL). On the scale of this diagram, the error bars representing the uncertainty are the same size as the symbols, and are thus not shown.

by a much lower slope (3.7 versus 11.9). Indeed, the snow without CSBD lost about 6.3 g to sublimation (~ 10 % of its initial mass). The inner chamber walls accumulated 6.6 g of frost during the experiment, yielding a mass balance error of 0.3 g (although no effort was made to account for the mass of water vapor in the chamber that had been derived from the snow without CSBD). The snow with CSBD lost about 3.8 g (~ 7 % of its initial mass) due to sublimation. The lower mass loss in this instance is due to the presence of the CSBD, which is an additional reservoir that can provide water to the atmosphere of the system. The CSBD lost 3.3 g during the run. The inner chamber walls accumulated 6.9 g of frost during the experiment, yielding a mass balance error of 0.2 g (although no effort was made to account for the mass of water vapor in the chamber that had been derived from the CSBD and snow with CSBD).

Interpretation

A Rayleigh distillation model (Lord Rayleigh, 1896) was used to predict the shift in isotope composition of the CSBD and snow with CSBD that would have resulted had they lost mass solely due to evaporation and sublimation (respectively). The mass fractions remaining at the end of the experiment were used in conjunction with the fractionation factors for the liquid-vapor (Majoube, 1971b) and ice-vapor systems (Majoube, 1971a; Merlivat and Nief, 1967) and the environmental conditions of the system. The results of the calculations (Figure 4-12) show that the CSBD became less enriched in δ D than predicted, but more enriched in $\delta\ ^{18}O$. For the snow with CSBD, the opposite occurred—it became less enriched in $\delta\ ^{18}O$ than predicted, but more enriched in δ D. This is consistent with isotope exchange between the two reservoirs via the atmosphere, as observed by Ingraham and Criss (1993) for a liquid-vapor-liquid system. Simple sublimation of the snow with CSBD would result in a low slope of evolution, but concurrent exchange with the CSBD would cause the slope to increase by enriching the snow with CSBD in D.

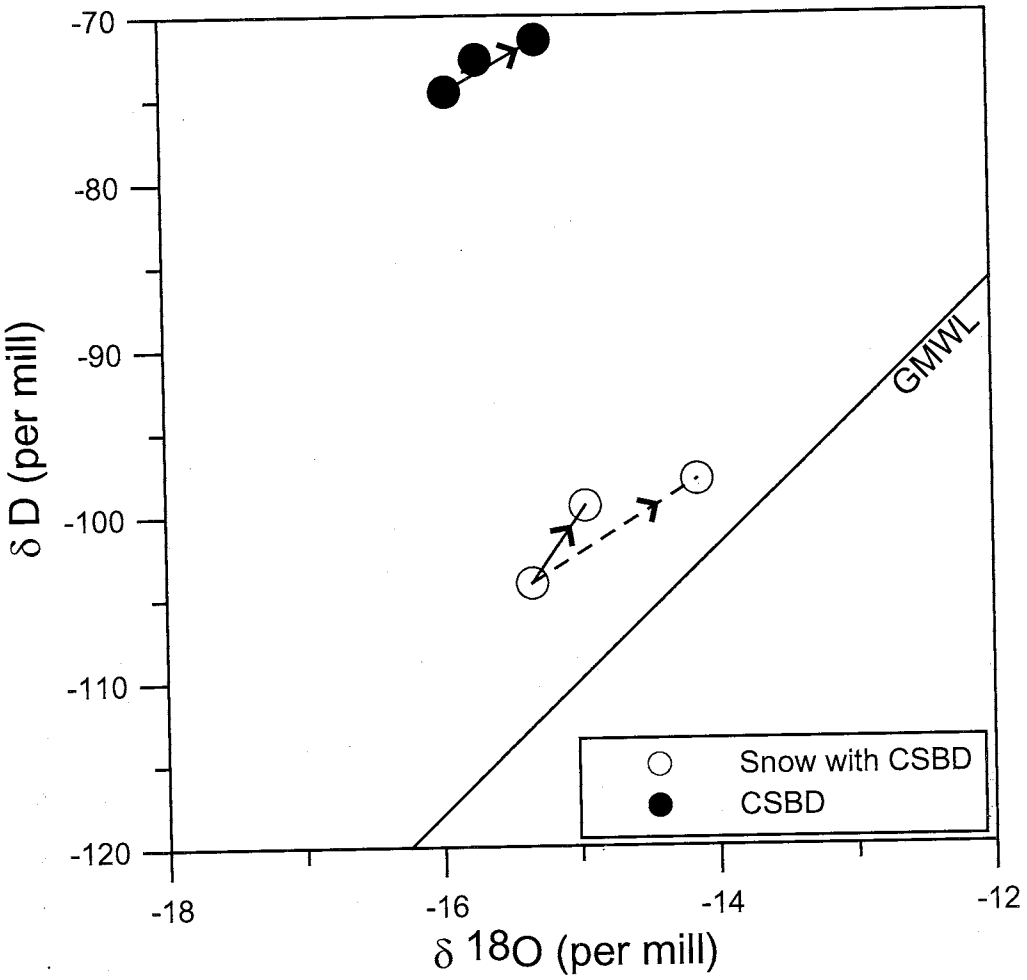

Figure 4-12. Plot of the observed isotope evolution of the snow with CSBD and CSBD (points connected by solid lines) and the evolution predicted to occur if only evaporation had affected the CSBD and only sublimation had affected the snow with CSBD (points connected by dashed lines; for the CSBD, the dashed line is the higher-slope upper line with no arrowhead), along with the global meteoric water line (GMWL). On the scale of this diagram, the error bars representing the uncertainty are the same size as the symbols, and are thus not shown.

The experimental results can be used to test a hypothesis regarding the isotope evolution of the snow with CSBD and the snow without CSBD. If the isotope evolution of snow below 0 °C is not influenced by exchange with atmospheric water vapor, then both the snow with CSBD and the snow without CSBD should be evolve along similar (if not identical within analytical error) low-slope paths on a δ D-δ ^{18}O plot, as sublimation should dominate in both cases, and this should cause low-slope evolution, as observed by Stichler *et alii* (2001). At the experimental temperature, the maximum slope that should result from sublimation of snow is 6.0 (using the vapor-ice equilibrium fractionation factors given by Majoube (1971a) and Merlivat and Nief (1967), and assuming no kinetic effects, which would reduce the slope). If isotope exchange with atmospheric water vapor can influence the evolution of snow, then snow with CSBD and snow without CSBD should evolve along different paths on a δ D-δ ^{18}O plot. In this case, the snow with CSBD would still evolve along its sublimation-caused low-slope path, but the snow without CSBD would along a much higher slope, as pure exchange with the CSBD would drive nearly-vertical evolution on a δ D-δ ^{18}O plot. The equilibration of temperatures prior to the start of each run and the fact that the snow with CSBD lost mass during the experiment indicate that condensation onto the snow with CSBD was not a significant process.

The (non-normalized) evolution of the snow with CSBD, CSBD, and snow without CSBD during the two runs are shown in Figure 4-11. The CSBD became enriched due to evaporation during the course of the experimental run. As both its initial and final isotope compositions are heavier in δ D and lighter in δ ^{18}O than those of the snow with CSBD, it is reasonable to infer that these relationships held throughout the run. Given the isotope compositions of the CSBD and snow with CSBD, the observed evolution of the snow with CSBD indicates that a combination of sublimation and exchange with atmospheric water vapor.

Due to experimental delays, the runs described here were conducted after the local snowfall season had ended. As a result, the snow used in these runs was older snow that, although maintained in sealed containers in a freezer, had undergone physical metamorphism, including increase of mean grain size. Because the snow grains used in these experiments had lower surface area/volume ratios than fresh snow, experiments using fresh snow would likely show greater influence of exchange than observed here. Similarly, while experimental design was being refined, archived snow underwent alteration in the freezer, as it plots significantly above the global meteoric water line. Fresh snow would have been more isotopically distinct from the CSBD than the old snow; because the rate of diffusive flux (which is an essential mechanism in the exchange process) is dependent on the concentration gradient between the exchanging reservoirs, a more isotopically-distinct snow sample would most likely have yielded a greater shift in isotope composition (assuming the same experimental duration).

Conclusions from the snow exchange experiment

Experimental investigation of the evolution of snow under controlled conditions in the laboratory shows that snow samples in a sealed chamber exposed to distinctive atmospheric water-vapor compositions manifested distinct changes in their isotope compositions. As the temperature of the system was maintained below 0 °C, no evidence of melt was observed, and snow-water temperatures were equalized prior to the start of the experiment, isotope exchange between the snow and the water vapor is the only factor that can reasonably explain the distinct shift in isotope signatures. Although the evolution of the snow with CSBD on a δ D-δ ^{18}O plot is not along the near-vertical slope that would have resulted from pure isotope exchange, the high slope of 11.9 it is consistent with a mix of exchange with the CSBD via the atmosphere and sublimation. The high slope of the snow with CSBD is

also distinct from that observed for the snow without CSBD (3.7, which is indicative of a kinetically-influenced process, such as sublimation). The distinct differences in isotope evolution of the snow with CSBD and the snow without CSBD meet the criteria outlined in the hypothesis discussed in the "Interpretations" section, showing that the isotope composition of snow is influenced by exchange with atmospheric water vapor.

CONCLUSIONS

The isotope composition of snow changes between snowfall and the conclusion of melt. Alteration during exposure causes the snow isotope composition to become heavier, and thus more similar to that of rain from the same area. The shift in isotope composition is due to a combination of factors, including evaporation/sublimation, partial melt and refreezing, and exchange with water vapor. The relative importance of the various processes depends on ambient conditions such as temperature and the amount of incoming solar radiation. Accounting for this shift can significantly increase estimates of the proportion of snowmelt in groundwater recharge. The results of the snow exchange experiment show that isotope exchange between snow and water vapor can account for a significant portion of this shift. In addition, different types of precipitation collectors can yield significantly different values if snow makes up a significant portion of precipitation. Collector design should be carefully considered when commencing a study to ensure that the results are applicable to the matter of interest (*exempli gratia* a study of isotope composition of meteoric water would probably call for a different collector design than a study to determine the isotope composition of water contributing to groundwater recharge).

Observations at four sites in the Southwest show that snowmelt accounts for approximately 40 to 70% of groundwater recharge; at these sites snow makes up 25 to 50% of the average annual precipitation. These high proportions of snowmelt

contribution to groundwater recharge at the sites monitored for this study, in conjunction with the work of Szecsody *et alii* (1983) and Winograd *et alii* (1998), suggest that in the Southwest, snowmelt is often a greater component of groundwater recharge than rain, and that snowmelt's contribution to recharge typically exceeds the proportion of snow in average annual precipitation.

Implications

A number of recent studies show that under generally-accepted climate-change scenarios resulting from increasing CO_2 in the atmosphere (increases of ~ 1.2 to 2 °C over the next 50 yr), the total amount of precipitation in the western USA will remain fairly constant, but the proportion of snow will decline significantly; many works also discuss the impacts of these predicted changes on surface water resources (Gleick and Chalecki, 1999; Hamlet and Lettenmaier, 1999; Hinzman and Kane, 1992; Leung *et alii*, 2004; Leung and Wigmosta, 1999; Miller and Russel, 1992; Mote, 2003; Ojima *et alii*, 1999). Despite the large impacts climate change could have on groundwater resources, there are relatively few studies dealing with this issue (Allen *et alii*, 2004; Beuhler, 2003; Kirshen, 2002; Loáiciga *et alii*, 2000; Vaccaro, 1992; Younger *et alii*, 2002; Yusoff *et alii*, 2002), and the majority of these works deal with areas outside the western USA, where the large snow-rain shifts are predicted.

If the results from our study sites are applicable to other areas of the Southwest, the loss of snowpack could have a significant impact on groundwater recharge. Because our results show that snowmelt has a higher recharge/fall ratio than rain, even if total precipitation remains constant, a shift from snow to rain could cause decreased recharge. While the lessened amount of snowfall would be one contributor to loss of recharge, the changed conditions could lessen the recharge efficiency of snow compared to that observed today. Thinner snowpacks subjected to

increased temperatures would have more rapid melt times, increasing the likelihood of runoff versus infiltration of snowmelt. Given the increasing burdens on Southwestern aquifers resulting from rapid population growth, further investigation of the potential impact of climate change on groundwater resources is important.

CONCLUSIONS

The research described here covers a wide range of topics, some of which may seem unrelated to each other. In fact, these areas of investigation all arose from one initial study, and they all relate to a common theme—the hydrogeology of the San Bernardino Valley.

The presence of a magmatically-active accommodation zone in a basin can have major impacts on its hydrogeologic properties. Although the San Bernardino Valley and its neighboring basins are bounded by highlands with of similar lithology, are of the same age, and share a common mode of formation, the San Bernardino Valley has distinct hydrogeologic properties, including groundwater chemical evolution, total dissolved solids content, groundwater ages, and storativity. The hydrogeologic differences are all related to the presence of the magmatically-active accommodation zone. The differences in hydrogeology between the San Bernardino Valley and its neighbors can be used as a basis for interpreting hydrogeological differences between other accommodation-zone basins and their neighbors.

The differences in water chemistry described above include a high ratio of $[HCO_3^-]$ to $[Ca^{2+}]$ in the San Bernardino aquifer due to injection of CO_2 related to the accommodation zone, which means that groundwaters from San Bernardino would form significant quantities of the mineral trona upon evaporation, but waters from its neighboring basins would not. Observation of this difference in mineral assemblages that would result from CO_2 injection led to an examination of other trona deposits and trona-forming waters around the world, suggesting that CO_2 injection appears to be a

necessary factor for trona formation. This refinement of the generally-accepted theory for trona formation helps to explain the limited distribution of trona deposits in the geologic record, and can aid future trona prospecting.

Given the importance of mountains as providers of water in the western USA and other parts of the world, groundwater recharge and movement in mountains is a topic that has received relatively little study. By combining a number of methods, including examination of the geology and hydraulics of the Chiricahua Mountains in southeastern Arizona, and of the major-ion solutes, stable isotopes, and dissolved gases in the range's groundwater, a conceptual model of water recharge and movement in the range was developed. Among other findings, the results show that high-elevation mountain springs are not necessarily hydraulically isolated from lower systems. In the Chiricahuas, the development of snowpack appears to be one of the factors that drives groundwater recharge. In addition, high-elevation zones of the range are the most important contributors of water to the mountain system and the adjacent San Bernardino aquifer. This is because factors such as high amounts of precipitation, high proportions of snow, and low evapotranspiration (compared to low-elevation zones) compensate for the low surface covered by the high-elevation zones.

Investigations of snow and snowmelt show that snow can experience significant changes in its isotope signature between fall and the conclusion of melt. This is driven by a complex interplay of a number of processes, including melt, sublimation, evaporation, and freeze/thaw cycling. Isotope exchange between snow and atmospheric (or soil) water vapor appears to be an influence as well. The isotope alteration of snow has important implications. Samples gathered by precipitation collectors of different designs in the same location allow different amounts of alteration to take place. For this reason, comparison of data gathered by different styles of collectors may yield misleading results if snow makes up a significant part

of the sample collected. The alteration of snow by precipitation collectors may not be evident, as even samples that have undergone significant alteration can plot on or above the global meteoric water line. The isotope signature of fresh snow is typically not representative of the bulk meltwater derived from the snow; because isotope evolution appears to increase with exposure time, samples of snow or melt collected on a given day are also unlikely to be representative of the bulk melt. As a result, isotope mixing models using fresh snow signatures as an end member contributing to groundwater recharge appear to underestimate the contribution of snowmelt. Mixing models using snowmelt isotope composition from a precipitation collector designed to provide an improved value for meltwater input (compared to fresh precipitation or a sample of snow or melt from a given day) show that snowmelt accounts for a significant proportion of groundwater recharge (typically 40-60%) at four sites in New Mexico and Arizona. The proportion of snowmelt in groundwater at these sites is typically higher than the proportion of snow in average annual precipitation, showing that snow has a greater recharge efficiency than rain.

FUTURE WORK

The presence of a magmatically-active accommodation zone in the San Bernardino valley causes significant hydrogeological distinctions compared to the neighboring basins; while it is logical to assume that a similar structure in other basins would produce many of the same differences, other accommodation-zone basins and their neighbors were not examined. Study via literature review and direct examination could show if such differences vary with the size, age, or other features of the accommodation zone.

Similarly, the investigation of trona formation relied entirely on modeling (although evaporites in the San Bernardino Basin's neighbors do show agreement

with those predicted by SNORM), and no evaporites have been identified in San Bernardino Basin that could allow direct confirmation of trona formation. The refinement suggested for the presently-accepted theory of trona formation could be tested in several ways. Waters from basins described in this report could be collected and evaporated to confirm the modeled results. Waters that have weathered granitic/ rhyolitic rocks but do not 'naturally' form trona could be exposed to CO_2 (by a means such as bubbling it through the water) before and/or during the evaporation process to see if this effects trona formation. PCO_2 values of waters in basins described here could be determined, and samples of gas emerging from faults or other possible conduits could be sampled to determine parameters such as the CO_2 content, the R/R_a value for $^3He/^4He$, and the $\delta\ ^{13}C$ of the CO_2. Using these field-measured values in mixing models would be superior to the application of 'generic' values, or the values from a nearby basin.

Because groundwater recharge and movement in mountains of the Southwest (and other parts of the world) has been the object of so little study, it is difficult to assess how widely applicable findings from the Chiricahuas may be to other ranges. In one sense, the geology and climate conditions of each range are unique. The mix of igneous and sedimentary rocks seen in the Chiricahuas (including the predominantly low-elevation presence of sedimentary outcrops) and the particular juxtaposition of igneous rocks with distinct permeabilities found near the crest of the Chiricahuas may not be observed in other ranges, so the importance of re-recharge in other ranges may be lower. However, other observations may be independent of such range-specific characteristics. One example is the apparent relationship of snowpack development and groundwater recharge in the Chiricahuas. Other ranges may show a similar relationship because snow appears to have a higher recharge efficiency than rain, and the presence of snowpack could tip the balance in favor of recharge for ranges

in arid or semi-arid regions. It might also be possible to delineate recharge zones using remote-sensing methods to examine areas of snowpack development along with characteristics such as the geology, vegetation, evapotranspiration, and topography. Such a method would be of value to water-resources planners.

The use of paired precipitation collectors appears to be a good method for determining the magnitude of alteration of stable isotope content in snow, and the samples gathered in extended funnel collectors likely yield a much better approximation of snowmelt input signature than samples of fresh snow or samples of snow or melt collected on a given day. Placing paired collectors at several sites in conjunction with soil lysimeters that would allow determination of the isotopic composition of infiltration water would show how closely a sample from an extended funnel collector represents the infiltration in the area, and would also provide a better understanding of the relative importance of recharge derived from melt at different points in time (for example, the issue of whether or not early, less altered melt is a bigger contributor to recharge than later, more altered melt could be examined). In addition, all the collectors emplaced during this study were placed in clearings. The degree of shading influences the isotope evolution of the snow, and snow intercepted by vegetation can have its isotope signature altered in a manner similar to that observed in the funnel collectors. To investigate these effects, sets of collector pairs could be placed at the same site in various conditions that could affect the sample isotope content, such as unshaded, shaded by vegetation, and subject to topographic shading for some portion of each day. Data from multiple collectors could be combined for broad estimates of isotope alteration based on remotely-sensed data such as the area covered by vegetation. Snowmelt is a significant contributor to groundwater recharge at the four sites examined with collector pairs during this study. Establishment of longer-term stations would provide more knowledge on year-to-year

REFERENCES

Abbott, M. D., Lini, A., and Bierman, P. R., 2000. δ ^{18}O, δD and ^{3}H measurements constrain groundwater recharge patterns in an upland fractured bedrock aquifer, Vermont, USA, *Journal of Hydrology*, v. 228, pp. 101-112.

Adams, A. I., Goff, F., and Counce, D., 1995. Chemical and Isotopic Variations of Precipitation in the Los Alamos Region, New Mexico, Los Alamos National Laboratory Report LA-12895-MS.

Aeschbach-Hertig, W., Peeters, F., Beyerle, U., and Kipfer, T., 1999. Interpretation of dissolved atmospheric gases in natural waters, *Water Resources Research*, v. 35, no. 9, pp. 2779-2792.

Aldrich, M. J., Jr., and Laughlin, W. A., 1984. A Model for the Tectonic Development of the Southeastern Colorado Plateau Boundary, *Journal of Geophysical Research*, v. 89, no. B12, pp. 12,207-10,218.

Allen, D. M., Mackie, D. C., and Wei, M., 2004. Groundwater and climate change: a sensitivity analysis for the Grand Forks aquifer, southern British Columbia, Canada, *Hydrogeology Journal*, v. 12, no. 3, pp. 270-290.

Anderholm, S. K., 2001. Mountain-Front Recharge Along the Eastern Side of the Middle Rio Grande Basin, Central New Mexico, Albuquerque, NM.

Anderson, O. J., Jones, G. E., and Green, G. N., 1997. Geologic Map of New Mexico, U. S. Geological Survey Open-File Report 97-52.

Anderson, T. W., Freethey, G. W., and Tucci, P., 1992. Geohydrology and Water Resources of Alluvial Basins in South-Central Arizona and Parts of Adjacent States, Washington, D. C., Professional Paper 1406-B.

Arculus, R. J., Dungan, M. A., Lofgren, G. E., and Rhodes, J. M., 1977. Lherzolite Inclusions and Megacrysts from the Geronimo Volcanic Field, San Bernardino Valley, Southeastern Arizona, Second International Kimberlite Conference, Santa Fe, NM.

Avon, L., and Durbin, T. J., 1994. Evaluation of the Maxey-Eakin Method for Estimating Recharge to Ground-Water Basins in Nevada, *Water Resources Bulletin*, v. 30, no. 1, pp. 99-111.

Bakker, M., Anderson, E. I., Olsthoorn, T. N., and Strack, O. D. L., 1999. Regional groundwater modeling of the Yucca Mountain site using analytic elements, *Journal of Hydrology*, v. 226, pp. 167-178.

Ballentine, C. J., and Hall, C. M., 1999. Determining paleotemperature and other variables by using an error-weighted, nonlinear inversion of noble gas concentrations in water, *Geochimica et Cosmochimica Acta*, v. 63, no. 16, pp. 2315-2336.

Barker, F. C., 1898. Irrigation in Mesilla Valley, New Mexico, Water-Supply and Irrigation Papers of the United States Geological Survey No. 10.

Barnes, R. L., 1991, Map Showing Groundwater Conditions in the San Simon Sub-Basin of the Safford Basin, Graham and Cochise Counties, Arizona, Hidalgo County, New Mexico--1987, Arizona Department of Water Resources Hydrologic Map Series Report Number 19.

Batu, V., 1998. *Aquifer Hydraulics: A Comprehensive Guide to Hydrogeologic Data Analysis*, John Wiley & Sons, Inc., New York, NY.

Beuhler, M., 2003. Potential impacts of global warming on water resources in Southern California, *Water Science and Technology*, v. 47, no. 7-8, pp. 165-168.

Biggs, T. H., Leighty, R. S., Skotnicki, S. J., and Pearthree, P. A., 1999. Geology and Geomorphology of the San Bernardino Valley, Southeastern Arizona, Tucson, Arizona Geological Survey Open-File Report 99-19.

Blake, W. D., Goff, F., Adams, A. I., and Counce, D., 1995. Environmental Geochemistry for Surface and Subsurface Waters in the Pajarito Plateau and Outlying Areas, New Mexico, Los Alamos National Laboratory Report LA-12912-MS.

Blasch, K., Ferré, T. P. A., Hoffmann, J., Pool, D., Bailey, M., and Cordova, J., 2004. Processes controlling recharge beneath ephemeral streams in southern Arizona, *in* Scanlon, B., ed., *Groundwater Recharge in a Desert Environment: The Southwestern United States*, American Geophysical Union, Washington, D. C.

Bodine, M. W., Jr., and Jones, B. F., 1986. THE SALT NORM: A Quantitative Chemical-Mineralogical Characterization of Natural Waters, Denver, CO, U. S. Geological Survey Water Resources Investigations Report 86-4086.

Bowser, C. J., and Jones, B. F., 2002. Mineralogic Controls on the Composition of Natural Waters Dominated by Silicate Hydrolysis, *American Journal of Science*, v. 302, pp. 582-662.

Bradley, W. H., 1964. Geology of Green River Formation and Associated Eocene rocks in southwestern Wyoming and adjacent parts of Colorado and Utah, Washington, D. C., U. S. Geological Survey Professional Paper 496-A.

Bryan, C. R., 1989. Mid-Tertiary volcanism in the eastern Chiricahuas: The Portal caldera, *in* Zidek, J., ed., *Field excursions to volcanic terranes in the western United States, Volume I: Southern Rocky Mountain Region*, New Mexico Bureau of Mines & Mineral Resources Memoir 46, Socorro, NM.

Búason, T., 1972. Equation of Isotope Fractionation Between Ice and Water in a Melting Snow Column With Continuous Rain and Percolation, *Journal of Glaciology*, v. 11, no. 63, pp. 387-405.

Caine, J. S., and Tomusiak, S. R. A., 2003. Brittle structures and their role in controlling porosity and permeability in a complex Precambrian crystalline-rock aquifer system in the Colorado Rocky Mountain Front Range, *GSA Bulletin*, v. 115, no. 11, pp. 1410-1424.

Campana, M. E., 1987. Generation of Ground-Water Age Distributions, *Ground Water*, v. 25, no. 1, pp. 51-58.

Chavez, A., Davis, S. N., and Sorooshian, S., 1994. Estimation of mountain front recharge to regional aquifers: 1. Development of an analytical hydroclimatic model, *Water Resouces Research*, v. 30, no. 7, pp. 2157-2167.

Clark, I., and Fritz, P., 1997. *Environmental Isotopes in Hydrogeology*, Lewis Publishers, Boca Raton, FL.

Coates, D. R., and Cushman, R. L., 1955. Geology and Ground-Water Resources of

the Douglas Basin, Arizona, U. S. Geological Survey Water-Supply Paper 1354.

Colbeck, S. C., 1987. Snow Metamorphism and Classification, *in* Orville-Thomas, W. J., ed., *Seasonal Snowcovers: Physics, Chemistry, Hydrology*, D. Reidel Publishing Company, Dordrecht, Netherlands.

Coleman, M. L., Shepherd, T. J., Durham, J. J., Rouse, J. E., and Moore, G. R., 1982. Reduction of Water with Zinc for Hydrogen Isotope Analysis, *Analytical Chemistry*, v. 54, no. 7, pp. 993-995.

Cooper, L. W., 1998. Isotopic Fractionation in Snow Cover, *in* McDonnell, J., ed., *Isotope Tracers in Catchment Hydrology*, Elsevier Science B. V., Amsterdam.

Craig, H., Gordon, L. I., and Horibe, Y., 1963. Isotopic Exchange Effects in the Evaporation of Water: 1. Low-Temperature Experimental Results, *Journal of Geophysical Research*, v. 68, pp. 5079-5087.

Cunningham, E. B., Long, A., Eastoe, C., and Bassett, R. L., 1998. Migration of recharge waters downgradient from the Santa Catalina Mountains into the Tucson basin aquifer, Arizona, USA, *Hydrogeology Journal*, v. 6, no. 1, pp. 94-103.

Cushman, R. L., Jones, R. S., and Hem, J. D., 1947. Geology and ground-water resources of the San Simon Basin, Cochise and Graham Counties, Arizona, U.S. Geological Survey Open-File Report (unnumbered).

D'Agnese, F. A., Faunt, C. C., Turner, A. K., and Hill, M. C., 1994. Hydrogeologic Evaluation and Numerical Simulation of the Death Valley Regional Ground-Water Flow System, Nevada and California, U. S. Geological Survey Water-Resources Investigations Report 96-4300.

Davis, J. M., Wilson, J. L., and Phillips, F. M., 1994. A Portable Air-Minipermeameter for Rapid In Situ Field Measurements, *Ground Water*, v. 32, no. 2, pp. 258-266.

Davis, L. A., Thomas Maddock, I., and Nish, R. M., 1997. Ground-water flow and interaction with surface water in San Bernardino Valley, Cochise County, Arizona and Sonora, Mexico, University of Arizona Department of Hydrology and Water Resources Report No. 97-030.

Dettinger, M. D., 1989. Reconnaissance Estimates of Natural Recharge to Desert Basins in Nevada, U.S.A., by Using Chloride-Balance Calculations, *Journal of Hydrology*, v. 106, pp. 55-78.

Drever, J. I., 1997. *The Geochemistry of Natural Waters (third edition)*, Prentice Hall, Inc., Upper Saddle River, NJ.

Drewes, H., 1980, Tectonic Map of Southeast Arizona, U.S. Geological Survey Miscellaneous Investigations Series Map I-1109.

Drewes, H. A., 1981. Tectonics of Southeastern Arizona, Washington, D.C., U.S. Geological Survey Professional Paper 1144.

du Bray, E. A., and Pallister, J. S., 1991. An Ash Flow Caldera in Cross Section: Ongoing Field and Geochemical Studies of the Mid-Tertiary Turkey Creek Caldera, Chiricahua Mountains, SE Arizona, *Journal of Geophysical Research*, v. 96, no. B8, pp. 13,435-13,457.

du Bray, E. A., and Pallister, J. S., 1995. Area Adjacent to the Turkey Creek Caldera,

Cochise County, Arizona--Analytic Data and Geologic Sample Catalog, U.S. Geological Survey Bulletin 2021-E.

du Bray, E. A., Pallister, J. S., and Yager, D. B., 1997. Geologic Map of the Turkey Creek Caldera, Chiricahua Mountains, Cochise County, Arizona, U.S. Geological Survey Miscellaneous Investigations Series Map I-2544.

DuBois, S. M., and Smith, A. W., 1980. The 1887 Earthquake in San Bernardino Valley, Sonora: Historic Accounts and Intensity Patterns in Arizona, Tucson, State of Arizona Bureau of Geology and Mineral Technology Special Paper No. 3.

Dyni, J. R., 1991. Descriptive Model of Sodium Carbonate in Bedded Lacustrine Evaporites; Deposit subtype: Green River, Model 35b.1 in Some Industrial Mineral Deposit Models: Descriptive Deposit Models, Orris, G. J. and Bliss, J. D., eds., U. S. Geological Survey Open-File Report 91-11A.

Dyni, J. R., 1996. Sodium Carbonate Resources of the Green River Formation, Denver, CO, U. S. Geological Survey Open-File Report 96-729.

Dyni, J. R., 1998. Prospecting for Green River-type sodium carbonate deposits, Proceedings of the First International Soda Ash Conference, Volume II, Rock Springs, WY, 1997.

Earman, S., McPherson, B. J. O. L., Phillips, F. M., Ralser, S., and Herrin, J. M., 2003. An Investigation of the Properties of the San Bernardino Groundwater Basin, Arizona and Sonora, Mexico, Technical Completion Report, Hydrology Program, New Mexico Institute of Mining and Technology.

Earman, S., and Phillips, F. M., 2003. Groundwater Recharge and Movement in the Central Chiricahua Mountains, Arizona, *Geological Society of America Abstracts with Programs*, v. 35, no. 7.

Elston, W. E., Deal, E. G., and Logsdon, M. J., 1983. Geology and geothermal waters of the Lightning Dock region, Animas Valley and Pyramid Mountains, Hidalgo County, New Mexico, New Mexico Bureau of Mines & Mineral Resources Circular 177.

Eugster, H. P., and Smith, G. I., 1965. Mineral Equilibria in the Searles Lake Evaporites, California, *Journal of Petrology*, v. 6, no. 3, pp. 473-522.

Evans, S. H., Jr., 1978. Studies in Basin and Range Volcanism, Ph. D. dissertation, Department of Geology and Geophysics, University of Utah, Salt Lake City.

Farrar, C. D., Sorey, M. L., Evans, W. C., Howle, J. F., Kerr, B. D., Kennedy, B. M., King, C.-Y., and Southon, J. R., 1995. Forest-killing diffuse CO_2 emission at Mammoth Mountain as a sign of magmatic unrest, *Nature*, v. 376, pp. 675-678.

Faulds, J. E., and Varga, R. J., 1998. The role of accommodation zones and transfer zones in the regional segmentation of extended terranes, *in* Stewart, J. H., ed., *Accommodation Zones and Transfer Zones: The Regional Segmentation of the Basin and Range Province*, Geological Society of America Special Paper 323.

Feng, X., Taylor, S., Renshaw, C. E., and Kirchner, J. W., 2002. Isotopic evolution of snowmelt 1. A physically-based one-dimensional model, *Water Resources Research*, v. 38, no. 10, pp. doi:10.1029/2001WR000814.

Feth, J. H., 1963. Hidden Recharge, *Ground Water*, v. 2, no. 4, pp. 14-17.

Fontes, J.-C., and Garnier, J.-M., 1979. Determination of the Initial ^{14}C Activity of the Total Dissolved Carbon: A Review of the Existing Models and a New Approach, *Water Resources Research*, v. 15, no. 2, pp. 399-413.

Francis, R. D., and Walker, C. T., 2001. The role of attenuation in the formation of the Railroad Valley structural basin, east-central Nevada; detachment control of petroleum reservoirs, *AAPG Bulletin*, v. 85, no. 7, pp. 1153-1182.

Freeze, R. A., and Cherry, J. A., 1979. *Groundwater*, Prentice Hall, Inc., Upper Saddle River, NJ.

Friedman, I., Benson, C., and Gleason, J., 1991. Isotopic changes during snow metamorphism, *in* Kaplan, I. R., ed., *Stable Isotope Geochemistry: A Tribute to Samuel Epstein*, Special Publication No. 3, The Geochemical Society, San Antonio, TX.

Friedman, I., and Smith, G. I., 1970. Deuterium Content of Snow Cores from Sierra Nevada Area, *Science*, v. 169, pp. 467-470.

Friedman, I., Smith, G. I., Gleason, J. D., Warden, A., and Harris, J. M., 1992. Stable Isotope Composition of Waters in Southeastern California, 1. Modern Precipitation, *Journal of Geophysical Research*, v. 97, no. D5, pp. 5795-5812.

Genik, G. J., 1993. Petroleum Geology of Cretaceous-Tertiary Rift Basins in Niger, Chad, and Central African Republic, *American Association of Petroleum Geologists Bulletin*, v. 77, no. 8, pp. 1405-1434.

Gleick, P. H., and Chalecki, E. L., 1999. The Impacts of Climatic Changes for Water Resources of the Colorado and Sacramento-San Joaquin River Basins, *Journal of the American Water Resources Association*, v. 35, no. 6, pp. 1429-1441.

Gonfiantini, R., 1986. Environmental Isotopes in Lake Studies, *in* Fontes, J. C., ed., *Handbook of Environmental Isotope Geochemistry, Volume 2: the Terrestrial Environment, B*, Elsevier Science Publishers B. V., Amsterdam.

Goodrich, D. C., Williams, D. G., Unkrich, C. L., Hogan, J. F., Scott, R. L., Hultine, K. R., Pool, D., Coes, A. L., and Miller, S., 2004. Comparison of methods to estimate ephemeral channel recharge, Walnut Gulch, San Pedro River Basin, Arizona, *in* Scanlon, B., ed., *Groundwater Recharge in a Desert Environment: The Southwestern United States*, American Geophysical Union, Washington, D. C.

Gross, G. W., and Wilcox, R., 1983. Groundwater Circulation in the Socorro Geothermal Area, *in* Callender, J. F., ed., *Socorro Region II*, New Mexico Geological Society 34th Annual Field Conference Guidebook.

Hage, K. D., Gray, J., and Linton, J. C., 1975. Isotopes in Precipitation in Northwestern North America, *Monthly Weather Review*, v. 103, no. 11, pp. 958-966.

Hamlet, A. F., and Lettenmaier, D. P., 1999. Effects of Climate Change on Hydrology and Water Resources in the Columbia River Basin, *Journal of the American Water Resources Association*, v. 35, no. 6, pp. 1597-1623.

Hanson, R. T., Martin, P., and Koczot, K. M., 2003. Simulation of Ground-Water/ Surface-Water Flow in the Santa Clara-Calleguas Ground-Water Basin, Ventra County, California, U. S. Geological Survey Water-Resources Investigations

Report 02-4136.
Hardie, L. A., and Eugster, H. P., 1970. The Evolution of Closed-Basin Brines, *in* Morgan, B. A., ed., *Fiftieth Anniversary Symposia: Mineralogy and Petrology of the Upper Mantle; Sulfides; Mineralogy and Geochemistry of Non-Marine Evaporites*, Mineralogical Society of America Special Paper Number Three.
Hawley, J. W., Hibbs, B. J., Kennedy, J. F., Creel, B. J., Remmenga, M. D., Johnson, M., Lee, M. M., and Dinterman, P., 2000. Trans-International Boundary Aquifers in Southwestern New Mexico, Las Cruces, NM, New Mexico Water Resources Research Institute Technical Completion Report.
Heald, W. F., 1975. *The Chiricahua Mountains*, University of Arizona Press, Tucson.
Helvaci, C., 1998. The Beypazari trona deposit, Ankara Province, Turkey, Proceedings of the First International Soda Ash Conference, Volume II, Rock Springs, WY, 1997.
Hem, J. D., 1992. Study and Interpretation of the Chemical Characteristics of Natural Water, Washington, D. C., U. S. Geological Survey Water-Supply Paper 2254.
Hermann, A., Lehrer, M., and Stichler, W., 1981. Isotope Input into Runoff Systems from Melting Snow Covers, *Nordic Hydrology*, v. 12, pp. 309-318.
Hershey, R. L., 1989. Hydrogeology and Hydrogeochemistry of the Spring Mountains, Clark County, Nevada, M. S. thesis, Geoscience Department, University of Nevada, Las Vegas.
Hevesi, J. A., and Flint, A. L., 2000. Evaluation of recharge processes affecting the Death Valley regional groundwater flow system, *Geological Society of America Abstracts with Programs*, v. 32, no. 7, pp. 338.
Hilton, D. R., 1996. The helium and carbon isotope systematics of a continental geothermal system: results from monitoring studies at Long Valley caldera (California, U.S.A.), *Chemical Geology*, v. 127, pp. 269-295.
Hinzman, L. D., and Kane, D. L., 1992. Potential Responses of an Arctic Watershed During a Period of Global Warming, *Journal of Geophysical Research*, v. 97, no. D3, pp. 2811-2820.
Hirschberg, D. M., and Pitts, G. S., 2000. Digital Geologic Map of Arizona, U. S. Geological Survey Open-File Report 00-409.
Hooper, P. R., 1990. The timing of crustal extension and the eruption of continental basalts, *Nature*, v. 345, pp. 246-249.
Hooper, R. P., and Shoemaker, C. A., 1986. A Comparison of Chemical and Isotopic Hydrograph Separation, *Water Resouces Research*, v. 22, no. 10, pp. 1444-1454.
Hulston, J. R., Taylor, C. B., Lyon, G. L., Stewart, M. K., and Cox, M. A., 1981. Environmental isotopes in New Zealand hydrology; 2, Standards, measurement techniques, and reporting of measurements for oxygen-18, deuterium, and tritium in water, *New Zealand Journal of Science*, v. 24, no. 3-4, pp. 313-322.
HydroSOLVE Inc., 2000. *AQTESOLV for Windows Users Guide*, Reston, VA.
Ingraham, N. L., and Criss, R. E., 1993. Effects of Surface Area and Volume on the Rate of Isotopic Exchange Between Water and Water Vapor, *Journal of Geophysical Research*, v. 98, no. D11, pp. 20547-20553.

Ingraham, N. L., Lyles, B. F., Jacobson, R. L., and Hess, J. W., 1991. Stable Isotopic Study of Precipitation and Spring Discharge in Southern Nevada, *Journal of Hydrology*, v. 125, pp. 243-258.

Jacobson, E. A., Wirganowicz, M., and Cochran, G. F., 2000. Importance of mountain block recharge in the numerical simulation of the Owens Lake basin groundwater system, *Geological Society of America Abstracts with Programs*, v. 32, no. 7, pp. 408?

James, E. R., Manga, M., Rose, T. P., and Hudson, G. B., 2000. The use of temperature and the isotopes of O, H, C, and noble gases to determine the pattern and spatial extent of groundwater flow, *Journal of Hydrology*, v. 237, pp. 100-112.

Jannik, N. O., Phillips, F. M., Smith, G. I., and Elmore, D., 1991. A ^{36}Cl chronology of lacustrine sedimentation in the Pleistocene Owens River systems, Eastern California, *Geological Society of America Bulletin*, v. 103, pp. 1146-1159.

Jones, B. F., 1965. The Hydrology and Mineralogy of Deep Springs Lake, Inyo County, California, U. S. Geological Survey Professional Paper 502-A.

Jones, B. F., 1966. Geochemical Evolution of Closed Basin Water in the Western Great Basin, *in* Rau, J. L., ed., *Second Symposium on Salt, Volume 1: Geology, Geochemistry, Mining*, Northern Ohio Geological Society, Cleveland, OH.

Jones, B. F., Eugster, H. P., and Rettig, S. L., 1977. Hydrochemistry of the Lake Magadi basin, Kenya, *Geochimica et Cosmochimica Acta*, v. 41, no. 1, pp. 53-72.

Jouzel, J., and Souchez, R. A., 1982. Melting-Refreezing at the Glacier Sole and the Isotopic Composition of the Ice, *Journal of Glaciology*, v. 28, no. 98, pp. 35-42.

Jull, A. J. T., Burr, G. S., McHargue, L. R., Lange, T. E., Lifton, N. A., Beck, J. W., Donahue, D. J., and Lal, D., 2004. New frontiers in dating of geological, paleoclimatic and anthropological applications using accelerator mass spectrometric measurements of ^{14}C and ^{10}Be in diverse samples, *Global and Planetary Change*, v. 41, no. 3-4, pp. 309-323.

Kalin, R. M., 2000. Radiocarbon Dating of Groundwater Systems, *in* Herczeg, A. L., ed., *Environmental Tracers in Subsurface Hydrology*, Kluwer Academic Publishers, Norwell, MA.

Kempton, P. D., 1984. Alkalic Basalts from the Geronimo Volcanic Field: Petrologic and Geochemical Data Bearing on their Petrogenesis; Petrography, Petrology and Geochemistry of Xenoliths and Megacrysts from the Geronimo Volcanic Field, Southeastern Arizona; and an Interpretation of Contrasting Nucleation and Growth Histories from the Petrographic Analysis of Pillow and Dike Chilled Margins, Hole 504B, DSDP Leg 83, Ph.D. dissertation, Southern Methodist University, Dallas.

Kempton, P. D., and Dungan, M. A., 1989. Geology and petrology of basalts and included mafic, ultramafic, and granulitic xenoliths of the Geronimo volcanic field, southeastern Arizona, *in* Zidek, J., ed., *Field excursions to volcanic terranes in the western United States, Volume I: Southern Rocky Mountain region*, New Mexico Bureau of Mines & Mineral Resources Memoir 46.

Kirshen, P. H., 2002. Potential Impacts of Global Warming on Groundwater in Eastern Massachusetts, *Journal of Water Resources Planning and Management*, v. 128, no. 3, pp. 216-226.

Labotka, T. C., and Albee, A. L., 1990. Uplift and exposure of the Panamint metamorphic complex, California, *in* Wernicke, B. P., ed., *Basin and Range Extensional Tectonics near the latitute of Las Vegas, Nevada*, Geological Society of America Memoir 176, Boulder, CO.

Langmuir, D., 1997. *Aqueous Environmental Geochemistry*, Prentice-Hall, Inc., Upper Saddle River, NJ.

Lawson, S. M., 1997. Sublimation From Snow Packs in Toiyabe National Forest, Nevada and Dixie National Forest, Utah, M. S. Thesis, Geoscience Department, University of Nevada, Las Vegas.

Lee, J., Rubin, C., Miller, M., Spencer, J., Lewis, O., and Dixon, T., 2000. Kinematics of the Eastern California shear zone north of the Garlock Fault, *Geological Society of America Abstracts with Programs*, v. 32, no. 7.

LeFevre, W. J., 1999. Geochemical Characterization of Geologically Complex Mountain Front Aquifers: Placitas, New Mexico, M. S. thesis, New Mexico Institute of Mining and Technology, Socorro.

Leung, L. R., Qian, Y., Bian, X., Washington, W. M., Han, J., and Roads, J. O., 2004. Mid-Century Ensemble Regional Climate Change Scenarios for the Western United States, *Climatic Change*, v. 62, pp. 75-113.

Leung, L. R., and Wigmosta, M. S., 1999. Potential Climate Change Impacts on Mountain Watersheds in the Pacific Northwest, *Journal of the American Water Resources Association*, v. 35, no. 6, pp. 1463-1471.

Leydecker, A., and Melack, J. A., 1999. Evaporation from Snow in the Central Sierra Nevada of California, *Nordic Hydrology*, v. 30, no. 2, pp. 81-108.

Lichty, R. W., and McKinley, P. W., 1995. Estimates of Ground-Water Recharge Rates for Two Small Basins in Central Nevada, U. S. Geological Survey Water-Resources Investigations Report 94-4104.

Loáiciga, H. A., Maidment, D. R., and Valdes, J. B., 2000. Climate-change impacts in a regional karst aquifer, Texas, USA, *Journal of Hydrology*, v. 227, pp. 173-194.

Long, A., 1966. Late Pleistocene and Recent Chronologies of Playa Lakes in Arizona and New Mexico, Ph.D. dissertation, Department of Geology, University of Arizona, Tucson.

Lord Rayleigh, 1896. Theoretical Considerations respecting the Separation of Gases by Diffusion and similar Processes, *The Philosophical Magazine and Journal of Science*, v. 42, pp. 493-499.

Lynch, D. J., 1972. Reconnaissance Geology of the Bernardino Volcanic Field, Cochise County, Arizona, M.S. thesis, Department of Geosciences, University of Arizona, Tucson.

Lynch, D. J., 1978. The San Bernardino Volcanic Field of Southeastern Arizona, *in* Clemons, R. E., ed., *Land of Cochise, Southeastern Arizona*, Twenty-ninth Field Conference Guidebook, New Mexico Geological Society.

Majoube, M., 1971a. Fractionnement en ^{18}O Entre la Glace et la Vapeur d'Eau, *Journal of Chemical Physics*, v. 68, pp. 625-636.

Majoube, M., 1971b. Fractionnement en Oxygène 18 et en Deutérium Entre l'Eau et sa Vapeur, *Journal of Chemical Physics*, v. 68, pp. 1423-1436.

Manning, A., and Solomon, D. K., 2003. Using noble gases to investigate mountain-front recharge, *Journal of Hydrology*, v. 275, pp. 194-207.

Manning, A. H., 2002. Using Noble Gas Tracers to Investigate Mountain-Block Recharge to an Intermountain Basin, Ph. D. dissertation, Department of Geology and Geophysics, University of Utah, Salt Lake City.

Mao, J., Kerrich, R., Li, H., and Li, Y., 2002. High $^{3}He/^{4}He$ ratios in the Wangu gold deposit, Hunan Province, China; implications for mantle fluids along the Tanlu deep fault zone, *Geochemical Journal*, v. 36, no. 3, pp. 197-208.

Mariner, R. H., and Nimz, G., 2000. Isotopic Composition of Snow at Medicine Lake Volcano, CA (USA) and Implications for Recharge to the 37 m^3s^{-1} Fall River Springs, *Geological Society of America Abstracts with Programs*, v. 32, no. 7.

Martinec, J., Moser, H., de Quervain, M. R., Rauert, W., and Stichler, W., 1977. Asessment of processes in the snowpack by parallel deuterium, tritium and oxygen-18 sampling, *Isotopes and Impurities in Snow and Ice: Proceedings of the Grenoble Symposium, August/September 1975*, International Association of Hydrological Sciences (IAHS) Publication No. 118.

Maulé, C. P., Chanasyk, D. S., and Muelenbachs, K., 1994. Isotopic determination of snow-water contribution to soil water and groundwater, *Journal of Hydrology*, v. 155, pp. 73-91.

Maurer, D. K., and Welch, A. H., 2001. Hydrogeology and Geochemistry of the Fallon Basalt and Adjacent Aquifers, and Potential Sources of Basalt Recharge, in Churchill County, Nevada, U. S. Geological Survey Water-Resources Investigations Report 01-4130 Carson City, NV.

McConnell, R. B., 1967. The East African Rift System, *Nature*, v. 215, pp. 578-581.

McIntyre, J. L., 1990. Late Cenozoic Structure of the Central Wassuk Range, Mineral County, Nevada, M.S. thesis, Oregon State University, Corvallis.

McKenna, L. W., Hodges, K. V., and Deaps, M. I. T., 1998. A Late Miocene Extensional Duplex, E. Panamint Range, Death Valley, CA, *Geological Society of America Abstracts with Programs*, v. 20, no. 3.

Merlivat, L., and Nief, G., 1967. Fractionnement isotopique lors des changements d'état solide-vapeur et liquide-vapeur de l'eau à des températures inférieures à 0 °C, *Tellus*, v. XIX, no. 1, pp. 122-127.

Miller, J. R., and Russel, G. L., 1992. The Impact of Global Warming on River Runoff, *Journal of Geophysical Research*, v. 97, no. D3, pp. 2757-2764.

Mohrbacher, C. J., 1984. Mountain-front recharge to the Tucson basin from the Santa Catalina Mountains, Arizona, M.S. thesis, University of Arizona, Tucson.

Morrison, R. B., 1991. Quaternary Geology of the southern Basin and Range province, *in* Morrison, R. B., ed., *Quaternary Nonglacial Geology: Conterminous U.S.*, Geology of North America volume K-2, Geological Society of America, Boulder, CO.

Moser, H., and Stichler, W., 1980. Environmental Isotopes in Ice and Snow, *in* Fontes, J. C., ed., *Handbook of Environmental Isotope Geochemistry: Volume I, The Terrestrial Environment, A*, Elsevier Science Publishers B. V., Amsterdam.

Mote, P. W., 2003. Trends in snow water equivalent in the Pacific Northwest and their climatic causes, *Geophysical Research Letters*, v. 30, no. 12, pp. 1601.

Nelson, S. T., and Dettman, D., 2001. Improving hydrogen isotope ratio measurements for on-line chromium reduction systems, *Rapid Communications in Mass Spectrometry*, v. 15, pp. 2301-2306.

Newman, B. D., Duffy, C. J., and Hickmot, D. D., 2001. Evaluating the hydrogeocehmical response of springs using singular spectrum analysis and phase-plane plots, *in* Wohnlich, S., ed., *New Approaches Characterizing Groundwater Flow: Proceedings of the XXXI International Association of Hydrogeologists Congress, Volume 2*, A.A. Balkema Publishers, Lisse, Netherlands.

Niewodniczanski, J., Grabczak, J., Baranski, L., and Rzepka, J., 1981. The Altitude Effect on the Isotopic Composition of Snow in High Mountains, *Journal of Glaciology*, v. 27, no. 95, pp. 99-111.

Ojima, D., Garcia, L., Elgaali, E., Miller, K., Kittel, T. G. F., and Lackett, J., 1999. Potential Climate Change Impacts on Water Resources in the Great Plains, *Journal of the American Water Resources Association*, v. 35, no. 6, pp. 1443-1454.

Olson, M. C., 1982. Mountain-front recharge to the Tucson basin from Tanque Verde Canyon, Arizona, M.S. thesis, University of Arizona, Tucson.

Oram III, P., 1993, Maps Showing Groundwater Conditions in the Willcox Basin, Graham and Cochise Counties, Arizona-1990, Arizona Department of Water Resources Hydrologic Map Series Report Number 25.

Oxburgh, E. R., O'Nions, R. K., and Hill, R. I., 1986. Helium isotopes in sedimentary basins, *Nature*, v. 324, pp. 632-635.

Pallister, J. S., and du Bray, E. A., 1989. Field guide to volcanic and plutonic features of the Turkey Creek Caldera, Chiricahua Mountains, southeast Arizona, *in* Zidek, J., ed., *Field excursions to volcanic terranes in the western United States, Volume I: Southern Rocky Mountain Region*, New Mexico Bureau of Mines & Mineral Resources Memoir 46, Socorro, NM.

Pallister, J. S., and du Bray, E. A., 1997. Interpretive Map and Guide to the Volcanic Geology of Chiricahua National Monument and Vicinity, Cochise County, Arizona, U. S. Geological Survey Miscellaneous Investigations Series Map I-2541.

Panichi, C., and Gonfiantini, R., 1981. Geothermal Waters, *in* Gonfiantini, R., ed., *Stable Isotope Hydrology: Deuterium and Oxygen-18 in the Water Cycle*, International Atomic Energy Agency Technical Reports Series No. 210, Vienna.

Papke, K. G., 1976. Evaporites and Brines in Nevada Playas, Nevada Bureau of Mines and Geology Bulletin 87.

Papke, K. G., 1987. Gypsum Deposits in Nevada, Nevada Bureau of Mines and

Geology Bulletin 103.
Papke, K. G., and Castor, S. B., 2003, Industrial Mineral Deposits in Nevada, Nevada Bureau of Mines and Geology Map 142.
Parry, W. T., Forster, C. B., Solomon, D. K., and James, L., 2000. Ownership of Mine-Tunnel Discharge, *Ground Water*, v. 38, no. 4, pp. 487-496.
Pearthree, P. A., 1986. Late Quaternary Faulting and Seismic Hazard in Southeastern Arizona and Adjacent Portions of New Mexico and Sonora, Mexico, Arizona Geological Survey Open File Report 86-8.
Pezzopane, S. K., and Weldon, R. J., 1990. Holocene Fault Activity Between the Basin and Range and High Cascades, Oregon, *Eos, Transactions of the American Geophysical Union*, v. 71, no. 43.
Phillips, F. M., 1981. Noble Gases in Ground Water as Paleoclimatic Indicators, Ph.D. dissertation, Department of Hydrology and Water Resources, University of Arizona, Tucson.
Phillips, F. M., 1994. Environmental Tracers for Water Movement in Desert Soils of the American Southwest, *Soil Science Society of America Journal*, v. 58, pp. 15-24.
Plummer, L. N., Prestemon, E. C., and Parkhurst, D. L., 1991. An Interactive Code (NETPATH) for Modeling Net Geochemical Reactions Along a Flow Path, U. S. Geological Survey Water-Resources Investigations Report 91-4078.
Polach, H., Calf, G., Harkness, D., Hogg, A., Kaihola, L., and Robertson, S., 1988. Performance of new technology liquid scintillation counters for ^{14}C dating, *The International Journal of Radiation Applications and Instrumentation, Part E, Nuclear Geophysics*, v. 2, no. 2, pp. 75-79.
Pouclet, A., and Durand, A., 1984. Structures cassantes cénozoïques d'aprés les phénomènes volcaniques et néotectoniques au nord-ouest du lac Tchad (Niger oriental), *Annales - Société Géologique du Nord*, v. 103, no. 2-3, pp. 143-154.
Pretti, V. A., and Stewart, B. W., 2002. Solute sources and chemical weathering in the Owens Lake watershed, eastern California, *Water Resources Research*, v. 38, no. 8.
Prudic, D. E., Harrill, J. R., and Burbey, T. J., 1995. Conceptual Evaluation of Regional Ground-Water Flow in the Carbonate-Rock Province of the Great Basin, Nevada, Utah, and Adjacent States, U. S. Geological Survey Professional Paper 1409-D.
Rascona, S. J., 1993, Maps Showing Groundwater Conditions in the Douglas Basin, Cochise County, Arizona-1990, Arizona Department of Water Resources Hydrologic Map Series Report Number 26.
Reeder, H. O., 1957. Ground Water in Animas Valley, Hidalgo County, New Mexico, New Mexico State Engineer Office Technical Report No. 11.
Robertson, F. N., 1991. Radiocarbon Dating in the San Pedro Valley, Southeastern Arizona, *Radiocarbon*, v. 33, no. 2, pp. 236-237.
Rodhe, A., 1981. Spring Flood: Meltwater or Groundwater?, *Nordic Hydrology*, v. 12, pp. 21-30.
Rose, T. P., 2003. Stable Isotope Investigation of Precipitation and Recharge Processes

in Central Nevada, *in* Kersting, A. B., ed., *Hydrologic Resources Management Program and Underground Test Area Project FY2001 - 2002 Progress Report*, Lawrence Livermore National Laboratory Report UCRL-ID-154357, Livermore, CA.

Rose, T. P., and Davisson, M. L., 1996. Radiocarbon in Hydrologic Systems Containing Dissolved Magmatic Carbon Dioxide, *Science*, v. 273, pp. 1367-1370.

Rose, T. P., Davisson, M. L., Criss, R. E., and Smith, D. K., 1999. Isotopic Investigation of Recharge to a Regional Groundwater Flow System, Great Basin, Nevada, USA, International Symposium on Isotope Techniques in Water Resources Development and Management, Vienna.

Scarborough, R. B., and Peirce, H. W., 1978. Late Cenozoic Basins of Arizona, *in* Clemons, R. E., ed., *Land of Cochise, Southeastern Arizona*, New Mexico Geological Society Twenty-Ninth Field Conference Guidebook.

Schreiber, J. F., Jr., 1978. Geology of the Willcox Playa, Cochise County, Arizona, *in* Clemons, R. E., ed., *Land of Cochise, Southeastern Arizona*, New Mexico Geological Society.

Schroeder, J. M., Lee, J., Owen, L. A., and Finkel, R. C., 2002. Quaternary dextral fault slip history along the White Mountains fault zone, California, *Geological Society of America Abstracts with Programs*, v. 34, no. 5, pp. A-87.

Schwab, K. J., 1992, Maps Showing Groundwater Conditions in the San Bernardino Valley Basin, Cochise County, Arizona, and Hidalgo County, New Mexico--1991, Arizona Department of Water Resources Hydrologic Map Series Report Number 24.

Schwennesen, A. T., 1919. Ground Water in the San Simon Valley, Arizona and New Mexico, *in* Grover, N. C., ed., *Contibutions to the Hydrology of the United States, 1917*, U. S. Geological Survey Water-Supply Paper 425.

Seaber, P. R., 1998. Hydrostratigraphic units, *in* Seaber, P. R., ed., *Hydrogeology*, Geology of North America volume O-2, Geological Society of America, Boulder, CO.

Sears, D. H., 1955. Geology of Central Panamint Range, *American Association of Petroleum Geologists Bulletin*, v. 39, no. 1, pp. 140.

Sherlock, M. G., Gettings, M. E., King, H. D., and Neuman, T. R., 1988. Mineral Resources of the Abert Rim Wilderness Study Area, Lake County, Oregon, U. S. Geological Survey Bulletin 1738-C.

Smalley, R. C., 1983. An Isotopic and Geochemical Investigation of the Hydrogeologic and Geothermal Systems in the Safford Basin, Arizona, M.S. Thesis, Department of Geosciences, University of Arizona, Tucson, AZ.

Smith, G. I., 1976. Origin of lithium and other components in the Searles Lake evaporites, California, *in* Vine, J. D., ed., *Lithium Resources and Requirements by the Year 2000*, U. S. Geological Survey Professional Paper 1005.

Smith, G. I., 1983. Core KM-3, a Surface-to-Bedrock record of late Cenozoic sedimentation in Searles Valley, California, U. S. Geological Survey Professional Paper 1256.

Smoot, J. P., and Lowenstein, T. K., 1991. Depositional Environments of Non-Marine Evaporites, *in* Melvin, J. L., ed., *Evaporites, Petroleum and Mineral Resources*, Elsevier Science Publishers B. V., Amsterdam.

Socki, R. A., Karlsson, H. R., and Gibson, E. K., Jr.,, 1992. Extraction Technique for the Determination of Oxygen-18 in Water Using Preevacuated Glass Vials, *Analytical Chemistry*, v. 64, no. 7, pp. 829-831.

Solomon, D. K., 2000. ^{4}He in Groundwater, *in* Herczeg, A. L., ed., *Environmental Tracers in Subsurface Hydrology*, Kluwer Academic Publishers, Norwell, MA.

Sommerfield, R. A., Clark, J., and Friedman, I., 1991. Isotopic changes during the formation of depth hoar in experimental snowpacks, *in* Kaplan, I. R., ed., *Stable Isotope Geochemistry: A Tribute to Samuel Epstein*, Special Publication No. 3, The Geochemical Society, San Antonio, TX.

Sorey, M., 1985. Evolution and Present State of the Hydrothermal System in Long Valley Caldera, *Journal of Geophysical Research*, v. 90, no. B13, pp. 11,219-11,228.

Sorey, M. L., Evans, W. C., Kennedy, B. M., Farrar, C. D., Hainsworth, L. J., and Hausback, B., 1998. Carbon dioxide and helium emissions from a reservoir of magmatic gas beneath Mammoth Mountain, California, *Journal of Geophysical Research*, v. 103, no. B7, pp. 15,303-15,323.

Spiegel, Z., 1957. Geology, *in* Reeder, H. O., Ground Water in Animas Valley, Hidalgo County, New Mexico, New Mexico State Engineer Office Technical Report No. 11.

Stephens, J. C., 2002. Response of Soil Mineral Weathering to Elevated Carbon Dioxide, PhD dissertation, California Institute of Technology, Pasadena.

Stewart, J. H., Anderson, R. E., Aranda-Gómez, J. J., Beard, L. S., Billingsley, G. H., Cather, S. M., Dilles, J. H., Dokka, R. K., Faulds, J. E., Ferrari, L., Grose, T. L. T., Henry, C. D., Janecke, S. U., Miller, D. M., Richard, S. M., Rowley, P. D., Roldán-Quintana, J., Scott, R. B., Sears, J. W., and Williams, V. S., 1998. Map Showing Cenozoic Tilt Domains and Associated Structural Features, Western North America, *in* Stewart, J. H., ed., *Accommodation Zones and Transfer Zones: The Regional Segmentation of the Basin and Range Province*, Geological Society of America Special Paper 323, Boulder, CO.

Stichler, W., 1987. Snowcover and Snowmelt Processes Studied by Means of Environmental Isotopes, *in* Orville-Thomas, W. J., ed., *Seasonal Snowcovers: Physics, Chemistry, Hydrology*, D. Reidel Publishing Company, Dordrecht, Netherlands.

Stichler, W., Rauert, W., and Martinec, J., 1981. Enviromental Isotope Studies of an Alpine Snowpack, *Nordic Hydrology*, v. 12, pp. 297-308.

Stichler, W., Schotterer, U., Frölich, K., Ginot, P., Kull, C., Gäggeler, H., and Pouyard, B., 2001. Influence of sublimation on stable isotope records recovered from high-altitude glaciers in the tropical Andes, *Journal of Geophysical Research*, v. 106, no. D19, pp. 22,613-22,620.

Stone, D. B., Moomaw, C. L., and Davis, A., 2001. Estimating Recharge Distribution by Incorporating Runoff from Mountainous Areas in an Alluvial Basin in the

Great Basin Region of the Southwestern United States, *Ground Water*, v. 39, no. 6, pp. 807-818.

Stute, M., and Schlosser, P., 2000. Atmospheric Noble Gases, *in* Herczeg, A. L., ed., *Environmental Tracers in Subsurface Hydrology*, Kluwer Academic Publishers, Norwell, MA.

Summers, W. K., Schwab, G. E., and Brandvold, L. A., 1972. Ground-Water Characteristics in a Recharge Area, Magdalena Mountains, Socorro County, New Mexico, New Mexico State Bureau of Mines and Mineral Resources Circular 124.

Szecsody, J. E., Jacobson, R. L., and Campana, M. E., 1983. Environmental Isotopic and Hydrogeochemical Investigation of Recharge and Subsurface Flow in Eagle Valley, Nevada, Desert Research Institute Water Resources Center Publication 42037.

Taylor, S., Feng, X., Kirchner, J. W., Osterhuber, R., Klaue, B., and Renshaw, C. E., 2001. Isotopic Evolution of a seasonal snowpack and its melt, *Water Resources Research*, v. 37, no. 3, pp. 759-769.

Taylor, S., Feng, X., Renshaw, C. E., and Kirchner, J. W., 2002. Isotopic evolution of snowmelt 2. Verification and parameterization of a one-dimensional model using laboratory experiments, *Water Resources Research*, v. 38, no. 10, pp. doi: 10.1029/2001WR000815.

Thomas, J. M., Hudson, G. B., Stute, M., and Clark, J. F., 2003. Noble gas loss may indicate groundwater flow across flow barriers in southern Nevada, *Environmental Geology*, v. 43, pp. 568-579.

Thomas, J. M., Welch, A. H., and Dettinger, M. D., 1996. Geochemistry and Isotope Hydrology of Representative Aquifers in the Great Basin Region of Nevada, Utah, and Adjacent States, U. S. Geological Survey Professional Paper 1409-C.

Unnikrishna, P. V., McDonnell, J. J., and Kendall, C., 2002. Isotope variations in a Sierra Nevada snowpack and their relation to meltwater, *Journal of Hydrology*, v. 260, pp. 38-57.

Vaccaro, J. J., 1992. Sensitivity of Groundwater Recharge Estimates to Climate Variability and Change, Columbia Plateau, Washington, *Journal of Geophysical Research*, v. 97, no. D3, pp. 2821-2833.

Vicat, J.-P., Ouclet, A., Bellion, Y., and Doumnang, J.-C., 2002. Les rhyolites hypercalines (pantellérites) du lac Tchad. Composition et signfication tectonmagmatique, *Comptes Rendu Geoscience*, v. 334, pp. 885-891.

Walvoord, M. A., Plummer, M. A., Phillips, F. M., and Wolfsberg, A. V., 2002. Deep arid system hydrodynamics 1. Equilibrium states and response times in thick desert vadose zones, *Water Resources Research*, v. 38, no. 12, pp. 1291-1302.

Waters, M. R., 1989. Late Quaternary Lacustrine History and Paleoclimactic Significance of Pluvial Lake Cochise, Southeastern Arizona, *Quaternary Research*, v. 32, no. 1, pp. 1-11.

Wertz, J. B., 1970. The Texas Lineament and Its Economic Significance in Southeast Arizona, *Economic Geology*, v. 65, pp. 166-181.

White, D. E., and Waring, G. A., 1963. Volcanic Emanations, U. S. Geological

Survey Professional Paper 440-K [Chapter K *in* Fleischer, M., *ed.*, *Data of Geochemistry, Sixth Edition* (U. S. Geological Survey Professional Paper 440)].

Wigley, T. M. L., Plummer, L. N., and Pearson, F. J. J., 1978. Mass transfer and carbon isotope evolution in natural water systems, *Geochimica et Cosmochimica Acta*, v. 42, pp. 1117-1139.

Wilson, J. L., and Guan, H., 2004. Mountain-Block Hydrology and Mountain-Front Recharge, *in* Scanlon, B., ed., *Groundwater Recharge in a Desert Environment: The Southwestern United States*, American Geophysical Union, Washington, D. C.

Wilson, L. G., DeCook, K. J., and Neuman, S. P., 1980. Regional Recharge Research for Southwest Alluvial Basins, unnumbered report, Arizona Water Resources Research Center.

Winograd, I. J., Riggs, A. C., and Coplen, T. B., 1998. The relative contributions of summer and cool-season precipitation to groundwater recharge, Spring Mountains, Nevada, USA, *Hydrogeology Journal*, v. 6, no. 1, pp. 77-93.

Wright, W. E., 2001. δD and $\delta^{18}O$ in Mixed Conifer Systems in the U.S. Southwest: The Potential of $\delta^{18}O$ in *Pinus ponderosa* Tree Rings as a Natural Environmental Recorder, Ph. D. dissertation, University of Arizona, Tucson.

Younger, P. L., Teutsch, G., Custudio, E., Elliot, T., Manzano, M., and Sauter, M., 2002. Assessments of the sensitivity to climate change of flow and natural water quality in four major carbonate aquifers of Europe, *in* Davison, R. M., ed., *Sustainable Groundwater Development*, Geological Society Special Publication No. 193, London.

Youxun, Z., 1985. Geology of the Wucheng Trona Deposit in Henan, China, *in* Harner, H. L., ed., *Sixth International Symposium on Salt, Volume One*, The Salt Institute, Alexandria, VA.

Yusoff, I., Hiscock, K. M., and Conway, D., 2002. Simulation of the impacts of climate change on groundwater resources in eastern England, *in* Davison, R. M., ed., *Sustainable Groundwater Development*, Geological Society Special Publication No. 193, London.

APPENDIX 1: Water chemistry and stable isotope data from San Bernardino Valley

Water Source	pH (field)	Temp (deg C)	DO (mg/L)	EC(µS/cm) (field)	Field Alkalinity (mg/L as $CaCO_3$)	pH (laboratory)	EC (µS/cm) (laboratory)	Hardness (CaCO3)	CO_3^{2-} (mg/L)
SBNWR									
Bath House Well	8.10	30.5	3.01	438	200	8.00	395	60	0
Bunting Well	8.34	26.4	2.52	392	177	8.00	365	46	0
Cottonwood Well	7.94	25.8	3.98	429	244	7.60	395	96	0
	7.90	27.3	4.54	438	-	-	-	-	-
East Border Well	7.83	26.9	3.88	435	216	7.70	400	84	0
Middle Well	7.79	26.3	3.84	437	208	7.60	385	112	0
North Well	7.96	26.1	3.51	426	200	7.70	395	82	0
Oasis Well	8.00	26.5	4.33	441	244	7.90	410	112	0
Old Twin Well	7.84	26.3	0.89	589	278	7.80	550	37	0
Twin II Well	7.89	28.0	3.51	451	214	7.90	410	67	0
West Border Well	7.91	28.2	3.78	443	224	7.70	390	75	0
Astin Spring	8.20	11.5	6.92	440	214	7.80	410	139	0
Goat Tank Spring	-	-	-	-	-	7.30	650	212	0
Headquarters Spring	-	-	-	-	-	7.10	700	242	0
House Spring	8.11	14.7	7.15	465	221	7.70	440	148	0
Mesa Seep	7.95	6.8	6.11	591	223	7.60	600	175	0
Snail Spring	7.58	19.7	3.80	482	212	7.50	450	128	0
Tule Spring	-	-	-	-	-	-	-	-	-
Black Draw Groundwater	7.21	22.3	3.17	1524	-	7.80	1390	549	0
Black Draw Piez.	9.15	21.0	3.10	374	-	9.13	369	-	2
Deep Border Piez.	10.43	21.1	0.02	361	-	10.74	407	-	44
Intermediate Border Piez.	10.08	20.8	1.40	381	-	10.45	358	-	21
Shallow Border Piez.	10.26	21.0	1.93	244	-	10.28	234	-	21
Hay Hollow Well	7.66	16.8	4.22	1009	-	7.85	1000	-	0
Deep Twin Piez.	7.64	22.5	1.52	316	-	7.92	328	-	0
Shallow Twin Piez.	7.89	22.1	1.62	118	-	7.27	120	-	0
Precipitation									
SBNWR Collector	-	-	-	-	-	-	-	-	-
SBNWR Collector	-	-	-	-	-	-	-	-	-
SBNWR Collector	-	-	-	-	-	-	-	15	0
SBNWR Collector	-	-	-	-	-	-	-	-	-
SBNWR Overnight Fall	-	-	-	-	-	-	-	-	-

Water Source	Calc. TDS (mg/L)	δ D (per mil)	δ ^{18}O (per mil)	^{14}C (pmc)	δ ^{13}C (per mil)	^{3}H (TU)	Date
SBNWR							
Bath House Well	390	-69	-9.2	-	-	-	01/06/98
Bunting Well	359	-71	-9.2	-	-	-	01/06/98
Cottonwood Well	400	-64	-8.6	-	-	-	01/06/98
	-	-	-	13.70	-8.3	0.7	03/16/00
East Border Well	408	-61	-9.4	-	-	-	01/06/98
Middle Well	412	-68	-8.9	-	-	-	01/06/98
North Well	392	-74	-9.3	-	-	-	01/06/98
Oasis Well	403	-65	-9.2	-	-	-	01/06/98
Old Twin Well	523	-73	-9.6	-	-	-	01/07/98
Twin II Well	406	-67	-9.3	-	-	-	01/07/98
West Border Well	413	-63	-9.4	-	-	-	01/06/98
Astin Spring	405	-67	-7.9	-	-	1.16 ± 1.03	01/07/98
Goat Tank Spring	576	-57	-8.6	-	-	-	01/07/98
Headquarters Spring	638	-65	-8.6	-	-	-	01/07/98
House Spring	413	-62	-7.4	-	-	1.83 ± 1.02	01/07/98
Mesa Seep	494	-57	-8.3	-	-	1.91 ± 0.96	01/07/98
Snail Spring	413	-66	-9.1	-	-	-	01/07/98
Tule Spring	-	-61	-8.7	-	-	-	01/07/98
Black Draw Groundwater	1535	-63	-7.6	-	-	-	06/10/99
Black Draw Piez.	333	-62	-8.4	-	-	-	12/13/01
Deep Border Piez.	262	-69	-9.6	25.5	-4.7	<0.9	12/13/01
Intermediate Border Piez.	227	-65	-8.9	-	-	-	12/13/01
Shallow Border Piez.	152	-63	-8.9	-	-	-	12/13/01
Hay Hollow Well	994	-60	-8.2	-	-	-	12/13/01
Deep Twin Piez.	329	-66	-9.2	16.2	0.8	0.6 ± 0.26	12/13/01
Shallow Twin Piez.	58	-65	-9.1	-	-	-	12/13/01
Precipitation							
SBNWR Collector	-	-55	-7.5	-	-	-	Jan 99
SBNWR Collector	-	-51	-6.7	-	-	-	March 00
SBNWR Collector	10	-43	-7.4	-	-	-	Jan 01
SBNWR Collector	-	-46	-7.7	-	-	-	July 01
SBNWR Overnight Fall	-	-48	-6.4	-	-	-	01/09/01

Water Source	pH (field)	Temp (deg C)	DO (mg/L)	EC(µS/cm) (field)	Field Alka-linity (mg/L as $CaCO_3$)	pH (laboratory)	EC (µS/cm) (laboratory)	Hardness (CaCO3)	CO_3^{2-} (mg/L)
Chiracahua Mts.									
Anita Spring	-	6.9	8.18	41	7	-	-	-	-
	6.73	9.2	-	-	-	-	-	-	-
Ash Spring	7.29	16.0	3.59	576	230	6.90	534	279	0
Bear Wallow Spring	-	8.8	8.43	70	4	-	-	-	-
	6.64	10.0	-	-	-	-	-	-	-
Birdsong Spring	-	-	-	-	5	6.30	47	11	0
	6.47	8.0	-	-	-	-	-	-	-
Booger Spring	-	7.3	8.32	83	6	6.20	92	22	0
	6.58	11.7	-	-	-	-	-	-	-
Cave Creek	8.03	12.9	8.71	176	52	7.30	168	64	0
Cima Spring	-	5.3	8.72	57	3	6.30	57	13	0
	6.60	12.0	-	-	-	-	-	-	-
Cottonwood Corral Spring	7.15	18.8	2.38	724		7.50	690	330	0
Hillside Spring	-	-	-	-	-	-	-	-	-
	-	9.8	7.98	89	-	-	-	-	-
	6.95	13.3	-	-	19	-	-	-	-
Seep near Hillside Sp.	-	-	-	-	-	-	-	-	-
Krentz Spring	7.07	24.3	2.09	729	265	7.00	732	339	0
Mormon Spring	6.83	9.9	8.73	72	16	6.90	71	18	0
Ojo Agua Fria	-	6.9	8.30	76	3	6.20	70	16	0
	6.34	8.9	-	-	-	-	-	-	-
Price Spring	6.39	15.2	3.17	129		7.00	120	42	0
Sycamore Spring	7.92	22.6	6.40	609	259	7.30	511	254	0
Lower Rustler Spring	-	7.9	7.83	110	-	6.40	99	20	0
	6.88	13.4	-	-	11	-	-	-	-
Upper Rustler Spring	-	-	-	-	-	-	-	-	-
	~7.10	-	-	-	-	-	-	-	-
Sulphur Spring	7.08	17.9	0.70	1466	68	6.90	1240	723	0
Tub Spring	-				4	-	-	-	-
	-	7.5	8.69	58	-	-	-	-	-
	6.53	7.5	-	-	-	-	-	-	-

Water Source	HCO_3^- (mg/L)	Cl^- (mg/L)	SO_4^{2-} (mg/L)	NO_3^- (mg/L)	F^- (mg/L)	Na^+ (mg/L)	K^+ (mg/L)	Mg^{2+} (mg/L)	Ca^{2+} (mg/L)	SiO_2 (mg/L)
Chiracahua Mts.										
Anita Spring	-	1.6	-	-	-	-	-	-	-	-
	-	-	-	-	-	-	-	-	-	-
Ash Spring	302	<4	58.0	<0.2	0.50	9.1	0.6	7.70	99.0	-
Bear Wallow Spring	-	<1	-	-	-	-	-	-	-	-
	-	-	-	-	-	-	-	-	-	-
Birdsong Spring	8	<1	10.0	3.10	<0.2	3.1	1.3	0.64	3.3	-
	-	-	-	-	-	-	-	-	-	-
Booger Spring	10	0.7	15.0	11.00	<0.2	3.4	1.9	1.60	6.0	-
	-	-	-	-	-	-	-	-	-	-
Cave Creek	74	1.3	17.0	1.60	0.24	5.8	1.4	2.70	21.0	-
Cima Spring	8	<1	9.0	7.10	<0.2	2.8	1.4	1.00	3.7	-
	-	-	-	-	-	-	-	-	-	-
Cottonwood Corral Spring	405	7.1	46.0	<0.2	0.24	15.0	2.0	8.60	118.0	43
Hillside Spring	-	<1	-	-	-	-	-	-	-	-
	-	-	-	-	-	-	-	-	-	-
	-	-	-	-	-	-	-	-	-	-
Seep near Hillside Sp.	-	-	-	-	-	-	-	-	-	-
Krentz Spring	407	7.7	39.0	1.10	0.31	15.0	1.4	9.60	120.0	50
Mormon Spring	24	<1	10.0	<0.2	<0.2	4.7	0.7	0.94	5.6	-
Ojo Agua Fria	6	1.8	10.0	10.00	<0.2	3.6	1.5	1.10	4.5	-
	-	-	-	-	-	-	-	-	-	-
Price Spring	57	4.0	12.0	<0.2	0.30	11.0	2.6	1.70	14.0	43
Sycamore Spring	307	<1	37.0	<0.2	0.56	18.0	0.8	7.70	89.0	-
Lower Rustler Spring	20	3.6	10.0	1.20	<0.2	4.0	2.3	1.30	6.0	-
	-	-	-	-	-	-	-	-	-	-
Upper Rustler Spring	-	<1	-	-	-	-	-	-	-	-
	-	-	-	-	-	-	-	-	-	-
Sulphur Spring	96	<4	765.0	<0.2	1.40	54.0	6.1	24.00	250.0	-
Tub Spring	-	2.5	-	-	-	-	-	-	-	-
	-	-	-	-	-	-	-	-	-	-
	-	-	-	-	-	-	-	-	-	-

Water Source	Calc. TDS (mg/L)	δ D (per mill)	δ ^{18}O (per mill)	^{14}C (pmc)	δ ^{13}C (per mill)	^{3}H (TU)	Date
Chiracahua Mts.							
Anita Spring	2	-70	-10.8	-	-	-	05/24/98
	0	-	-	-	-	-	05/28/98
Ash Spring	477	-71	-10.3	-	-	-	05/30/98
Bear Wallow Spring	0	-65	-10.0	-	-	-	05/23/98
	-	-	-	-	-	-	05/28/98
Birdsong Spring	29	-67	-10.6	-	-	-	05/23/98
	-	-	-	-	-	-	05/28/98
Booger Spring	50	-67	-10.6	-	-	-	05/23/98
	0	-	-	-	-	-	05/28/98
Cave Creek	125	-65	-9.7	-	-	-	05/30/98
Cima Spring	33	-67	-9.7	-	-	-	05/24/98
	0	-	-	-	-	-	05/28/98
Cottonwood Corral Spring	645	-66	-8.7	-	-	-	05/30/99
Hillside Spring	0	-68	-10.2	-	-	-	05/22/98
	0	-	-	-	-	-	05/23/98
	0	-	-	-	-	-	05/29/98
Seep near Hillside Sp.	-	-64	-9.9	-	-	-	05/22/98
Krentz Spring	651	-69	-8.9	-	-	-	05/24/00
Mormon Spring	46	-70	-10.4	-	-	-	06/02/98
Ojo Agua Fria	39	-69	-9.9	-	-	-	05/24/98
	0	-	-	-	-	-	05/28/98
Price Spring	146	-64	-10.1	-	-	-	05/30/99
Sycamore Spring	460	-65	-9.0	-	-	-	06/02/98
Lower Rustler Spring	48	-65	-10.5	-	-	-	05/22/98
	-	-	-	-	-	-	05/29/98
Upper Rustler Spring	0	-72	-10.4	-	-	-	05/22/98
	-	-	-	-	-	-	05/29/98
Sulphur Spring	1197	-79	-10.9	-	-	-	05/31/98
Tub Spring	3	-67	-10.5	-	-	-	05/22/98
	-	-	-	-	-	-	05/23/98
	-	-	-	-	-	-	05/28/98

Water Source	pH (field)	Temp (deg C)	DO (mg/L)	EC(µS/cm) (field)	Field Alkalinity (mg/L as $CaCO_3$)	pH (laboratory)	EC (µS/cm) (laboratory)	Hardness (CaCO3)	CO_3^{2-} (mg/L)
Chiracahua Mts.									
Turkey Creek (East)	8.09	17.9	7.87	196	45	6.40	139	54	0
Turkey Creek (West)	7.32	16.7	7.38	77	18	7.50	85	21	0
Turkey Seep	6.95	14.3	5.18	114	29	6.80	112	33	0
Welch Seep	6.81	18.0	0.89	1595	242	6.60	1360	827	0
San Bernardino Valley									
Anderson Well	7.55	27.4	1.98	250	77	7.40	272	76	0
Ashurst Well	7.82	25.2	5.89	310	145	7.80	331	124	0
Austin Flowing Artesian Well	-	-	-	-	-	-	-	-	-
Austin Ranch House Well	7.86	28.8	4.51	544	-	7.50	560	103	0
	-	-	-	-	-	-	-	-	-
Gibbons Well	7.75	31.8	5.12	395	160	7.70	422	164	0
Kimble Well	7.88	26.8	4.83	369	120	8.00	384	61	0
Krentz Well	8.31	28.6	2.60	336	165	8.30	361	83	0
Magoffin Well	6.50	32.2	1.50	1731	-	6.60	1660	493	0
Peterson #2 Well	6.73	28.3	2.47	1763	670	6.70	1790	470	0
Peterson #3 Well	7.86	29.2	5.87	394	142	8.00	417	145	0
Ranchita Well	8.13	25.0	4.87	341	115	8.20	351	96	0
Snure Well	7.88	32.8	4.47	386	140	7.80	400	138	0

Water Source	HCO_3^- (mg/L)	Cl^- (mg/L)	SO_4^{2-} (mg/L)	NO_3^- (mg/L)	F^- (mg/L)	Na^+ (mg/L)	K^+ (mg/L)	Mg^{2+} (mg/L)	Ca^{2+} (mg/L)	SiO_2 (mg/L)
Chiracahua Mts.										
Turkey Creek (East)	54	2.5	20.0	2.80	<0.2	5.7	1.1	3.40	16.0	-
Turkey Creek (West)	21	1.0	16.0	<0.2	<0.2	4.8	0.8	1.40	6.2	-
Turkey Seep	40	<1	12.0	<0.2	0.23	4.6	0.4	2.60	9.0	-
Welch Seep	341	<4	561.0	2.60	<0.2	30.0	1.6	25.00	290.0	-
San Bernardino Valley										
Anderson Well	131	4.4	9.1	1.40	3.10	21.0	2.8	2.00	27.0	112
Ashurst Well	170	5.8	5.8	4.60	0.96	12.0	5.7	5.80	40.0	95
Austin Flowing Artesian Well	-	-	-	-	-	-	-	-	-	-
Austin Ranch House Well	312	6.2	11.0	4.70	0.44	71.0	6.2	14.00	18.0	64
	-	-	-	-	-	-	-	-	-	-
Gibbons Well	218	5.9	8.0	2.10	2.10	14.0	3.8	6.40	55.0	94
Kimble Well	179	5.2	23.0	1.40	3.20	53.0	2.6	0.77	23.0	86
Krentz Well	197	5.0	4.6	5.70	0.62	37.0	7.1	11.00	15.0	55
Magoffin Well	1056	20.0	32.0	<0.1	2.90	185.0	32.0	50.00	115.0	27
Peterson #2 Well	1131	18.0	35.0	0.54	0.98	241.0	35.0	31.00	137.0	75
Peterson #3 Well	234	4.8	6.0	8.10	0.26	25.0	6.8	20.00	25.0	130
Ranchita Well	186	6.1	4.8	7.30	0.39	29.0	7.6	13.00	17.0	65
Snure Well	226	5.3	3.5	7.60	0.22	24.0	5.0	19.00	24.0	98

Water Source	Calc. TDS (mg/L)	δ D (per mill)	δ ^{18}O (per mill)	^{14}C (pmc)	δ ^{13}C (per mill)	^{3}H (TU)	Date
Chiracahua Mts.							
Turkey Creek (East)	105	-66	-9.6	-	-	-	05/29/98
Turkey Creek (West)	51	-67	-10.0	-	-	-	06/01/98
Turkey Seep	69	64	-9.7	-	-	-	06/01/98
Welch Seep	1251	-68	-10.2	-	-	-	05/29/98
San Bernardino Valley							
Anderson Well	314	-66	-9.3	35.60	-10.7	<1.1	05/24/00
Ashurst Well	346	-65	-8.9	31.70	-8.6	<0.9	05/22/00
Austin Flowing Artesian Well	-	-64	-0.9	-	-	-	01/14/01
Austin Ranch House Well	508	-67	-9.1	21.40	-7.4	0.5	03/16/00
	-	-61	-8.4	-	-	-	01/14/01
Gibbons Well	409	-62	-9.1	43.20	-9.6	<0.8	05/22/00
Kimble Well	377	-64	-9.6	29.30	-9.0	<0.7	05/17/00
Krentz Well	338	-61	-9.3	8.60	-8.3	<1.2	05/24/00
Magoffin Well	1520	-76	-10.8	1.20	-3.3	1.7 ± 0.4	02/24/01
Peterson #2 Well	1705	-72	-10.1	1.60	-0.9	<1.0	05/26/00
Peterson #3 Well	460	-60	-7.7	46.80	-7.2	<1.8	05/26/00
Ranchita Well	336	-70	-9.2	21.50	-7.6	<1.8	05/26/00
Snure Well	413	-61	-7.8	31.40	-8.4	<1.2	05/23/00

APPENDIX 2: Description of NETPATH models

Description of NETPATH modeling

NETPATH is calculate mass balance reactions based on a plausible set of reactants. User knowledge of the reactions that control the water chemistry in the area being modeled are thus important, as selection of a proper set of reactants is necessary to provide NETPATH with the tools to accurately simulate the chemical evolution observed. NETPATH requires user input of the concentrations of the ions in solution in an "initial well" and a "final well" on a flowpath, and input of sets of "constraints" and "phases" with which the change in water chemistry between the wells is measured. Constraints are elements that are found in the common rock-forming minerals (and are thus typically found in natural waters), such as carbon, calcium, and sulfur. Phases are minerals that can dissolve into or precipitate out of the water, such as calcite and gypsum.

To model the chemical evolution of water as it moves along the defined flowpath in the San Bernardino aquifer (see Chapter 1), a separate model was constructed for each well on the flowpath. That well was used as the 'final' flowpath well and NETPATH was used to simulate the mass transfers that occurred between the initial flowpath well and the well that was the subject of the simulation. The constraints used for the San Bernardino simulations consisted of carbon, calcium, magnesium, aluminum, sodium, and silica. The phase list for all wells included calcite, dolomite, potassium feldspar, sodium plagioclase, SiO_2, CO_2 gas, and illite. For simulations in which the 'final' well is on the latter portion of the flowpath, olivine was added as a phase (olivine is not a default phase in the NETPATH database, so the database was updated to include it). These phases are those likely to be transferred by the major reactions that can result from interaction with the materials that make up the San Bernardino aquifer (and 'external' process that can affect it)—sediments derived from rhyolitic rocks and carbonate minerals, clays

produced from weathering (numerous clay lenses are found in the basin fill), CO_2 injection, and (for the wells on the latter part of the flowpath) basalts. The results of the models are given below. The numeral in parentheses after each well name corresponds to the "Flowpath Well" description in Table 1-1. The numbers associated with each phase represent the number of millimoles per liter of water that NETPATH models as having been transferred into the water (positive values) or out of the water (negative values) as it traveled the flowpath.

Anderson (1)-Gibbons (2)

Calcite	0.80046
Illite	0.72424
K-Spar	-0.66063
Na-Plagiocl	-0.40603

Anderson (1)-Ashurst (3)

Calcite	0.38100
Dolomite	0.07401
Illite	0.32939
CO_2 gas	0.06025
Na-Plagiocl	-2.2212

Anderson (1)-Krentz (4)

Calcite	-1.1072
Dolomite	0.85809
Illite	-1.95108
CO_2 gas	0.32871
Na-Plagiocl	-2.2212

Anderson (1)-Ranchita (5)

Calcite	-1.17517
Dolomite	0.80956
Illite	-1.42782
CO_2 gas	0.34543
K-Spar	0.97949
Na-Plagiocl	0.46416

Anderson (1)-Cottonwood (6)

Calcite	-1.19337
Dolomite	0.43207
CO_2 gas	2.31761
K-Spar	0.81511
Na-Plagiocl	2.14685
Illite	-1.34053

Anderson (1)-Austin (7)

Calcite	-1.77308
Dolomite	0.82315
CO_2 gas	2.07648
K-Spar	1.27733
Na-Plagiocl	2.90156
Illite	-2.13172

APPENDIX 3: Chemistry data used for Figure 1-5

Sample ID	Ca^{2+}	Mg^{2+}	Na^{+}	K^{+}	HCO_3^{-}	SO_4^{2-}	Cl^{-}
Lower Chiricahauas recharge to San Bernardino							
Ash Spring	99	7.7	9.1	0.6	302	58	< 4
Cottonwood Corral Spring	118	8.6	15	2	405	46	7.1
Krentz Spring	120	9.6	15	1.4	407	39	7.7
Sycamore Spring	89	7.7	18	0.8	307	37	< 1
San Bernardino groundwaters							
Anderson Well	27	2	21	2.8	131	9.1	4.4
Ashurst Well	40	5.8	12	5.7	170	5.8	5.8
Astin Spring	21	21	40	8.5	265	9	7
Austin Ranch House Well	18	14	71	6.2	312	11	6.2
Bath House Well	11	8	74	4.2	250	10	6
Bunting Well	9	5.6	72	2.4	230	9	6
Cottonwood Well	18	12.5	58	2.6	255	10	6
East Border Well	18	9.5	65	2.7	260	10	6.2
Gibbons Well	55	6.4	14	3.8	218	8	5.9
Goat Tank Spring	27	35	56	12.6	345	30	18
Hay Hollow Well	76	47	85	19	657	57	19
Headquarters Spring	31	40	60	14	375	38	22
House Spring	18	25	40	11	270	13	10
Kimble Well	23	0.77	53	2.6	179	23	5.2
Krentz Well	15	11	37	7.1	197	4.6	5
Magoffin Well	115	50	185	32	1056	32	20
Mesa Seep	24	28	55	12	255	70	24
Middle Well	20	15	54	2.7	265	10	6
North Well	13	12	63	2.9	250	10	6
Oasis Well	20	15	53	2.5	260	9	6
Old Twin Well	10	2.9	118	2.6	330	14	11
Peterson #2 Well	137	31	241	35	1131	35	18
Peterson #3 Well	25	20	25	6.8	234	6	4.8

Major-ion data from the San Bernardino Valley and vicinity. All values are reported as mg/L.

APPENDIX 4: Description of mass-balance calculation methodology

All mixing calculations described in the text (which are simple two-end-member mixes) were performed using the 'Solver' tool of Microsoft Excel. An example is provided here for determining what proportion of two end members of known values would be needed to form a mixture with a known value (the 'value' could be any analytical value for which mixing will proceed linearly, such as the $\delta\ ^{18}O$ or $\delta\ ^{13}C$ of a water sample). The same principle used in the example problem can also (with only slight modification) be used to solve for the unknown value of a second end member when the proportions of the two end members, the value of one end member, and the value of the mixture are known.

As shown in Tables A4-1A and A4-1B (Table A4-1A shows the values or formulae entered into the various cells, Table A4-1B shows the resultant values displayed by Excel) the analytical values of the two end members and the mix are entered into cells A2, A3, and A5 of a spreadsheet. Seed values of mix proportions are provided in cells B2 and B3 (a 50-50 mix was used for the seed). Seed values are simply dummy variables that will allow the Solver function to work, they are not meant to be estimates of the actual proportion of each end member in the mix). The seed values are entered such that the first end member's fractional percentage is entered directly, while the second end member's fractional percentage is dependant on the fractional percentage entered for the first end member (*exempli gratia*, if the first end member's fractional percentage in the mixture is 0.97, the fractional percentage is automatically set to 0.3). In cells C2 and C3, the value for each end member of is multiplied by its fractional percentage in the mixture. The value-proportion product for the two end members is summed in cell C5, which yields the value that a mix of the entered proportions would have.

The Solver tool is then activated. It is instructed to find a mix proportion for the two end member that will cause the calculated value of the mix to equal the

observed value. Solver is instructed to estimate the value by changing the fractional percentage of the first end member (which automatically causes the proportion of the second end member to change). For linear problems, the Solver tool uses the branch-and-bound method and the simplex method with bounded variables to converge on a solution. Table A4-1C shows the solution produced for the Solver tool for the hypothetical scenario shown in Table A4-1A.

	A	B	C	D
1		**Analytical value**	**Fractional mixture percent**	**Contribution to mixture**
2	End member 1	5	0.5	2.5
3	End member 2	20	0.5	10
4				
5	Final composition	10		12.5

	A	B	C	D
1		**Analytical value**	**Fractional mixture percent**	**Contribution to mixture**
2	End member 1	5	0.5	=B2*C2
3	End member 2	20	=1-C2	=B3*C3
4				
5	Final composition	10		=SUM(D2:D3)

	A	B	C	D
1		**Analytical value**	**Fractional mixture percent**	**Contribution to mixture**
2	End member 1	5	0.66666667	3.333333333
3	End member 2	20	0.33333333	6.666666667
4				
5	Final composition	10		10

APPENDIX 5: Stable isotope data and elevation data, Chiricahua Mountains

Site	$\delta^{18}0$ (‰)	δ D (‰)
Chiricahua Mountains		
Anita Spring	-10.79	-70
Ash Spring	-10.25	-71
Bear Wallow Spring	-9.97	-65
Birdsong Spring	-10.58	-67
Booger Spring	-9.59	-67
Cave Creek	-9.66	-65
Cima Creek	-9.69	-67
Cottonwood Corral Spring	-8.73	-66
Hillside Seep	-9.94	-64
Hillside Spring	-10.18	-68
Krentz Spring	-8.94	-69
Lower Rustler Spring	-10.48	-65
Mormon Spring	-10.35	-70
Ojo Agua Fria	-9.87	-69
Price Can Dr #1	-9.95	-59
Price Spring	-10.13	-64
Sulphur Spring	-10.89	-79
Sycamore Spring	-9.04	-65
Tub Spring	-10.50	-67
Turkey Creek (East)	-9.55	-66
Turkey Creek (West)	-10.04	-67
Turkey Seep	-9.65	-64
Upper Rustler Spring	-10.36	-72
Welch Seep	-10.20	-68
San Bernardino springs		
Astin Spring	-7.88	-67
Black Draw	-7.80	-63
Goat Tank Spring	-8.64	-57
Headquarters Spring	-8.56	-65
House Spring	-7.39	-62
Mesa Seep #1	-7.54	
Mesa Seep #2	-8.34	-57
Snail Spring	-9.08	-66
Tule Spring	-8.65	-61
San Bernardino basin-center wells		
Bathhouse	-9.21	-69
Bunting	-9.18	-71
Cottonwood Well	-8.64	-64
East Border Well	-9.35	-61
Middle Well	-8.94	-68
North Well	-9.25	-74
Oasis Well	-9.17	-65
Old Twin Well	-9.56	-73
Twin II Well	-9.29	-67
West Border Well	-9.35	-63

Site	$\delta^{18}0$ (‰)	δ D (‰)
San Bernardino wells		
Anderson Well	-9.34	-66
Ashurst Well	-8.89	-65
Gibbons Well	-9.06	-62
Krentz Well	-9.27	-61
San Bernardino precipitation		
SB precip 1-99	-7.53	-55
SB precip 3-00	-6.71	-51
SBP 1/01	-7.4	-43
SBP 1/01 #2	-7.65	-46
SB ONP	-6.4	-48
Chiricahua precipitation		
Chiricahua Crest (Funnel) 10/02	-6.30	-44.11
Chiricahua Crest PVC 5/03	-10.90	-69.87
Chiricahua Crest Funnel 5/03	-10.48	-67.44
Chiricahua Crest PVC 10/03	-9.53	-62.10
Chiricahua Crest Funnel 10/03	-9.33	-59.10
Chiricahua Crest PVC 6/04	-10.20	-68.90
Chiricahua Crest Funnel 6/04	-10.26	-71.67
SWRS (Funnel) 10/02	-5.00	-33.33
SWRS PVC 5/03	-9.13	-60.47
SWRS Funnel 5/03	-8.70	-58.27
SWRS PVC 10/03	-6.85	-51.59
SWRS Funnel 10/03	-6.78	-51.07
SWRS PVC 6/04	-11.54	-77.52
SWRS Fun [ext.blk] 6/04	-12.06	-77.91

APPENDIX 6: Results of SNORM models

	SBB	Willcox	Animas	SSB	Douglas
Trona	62.75	0	0.69	0	0
Misc.	6.63	4.33	1.37	0.13	0.2
Gypsum	2.94	26.96	59.73	70.24	31.63
Halite	2.83	30.55	13.62	21.48	64.81
Calcite	24.85	38.16	24.59	8.15	3.36

Percent (by mass) of the normative evaporite mineral assemblage accounted for by each mineral family (*exempli gratia* "Gypsum" accounts for gypsum and anhydrite), San Bernardino and neighboring basins.

Source	Calcite + Dolomite	Trona	Pirssonite	Burkeite	Apthitalite + Thenardite	Gypsum + Glauberite + Syngenite	Halite	Significant Misc.	Plot ID
Deadman	46	35.5	4.2	0	7.5	0	0		1
Hot	19.38	37.5	4.8	7.8	7.8	0	20.9		2
Casa Diablo Well	0.06	35.45	0.33	8.4	9.7	0	34.6	Borax = 10	3
Colton	0.19	6.69	0.43	25.12	5.97	0	48.44	Borax = 11	4
Hot Creek Gorge	0.12	44.79	0.79	9.48	5.57	0	30.22	Borax = 8	5
Little Hot Creek	0.39	40.95	9.7	9	5.83	0	27.01	Borax = 6	6
Sorey Meadow	0.63	9.98	2.6	16.94	14.3	0	43.34	Borax = 10	7
Big Springs	7.08	46.23	22.99	1.67	11.76	8.95	0		8
Laurel Springs	51.52	0	0	0	17.75	28.75	1.29		9
Casa Diablo Hot Springs	2.31	0	2.63	0	29.34	0	50.99	Borax = 13	10
[blank]	0	0	0	0	0	0	0		11
Convict	75	0	0	0	0	19.98	1		12
McGee	63.11	0	0	0	0	28.08	2.2		13
Hilton	55	0	30.1	0	7.5	0	3.9		14
Rock	21.2	0	57	0	15.9	0	3.9		15
Pine	12.5	0	0	0	57	27.1	1.2		16
Bishop	69	0	0	0	23.4	0	4.1		17
Big Pine	56	0	16.9	0	18.7	0	8.2		18
Birch	59	0	14	0	20.6	0	5.7		19
Goodale	45.6	0	0	0	0	49.5	2.2		20
Sawmill	58	0	0	0	4.5	32.5	1.7		21
Independence	52.5	0	0	0	30.66	1.1	15		22
Shepherd	61.19	0	0	0	0	29.62	4.8		23
Lone Pine	62.33	0	14.7	0	14.92	0	5.79		24
Cottonwood	55.11	0	27.48	0	13.85	0	2.96		25
Ash	51.63	0	0	0	0	41.1	1.85		26
Summit	59.47	0	20.74	0	15.51	0	3.68		27
Nine Mile Canyon	64.63	0	3.66	18.43	5.56	0	7.33		28

Percent (by mass) of the normative evaporite mineral assemblage accounted for by each mineral family, Owens River Basin.

APPENDIX 7: Average annual temperature data and elevation data for southeastern Arizona

Station	Elevation (m)	Mean Temp (°C)
Portal	1524	14.6
Chiricahua NM	1625	14.6
Portal 4SW	1643	12.3
Paradise	1655	12.8
Tuson Magnetic Observatory	771	19.4
Sabino Canyon	796	20.4
Benson	1094	17.1
San Simon	1100	16.7
Apache Powder Company	1125	16.8
Bowie	1146	17.8
San Simon 9 ESE	1183	17.1
Douglas Smelter	1210	17.1
Douglas FAA AP	1250	16.7
Douglas	1262	16.6
Cochise 4 SSE	1274	15.6
Wilcox	1280	15.2
Pearce Sunsites	1366	16.5
Tombstone	1384	17.4
Cochise Stronghold	1500	15.5
Bisbee 2	1530	16.7
Kitt Peak	2085	12.8
Palisade Ranger Station	2426	9.3

APPENDIX 8: Water chemistry data, Chiricahua Mountains

Sample ID	Ca^{2+}	Mg^{2+}	Na^{+}	K^{+}	HCO_3^{-}	SO_4^{2-}	Cl^{-}
Chiricahua Crest							
Birdsong Spring	3.3	0.64	3.1	1.3	8	10	< 1
Cima Spring	3.7	1	2.8	1.4	8	9	< 1
Lower Rustler Spring	6	1.3	4	2.3	20	10	3.6
Booger Spring	6	1.6	3.4	1.9	10	15	0.7
Ojo Agua Fria	4.5	1.1	3.6	1.5	6	10	1.8
Chiricahua Southest							
Cottonwood Corral Spring	118	8.6	15	2	405	46	7.1
Sycamore Spring	89	7.7	18	0.8	307	37	< 1
Krentz Spring	120	9.6	15	1.4	407	39	7.7
Burro Spring	8	1.3	11	5.9	46	2.6	6.5
Price Spring	14	1.7	11	2.6	57	12	4
Chiricahua Mineral-ized							
Sulphur Spring	250	24	54	6.1	96	765	< 4
Welch Seep	290	25	30	1.6	341	561	< 4
Hilltop Mine Spring	163	20	4.7	0.9	239	296	3.6
Chiricahua Mid-East							
Ash Spring	99	7.7	9.1	0.6	302	58	< 4
Cave Creek	21	2.7	5.8	1.4	74	17	1.3
Turkey Creek (East)	16	3.4	5.7	1.1	54	20	2.5
Chiricahua Mid-West							
Mormon Spring	5.6	0.94	4.7	0.7	24	10	< 1
Turkey Seep	9	2.6	4.6	0.4	40	12	< 1
Turkey Creek (West)	6.2	1.4	4.8	0.8	21	16	1
San Bernardino							
Anderson Well	27	2	21	2.8	131	9.1	4.4
Ashurst Well	40	5.8	12	5.7	170	5.8	5.8
Gibbons Well	55	6.4	14	3.8	218	8	5.9

Major-ion data from the Chiricahuas and vicinity. All values are reported as mg/L.

APPENDIX 9: Stable isotope data from individual precipitation events, Chiricahua Mountains

Sample	δ D (‰)	Elevation (m)
Chir Rain ~4800 2/13/03	-62.0	1463
Chir Rain ~5519 2/13/03	-16.3	1682
Chir Rain ~5600 2/13/03	-49.7	1707
Chir Rain 2/13/03 ~6553	-47.1	1997
Chir Rain ~7058 2/13/03	-50.9	2151
Chir Rain ~7600 2/13/03	-63.5	2316
Chir Snow ~6509 2/27/03	-58.4	1984
Chir Snow ~7018 2/27/03	-58.1	2139
Chir Snow ~7442 2/27/03	-61.5	2268
Chir Snow ~8006 2/27/03	-53.5	2440
Chir Snow ~8590 2/27/03	-51.7	2618
Snow from Gate ~4400 1/01	-87.7	1347
Snow from Idlewilde 1/01	-94.7	1522
Snow from H. Martyr 1/01	-108.8	1667

APPENDIX 10: Recharge temperature-elevation calculation results, Chiricahua Mountains

Anderson Well		Ashurst Well		Ranchita Well		Twin II Well		Ash Spring		Cottonwood Corral	
Elev. (m)	Temp. (° C)	Elev. (m)	Temp. (° C)	Elev. (m)	Temp. (° C)	Elev. (m)	Temp. (° C)	Elev. (m)	Temp. (° C)	Elev. (m)	Temp. (° C)
1561	19.79	1423	24.05	1350	28.89	1140	40.25	1881	13.28	1835	11.46
2000	17.61	1500	23.49	1500	28.06	1500	37.18	2000	12.76	2000	10.77
2500	15.29	2000	21.03	2000	25.49	2000	34.02	2500	10.62	2500	8.71
2946.5	13.29	2500	18.69	2500	22.71	2500	30.71	2946.5	8.79	2946.5	6.92
		2946.5	16.6	2946.5	20.59	2946.5	27.96				

Lower Rustler		Sulphur Spring		Sycamore Spring		Tub Spring		Welch Seep	
Elev. (m)	Temp. (° C)	Elev. (m)	Temp. (° C)	Elev. (m)	Temp. (° C)	Elev. (m)	Temp. (° C)	Elev. (m)	Temp. (° C)
2551	2.95	1600	9.87	1876	10.8	2774	2.51	1423	10.93
2750	2.21	2000	8.3	2000	10.1	2946.5	1.86	1500	10.61
2946.5	1.49	2500	6.27	2500	7.37			2000	8.59
		2946.5	4.55	2946.5	5.1			2500	6.52
								2946.5	4.96

Calculated recharge temperatures based on assumed recharge elevations.
The lapse curve equation used to determine recharge elevation is:
Temp (° C) = Elevation (m) * 0.00955215991 + 29.31855235

APPENDIX 11: Snow pan data, Magdalena Mountains

Unshaded (US) Pan

Date	Avgerage temperature (°C)	Minimum temperature (°C)	Maximum temperature (°C)	Total mass loss (g)	Melt mass (g)	Evap/Sub loss (g)	Snow δ D (‰)	Melt δ D (‰)	Snow δ 18O (‰)	Melt δ 18O (‰)
1/21/2004	-7.4	-9.1	-5.2	-	-	-	-109.7	-	-16.78	-
1/22/2004	-5.6	-9.6	-1.4	-	-	-	-106.5	-	-16.54	-
1/23/2004	-3.7	-7.8	-0.2	439	372	67	-101.8	-112.9	-16.74	-17.68
1/24/2004	-5.7	-7.3	-3.7	775	719	56	-95.0	-103.6	-15.02	-16.22
1/25/2004	-9.2	-16.6	-7.2	57	157	-	-92.1	-103.6	-14.09	-16.11
1/27/2004	-16.1	-20.3	-12.1	124	124	-	-86.3	-78.8	-13.07	-12.63
1/29/2004	-9.7	-14.1	-5.6	771	574	197	-82.5	-79.5	-12.30	-10.60
1/31/2004	-6.2	-8.9	-3.1	850	775	75	-	-78.6	-	-11.78

Shaded (S) Pan

Date	Avgerage temperature (°C)	Minimum temperature (°C)	Maximum temperature (°C)	Total mass loss (g)	Melt mass (g)	Evap/Sub loss (g)	Snow δ D (‰)	Melt δ D (‰)	Snow δ 18O (‰)	Melt δ 18O (‰)
1/21/2004	-7.4	-9.1	-5.2	-	-	-	-110.8	-	-17.44	-
1/22/2004	-5.6	-9.6	-1.4	-	2	-	-108.4	-	-17.23	-
1/23/2004	-3.7	-7.8	-0.2	91	0	91	-103.2	-	-15.46	-
1/24/2004	-5.7	-7.3	-3.7	655	468	187	-97.0	-109.0	-14.31	-17.08
1/25/2004	-9.2	-16.6	-7.2	218	132	86	-96.5	-107.6	-14.19	-15.99
1/27/2004	-16.1	-20.3	-12.1	160	1	159	-95.3	-	-13.64	-
1/29/2004	-9.7	-14.1	-5.6	451	253	199	-95.5	-90.8	-13.52	-13.06
1/31/2004	-6.2	-8.9	-3.1	680	602	78	-	-93.8	-	-13.04